Dissecting and Modeling Oncogene Dependent Molecular Mechanisms in Lymphoma Genesis and Progression

Doctoral Thesis

In partial fulfillment of the requirements for the degree

“Doctor rerum naturalium (Dr. rer. nat.)”

in the Molecular Medicine Study Program

at the Georg-August University Göttingen

submitted by Elisabeth Hand

born in Berlin

Göttingen, 2013

Thesis Committee

Prof Dr. Dieter Kube (Supervisor)

E-Mail	dkube@med.uni-goettingen.de
Phone	0049-551-391537
Postal Address	Universitätsmedizin Göttingen Zentrum Innere Medizin Abteilung Hämatologie und Onkologie Robert-Koch-Straße 40 37075 Göttingen

Prof Dr. Mikael Simons

E-Mail	msimons@gwdg.de
Phone	0049-551-3899533
Postal Address	Max-Planck-Institut für experimentelle Medizin Hermann-Rein-Str. 3 37075 Göttingen

Prof Dr. Peter Burfeind

E-Mail	pburfei@gwdg.de
Phone	0049-551-397595
Postal Address	Universitätsmedizin Göttingen Zentrum Hygiene und Humangenetik Institut für Humangenetik Heinrich-Düker-Weg 12 37073 Göttingen

Date of Disputation:

Affidavit

By this I declare that I independently authored the presented thesis:

“Dissecting and modeling oncogene dependent molecular mechanisms in lymphoma genesis and progression”

and that I did not use other auxiliary means than indicated. Paragraphs that are taken from other publications, by wording or by sense, are marked in every case with a specification of the literary source.

Furthermore I declare that I carried out the scientific experiments following the principles of Good Scientific Practice according to the valid “Richtlinien der Georg-August-Universität Göttingen zur Sicherung guter wissenschaftlicher Praxis”.

_____

Elisabeth Hand

Göttingen, August 2013

Table of Contents

Abstract

Aggressive Non-Hodgkin lymphomas (aNHL) are a heterogeneous group of lymphomas. The constellation of oncogenic pathway activities can vary in patients with the same malignant disease. The pathological mechanisms behind the current criteria to distinguish individual aNHL subtypes are still poorly understood. Molecular models depicting the dynamics of oncogenic signaling and cross talk of the pathways can help to obtain a better understanding of lymphoma pathogenesis. Thereby the development of future targeted therapies, that will have to intervene with specific signaling modules to reverse pathway deregulation, will be enabled. We postulate that the description of a time-resolved global gene expression change provides new insights into the dynamics of oncogenic signaling and that the intervention into pathway intersections allows identifying new essential pathway nodes and cross talks for targeted therapies.

To gain closer insight into distinct cell signaling networks and their relevance for NHL subtypes, firstly, high-dimensional data of time-resolved gene expression changes in BL2 cells induced by BCR or CD40 activation were generated. By using a newly established computational method we were able to describe 20 disjoint sets of genes to group their time courses. 15 significant sets of genes were identified for BCR stimulated samples and 5 significant sets of genes for CD40 activated samples, all displaying distinct time courses. We discovered a co-repression of *LEF1*, *PTCH1* and *NOTCH1* by activation of the B cell receptor. Functional assays revealed that BL cells are not responsive to Sonic hedgehog stimulation, but evidence is provided for a c-Myc-driven non-canonical regulation of this pathway. Furthermore, a working model for a causality network of BCR induced gene expression correlations was compiled. In addition, sustained activated BCR signaling induced a change of the gene expression profile towards a certain 'DLBCL-likeness'. Therefore, a first step to develop a model displaying the causative factors for the non-mBL signature is provided. Secondly, the gene expression changes of BCR or CD40L stimulated BL2 cells after chemical inhibition of Tak1, JNK, p38 and IKK2 were monitored on the whole genome level. In BCR stimulated cells the activity of PI3K and Mek1/2 was as well inhibited. Additional biochemical analyses supported the view that Tak1 is a pivotal modulator of both CD40 and BCR mediated p38 and NF-κB signaling. Moreover, using (5Z)-7-Oxozeanol as well as *TAK1*-directed siRNA to inhibit Tak1 activity, a corresponding Tak1-Erk1/2 subnetwork was described.

Thus, the present study and the herein allocated data provide deep insight into oncogenic pathway activities and enable a large variety of continuing studies, which may help to obtain a better understanding of the biology of lymphoma.

List of Figures

List of Tables

1 Introduction

Approved living circumstances in the Western World as well as the demographic change and prolonged life expectancies have favored cancer becoming a leading cause of mortality worldwide. According to the World Health Organization (WHO), cancer accounted for 13 % of all deaths in Europe in 2008 (Ferlay et al., 2010). Non-Hodgkin lymphoma (NHL) is estimated to be the tenth most common cancer worldwide, with an increasing incidence over the last decades and highest rates being reported in the most economically developed countries (Cancer Research UK, 2010). NHLs are a subgroup of lymphoma, which comprise a heterogeneous group of hematological malignancies that originate mainly from B cells (95 %) and usually form solid tumors. NHL can be divided into indolent (slow-growing) and aggressive (fast-growing) subtypes (Jaffe et al., 1998). B cell aggressive NHL (aNHL) is a very heterogeneous group of malignancies. In the last decade, clinical and experimental investigations complemented by novel molecular genome-wide investigations like gene expression profiling and whole-genome sequencing have helped to expand our understanding of the biology and diversity of different types of aNHL.

1.1 Development and transformation of germinal center B cells in lymph nodes

In the past 20 years, exciting progress has been made to elucidate the cellular origin of B cell lymphomas as well as the key events leading to transformation. Furthermore, large efforts were made to characterize the pathogenesis of lymphoma (reviewed in Klein and Dalla-Favera, 2008; Küppers, 2005). The development of B cells as part of the adaptive immune response is strictly dependent on their surrounding microenvironment. To achieve optimal antigen recognition by their surface antigen receptor, B cells undergo several maturation, differentiation and proliferation steps in different compartments of the body. Early B cell development occurs in the bone marrow, consists of rearrangement of the heavy and light chain immunoglobulin (Ig) genes and concludes with a B cell carrying a functional, non-autoreactive B cell receptor (BCR). Those cells differentiate into mature naïve B cells, leave the bone marrow and circulate in the blood and lymphatic system to performe the role of immune surveillance. In contrast, precursor B cells, which were unable to maturate a functionally active BCR, undergo apoptosis.

Upon antigen binding to the BCR, mature naïve B cells can be activated. In the T-cell-dependent response to exogenous antigens, proliferating B cells form so called ‘germinal centers’ (GCs) in the follicles of peripheral lymphoid tissues including lymph nodes. In the early 1990 it was shown that GCs are the main site where the immunoglobulins are modified and finalized through somatic hypermutation (SHM) and class-switch recombination (CSR) (Berek et al., 1991; Jacob et al., 1991).

Today, it is broadly accepted, that the GC microenvironment is the general source of memory B cells and plasma cells (Figure 1-1), producing high-affinity antigen receptors and therefore being essential for an effective protection against invading microorganisms (MacLennan, 1994). In addition, the GC micromilieu seems to play an important role in lymphoma pathogenesis, since several studies observed that most types of malignant B cells forming B cell lymphomas reflect their origin by being 'frozen' at that particular differentiation status. In fact, nearly all B cell aNHLs display somatically mutated IgV genes, indicating that they are derived from GC or post-GC B cells (Küppers et al., 1999; Stevenson et al., 2001).

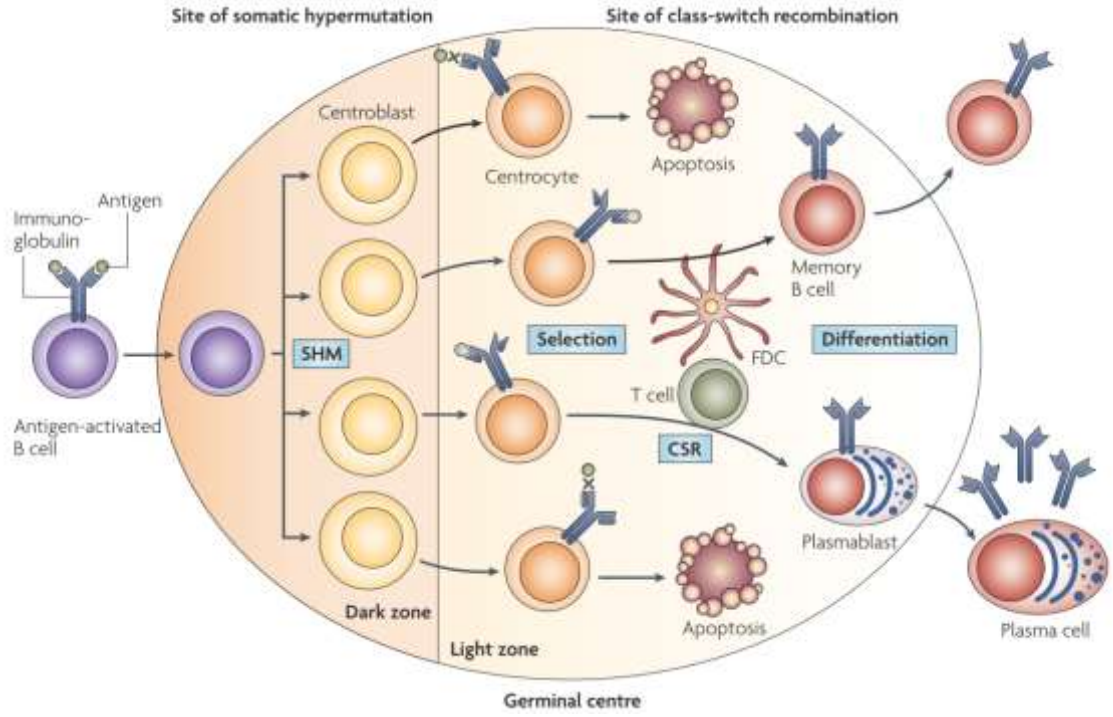

Figure 1-1 Simplified scheme of B cell differentiation in the germinal center. Antigen-activated B cells enter peripheral lymphoid organs and form a germinal center (GC). GCs are polarized into dark and light zones. The dark zone mainly consists of proliferating GC B cells, in which somatic hypermutation (SHM) occurs. By this a high rate of mutations in the variable (V)-region of Ig genes are introduced. GC B cells with mutated BCRs can then enter the light zone (now mainly consisting of resting cells) and are positively selected for high affinity antigen receptors. GC B cells exhibiting a BCR with lower affinity for the antigen undergo apoptosis. The selection process is presumably controlled through the close contact to T cells and follicular dendritic cells (FDCs). A fraction of the positively selected cells encounter class-switch recombination (CSR). Finally, GC B cells differentiate into plasma cells or memory B cells and leave the germinal center microenvironment into the periphery. Figure taken from (Klein and Dalla-Favera, 2008).

Indeed, both of the germinal center-intrinsic processes somatic hypermutation and class-switch recombination may lead to genetic aberrations promoting lymphomagenesis (reviewed in Küppers et al., 1999). Thus, mistakes or malfunctions in the immunoglobulin gene remodeling mechanisms – chromosomal translocations and aberrant SHM – can be found as the main causes for genetic lesions in B cell NHLs (reviewed by Küppers and Dalla-Favera, 2001). A typical functional consequence is the

deregulated expression of proto-oncogenes, because regulatory sequences have been juxtaposed in close proximity to the intact coding domain of the target gene from heterologous chromosomes by translocations.

Thus, chromosomal translocations, which involve for example *BCL-6* (B cell lymphoma 6), result in prevention of gene silencing at the end of the GC reaction and can be frequently found in diffuse large B cell lymphoma (DLBCL) (see chapter 1.3.1 for more detail). Enhanced expression of the proto-oncogene *c-MYC* results from the translocation into the immunoglobulin heavy chain or light chain loci and is associated with 100 % of Burkitt's lymphoma cases (see chapter 1.3.2 for more details on Burkitt's lymphoma) and up to 10 % of DLBCL cases (Klein and Dalla-Favera, 2008). Moreover, additional genetic alterations occur in the different subtypes of aNHL, altogether leading to deregulated signaling events promoting oncogenic transformation.

1.2 Paracrine and autocrine signaling influence B cell development and transformation

Proliferation, differentiation and survival of activated B cells in secondary lymphatic organs rely tremendously on paracrine signals mediated by the microenvironment. This is provided in the GC, for example by T cells and follicular dendritic cells (FDCs). These bystander cells supply the maturating B cells with important survival signals, as for example CD40L expressed by $CD4^+$ T cells (see chapter 1.2.2 for further details) or Sonic hedgehog (Shh) expressed by FDCs in the GC (see chapter 1.2.3 for more information). On the other hand, autocrine signaling that is not dependent on surrounding microenvironmental cells determines the B cell fate in a similar manner. One central player includes the B cell receptor. Normal B cells depend on BCR expression for survival and undergo stringent selection for expression of the appropriate BCR throughout their lives. Moreover, the selection for expression of a functional BCR also seems to occur in most aNHL subtypes (Gunvén et al., 1980; Segal et al., 1991; Yano et al., 1992). Additionally, deregulations of BCR signaling or signaling mediated through BCR or CD40 activation seem to operate in BL and DLBCL (chapter 1.2.1 and 1.2.2). In the following paragraphs a brief overview will be given of BCR, CD40 and Hedgehog activated signaling pathways and the distinct mechanism involved in the respective pathway activations. As NF-κB (nuclear factor of kappa light polypeptide enhancer in B cells) and MAPK (mitogen-activated protein kinase) signaling are central to most of the here described signaling pathways, they will be described in more detail.

1.2.1 B cell receptor activated signaling and its implications in lymphomagenesis

Every normal B cell and consequently every lymphoma has a unique BCR, whose signaling results in activation of the NF-κB, phosphoinositol 3-kinase (PI3K), MAPK, nuclear factor of activated T cells (NFAT) and RAS pathways, which foster proliferation and survival of normal and malignant B cells (Dal Porto et al., 2004). The BCR is a multimeric complex, consisting of an antigen-recognition structure and a membrane-bound immunoglobulin (Ig), which itself lacks signaling capacity. Therefore, the BCR is non-covalently associated with CD79A (Igα) and CD79B (Igβ), each bearing an immunoreceptor tyrosine-based activation motif (ITAM) (Cambier, 1995; Reth, 1989), which transduces signals intracellularly (Figure 1-2). Antigen induced aggregation of the BCR induces ITAM phosphorylation by SRC-family kinases, which in turn leads to recruitment and activation of the tyrosine kinase SYK (Rowley et al., 1995; Saijo et al., 2003). The hereupon nucleated multiprotein complex consisting of various other kinases and adaptor proteins activates downstream kinases like Bruton's tyrosin kinase (Btk) and phospholipase Cγ2 (PLCγ2) (Takata and Kurosaki, 1996). As consequence numerous signal transducers and second messengers are activated. Thus, for example PLCγ2 triggers the release of calcium from the endoplasmatic reticulum thereby activating

calcineurin and the transcription factor NFAT (Antony et al., 2004). Additionally, the increased calcium levels activate protein kinase Cβ (PKCβ), which in turn phosphorylates many substrates, including caspase recruitment domain-containing protein 11 (CARD11), a key signaling adaptor mediating NF-κB activation (Shinohara et al., 2005).

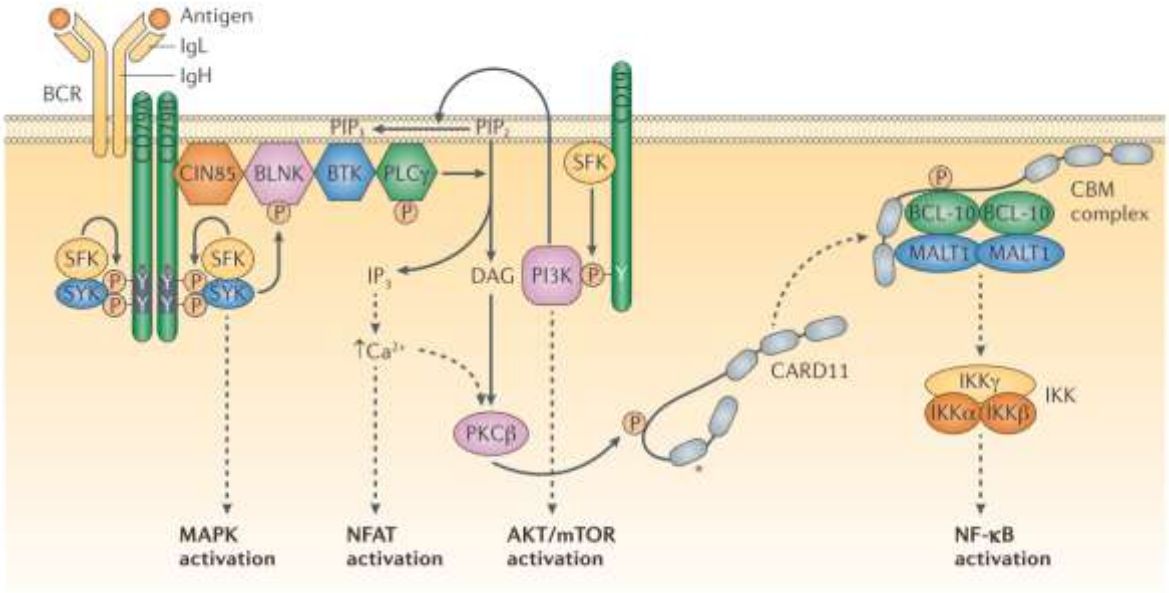

Figure 1-2 Simplified scheme of the basics of B cell receptor signaling. The scheme depicts the BCR, consisting of pairs of immunoglobulin heavy (IgH) and light (IgL) chains, whose variable region allows the BCR to bind to diverse antigens. The antibody portion of the BCR is coupled non-covalently with CD79A and CD79B, which mediate plasma membrane expression, signal transduction and receptor internalization. The ITAM region, containing two tyrosine residues (Y) is phosphorylated by SRC-family kinases (SFK) upon antigen-induced aggregation of the BCR following SYK recruitment. Several signaling mediators are engaged and lead to the activation of various downstream signaling pathways, as indicated (refer to main text for details). CIN85, Cbl-interacting protein of 85 kDa; BLNK, B cell linker protein; BTK, Bruton tyrosine kinase; PLCγ, phospholipase Cγ; PIP2, phosphatidylinositol-4,5-biphosphate; PIP3, phosphatidylinositol-3,4,5-triphosphate; IP_3, inositol triphosphate; DAG, diacylglycerol; PKCβ, protein kinase Cβ; PI3K, phosphoinositol 3-kinase; CARD11, caspase recruitment domain-containing protein 11; CBM, CARD11-BCL-10-MALT1; IKK, inhibitor of NF-κB. The asterisks indicate recurrently mutated protein regions in human lymphoma. Figure taken from (Young and Staudt, 2013).

Furthermore, PI3K is activated through BCR crosslink and catalyzes the phosphorylation of phosphatidylinositol-4,5-biphosphate (PIP2) to phosphatidylinositol-3,4,5-triphosphate (PIP3), which acts as docking site for Akt (also known as protein kinase B, PKB) and phosphoinositide-dependent kinase 1 (PDK1). PDK1 phosphorylates Akt at threonine-308 in its kinase domain and subsequent phosphorylation of serine-473 by the mTor-rictor complex (mTORC2) leads to full activation of Akt (Sarbassov et al., 2005). Akt is the main mediator of the PI3K pathway. Through subsequent activation of mTor and resulting phosphorylation of ribosomal S6 kinases as well as the eukaryotic initiation factor 4E (eIF4E)-binding protein 1, components of ribosomal biogenesis and mRNA translation, protein synthesis and cell growth are promoted (reviewed in Markman et al., 2010). In

addition, Akt influences the transcription factor FOXO (forkhead box transcription factor), thus inactivating cell cycle inhibitors and promoting cellular proliferation (reviewed in Burgering and Medema, 2003). PI3K activity is counteracted by phosphatase and tensin homologue (PTEN), which is a PIP_3 3-phosphatase (Di Cristofano et al., 1998; Salmena et al., 2008). Aberrant activation of the PI3K/Akt-pathway can be found in a wide array of cancers, including hematological malignancies (reviewed in Chalhoub and Baker, 2009; Markman et al., 2010).

In contrast to the 'activated', antigen-induced B cell receptor signaling, a second form of BCR signaling mainly utilized by mature B cells to ensure B cell survival exists: so-called 'tonic' BCR signaling (Lam et al., 1997). Although several investigations implicate the PI3K pathway as a key component of tonic BCR signaling, the biochemical and biophysical basis of tonic BCR signaling and PI3K involvement is still debated (Cambier and Johnson, 1995; Delgado et al., 2009; Kraus et al., 2004; Lam et al., 1997; Monroe, 2006; Wienands et al., 1996).

BCR expression is maintained on the cell surface of most B cell lymphomas (reviewed in Küppers, 2005), although immunoglobulin loci are disrupted in favor of placing oncogenes under the control of the immunoglobulin enhancers (reviewed in Nussenzweig and Nussenzweig, 2010). Many B cell lymphomas utilize IgM constant regions to form their BCR, because IgM-BCR signaling seems to promote the survival and proliferation of B cells, instead of IgG-BCR signaling, which favors differentiation into plasma B cells (Dogan et al., 2009; Horikawa et al., 2007; Martin and Goodnow, 2002).

1.2.2 CD40 mediated signaling

CD40, a member of the TNFR (tumor necrosis factor receptor) superfamily, is expressed on the cellular surface of virtually all mature B lymphocytes. Upon binding to its ligand CD40L/CD154, CD40 activates multiple signaling pathways promoting B cell activation, proliferation and survival (reviewed in Van Kooten and Banchereau, 2000). CD40L is primarily expressed by activated ($CD4^+$) T cells. The CD40-CD40L interaction is regarded as the 'classical' co-stimulatory signal, contributing to GC formation, memory B cell formation, Ig isotype switching and affinity maturation (DiSanto et al., 1993; Kawabe et al., 1994; Xu et al., 1994). A soluble form of CD40L exhibiting comparable activating features as the membrane-bound ligand has been reported as well (Graf et al., 1995; Mazzei et al., 1995).

Upon CD40-CD40L binding a multi-component protein complex is assembled, containing the adaptor molecules TNF receptor-associated factor 2 and 3 (TRAF2, TRAF3), ubiquitin conjugating enzyme Ubc13, cellular inhibitor of apoptosis proteins 1 and 2 (c-IAP1/2), IKKγ/NEMO and MAPK kinase kinase 1 (MEKK1) (Matsuzawa et al., 2008). c-IAP1/2 mediated degradation of TRAF3 leads to

translocation of the 'cytokine receptor-assembled signaling complex' to the cytosol and thus to the activation of MEKK1-mediated MAPK signaling *via* p38 and JNK (Gallagher et al., 2007). In addition IKK-promoted canonical and non-canonical NF-κB activation can occur. Moreover, recruitment of TRAF6 and Tak1 to CD40 upon its engagement was also suggested, providing a second mechanism to activate MAPK and NF-κB signaling in response to CD40 activation (Matsuzawa et al., 2008).

As in normal B cells, CD40 activation induces in certain B cell malignancies an increase in anti-apoptotic factors such as Bcl-XL (B cell lymphoma-extra large), A20 (tumor necrosis factor, alpha-induced protein 3 - TNFAIP3), survivin and CFLAR (CASP8- and FADD-like apoptosis regulator) (reviewed in Elgueta et al., 2009). Some *in vitro* investigations suggested that low-level constitutive engagement of CD40 may facilitate malignant cell growth. Studies with non-Hodgkin's lymphoma cells including Burkitt's lymphoma cells have shown that these cells express low levels of CD40L, which in turn leads to sustained cell proliferation through autocrine pathway activation and protection from apoptosis (Challa et al., 2002; Pham et al., 2002). Conversely, transient *in vitro* and *in vivo* activation of CD40 in Burkitt's lymphoma, multiple myeloma and primary high-grade B cell lymphoma resulted in reduction of tumor cell proliferation (Funakoshi et al., 1994; Pellat-Deceunynck et al., 1996). Thus, not only the activation status but also the quantitative level of CD40 activation might play a role in cell fate determination.

1.2.3 Hedgehog signaling pathway

The Hedgehog (Hh) signaling pathway was first identified in 1980 in *Drosophila melanogaster* as essential developmental signaling pathway regulating proliferation, differentiation and migration of embryonic cells (Nüsslein-Volhard and Wieschaus, 1980). In humans, the Hh family of proteins comprises three distinct ligands which are processed from the same precursor protein: Sonic hedgehog (Shh), Indian hedgehog (Ihh) and Desert hedgehog (Dhh). In the absence of Hh ligands, the transmembrane receptor Patched1 (Ptch1) inhibits the activation of Smoothened (Smo), a transmembrane G-like protein coupled receptor and thereby prevents active Hh signaling. Once Hh binds to Ptch, the inhibition of Smo is abated, thus allowing Smo to translocate to the cytoplasm. Smo activation triggers a cascade of signaling events, leading to the activation of members of the glioma-associated oncoproteins (Gli) family of zinc-finger transcription factors (Gli1 and Gli2, which function mostly as activators while Gli3 as repressor). Gli then translocates to the nucleus and initiates transcription of Hh target genes, including *GLI1*, *GLI2* and *PTCH1* as well as regulators of cell proliferation and survival (Ikram et al., 2004; Lee et al., 1997). The exact details of these processes still have to be further investigated for mammalian cells. Since all Hh signaling *via* the canonical pathway require Smo, small molecule inhibitors as cyclopamine, which block Smo function,

completely abrogate all Hh signaling regardless of the ligand (Incardona et al., 1998; Taipale et al., 2000).

The identification of point mutations in *PTCH1* and *SMO* in patients with medulloblastomas, basal cell carcinomas and rhabdomyosarcomas (Aszterbaum et al., 1999; Goodrich and Scott, 1998; Marino, 2005; Xie et al., 1998) has linked the Hh signaling pathway to cancer. Recent investigations suggest that several cancers including B cell lymphoma abnormally express Hh ligands and activate the Hh signaling pathway in an autocrine manner (Singh et al., 2010). In addition to Shh production by follicular dendritic cells in the lymph node and its necessity for proliferation, survival and antibody production of germinal center B cells (Sacedón et al., 2005), another study demonstrated *in vitro* and *in vivo* secretion of Hh ligands by stromal cells in non-Hodgkin lymphoma, which promoted survival of the malignant cells in an inverse paracrine manner (Dierks et al., 2007).

1.2.4 NF-kB signaling pathway

The Rel/NF-κB-family of transcription factors plays a central role in the immune system by regulating various processes, including development and survival of B and T cells, as well as the control of immune responses and malignant transformation (reviewed in Vallabhapurapu and Karin, 2009). The NF-κB family comprises five subunits: NF-κB1 (p50 and its precursor p105), NF-κB2 (p52 and its precursor p100), p65 (RelA), c-Rel and RelB. These subunits form homo- and heterodimeric complexes that can bind to DNA and regulate NF-κB specific target genes. Inhibitors of NF-κB (IκBα, IκBβ and IκBε) hold NF-κB complexes in an inactive state in the cytoplasm (reviewed in Yamamoto and Gaynor, 2004). The release of NF-κB subunits from the IκBs is controlled by IκB kinases (IKKα/IKK1, IKKβ/IKK2 and IKKγ/NEMO) in a signal dependent manner. Many different stimuli activate the NF-κB transcription factors to induce their nuclear translocation. Here, two different pathways exist: the classical (canonical) and the alternative (non-canonical) pathway. The major and most-well studied pathway used by most stimuli (including antigen receptors (see chapter 1.2.1 for more detailed description), tumor necrosis factor receptors as CD40 (chapter 1.2.2), toll-like receptors (TLRs), IL-1R and others) is the canonical NF-κB pathway, which mainly employs the p65:p50 and c-Rel:p50 heterodimers. This pathway mainly centers on activation through a trimeric IKK-complex, where IKK1 and IKK2 function as catalytic subunits that phosphorylate the IκBs leading to their subsequent degradation, while IKKγ/NEMO comprises the regulatory subunit of the IKK complex. The IKK2 subunit is referred to exhibit the majority of IκB kinase activity in most cell lines. In the absence of IKK2, IKK1 can adopt residual IκB kinase activity (Li et al., 1999), whereas deletion of IKK1 in IKK2-expressing cells has nearly no effect on classical IKK activity (Hu et al., 1999). An important and unique function of IKK1 is the activation of the alternative NF-κB signaling pathway by activation through NIK (NF-κB-inducing kinase) (Senftleben et al., 2001). The non-canonical pathway is based on

processing of the p100 precursor and subsequent activation of RelB:p52 dimers (Yilmaz et al., 2003). This alternative pathway is activated in response to a small subset of tumor necrosis factor (TNF) family members, including CD40L, but also regulated through the canonical NF-κB pathway, which upregulates NF-κB2 expression (Senftleben et al., 2001).

As mentioned above, NF-κB signaling is induced through a variety of different stimuli and positively as well as negatively regulated. Thus, it is not surprising that deregulated NF-κB signaling leads to aberrant expression of its target genes, which predominantly regulate cell survival, proliferation or growth and occupies an important role in many types of cancer. Hence, constitutively active NF-κB signaling can be found in several lymphoma subtypes including ABC (activated B cell-like) DLBCL (see also chapter 1.3.1) or Epstein-Barr virus positive Burkitt's lymphoma (chapter 1.3.2).

1.2.5 Mitogen activated protein kinase (MAPK) signaling pathways

Mitogen activated protein kinases (MAPKs) are serine/threonine-specific protein kinases directing the cellular response to a diverse array of stimuli, such as mitogens, pro-inflammatory cytokines or stress signals. Amongst others they regulate proliferation, gene expression, differentiation, mitosis, cell survival and apoptosis (reviewed by Pearson, 2001). The best studied MAPKs are extra-cellular signal related kinases 1 and 2 (Erk1/2), the Jun-N-terminal kinases (JNKs) and p38 kinases. MAPKs are activated by phosphorylation cascades. The two upstream protein kinases MAPK kinase kinases (MKKs) and MKK kinases (MAP3Ks) are activated in series and regulate MAPKs. Furthermore, additional kinases may be required upstream of this three-kinase module. Erk1/2, JNK and p38 are predominantly regulated by different MKKs (Raman et al., 2007), thus resulting in distinct responses to a specific stimulus. Another characteristic of the phosphorylation cascade is signal amplification provided if the successive protein is more abundant than its regulator. In case of the Erk1/2 pathway, Raf and MEK1/2 are the relevant upstream protein kinases. MEK1/2 inhibitors have been used extensively to elucidate the biological relevance of Erk1/2 in a wide array of events. One of the most often used inhibitors is U0126 (Favata et al., 1998), which interacts preferentially with the inactive, unphosphorylated kinase, thus preventing activation of MEK1/2. Upon stimulation Erk1/2 phosphorylates a large number of substrates (reviewed in Yoon and Seger, 2006), among others the transcription factor Elk-1, which is thereby activated and is known to induce expression of immediate early response genes such as c-Fos (Gille et al., 1995).

In contrast to the relatively well-insulated Erk1/2 pathway, p38 and JNK share most of their activators at the MAP3K level (MEKK1, MEKK4, Tak1 and others). In addition, some of the MKKs directly activate both p38 and JNK (MKK4), whereas others are specific for either p38 (MKK3 and MKK6) or JNK (MKK7). Due to this interlacing there are few stimuli that can induce JNK activation without simultaneously regulating p38 or *vice versa* (Cargnello and Roux, 2011). Identification of the

p38α-specific inhibitor SB203580 (Lee et al., 1994), which was exploited in a huge number of studies, revealed the pivotal functions of p38 in immune and inflammatory responses. P38 excerts its function through phosphorylation of many substrates in the cytoplasm and the nucleus, thereby modulating the activity of kinases as well as transcription factors (reviewed in Cuadrado and Nebreda, 2010).

To elucidate the role of JNK in inflammatory diseases, apoptotic cell death and cancer, the reversible ATP-competitive inhibitor SP600125 has been invented (Bennett et al., 2001). The transcription factor c-Jun is a well-known target of JNK, as well as other transcription factors including p53, Elk-1, JunB, Stat3 and c-Myc (reviewed in Weston and Davis, 2002).

Both MAPKs, p38 and JNK, are activated through the MAP3K Tak1 (transforming growth factor-β activated kinase 1). Tak1 was originally identified as a protein kinase involved in TGF-β (transforming growth factor -β) signaling (Yamaguchi et al., 1995), but has emerged in several studies for being activated through several external stimuli and thus being a key modulator of the cellular response to a variety of signals. These stimuli include IL-1R, TNF, bacterial lipopolysaccharide (LPS), CD40 and its viral counterpart LMP1, as well as BCR signaling in various types of cells (Arcipowski and Bishop, 2012; Irie et al., 2000; Ninomiya-Tsuji et al., 1999; Schuman et al., 2009; Shkoda et al., 2012; Sorrentino et al., 2008; Takaesu et al., 2012; Wan et al., 2004; Yamaguchi et al., 1995).

1.3 Strategies to describe and stratify lymphoma cases based on gene expression profiling

As described before, aNHL comprise a very heterogeneous group of malignancies. This is reflected in an increased number of distinct entities specified in the recent WHO classification (Campo et al., 2011; Jaffe, 2009; Swerdlow et al., 2008). The WHO classifications attempts to define disease entities according to their histology, morphology, clinical behavior and molecular characteristics to help clinicians and pathologists to recognize the specific entity. In the 1950s, all NHL diversities were pooled together and treated – clinically and experimentally – as one disease. With the help of the WHO classification and the rise of new molecular methods, multiple novel therapeutic options have emerged in the treatment of aNHL and the distinct subtypes of aNHL are treated differentially nowadays.

1.3.1 Diffuse large B cell lymphoma (DLBCL)

The most common subtype of B cell NHL in Western countries is the diffuse large B cell lymphoma, which comprises 25 % to 35 % of new cases annually (Cancer Research UK, 2010). Although historically assembled into one category both pathologically and clinically, patients with DLBCL vary tremendously in clinical presentation, prognosis and response to current therapies. Patients often present with a rapidly progressing lymphadenopathy. Standard chemotherapy regimen includes cyclophosphamide, doxorubicin, vincristine and prednisone and the monoclonal antibody rituximab (R-CHOP). Response rates in patients with low-risk disease range from 80 % to 90 % (Feugier et al., 2005), however the 5-year overall survival rate ranges between 30 % and 50 % in all DLBCL patients, indicating a large clinical spectrum of sensitivity to the standard treatment (reviewed in Cultrera and Dalia, 2012).

Advances in molecular diagnostics went along with the definition of prognostic factors for DLBCL. DLBCL tumors present with large B cells with a very high percentage of tumor infiltrate. Most of the tumor cells resemble germinal center centroblasts, carrying complex chromosomal aberrations (Dave et al., 2002). Chromosomal alterations leading to aberrant expression of proto-oncogenes as *BCL-6*, *c-MYC*, *BCL-2* and *P53* are associated with poor outcome (Friedberg, 2011). The most common chromosomal alteration, leading to constitutive activation, is the translocation of BCL-6, a critical transcriptional repressor, whose down regulation is essential for the exit from the germinal center reaction (Ci et al., 2008, 2009; Fukuda et al., 1997; Iqbal et al., 2007; Kusam et al., 2009; Parekh et al., 2007; Polo et al., 2004, 2007; Saito et al., 2009).

Identification of several subgroups of DLBCLs by global gene expression profiling

The availability of an ever-growing panel of new genetic technologies, including gene expression profiling, array comparative genomic hybridization, methylation profiling, miRNA profiling as well as deep sequencing has led to an exponential growth in the discovery of the genetic basics of DLBCL's heterogeneity. Based on gene expression profiling, Alizadeh and colleagues identified a stratification for DLBCLs subgroups established by their comparison of healthy B cells from distinct differentiation and activation statuses. Thereby two major molecular subtypes have emerged: germinal center B cell-like (GCB) DLBCL and activated B cell-like (ABC) DLBCL (Alizadeh et al., 2000). This classification helped to underline several diverse signaling properties of DLBCLs in further studies. Based on gene expression profiling, ABC DLBCL were identified to be hallmarked by a constitutive active NF-κB signal (Lam et al., 2005). Subsequent studies confirmed the activity of NF-κB to be required for ABC DLBCL survival in contrast to GCB DLBCLs (Davis et al., 2001). Further studies revealed dependency of ABC DLBCL cells on constitutive active BCR signaling, either in form of mutations in CARD11 (Ngo et al., 2006) or mutations affecting the ITAM motifs of CD79A and CD79B (Davis et al., 2010). Both mutations lead to constitutive activation of NF-κB through the CARD11-BCL10-MALT1 (CBM) complex (Bidère et al., 2009). Due to these very recent findings, ABC DLBCL are now considered to be hallmarked by 'chronic active BCR signaling' (Davis et al., 2010) in contrast to other lymphoma entities which harbor tonic BCR signaling (compare chapter 1.2.1). Further on, the large number of downstream targets of NF-κB contribute to the poor prognosis of ABC DLBCL by collectively preventing apoptosis and rendering cells insensitive to chemotherapy (Baldwin, 2001; Rosenwald et al., 2002). By blocking the JAK signaling pathway in ABC DLBCL cells *in vitro*, resulting in apoptosis, it was shown that NF-κB signaling also induces cytokines, which act in an autocrine fashion resulting in activation of JAK/STAT signaling (Lam et al., 2008).

1.3.2 Burkitt's lymphoma (BL)

In the WHO's classification of lymphoid tumors, Burkitt's lymphoma (BL) is listed as an aggressive non-Hodgkin B cell lymphoma, characterized by a high proliferation rate of the malignant cells and deregulation of the *c-MYC* gene (Swerdlow et al., 2008). BL was first characterized by Denis Burkitt in 1958 as the most prevalent childhood lymphoma in Africa mostly localized at the jaw (Burkitt, 1958). Nowadays BL is classified in 3 clinical variants, differing in geographical distribution and Epstein-Barr virus (EBV) association. The endemic form of BL is found in equatorial Africa and is in 98 % of cases associated with an EBV infection (Blum et al., 2004; van den Bosch, 2004; Brady et al., 2008; Ferry, 2006; Pattle and Farrell, 2006). The immunodeficiency-associated BL is related to an EBV infection in 30 % of the cases and mainly presents in HIV carriers, where tumors can arise due to the severe immunosuppression coincident with the onset of AIDS (Powles et al., 2000). The sporadic form of BL, predominantly presented in Western countries, accounts for 2 % of all lymphomas in European

countries and the United States and is rarely associated with EBV infection (Blum et al., 2004; Brady et al., 2008; Ferry, 2006; Pattle and Farrell, 2006; Perkins and Friedberg, 2008). However, as the central leading event of pathogenesis all three forms share the activation of the *c-MYC* gene at 8q24, usually through translocation with an immunoglobulin locus, which introduces a transcriptional enhancer element (reviewed in Hecht and Aster, 2000).

So far, for management of sporadic BL more intensive chemotherapy regimens are required than for treatment of DLBCLs (Blum et al., 2004; Magrath et al., 1996; Mead et al., 2002). Furthermore, because of the high risk of involvement of the central nervous system systemic chemotherapy crossing the blood-brain barrier is often essential (Bishop et al., 2000). The diagnosis of BL mainly relies on morphologic findings, cytogenetic features and immunophenotyping results (Jaffe, 2009; Swerdlow et al., 2008). However, the main diagnostic challenge in BL is to distinguish it from DLBCL, which may present with similar histological features. Additionally, the characteristic t(8;14) translocation of BLs, juxtaposing the *c-MYC* gene with an immunoglobulin enhancer also occurs in 5 to 10 percent of DLBCL cases (Kramer et al., 1998). Since the prevalence for DLBCLs is 20 times higher than for BL, a lymphoma presenting with a t(8;14) translocation may raise diagnostic challenge.

Molecular Diagnosis of BL with the index of 'Burkitt-likeness'

In 2006, two major DNA microarray studies were published using whole genome gene expression profiling to distinguish BL from DLBCL on the molecular level (Dave et al., 2006; Hummel et al., 2006). Using a new statistical approach, Hummel and colleagues developed a molecular classifier to achieve a clear discrimination of BL from other mature aggressive B-NHL. Based on the gene expression profile of 220 NHL tumors, they identified 58 genes that constituted a molecular Burkitt's lymphoma (mBL) signature. This mBL signature was used to establish a continuous index score (I) of 'Burkitt-likeness' that allows the stratification of aNHL cases either into mBL ($I > 0.95$), non-mBL ($I < 0.05$) or intermediate lymphomas ($0.95 < I > 0.05$) (Hummel et al., 2006). Array-based comparative genomic hybridization (CGH) further revealed that mBLs had very few genetic alterations in addition to an IG-*MYC* translocation (simple karyotype), whereas intermediate and non-mBL cases displayed a higher genetic complexity (non-IG-*MYC* translocations and other genetic aberrations on the background of a complex karyotype). At the same time, Dave and colleagues established a classifier for Burkitt's lymphoma based on gene expression profiling with the help of c-Myc target genes identified by siRNA-mediated knock down of *c-MYC* in an ABC DLBCL cell line (OCI-Ly10). Tumor biopsies from Burkitt's lymphomas could be distinguished to a certain extend from DLBCLs by high expression of c-Myc target genes, the expression of a subgroup of germinal-center B cell genes and decreased expression of NF-κB target genes and major-histocompatibility-complex (MHC) class I genes. In summary, four different gene expression profiles were used to distinguish BL from DLBCL, but the

molecular mechanisms underlying those differences in gene expression are still unclear (Dave et al., 2006).

1.3.3 Surrogate markers for oncogenic pathway activation

Multiple studies demonstrated that DNA-microarray based gene expression profiling (GEP) provides the ability to define cancer subtypes, recurrence of disease and response to specific therapies. Various studies have also shown the potential of gene expression profiles for the analysis of oncogenic pathways. Hence, its stands to reason to use gene expression signatures, obtained through specified manipulation of target cells *in vitro,* to identify and model patterns of oncogene activity, which underlie the development of the oncogenic phenotype and reflect the biology and outcome of specific cancers (Bentink et al., 2008; Bild et al., 2006). Thus, the gene expression data established from ectopic expression of several oncogenes (including *RAS*, *SRC*, *β-catenin*, *E2F3* and *MYC*) in primary human epithelia cells (Bild et al., 2006) has been used to model gene modules, representing the activity of a defined proto-oncogene (Bentink et al., 2008). These data were then combined to so-called 'pathway activation patterns' (PAPs), which stratified mature aggressive B cell lymphomas into distinct groups. One of the identified PAPs comprised mainly aNHL cases, which were characterized as 'intermediate' by the mBL index and present mainly cases carrying a complex karyotype and being situated in the transitional zone between mBL and non-mBL (Hummel et al., 2006). The underlying pathway activities were largely undefined. In the meantime, GEP was used to demonstrate that outcome in DLBCL patients seems to be influenced by differences in stromal factors supplied by the microenvironment of the tumor, such as differences in immune cells, fibrosis and angiogenesis (Lenz et al., 2008).

Driven by these investigations, the group of Dr. Kube started to identify and characterize new gene expression patterns that harbor information about relevant oncogenic pathway activities. In order to better understand the pathogenesis, implicated diagnostic and therapeutic possibilities of lymphomas, gene expression profiling of lymphomas was used to reveal oncogenic pathway activities. Therefore, one study focused on the effect of aberrant *MYC* activity in lymphoma precursor cells and its role in aNHL. Schrader and colleagues could later on demonstrate that high c-Myc activity constitutes a negative prognostic marker in DLBCLs independent of established risk factors and of the presence of a *MYC* translocation (Schrader et al., 2012a). Additionally, A. Schrader also investigated the possibility to identify novel pathway activities in malignant lymphoma by transferring gene expression data from *in vitro* perturbation assays performed in lymphoma cell lines to primary lymphoma gene expression profiles (Schrader, 2011) and thus was instrumental in preparing the present study.

Aim of the Study

A major step fostering the understanding of the clinical heterogeneity of aNHL was the recent molecular classification of aNHL based on global gene expression analyses of individual lymphomas. These transcriptome based analyses aimed to describe oncogenic events to identify new biomarkers and potential targets for individualized therapies of aNHL. However, the mechanisms behind the current criteria to distinguish individual NHL subtypes are still poorly understood. A more functional characterization of deregulated pathways in aNHL needs to be elucidated in order to improve our knowledge of the molecular mechanisms of malignant transformation of B cells.

We postulate that the description of time-resolved global gene expression changes provides new insights into the dynamics of oncogenic signaling. Furthermore, the intervention into pathway intersections by chemical inhibitors will allow us to describe the pathways interplay and cross talk.

Based on in vitro experiments, it was concluded that subsets of aNHLs are characterized by aberrantly activated NF-κB and JAK-STAT signals. Using stimulation-mediated gene expression changes, specific pathway activities in individual NHL were predicted. Regardless these achievements, a number of open questions still exist and need to be answered.

1) How is the activation of distinct pathway networks by BCR and CD40 activation reflected in the gene expression changes occurring over time?
    a. Identify groups of genes which are regulated in a comparable way in response to BCR and CD40 activation.
    b. Identify gene expression changes which reflect the immediate early and the late pathway activation triggered by BCR / CD40 activation.
    c. Identify networks of genes which reflect a dependency of gene expression regulations and could thereby represent regulatory circuits or feedback loops that stand in causal relationships within oncogenic pathways.
2) Is the gene expression profile of DLBCL cells, in contrast to that of BL cells, dominantly shaped by constitutive active micromilieu signals?
    a. Evaluate how sustained activation of micromilieu derived signals influences the Burkitt-likeness of human transformed germinal center B cells.
    b. Interrogate whether it is possible to resemble the activated gene expression profile of DLBCL by stimulating BL cells *in vitro*.
3) What is the functional background of the observed pathway activities?
    a. Interrogate which differentially regulated genes could be involved in the oncogenic function of the identified gene groups / signatures.

b. Identify new functions of signaling molecules that are involved in mediating these pathway activities.

In order to answer these questions, a prototypical cell line characteristic for human transformed germinal center B cells was used to analyze the temporal pattern of global gene expression changes upon signaling pathway activation by factors of the microenvironment. Secondly, several potential oncogenic signaling pathways were inactivated at different levels in the signaling cascade in order to dissect intersections in the complex signaling network evolving in a lymphoma cell.

2 Material and Methods

2.1 Biological Material

2.1.1 Primary Material

Primary material of human pediatric patients was obtained with consent and ethical approval from tonsillectomies performed in the University Medical Center Göttingen, Germany.

2.1.2 Cell Lines

Cell lines used in this work are listed in Table 2-1.

Table 2-1 Cell lines

Cell line	Source	Distributor	Reference
BL2	B cell, Burkitt Lymphoma (EBV negative)	DSMZ	(Kube et al., 1995; Nilsson and Pontén, 1975)
BL41	B cell, Burkitt Lymphoma (EBV negative)	DSMZ	(Lenoir et al., 1985)
BL70	B cell, Burkitt Lymphoma (EBV negative)	DSMZ	(Lenoir et al., 1985)
DG-75	B cell, Burkitt Lymphoma (EBV negative)	DSMZ	(Ben-Bassat et al., 1977)
HT	B cell, Diffuse Large B cell Lymphoma (GCB)	DSMZ	(Beckwith et al., 1990)
Ramos	B cell, Burkitt Lymphoma (EBV negative)	DSMZ	(Klein et al., 1975)
SuDHL4	B cell, Diffuse Large B cell Lymphoma (GCB)	DSMZ	(Epstein et al., 1976)
SuDHL5	B cell, Diffuse Large B cell Lymphoma (GCB)	DSMZ	(Epstein et al., 1978)
SuDHL6	B cell, Diffuse Large B cell Lymphoma (GCB)	DSMZ	(Epstein et al., 1978)
OCI-Ly1	B cell, Diffuse Large B cell Lymphoma (GCB)	Ontario Cancer Institute, Toronto	(Chang et al., 1995)
OCI-Ly3	B cell, Diffuse Large B cell Lymphoma (ABC)	Ontario Cancer Institute, Toronto	(Tweeddale et al., 1987)

OCI-Ly7	B cell, Diffuse Large B cell Lymphoma (GCB)	Ontario Cancer Institute, Toronto	(Chang et al., 1995)
U2932	B cell, Diffuse Large B cell Lymphoma (ABC)	DSMZ	(Amini et al., 2002)

2.2 Chemicals and Consumable Supplies

Chemicals and consumables used in the present study are listed in Table 2-2 and Table 2-3.

Table 2-2 Chemicals

Chemical	**Manufacturer**
α-Thiolglycerol	Sigma-Aldrich, Munich GER
Acrylamid/Bisacrylamid 40%	BioRad, Munich GER
Ammonium persulphate	Sigma-Aldrich, Munich GER
Bradford solution	RotiQuant-Roth, Karlsruhe GER
Bromphenol Blue	Sigma-Aldrich, Munich GER
Bovine serum albumin (BSA)	Serva, Heidelberg GER
Diethylpyrucarbonate (DEPC)	Roth, Karlsruhe GER
Dimethyl sulfoxide (DMSO)	Sigma-Aldrich, Munich GER
deoxyribonucleoside triphosphates (dNTPs: 100 mM dATP, dCTP, dGTP, dTTP)	PrimeTech LTD, Minsk BY
Ethanol (100 %)	J.T. Baker, Deventer NL
Ethylenediaminetetraacetic acid (EDTA)	Riedel-de Haën, Seelze GER
Full Range Rainbow Molecular Weight Marker RPN800	GE Healthcare, Munich GER
Formaldehyde	Sigma-Aldrich, Munich GER
Glycerol	Roth, Karlsruhe GER
Glycine	Roth, Karlsruhe GER
HEPES	Sigma-Aldrich, Munich GER
Hot FIREpol DNA polymerase (5 U/µl)	PrimeTech LTD, Minsk BY
Hydrogen Peroxide	Sigma-Aldrich, Munich GER

Isopropanol	Sigma-Aldrich, Munich GER
Luminol	Sigma-Aldrich, Munich GER
Magnesium chloride (25 mM)	PrimeTech LTD, Minsk BY
Methanol 100 % (p.a.)	J.T. Baker, Deventer NL
Milk powder	Roth, Karlsruhe GER
Nonidet P-40	Sigma-Aldrich, Munich GER
Phosphatase inhibitor Phospho- STOP	Roche, Mannheim GER
Phenylmethylsulfonyl fluoride (PMSF)	Sigma-Aldrich, Munich GER
Proteaseinhibitor-Mix Complete™	Santa Cruz biotechnology, Heidelberg GER
RPMI-1640	Lonza, Basel CH
Sodium dodecyl sulfate (SDS)	Merck, Darmstadt, GER
Sodium chloride	Merck, Darmstadt, GER
Sodium deoxycholate	Merck, Darmstadt, GER
Sodiumvanadat	Sigma-Aldrich, Munich GER
Spectra Multicolor Broad Range Protein Ladder	Fermentas, Frankfurt GER
SYBR Green I Nucleic Acid Gel Stain	Roche, Grenzach GER
Tetramethylethylenediamine (TEMED)	Sigma-Aldrich, Munich GER
Trehalose	Roth, Karlsruhe GER
Trisbase	Sigma-Aldrich, Munich GER
TritonX-100	Roth, Karlsruhe GER
Trypanblue 0.4 % in PBS	GIBCO BRL, Life Technologies, Eggenstein GER
Tween-20	Merck, Darmstadt GER
Water HPLC grade	Merck, Darmstadt GER

Table 2-3 Consumables

Consumables	**Manufacturer**
ABI PRISM® 384-Well Clear Optical Reaction Plate	Applied Biosystems, Foster City USA
ABI PRISM® Optical Adhesive Covers	Applied Biosystems, Foster City USA
Cell culture flasks	Sarstedt, Nümbrecht GER
Cryo Box	Nunc, Wiesbaden GER
Cryotubes	Nunc, Wiesbaden GER
Diethylaminoethyl-Cellulose	Whatman®, International Ltd UK
Electroporation Cuvettes	BioRad, Munich GER
Falcon Tubes 15 ml	Sarstedt, Nümbrecht GER
Falcon Tubes 50 ml	Sarstedt, Nümbrecht GER
Filter Tips, 10 µl, 100 µl, 200 µl, 1000 µl	Starlab, Ahrensburg GER
Micro Touch Examination Gloves	Ansell, München GER
Pasteurpipettes	Sarstedt, Nümbrecht GER
Pipette Tips w/o filters	Sarstedt, Nümbrecht GER
Reaction tubes 0.5 ml, 1.5 ml, 2.0 ml	Sarstedt, Nümbrecht GER
Serological pipettes 5 ml, 10 ml, 25 ml	Sarstedt, Nümbrecht GER
Tissue culture dish	Sarstedt, Nümbrecht GER
Tissue culture plates, 6 well, 12 well, 24 well	Nunc, Wiesbaden GER
96 well plate, Round/Flat bottom	Nunc, Wiesbaden GER

2.3 Buffers, Solutions and Media

Buffers, solutions and media used for this study are listed in Table 2-4.

Table 2-4 Buffers, solutions and media

Liquid	Receipt / Manufacturer
4x loading buffer Roti®-Load	Roth, Karlsruhe GER
Cell culture medium I (cell lines - BL)	RPMI-1640 10 % (v/v) FBS (Sigma-Aldrich, Munich GER) 200 U/ml Penicilin + 200 µg/ml Streptomycin + 4 mM L-Glutamine (PSG) (Sigma-Aldrich, Munich GER) 50 µM α-Thiolglycerol, 20 nM BCS, 1 mM Sodium pyruvat
Cell culture medium II (cell lines - DLBCL)	RPMI-1640 10 % (v/v) FBS 200 U/ml Penicilin +200 µg/ml Streptomycin + 4 mM L-Glutamine (PSG)
Cell culture medium III	IMDM (PAA) 10 % (v/v) FBS 200 U/ml Penicilin +200 µg/ml Streptomycin + 4 mM L-Glutamine (PSG) OCI-Ly3 cells were cultivated with 20 % FBS
EDTA cell culture grade	0.5 M (Sigma Aldrich, Munich GER)
Freezing medium	90 % (v/v) FCS 10 % (v/v) DMSO
Nuclear Extract Buffer A	10 mM HEPES pH 7.9 10 mM KCl 10 µM EDTA 10 µM EGTA 1 mM DTT 1 x Complete Mini Protease Inhibitor 1 x PhosStop

Nuclear Extract Buffer B	20 mM HEPES pH 7.9 400 mM KCl 1 mM EDTA 1 mM EGTA 1 mM DTT 1 x Complete Mini Protease Inhibitor 1 x PhosStop
PCR buffer (10x) for qRT	750 mM Tris-HCl pH 8.8 200 mM Ammonium sulfate 0.1 % Tween-20 in depc water
PBS (Phosphate Buffered Saline)	137 mM NaCl 10 mM Phosphate 2.7 mM KCl, pH 7.4.
PBS pH 7.4 (cell culture grade)	Lonza, Verviers BEL
Ponceau-S	5 % (v/v) glacial acetic acid 0.5 % (w/v) Ponceau-S
ReBlot plus mild	Millipore, Schwalbach/Ts. GER
RIPA buffer	150 mM NaCl 1 % NP-40 0.1 % SDS 50 mM TrisHCl pH 7,4 0.25 % Sodium-Deoxycholat
Running buffer (1x):	25 mM Tris-Base 192 mM Glycin 34.67 mM SDS
Separation Gel Mix	31.3 % (v/v) Acrylamid/Bis Solution (40 %) 332 mM Tris Base, pH 8.9 3.33 mM EDTA
Stacking Gel Mix	15 % (v/v) Acrylamid/Bis Solution (40 %) 125 mM Tris Base pH 6.8 0.1 % (w/v) SDS 5 mM EDTA

Solution 1 Chemiluminescence – Luminol	100 mM Tris/HCl pH 8.8 2.5 mM Luminol (Sigma-Aldrich, Munich GER) 4 mM 4-IPBA (Sigma-Aldrich, Munich GER)
Solution 2 Chemiluminescence – Peroxide	100 mM Tris/HCl pH 8.8 10.6 mM H2O2
SybrGreenMix	1 x PCR buffer 3 mM MgCl2 1:80000 SybrGreen 0.2 mM dNTP each 20 U/ml Hot FIREpol DNA polymerase 0.25 % TritonX-100 0.5 mM Trehalose in depc water
TBS (1x)	20 mM Tris-Base, 137 mM Sodium Chloride, pH 7.6
TBS-T	1 x TBS 0.1 % (v/v) Tween-20
Transferbuffer (1x):	25 mM Tris-Base 192 mM Glycin 15 % (v/v) MeOH

2.4 Equipment

Table 2-5 lists the equipment used in the present study.

Table 2-5 Equipment

Instrument	**Manufacturer**
ABI PRISM 7900HT	Applied Biosystems, Foster City USA
Accu-jet	Brand, Hamburg GER
Biofuge Pico	Heraeus Instruments, Hanau GER
Biofuge Primo R	Heraeus Instruments, Hanau GER
Consort E734 Power Supply	Schütt Labortechnik, Göttingen GER
CAT RM 5 horizontal roller	CAT M Zipperer, Staufen GER

Centrifuge 5451D	Eppendorf, Hamburg GER
GenePulser Xcell	Bio-Rad, Munich GER
Hera freeze -80°C freezer	Heraeus Instruments, Hanau GER
IKA KS 260 shaker	IKA, Staufen GER
IKAMAG RCT magnetic stirrer	IKA, Staufen GER
Incubator Cytoperm	Heraeus Instruments, Hanau GER
Incudrive incubator	Schütt Labortechnik, Göttingen GER
LAS-4000 Image Reader	Fujifilm, Düsseldorf GER
Microflow Laminar Downflow Workstation	Bioquell, UK
Microcoolcentrifuge 1-15k	Sigma, Munich GER
Multifuge 3 L-R	Heraeus Instruments, Hanau GER
ND-1000 UV/Vis-Spectrophotometer	NanoDrop™, Wilmington USA
Neubauer Counting Chamber Improved	Lo Labor Optik, Friedrichsdorf GER
Power Pac 300 Power Supply	Bio-Rad, München GER
Reax2 shaker	Heidolph, Schwabach GER
SunriseTM Microplate Reader	Tecan, Crailsheim GER
Thermocycler Mastercycler	Eppendorf, Hamburg GER
Thermocycler 60	Biomed, Theres GER
Thermocycler T3000	Biometra, Göttingen GER
Thermomixer Compact	Eppendorf, Hamburg GER
Vortex Genie 2	Schütt Labortechnik, Göttingen GER
Water bath	Köttermann Labortechnik, Hänigsen GER

2.5 Recombinant Proteins

BL and DLBCL cell lines as well as primary B cells were stimulated with either sCD40L (#ABC159; AutogenBioclear, Calne, Wiltshire UK) or goat anti human IgM $F(ab)_2$ fragment (#109006129; Jackson ImmunoResearch / Dianova, Hamburg GER).

2.6 Inhibitors

The chemical inhibitors used in this study are listed in Table 2-6. The final concentration listed for each inhibitor was used, if not stated differentially in the text.

Table 2-6 Chemical inhibitors

Description (target)	Manufacturer	Final concentration
10058-F4 (c-Myc)	Sigma-Aldrich, Munich GER	60 µM
5Z-7-oxozeaenol (TAK1/MAP3K7)	Calbiochem/Merck, Darmstadt GER	100 nM
Akti-1/2 (Akt)	Calbiochem/Merck, Darmstadt GER	2.5 µM
AZ-Tak1 (TAK1)	Tocris Biosciences, Toronto, CA	500 nM
Bisindolylmaleimide I (PKC)	Calbiochem/Merck, Darmstadt GER	1 µM
BKM-120 (PI3K)	Selleckchem, Munich GER	1 µM
BX-912 (PDK1)	Selleckchem, Munich GER	250 nM
Compound 15e (PI3K)	Enzo Life Sciences, Lörrach GER	400 nM
Cyclopamine (SMO)	Calbiochem/Merck, Darmstadt GER	5 µM
Everolimus (mTOR)	Sigma-Aldrich, Munich GER	1 µM
IKK2 inhibitor VIII (IKK2)	Calbiochem/Merck, Darmstadt GER	7 µM
Ly294002 (PI3K)	Calbiochem/Merck, Darmstadt GER	10 µM
SB203580 (p38/MAPK14)	Sigma-Aldrich, Munich GER	2 µM
SP600125 (JNK)	Calbiochem/Merck, Darmstadt GER	10 µM
U0126 (MEK1/2)	Sigma-Aldrich, Munich GER	10 µM
U73122 (PLCγ)	Tocris Biosciences, Toronto CA	1 µM

2.7 Antibodies

Antibodies used for immunoblotting are summarized in Table 2-7.

Table 2-7 Antibodies used for immunoblotting.

Antibody	Source	Working dilution
mouse monoclonal anti α-tubulin (#05-829)	Upstate/Millipore, Schwalbach GER	1:5000 in 3 % milkpowder in TBS-T
rabbit anti p-AKT (S473) (#9271)	Cell Signalling/ New England Biolabs, Frankfurt am Main GER	1:1000 in 5 % BSA in TBS-T
rabbit anti p-AKT (S473) (D9E) (#4060)	Cell Signalling/ New England Biolabs, Frankfurt am Main GER	1:1000 in 5 % BSA in TBS-T
rabbit p-Akt (T308) (C31E5E)	Cell Signalling/ New England Biolabs, Frankfurt am Main GER	1:1000 in 5 % BSA in TBS-T
rabbit anti pan AKT (C67E7) (#4691)	Cell Signalling/ New England Biolabs, Frankfurt am Main GER	1:1000 in 5 % BSA in TBS-T
rabbit anti c-myc (#9402)	Cell Signalling/ New England Biolabs, Frankfurt am Main GER	1:1000 in 5 % BSA in TBS-T
rabbit anti c-Rel (G57) (#4774)	Cell Signalling/ New England Biolabs, Frankfurt am Main GER	1:1000 in 5 % BSA in TBS-T
rabbit anti HDAC1 (#2062)	Cell Signalling/ New England Biolabs, Frankfurt am Main GER	1:1000 in 5 % BSA in TBS-T
rabbit anti p-p38 (T180/Y182)(#9211)	Cell Signalling/ New England Biolabs, Frankfurt am Main GER	1:1000 in 5 % BSA in TBS-T
rabbit anti p38 (#9212)	Cell Signalling/ New England Biolabs, Frankfurt am Main GER	1:1000 in 5 % BSA in TBS-T
rabbit anti p-p44/p42 (p-ERK1/2) (#4372)	Cell Signalling/ New England Biolabs, Frankfurt am Main GER	1:1000 in 5 % BSA in TBS-T
rabbit anti p44/p42 (ERK1/2) (#4695)	Cell Signalling/ New England Biolabs, Frankfurt am Main GER	1:1000 in 5 % BSA in TBS-T
rabbit anti p65 (C22B4) (#4764)	Cell Signalling/ New England Biolabs, Frankfurt am Main GER	1:1000 in 5 % BSA in TBS-T
rabbit anti p-p70 S6 Kinase (T389) (108D2) (#9234)	Cell Signalling/ New England Biolabs, Frankfurt am Main GER	1:1000 in 5 % BSA in TBS-T
rabbit anti p70 S6 Kinase (49D7) (#2708)	Cell Signalling/ New England Biolabs, Frankfurt am Main GER	1:1000 in 5 % BSA in TBS-T

rabbit anti p100/p52 (NF-KB2) (#4882)	Cell Signalling/ New England Biolabs, Frankfurt am Main GER	1:1000 in 5 % BSA in TBS-T
rabbit anti p-IκBα (S32) (14D4) (#2859)	Cell Signalling/ New England Biolabs, Frankfurt am Main GER	1:1000 in 5 % BSA in TBS-T
rabbit anti IκBα (44D4) (#4812)	Cell Signalling/ New England Biolabs, Frankfurt am Main GER	1:1000 in 5 % BSA in TBS-T
rabbit anti p-SAPK/JNK (T183/Y185) (81E11) (#4668)	Cell Signalling/ New England Biolabs, Frankfurt am Main GER	1:1000 in 5 % BSA in TBS-T
rabbit anti JNK1/3 (C-17) (#sc-474)	Santa Cruz, Heidelberg GER	1:1000 in 5 % BSA in TBS-T
rabbit anti RelB (C1E4) (#4922)	Cell Signalling/ New England Biolabs, Frankfurt am Main GER	1:1000 in 5 % BSA in TBS-T
rabbit anti p-S6 ribosomal protein (S240/244) (#2215)	Cell Signalling/ New England Biolabs, Frankfurt am Main GER	1:1000 in 5 % BSA in TBS-T
rabbit anti S6 ribosomal protein (54D2) (#2317)	Cell Signalling/ New England Biolabs, Frankfurt am Main GER	1:1000 in 5 % BSA in TBS-T
rabbit anti Tak1 (D94D7) (#5206)	Cell Signalling/ New England Biolabs, Frankfurt am Main GER	1:1000 in 5 % BSA in TBS-T
goat anti mouse HRP polyclonal (D1609)	Santa Cruz, Heidelberg GER	1:5000 in 5 % BSA in TBS-T
goat anti rabbit HRP polyclonal (E1710)	Santa Cruz, Heidelberg GER	1:5000 in 5 % BSA in TBS-T

2.8 Oligonucleotides

Primers used for qRT-PCR are summarized in Table 2-8.

Table 2-8 Oligonucleotides used for qRT-PCR.

Oligo	Sequence
ABL	fwd: 5'-AGCCTGGCCTACAACAAGTTCTC-3' rev: 5'-GACATGCCATAGGTAGCAATTTCC-3'
B2M	fwd: 5'-CTATCCAGCGTACTCCAAAGATTCA-3' rev: 5'-TCTCTGCTGGATGACGTGAGTAAA-3'
CCND2	fwd: 5'-CTGCGCAGGCAAGCACTAT-3' rev: 5'-TCTTATCCTGCCAATTCAGTGTGA-3'
CDK4	fwd: 5'-AGGCGACTGGAGGCTTTTG-3' rev: 5'-GTGGCACAGACGTCCATCAG -3'
CDKN1_P21	fwd: 5'-TGGAGACTCTCAGGGTCGAAA-3' rev: 5'-GCGTTTGGAGTGGTAGAAATCTG-3'
c-MYC	fwd: 5'-AAGAGGGTCAAGTTGGACAGTTGC-3' rev: 5'-TTTCGGTTGTTGCTGATCTGTCT-3'
GAPDH	fwd: 5'-ACCACTTTGTCAAGCTCATTTCCT-3' rev: 5'-GTTGCTGTAGCCAAATTCGTTGT-3'
hGLI1	fwd: 5'-CTGTGGGCAACATGAGTGTCTTAC-3' rev: 5'-AATTCTGTTTCCCCAGGTAGGG-3'
hSHH	fwd: 5'-TTAAGGATGAAGAAAACACCGGAG-3' rev: 5'-AGCGTTCAACTTGTCCTTACACCT-3'
hSMO	fwd: 5'-GTGACAAAGCCTCTGAAAGATGC-3' rev: 5'-CCCACTAAATGGGTGTGAGGAA-3'
PTCH1	fwd: 5'-TCGACATCAGCCAGTTGACTAAAC-3' rev: 5'-TTAATGATGCCATCTGCATCCA-3'
RNAPOLII	fwd: 5'-CACTATTAAGAAGGCCAAGCAGGA-3' rev: 5'-TGTTGTGTGCCTTCTCGATGAC-3'
TAK1	fwd: 5'-ACAGCCTATTCCAAGCCTAAACG-3' rev: 5'-CAGAATGTTGCCAAATGAAGCA-3'

ICAM1	fwd: 5’-TTCACAATGACACTCAGCGGTC-3’ rev: 5’-AGTGCAAGCTCCCAGTGAAATG-3’
ANK3	fwd: 5’-CGTAACAGCGAACGGTCAGTC-3’ rev: 5’-TACTTCCTGCTGACATTTCTTCCAC-3’
SIRPA	fwd: 5’-CTTCTTCTACAAGGTTGCATGAGCC-3’ rev:5’-GTCTGAATGCTGGCATACTCCG-3’
RFTN1	fwd: 5’-GAGTGTATCCACCAAGCAGATTGT C-3’ rev: 5’-CCTCATCTGCCTGTTGTGCAT-3’
LINC00158	fwd: 5’-GAACCCTGAGCAGAACACATGC-3’ rev: 5’-GACGACCGCTTTCTTAAACTTTCTC-3’
CTDSPL	fwd: 5’-TATTGTTCCGGTTGAAATCGATG-3’ rev: 5’-GGCCAAGCTGGCAGTAAAGAG-3’

2.9 Ready to Use Reaction Systems

In Table 2-9 the Ready to use reaction systems applied during this study are listed.

Table 2-9 Reaction Systems

Description	**Manufacturer**
RNA Isolation Kit	Machery+Nagel, Düren GER
Rneasy® Mini Kit	Qiagen, Hilden GER
SuperscriptII™ RT Kit	Invitrogen, Karlsruhe GER
SignalBoostTM Immunoreaction Enhancer Kit	Calbiochem *via* Merck, Darmstadt GER

2.10 Software used

If not stated elsewhere the following software products were used: the present thesis was written in Microsoft® Office Word 2013 and 2007. Literature-management and bibliography was generated using Mendeley Desktop Version 1.8.4. Graphs were created using GraphPad PRISM 5.04 and figures were assembled using Adobe® Photoshop® CS2 and Microsoft® Office PowerPoint 2013 and 2007. Gene expression data were manually compared and analyzed using VENNY (Oliveros, 2007).

2.11 Cell Biology

2.11.1 Cell Culture Techniques

Burkitt Lymphoma cell lines were cultured in RPMI-1640, 10 % (v/v) FCS, 200 U/ml Penicilin, 200 µg/ml Streptomycin, 20 nM BCS, 50 µM α-Thioglycerol, 1 mM Sodium pyruvate. Cells were cultured at 37°C, 5 % CO_2 and splitted daily depending on the observed cell proliferation (cell density: $0.3x10^6$ cells/ml - $1x10^6$ cells/ml). The day before the experiment $0.3x10^6$ cells/ml were seeded.

DLBCL cell lines, except OCI-Ly1, OCI-Ly3 and OCI-Ly7, were cultured in RPMI-1640, 10 % (v/v) FCS, 200 U/ml Penicilin, 200 µg/ml Streptomycin and kept in a cell density of $0.5x10^6$ - $1x10^6$ cells/ml. OCI-Ly1 and OCI-Ly7 were cultured in IMDM, 10 % (v/v) FCS, 200 U/ml Penicilin, 200 µg/ml Streptomycin, 4 mM L-Glutamine and OCI-Ly3 were cultured in IMDM, 20% (v/v) FCS, 200 U/ml Penicilin, 200 µg/ml Streptomycin, 4 mM L-Glutamine.

Cells were counted in 0.4 % Trypan blue using a Neubauer counting chamber. To cultivate cells from a frozen aliquot, thawed cells were washed with 10 ml of the respective cell culture medium (centrifugation 250 x g, 7 min at RT). The cell pellet was resuspended in 5-10 ml medium and cells were incubated at 37°C, 5 % CO_2. To freeze cells approximately $1x10^7$ cells were sedimented as described above and resuspended in 1 ml freezing medium (90 % FCS, 10 % DMSO). Cells were frozen in cryo boxes containing isopropanol to obtain a constant cooling of approximately 1°C/min and stored immediately at -80°C for 24 hours before permanent storage at -150°C.

2.11.2 Activation of B cells with Soluble Stimulating Factors

Burkitt lymphoma cell lines were seeded in fresh media in a density of $3x10^5$ cells/ml (DLBCLs: $5x10^5$ cells/ml) the day prior to experimental handling. In order to stimulate the cells, they were counted, centrifuged at 250 x g for 7 min, resuspended in fresh corresponding medium supplied with 10 mM Hepes ($1x10^6$ cells/ml) and supplemented with sCD40L (200 ng/ml) or anti human IgM $F(ab)_2$ fragment (13 µg/ml). Cells were incubated at 37°C, 5 % CO_2 for 15 min, 30 min, 60 min, 90 min, 120 min, 150 min, 180 min, 210 min, 240 min, 360 min, 480 min and 24 hours for microarray analyses. Cells were harvested (10 min, 300 x g, 4°C) and washed with PBS containing 100 mM sodium orthovanadate. Samples were frozen at -80°C and RNA was isolated with the RNeasy Kit

(Qiagen) for microarray analyses or with the NucleoSpin® RNA II Kit (Macherey-Nagel, Düren Germany).

2.11.3 Inhibitor Treatment

16 hours prior to inhibitor treatment cells were seeded in serum-reduced media (0.5 % FCS) at $3x10^5$ cells/ml (BL cell lines) or at $5x10^5$ cells/ml (DLBCL cell lines). Before inhibitor treatment, cells were counted, centrifuged (250 x g, 7 min) and seeded in a density of $1x10^6$ cells/ml in fresh serum-reduced media containing 25 mM Hepes. For microarray analyses, cells were treated with 100 nM (5Z)-7-Oxozeaenol (TAK1/MAP3K7 inhibitor), 7 µM IKK2-VIII inhibitor, 10 µM Ly294002 (PI3K inhibitor), 2 µM SB203580 (p38/MAPK14 inhibitor), 10 µM SP600125 (JNK inhibitor) or 10 µM U0126 (MEK1/2 inhibitor) for 3h prior to BCR or CD40 activation. The stimulation was performed for 3 hours to monitor gene expression changes, or for 30 minutes to validate pathway activation *via* WB respectively. Cells were harvested at 300 x g at 4°C for 10 min and resuspended in ice-cold PBS, supplemented with 1 mM sodium orthovanadate. Dry pellets were frozen at -20°C for protein analyses or -80°C for RNA processing.

2.11.4 Transfection of siRNA

Small-interfering RNA (siRNA) is a short (20-25bp) double-stranded RNA molecule, which can be theoretically used to knock down any gene of interest when synthetically engineered. siRNA can be introduced in mammalian cells by transfection. Transfection can be carried out using calcium phosphate by mixing a cationic lipid with the siRNA to produce liposomes, which fuses with the cell membrane. Another transfection method is electroporation. For electroporation, the cells are exposed to short pulses of an intense electric field, which transiently increases the permeability of the cell membrane.

To achieve a knock down of Tak1, corresponding siRNAs (Silencer® Select, Invitrogen, Darmstadt GER) were transfected into Burkitt's and Diffuse large B cell lymphoma cell lines using the GenePulser Xcell (Bio-Rad, Munich GER). 2 µg of corresponding siRNA were transfected by electroporation (300 V, 150 µF, 1540 Ω) in $2.5x10^6$ cells/ml lymphoma cell lines in 200 µl Opti-MEM® (Invitrogen, Darmstadt GER) and transferred into 5 ml pre-warmed RPMI 1640, supplemented with 10 % (v/v) FCS, 200 U/ml Penicilin, 200 µg/ml Streptomycin, 20 nM BCS, 50 µM α-Thioglycerol, 1 mM Sodium pyruvate and 25 mM Hepes. Transfected cells were incubated for 24 hours at 37°C, 5 % CO_2 and subsequently transfected a second time. A non-sense siRNA without a human target was used as control (scrbl). Upon two transfections and subsequent 24 hours of incubation, control-transfected cells were subjected to inhibitor treatment and stimulation with sCD40L (200 ng/ml) or α-IgM (13 µg/ml).

2.12 Protein Biochemistry

2.12.1 Preparation of Cell Lysates

Cells were harvested using sedimentation (300 x g, 7 min, 4°C) and washed once with PBS containing 1 mM Sodium orthovanadate. Dry pellets were stored at -20°C until further preparation.

Whole cell lysates

Whole cell lysates were prepared by resuspending a cell pellet corresponding to $1x10^6$ cells in 50 µl RIPA buffer. The cell suspension was incubated for 30 min on ice, subsequently residual cell debris was sedimented at 13000 rpm for 15 min at 4°C. The supernatant, containing the whole cell lysate, was transferred into a fresh tube and protein concentration was determined using the RotiQuant® assay (Roth, Karslruhe GER). Protein concentration was measured with a microplate reader (Infinite® F50, Tecan, Männedorf CH).

Cell fractionation

To demonstrate activation of the NF-kB pathway, nuclear translocation of NF-kB family members was monitored. Therefore, separation of cytosolic protein from nuclear protein was necessary. To obtain nuclear extracts from freshly harvested cell pellets, cell fractionation according to Schreiber et al. (Schreiber et al., 1989) was accomplished. Therefore $1x10^7$ cells were harvested (300 x g, 10 min, 4°C) and washed twice with PBS containing 1 mM Sodium orthovanadate. Pellets were lysed in 400 µl buffer A and incubated 15 min on ice. 25 µl 10 % NP-40 were added and vigorously vortexed for 10 s. Samples were sedimented for 5 min, 4°C at 13000 rpm and the supernatant containing cytosolic protein was transferred to a new tube. The pellet was covered with 50 µl buffer B and shaked strongly for 25 min at 4°C in the cold room. Upon sedimentation for 5 min at 13000 rpm, 4°C, the supernatant containing the nuclear proteins was transferred into a new tube. Protein concentration was determined using the RotiQuant® assay (Roth, Karslruhe GER).

2.12.2 SDS-PAGE and Western Blot

For separation of proteins depending on their molecular weight sodium dodecyl sulphate polyacrylamide gelelectrophoresis (SDS-PAGE) was used (Ahn et al., 2001; Laemmli, 1970). Using the BioRad System (Munich, GER), polyacrylamide gels comprised of a 10 % separation gel and a 5 % stacking gel were prepared. 20-30 µg of protein samples were loaded with 4x RotiLoad®-loading dye, denaturized at 95°C for 5 min and loaded onto the gel. For protein size determination, Rainbow-FullRange™ marker was loaded additionally. Gels were run with 20 mA per gel for 1 hour and subsequently proteins were transferred to a nitrocellulose membrane (Hybond™-C extra, GE Healthcare, Munich, Germany) using the Tank Blot System (BioRad, Munich, Germany). The separating gel was cut from the stacking gel and equilibrated for one minute in Transfer Buffer. For

protein transfer a pile was carefully prepared as follows: cathode (-), foam pad, 2 Whatman™-papers, separating gel, nitrocellulose membrane, 2 Whatman™-papers, foam pad, anode (+). Transfer was conducted at 100 V for 1 hour at 4°C.

2.13 Molecular Biology

2.13.1 mRNA Isolation

mRNA was isolated from cell pellets using the RNeasy® Mini Kit (Qiagen, Hilden, Germany) or NucleoSpin® RNA Kit (Macherey&Nagel, Düren, Germany) according to manufacturer instructions. mRNA was eluted using 40 µl RNAse-free water. Concentrations were measured by NanoDrop™ measurement.

2.13.2 Reverse Transcription

In order to obtain cDNA, 1 - 2 µg mRNA was reversely transcribed using the SuperScriptII™ RT Kit (Invitrogen, Darmstadt GER). Reverse transcription was initiated with random hexamer primer. 2 µl random hexamer primer (100 µM) and 1 - 2 µg mRNA in 10 µl H_2O were added to each cup. The mix was denaturated for 10 min at 70°C in a thermocycler (Biometra). Subsequently 8 µl of Master Mix (Table 2-10) was added and the complete mixture was incubated in a thermocycler with the following program (Table 2-10).

Table 2-10 Master Mix and thermocycler program for reverse transcription of mRNA

Master Mix	thermocycler program
4 µl 5x First Strand Buffer	
2 µl DTT (0.1M)	42°C 60 min
1 µl dNTPs (10 mM each)	65°C 10 min
1 µl SuperScript RT II	4°C ∞

2.13.3 qRT-PCR (quantitative Real Time – Polymerase Chain Reaction)

For the quantification of transcripts, a SYBR® Green based system was used. The cyanine dye SYBR® Green intercalates in double-stranded DNA. The resulting DNA-dye-complex absorbs blue light (λ_{max} = 488 nm) and emits green light (λ_{max} = 522 nm) and can therefore be used to quantify double-stranded PCR products over time during a PCR reaction. The number of PCR cycles at which a certain threshold of fluorescence intensity is achieved (Ct - value, cycle threshold), directly correlates to the number of DNA templates present in the reaction.

Transcript quantification was performed with Fast SYBR® Green (Applied Biosystems, Foster City USA) for GC B samples and a self-made SYBR Green Mix (see section Materials) for all samples obtained from cell lines. To carry out the PCR reaction and fluorescence detection an ABI PRISM 7900HT sequence detection system (Applied Biosystems, Foster City USA) was used (SDS 2.4). For GC B samples, cDNA corresponding to 2.5 µg RNA was used as template. For cDNA obtained from cell line experiments a corresponding amount of 10 - 20 µg RNA was used. PCR reactions were performed in a 384-well clear optical plate. The relative mRNA expression levels were determined by normalizing the mean Ct-values of triplets to the Ct values of a housekeeping gene:

$$\Delta Ct = Ct_{\text{gene of interest}} - Ct_{\text{housekeeping gene}}$$

The ΔCt values of the modified sample and the control sample can then be compared by calculating ΔΔCt:

$$\Delta\Delta Ct = \Delta Ct_{\text{modified sample}} - \Delta Ct_{\text{control}}$$

ΔΔCt is a relative measurement, giving the values for the differences of cycles of the amplicon of the gene of interest after treatment in comparison to control. Assuming that the efficiency for both genes (household gene and gene of interest) is 100 %, one can calculate the n-fold change = $2^{-\Delta\Delta Ct}$. As housekeeping gene, *ABL* was chosen in this study. All primers for the qRT-PCR reactions were designed with the use of PrimerExpress™ software (Applied Biosystems, Foster City USA) on the basis of the published NCBI mRNA sequence (http://www.ncbi.nlm.nih.gov/sites/entrez/). Specificity was tested with the help of BLAST software (http://www.ncbi.nlm.nih.gov/blast/Blast.cgi). In addition, the efficiency of each pair of primers was assessed, running a qRT-PCR on a dilution series of template DNA and calculating the slope m of the linear regression of the standard curve. The efficiency was calculated by

$$E = 10^{-1/m} - 1.$$

Thus, an efficiency of 100 % results in a slope of -3.32 which corresponds to a doubling of the amount of amplicon with one cycle. Primer pairs with an efficiency lower than 93 % were abolished. Analyses were accomplished using Microsoft® Office Excel 2007.

2.14 Microarray Analyses

Two different types of Affymetrix GeneChip® microarray platforms were used in the present study. For pathway perturbation analyses *via* inhibitor use (chapter 3.3), the Affymetrix GeneChip Human Genome U133 Plus 2.0 array was used to ensure comparability to former derived data sets. The time course analyses were hybridized on Affymetrix Human Gene 1.0 ST microarrays. In contrast to the classical 3' gene expression arrays, the Human Gene 1.0 ST microarray platform is a whole-transcript

expression array, including approx. 26 probes per annotated gene, spread across the whole length of the gene.

For both microarray platforms, cDNA was synthesized using 1 µg corresponding RNA and including Poly-A RNA controls with the help of the Affymetrix GeneChip® Poly-A RNA control Kit. Secondly, cRNA synthesis and cleanup was carried out using the Affymetrix GeneChip® IVT Labelling Kit. Subsequently, fragmentation and labeling for microarray hybridization was accomplished with the corresponding kits according to manufacturer's instructions. The whole process, including final hybridization, washing, staining and scanning was executed in the DNA Micorarray and Deep-Sequencing Facility of the University Medical Center Göttingen (UMG) with the help of Dr. G. Salinas-Riester and S. Luthin. Raw data were transferred to the Institute of Functional Genomics, University Regensburg, and statistically analyzed by K. Meyer, M. Pirkl and Prof. Dr. R. Spang.

Microarray data preprocessing - Data analysis was performed using the statistical computing environment R and the life-science related extension Bioconductor (http://www.bioconductor.org). Gene expression profiles were background corrected and normalized on probe level using a variance stabilization method (Huber et al., 2002). Normalized probe intensities were summarized into gene expression levels using an additive model described in (Irizarry, 2003) and fitted by a median polish routine. Additionally, batch effects were corrected using ComBat (Johnson et al., 2007) by estimating additive and multiplicative effects for each batch and normalizing accordingly.

Differential gene expression - An additive linear model approach (Smyth, 2005) was used to calculate effects of experimental conditions on each probe set. The experiments with single inhibitors/stimulations are used to calculate the individual effect. Synergetic effects are then inferred from the combinatorial experiments.

Nested Effects Models – The effects of gene perturbation *via* inhibitor use and subsequent stimulation on the whole genome gene expression level were analyzed using a class of probabilistic models called 'Nested Effects Models' (NEMs) (Fröhlich et al., 2007; Markowetz et al., 2005).

GO KEGG and GSEA - Gene set enrichment analysis (GSEA) of ranked gene lists was performed using the Java implementation of GSEA obtained from http://www.broadinstitute.org/gsea/. GSEA was conducted in the mode for pre-ranked gene lists on the C2 set of curated gene signatures from the Molecular Signature Database (MSigDB). GO and KEGG pathway enrichment analyses were performed using the gokeggLister method implemented in the package compdiagTools.

3 Results

3.1 Temporal pattern of whole genome gene expression changes upon signaling pathway activation

In the last decade, global gene expression analyses have been excessively used for developing strategies to describe and stratify lymphoma cases. Hence, a molecular definition of BL was identified, distinguishing mBL from non-mBL, including DLBCLs (Dave et al., 2006; Hummel et al., 2006). However, it remains unclear to which extent distinct signaling pathways of the immune response are in charge of the differences in gene expression that distinguish lymphoma. In former analyses in the group of D. Kube, BL cells were stimulated with factors known to be involved in B cell signaling, microenvironment and lymphoma pathogenesis and subjected to microarray analysis. Thereby, distinct *in vitro* stimuli could characterize individual NHL and signaling pathways dominantly involved in these global gene expression patterns have been identified (Schrader et al., 2012b). In the present study, two of the stimuli inducing the strongest gene expression changes (CD40 and B cell receptor activation) were used in a time-resolved analysis to provide data allowing the prediction of regulatory feedback loops of certain oncogenic pathways.

In order to obtain a defined time course of pathway perturbation at the global level, we used human transformed GC B cells as a model system *in vitro* (BL2). Stimulation of cells *in vitro* was done in triplicates by adding α-IgM $F(ab)_2$-fragment to activate BCR signaling or sCD40L to activate CD40 mediated signaling, respectively. Samples were collected in defined time intervals until 480 min (Figure 3-1 A). The corresponding RNA samples were hybridized to Human Gene 1.0 ST arrays (Affymetrix, Santa Clara). Respective bioinformatical and high-dimensional statistical data analysis was performed in parallel by several statisticians belonging to the HaematoSys-consortium. Data preparation (background correction, normalization, estimation of gene expression levels by a median polish routine: Katharina Meyer, Regensburg) exhibited a unique gene expression pattern (Figure 3-1 B + D). Upon α-IgM stimulation 2509 genes with fold change ≥3 were altered in their expression level, while CD40 activation led to change of expression level in 2447 genes (here fold change ≥ 1.5 was chosen, since the overall variance of expression changes was smaller than in α-IgM stimulated cells).

In parallel, CD40 and BCR mediated signaling was monitored on the protein level by detecting changes in protein phosphorylation and degradation (Figure 3-1 C + E). To describe the effects and their time courses, activation of the following pathways was monitored by Western Blot analyses: MAPK signaling (phosphorylation of Erk and p38), NF-κB signaling (*via* the degradation of IκBα) and PI3K/Akt signaling (phosphorylation of Akt).

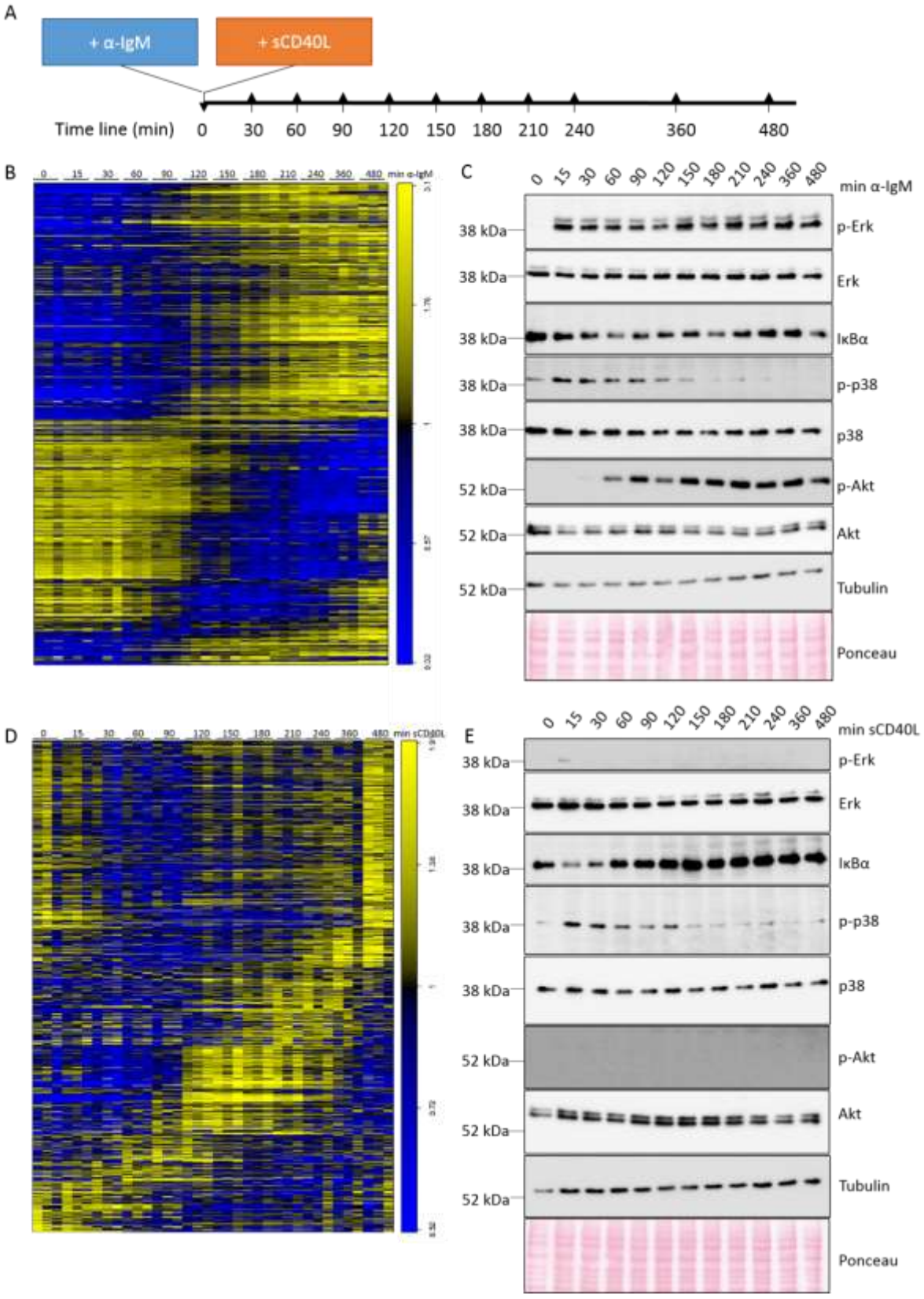

Figure 3-1 Time course analyses of gene expression changes on the whole genome level upon stimulation of human transformed germinal center B cells. A BL2 cells were stimulated with 200 ng/ml sCD40L or 13 µg/ml anti-IgM F(ab)$_2$ fragment respectively and samples were harvested every 30 minutes for up to 4 hours, plus additional later time points at 6 and 8 hours, **B + D** Heatmaps displaying gene expression changes on the whole genome level. Each row represents one of the TOP100 most highly responding genes. Each column represents

one sample. Three biological replicates of each sample either with BCR (**B**) or CD40 activation (**D**) were hybridized to HU Gene 1.0 (Affymetrix). Additionally, changes in protein phosphorylation and degradation were documented by Western Blot analyses (**C + E**).

As shown in Figure 3-1 C, α-IgM stimulation of BL cells induced a rapid and sustained phosphorylation of Erk as well as an equally rapid activation of p38 (p-p38). However, the phosphorylation status of p38 declined 90 min after BCR crosslink and reached basal level upon 150 min after stimulation. CD40 activation of BL cells showed a similar phosphorylation course of p38, although an activation of MAPK signaling through phosphorylation of Erk was hardly detectable upon 15 min after CD40 stimulation, but not at any other time point after stimulation (Figure 3-1 E). The activation of NF-κB signaling was detected by monitoring the degradation of the NF-κB inhibitor IκBα. CD40L strongly activated canonical NF-κB signaling rapidly after stimulation (15 min – 30 min), whereas α-IgM stimulation of BL cells resulted only in a marginal degradation of IκBα at a later time point (60 min after BCR activation). In contrast, BCR crosslink led to a pronounced activation of the PI3K/Akt pathway (p-Akt, Figure 3-1 C), whereas upon CD40L stimulation a phosphorylation of Akt was not detectable. Thus, we confirm that α-IgM and CD40L treatment activate, although with distinct kinetics, partially overlapping pathways.

3.1.1 α-IgM stimulation of BL cells changes the mBL index towards non-mBLs

To further prove the functional relevance of CD40L and α-IgM stimulated BL cells *in vitro,* it was investigated how the activation of the BL cells influences their mBL index. The mBL index value summarizes the expression of the 58 mBL signature genes and represents a measure for 'Burkitt-likeness' (Hummel et al., 2006). Designated mBL and non-mBL patient samples from the MMML study were hybridizied to HU Gene 1.0 (Affymetrix, Santa Clara, US) to achieve comparability to the time course data. Subsequently, the expression of the 58 mBL signature genes in the experimental time course samples was determined and each sample was assigned an mBL-signature index score, with a higher score reflecting a higher similarity of gene expression in comparison to the mBL core samples (Hummel et al., 2006). One can observe, as expected, that untreated BL2 cells showed a similar mBL index as proven BL NHL cases (Figure 3-2). Sustained CD40L stimulation for up to 8 hours reduced the mBL index score slightly, but did not change the expression of the mBL signature genes in an intense manner. In contrast, anti-IgM stimulation of BL2 cells for up to 8 hours led to a more intense reduction in the mBL index score over time. One could conclude that the stimulation of BL2 cells with α-IgM $F(ab)_2$ fragments shifts the gene expression profile of the former mBL cells towards a gene expression profile of DLBCLs. Thus, signaling pathways, which are activated in consequence of B cell receptor cross linking, seem to induce gene expression changes, which in turn are relevant for a certain "DLBCL-likeness". To further illuminate the substantial differences, which characterize DLBCL

and BL, their clinical manifestations and inevitable therapies, a closer view into BCR mediated signaling events in transformed germinal center B cells will be very helpful.

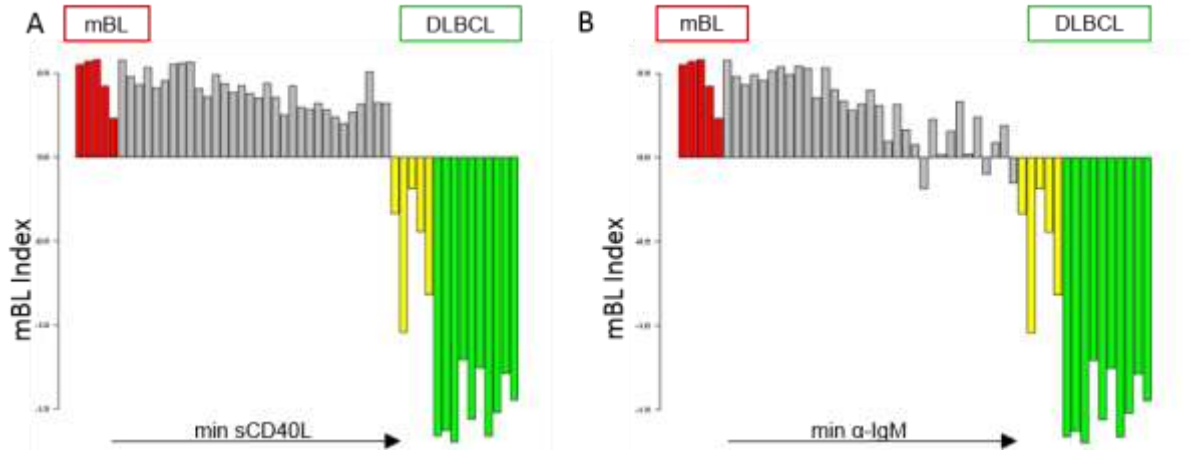

Figure 3-2 Sustained BCR activation in BL cells shifts mBL index towards the index of non-mBLs. mBL index (Hummel et al., 2006) of time course microarray data (grey bars) upon (**A**) CD40L stimulation and (**B**) BCR crosslink was calculated and compared to defined mBL (red bars), intermediate (yellow bars) and non-mBL cases (green bars, DLBCL). Each bar represents one sample hybridized to HU Gene 1.0 (Affymetrix).

3.1.2 Causality Network of BCR induced gene expression correlations

A time course of signaling events is especially interesting to analyze in order to find interdependent groups of genes. Data obtained in the present study were taken for network modeling to display correlations and causalities between subsets of genes. Normalized and calibrated raw data were taken and data were subsequently pre-filtered in two independent steps to exclude genes, which (step 1) can be assigned to noise and which (step 2) don't show any changes in expression over time. Noise-cancellation was accomplished assuming a Gaussian distribution of the expression values and modeling the overall signal through heuristic fitting of a two-component-mixture. Thereby, noise was cancelled and the signal remained. For anti-IgM stimulated data 8012 out of 21995 genes represented on the array remained. Secondly, genes which don't change their expression level with time elapsed, were excluded. Therefore, Fisher's g-test, testing on white noise of unknown frequency was used (Wichert et al., 2003). Using a False-Discovery-Rate of 0.1, 2832 genes remained, significantly changing their expression upon BCR crosslink. Using Bayesian Hierarchical Clustering (Cooke et al., 2011; Heller and Ghahramani, 2005; Savage et al., 2009) clustering of genes with a very similar time course was computed. This method reduced the dimensions to 22 clusters of genes. Subsequently, clusters with marginal changes over time were observed. All clusters of genes with an expression range less than 0.5 and less than 10 % highly significant genes (FDR < 0.05) were excluded. Finally based on an algorithm calculating partial correlation between the clusters (SIMoNe (Charbonnier et al., 2010)) a network displaying causal relationships was modeled (Figure 3-3).

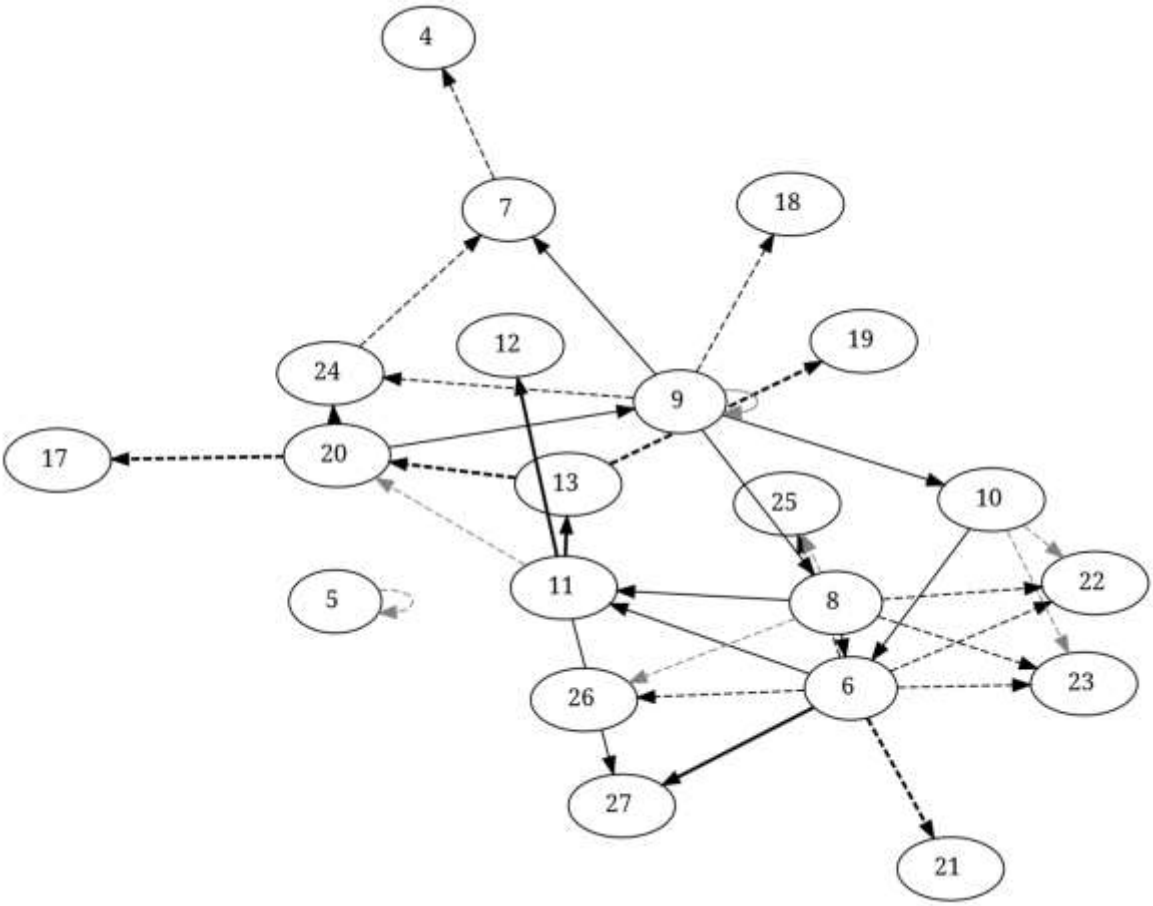

Figure 3-3 Causality network displaying anti-IgM stimulated gene expression correlations. Network modelled by B. Klaus (AG Strimmer, IMISE Leipzig), based on partial correlation using the 'R' package SIMoNe (Statistical Inference for Modular Networks (Chiquet et al., 2009)) displaying causal relationships between clusters of genes. Genes combined in one cluster display the same time course (Bayesian Hierarchical Clustering). A complete list of genes contained in each cluster can be found in Table A-1. Arrows indicate the causal relationship; bold arrows display a strong positive correlation between two clusters, whereas dashed arrows indicate a negative correlation.

In this directed graph, partial correlation between the expression courses of two clusters of genes may infer a regulatory link between the clusters. Continuous arrows indicate here a positive regulation, whereas dashed arrows represent a negative regulation. Additionally, stronger partial correlation between two nodes is depicted with bold arrows, whereas weak partial correlation is displayed with narrow arrows.

Having a closer view to the network, it becomes clear that there is no 'cluster of initiation'. All clusters depicted in Figure 3-3 are conditionally dependent on another cluster. This suggests that the anti-IgM stimulation triggered several independent processes at the same time. In contrast, several clusters are influenced by others, but do not influence a third cluster. This may be due to the limited period of time of observation and the statistical limitations in cluster generation.

Interestingly, cluster 6 and 8 seem to influence numerous other clusters. Apparently, cluster 8 is only conditionally dependent on one Cluster (#9) and cluster 6 is dependent on cluster 8 and 10. Both clusters (6 and 8) contain genes, which are slightly up regulated in the first 30 to 90 minutes after stimulation (Figure A-1). Both of the clusters then follow a time course, which depicts a down regulation of the harboring genes upon 90 to 240 minutes after BCR stimulation. Cluster 6 comprises 102 genes and cluster 8 harbors 58 genes. In both clusters, genes being mainly associated with signal transduction, protein modifications, transcriptional regulation and metabolic processes can be found. Cluster 6 and 8 contain amongst others genes encoding kinases (cl 6: *NADK*, *CAMK2G*, *PIP4K2B*, *PXK*, *DCK*, *FASTK,* cl 8: *AURKA*, *P38*) and genes encoding G-proteins and related proteins (cl 6: *CDC20*, *RASGRP1*, *ARGHAP35*, *ERC1*, *TBC1D14,* cl 8: *GOPC*, *FPGT*, *ARHGEF3*) (Table A-2). Both clusters 6 and 8 seem to influence the expression of genes in cluster 11, which contains 126 genes. Those genes show a similar expression course as genes from clusters 6 and 8, but with a higher expression rate, thus resulting in a distinct cluster of genes. Cluster 11 comprises genes associated with transcription, such as transcriptions factors (*MYC, BCL6, ID4*), transcriptional cofactors (*BCL9, BCL3*) and others, being involved in regulation of RNA and DNA metabolic processes (Table A-2).

Apparently, statistical analysis of the here obtained time course data enable the construction of a comprehensive causality network. Unfortunately, the biological interpretation of this huge data set remains difficult, since the distinct clusters comprise large lists of genes, which cannot be assembled to one specific function (a complete overview of the GO-analyses can be found on external CD ROM \\time course analyses\Network\GO-Enrichment). Thus, the conflation of our time course specific gene expression data set with other sources of high-throughput data may be useful to fathom the biological meaning of such a causality network. In order to shed some light on the complexity of the gene expression changes and their causal correlation induced through α-IgM stimulation, ongoing analyses are supposed to integrate genome-wide chromatin immunoprecipitation assays in our cell perturbation assays. Therewith, we aim to use such a causality network for identification of, for example, transcription factor targets.

3.1.3 A mathematically new method to analyze time courses identifies differentially expressed clusters of genes

Simultaneously to the network modeling of causalities and regulations in gene expression changes over time, a second group around Prof. Dr. J. Läuter (University Magdeburg) established a new method to analyze high-dimensional time course gene expression data. The here presented strategy to provide a mathematically stringent and effective procedure to describe time course data is based on spherical tests (Läuter et al., 1996, 1998). These aim to select the variables which exhibit a statistically firm unsteady distribution over time (Läuter et al., 2012). Thereby, the following stabilizing strategy was used: genes with similar time course were pooled in one set or cluster and tested for stationarity. Those clusters of genes, which emerged to be significant (multiple Beta-testing according to (Läuter et al., 1998) with alpha error $\alpha = 0.05$ and abort of the testing at $k = 5$ non-significant non-spherical tests (Hommel and Kropf, 2005)), can be taken for biological consideration. Hereby, the algorithm presumes that genes, which exhibit a uniform process, are potentially regulated through the same elicitor. In addition, in the case of several distinct clusters of genes, the specific shape of the serial data curves may be due to mutual regulatory dependence.

Via the adaptation and advancement of the test for stationarity, 500 sets of genes were built. Upon α-IgM stimulation 21 sets of genes were disjoint and CD40 activation led to 20 disjoint sets of genes. 15 significant sets of genes out of 21 displaying disjoint time courses were identified for α-IgM stimulated samples and 5 significant sets of genes for sCD40L-stimulated samples. 8 positively regulated gene groups and 7 gene groups suppressed through α-IgM are described. CD40 activation in turn led to 4 sets of up regulated genes and one gene set showing a suppression of gene expression.

Additionally, a combined analysis of CD40 and BCR induced gene expression changes allows the comparison of congenial reactions or differences in response to the distinct stimuli. Here, gene sets were identified, in which significant differences of gene expression changes upon BCR or CD40 or in both stimulations were observable. In Figure 3-4, the blue dashed line shows the mean gene expression changes over time for CD40L-stimulated cells, whereas the red curve shows the changes upon anti-IgM antibody stimulation. Group #1 illustrates genes highly up regulated through BCR crosslink, but not changed at all through CD40 stimulation. Additionally, group #2 depicts genes, which showed the same course of expression changes over time, regardless which stimulus the cells experienced. Finally 10 more groups of genes could be computed showing the same directionality of gene regulation through the different stimuli, but differentiating in intensity or course after a certain time has passed. For a complete list of genes please refer to Table A-3.

All of the computed gene sets display distinct expression changes over time, allowing discrimination between immediate-early activated gene sets, late events or immediately up regulated and later in time course down regulated gene sets.

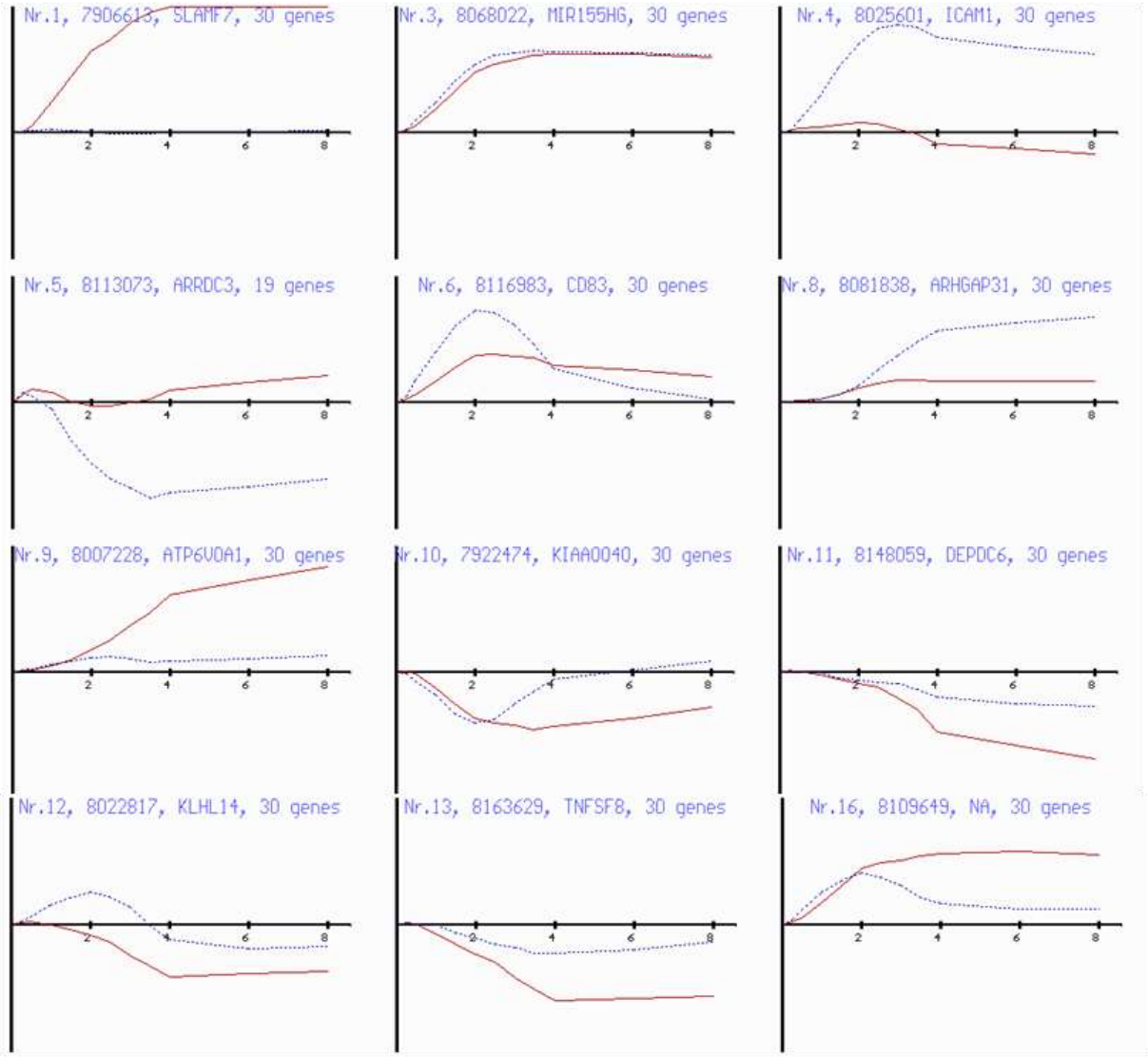

Figure 3-4 Comparison of time courses of genes commonly regulated through BCR and CD40. 12 significant, distinct groups of genes were computed, when taking commonly regulated genes by CD40L and BCR crosslink into calculation. red curve – time course of gene expression changed through anti-IgM stimulation, blue curve – time course of gene expressions stimulated through sCD40L. The y-axis displays changes in gene expression levels (not scaled), x-axis shows the hours of specific treatment.

Testing for stationarity in differential gene expression changes from CD40L stimulated BL cells computed 5 disjoint and distinct gene sets (Figure 3-5 A). GO analysis was used to characterize the sets of genes. A complete overview of the GO results for each cluster of genes is provided as external data stored on a CD ROM (\\time course analyses\Stationarity\GoKeggLister). Gene set #2 was the only group of genes, which comprised solely repressed genes. Interestingly, the majority of the gene products display tyrosine kinase or transferase activity. Taken together with the observations from

gene set #4, including mainly negative regulators of signaling as phosphatases, one can postulate that CD40 mediated signaling happens very rapidly on the proteome level, leading to a fast feedback loop mediated by gene expression changes. The second group of up regulated genes upon CD40L stimulation displayed a late onset of increased expression (> 2 hours) and may represent a second wave of target genes. In this group, GO analyses did not reveal enrichment in molecular function of different gene products, but the list contains target genes of NF-κB signaling (*WNT5a, CFLAR*) (Katoh and Katoh, 2009) and cytokines as *TNFSF4* (*OX-40L*), providing co-stimulatory signals to T-cells (Akiba et al., 1999; Brocker et al., 1999). Thus, activation of target genes affecting proliferation, differentiation and paracrine signaling occurs 2 hours after CD40L activation.

To afford the massive necessity of transcriptional regulators, a second intermediate step is imperative. Group #8 displayed a strong increase in gene expression for the first 90 min after stimulation paired with a rapid inhibition back to basal level after 180 min after stimulation. This gene group comprised mainly DNA-binding and transcription factor activity (Table A-4 and external data on CD ROM \\time course analyses\Stationarity\GoKeggLister\CD40.3_cluster_8). In contrast, gene group #5, showing a similar bi-phasic course with the highest expression change upon 2 to 2.5 hours after CD40L stimulation and following decline in expression levels up to basal levels upon 6 hours after stimulation, illustrated several processes as positive regulation of protein kinase activity, response to stress (unfolded proteins etc.) and expression of signaling molecules as CD40 itself (Table A-4 and external data on CD ROM \\time course analyses\Stationarity\GoKeggLister \CD40.3_cluster_5).

Enhanced gene expression as a response to α-IgM was found in 8 gene sets. Those groups of genes can be additionally subdivided in groups, which display an 'immediately-up' course (#1, #2, #5) or 'late-up' gene expression (#3, #9, #11, #13, #19). Additionally genes responding with reduced expression to α-IgM treatment (#4, #6, #12, #17) could be computed (Table A-5). Genes in group #1 were commonly activated upon α-IgM stimulation and reached their highest expression level after 4 hours of stimulation (Figure 3-5 B, #1). *SLAMF7* (also known as *CS1, CRACC, CD319*), the center gene of the set, was strongly up regulated upon BCR crosslink, but did not respond to CD40L stimulation (compare Figure 3-4). *SLAMF7* is a lymphocyte cell surface receptor, which has been shown to be strongly up regulated in response to BCR crosslink in Ramos cells and to induce proliferation and autocrine signaling of cytokines in human B lymphocytes (Lee et al., 2007). Genes in this group could not be integrated in a specific function or process, but represent the diversity of B cell receptor signaling, immune response activating signaling and protein tyrosine kinase activity.

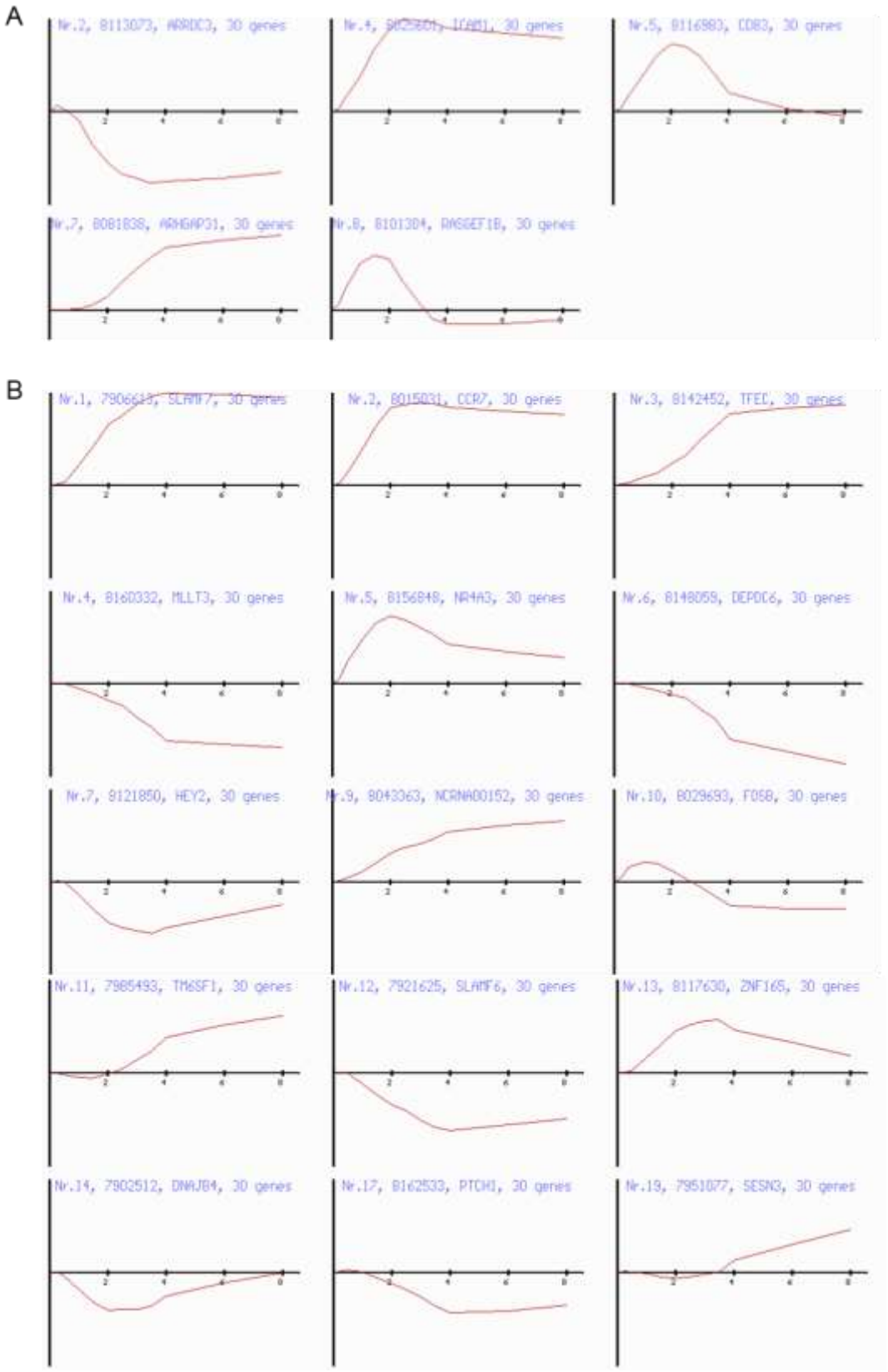

Figure 3-5 Distinct time courses for anti-IgM and CD40 stimulated BL2 cells can be determined by testing for stationarity. Testing for stationarity by reducing the number of genes in each group to 30 genes leads to (**A)** 5 unique and disjoint groups of genes upon sCD40L stimulation, (**B**) 15 significant unique time courses upon α-IgM stimulation of BL2 cells. The y-axis displays changes in gene expression levels (not scaled), x-axis shows the hours of specific treatment.

The set of genes #2 displayed a sharper increase in gene expression, reaching approx. 90% of highest expression level upon 2 hours of α-IgM treatment (Figure 3-5 B, #2). Center gene of the set is *CCR7*, a pivotal player in homing tumor cells into lymphoma-supporting niches in secondary lymphoid organs (Rehm et al., 2011) and known to be highly up regulated upon BCR stimulation (Calpe et al., 2011). Additionally this group comprised lots of genes actively sustaining immune response and playing part in MAPK signaling and G-protein-coupled signaling (\\time course analyses\Stationarity\ GoKeggLister\BCR.3_cluster_2). Set #5 displayed a bi-phasic course of gene expression changes. Gene expression was immediately up regulated upon α-IgM stimulation, whereas after 2 hours expression of those genes was reduced again. This particular set of genes mainly comprised regulators of gene transcription like DNA-binding factors (*PRDM2, MFSD2A, JUND, PIM3, E2F3*) and genes affecting transcription factor activity (one example: *NR4A3*, the center gene of the set involved in steroid hormone receptor activity and positively regulating DNA-binding transcription factor activity). This time course perfectly fits with the estimation that upon stimulation of the cell, the signal is transduced in the nucleus and gene expression is affected in a very pronounced manner, leading to feedback signals negatively regulating transcriptional activity.

A similarly interesting gene set #10, displaying a bi-phasic time course with a slight induction of gene expression in the first hour and subsequent transcriptional repression, harbored the center gene *FOSB*. *FOSB*, belonging to the *FOS* gene family, encodes a leucine zipper protein, dimerizing with proteins of the *JUN* family, thereby forming the AP-1 transcription factor complex and regulating cell proliferation, differentiation and transformation (Entrez Gene: *FOSB* FBJ murine osteosarcoma viral oncogene homolog B). The proto-oncogene *JUNB*, dimerizing partner for FosB, was as well regulated in gene set #10 and displayed the same time course in gene expression. Additionally, this group harbored proto-oncogenes like *PIM-1* and *PIM-2*, both exerting their oncogenic activity through the regulation of *MYC* transcriptional activity (van der Lugt et al., 1995; Shirogane et al., 1999).

Supporting this issue, the expression of *MNT*, a MAX-binding protein, seems to be co-regulated since it displayed the same time course. The protein encoded by this gene has a basic-Helix-Loop-Helix-zipper domain, whereby it binds the E-box, following heterodimerization with Max proteins, thereby repressing transcription of *MYC* target genes (Hurlin et al., 1997a, 1997b; Sommer et al., 1998). Upon BCR stimulation, this repression is likely to be abolished, since *MNT* expression levels were decreasing (Figure 3-5 B, #10). The gene groups #3, #9 and #13 comprise genes whose expression was up regulated after α-IgM stimulation later in time. In general, the increase in gene expression took a longer period of time than in the groups mentioned above. Gene set #9 displayed a continuous gain of gene expression, reaching a saturation level after 4 hours of stimulation with α-IgM antibody. Genes encountered in this group could not be assigned to one single specified

biological process, but their products were mainly membrane- and organelle-bound proteins. One example is *LRMP* (lymphoid-restricted membrane protein, Jaw1), an endoplasmic reticulum-associated protein, which was originally identified as differentially regulated transcript in B and T cells (Behrens et al., 1994). Subsequently, *LRMP* was reported as marker for diffuse large B cell lymphoma of the GCB subtype (Tedoldi et al., 2006).

In gene set #3, gene expression was constitutively increasing for 2 hours after BCR crosslink reaching a point of inflection after 4 hours of stimulation. Genes comprised in this particular gene set comprised mainly regulating kinase or transferase activity (\\time course analyses\Stationarity\GoKeggLister\BCR.3_cluster_3), thus maybe inducing a "second wave of activity". Such kinases might act as feedback loop for the immediate-early response genes. The expression of genes in group #13 increased slowly upon BCR crosslink, reaching the maximum after 4 hours of stimulation before being reduced again in direction to basal level of expression. The high diversity of genes comprised in this group impeded the assignment of one specific function to this cluster. Among them, we found genes whose products represent several functions such as Rho protein signal transduction (*ARAP2*), DNA binding components (*ZNF165, PHF13, ZNF643*), helpers in protein unfolding (*TOR3A*) and others (\\time course analyses\Stationarity\GoKeggLister \BCR.3_cluster_13). Finally, group #11 and #19 show the genes, whose expression was increased at very late stages in the observation period. In group #11, genes preparing the cellular machinery for translational processes were enriched (*AGA, TARS, WARS, UGDH*), whereas in group #19 the negative regulation of the cellular response to growth stimuli was activated (*NEK7, CLCC1*). Thereby, negative feedback loops of early-activated genes are potentially activated.

Additionally, 6 groups of genes showed a decrease in gene expression upon anti-IgM stimulation. The groups #4 and #6 showed a similar course where expression continuously diminished as time went on. In contrast, in groups #7, #12, #14 and #17, a bi-phasic expression course could be observed. In the first phase, gene expression decreased to be returned after a certain period of time to the initial expression level. Since the basal expression level was not reached during the period of observation and the gain in expression took place very slowly, one might postulate that this time course depicts the time-resolved turnover of mRNA abundance in the cell: after initial regulation (here repression), the inhibitory effect is released and slowly mRNA expression is increased again, leading back to the point of departure.

In gene set #7, center gene of the set was HEY2, which encodes a bHLH transcription factor. The encoded protein acts as a transcriptional repressor and binds preferentially to the canoncical E box sequence 5'-CACGTG-3' (Heisig et al., 2012; Wu et al., 2011). Interestingly, the expression of this gene was down regulated following anti-IgM stimulation, thus promoting a preexisting release of

transcriptional repression. GO analysis also showed enrichment for transcriptional regulation and negative regulation of cell growth (\\time course analyses\Stationarity\GoKeggLister \BCR.3_cluster_7) in gene set #7. A similar enrichment could be found in gene sets #12, #14 and #17. Thus, negative regulators of gene transcription were down regulated through BCR crosslink, promoting active gene transcription. Interestingly, gene set #17 harbored the genes *PTCH1, LEF1* and *NOTCH1*. All three genes are known to be evolutionary important for developmental processes as hematopoiesis. Notch1, the transmembrane receptor for the Notch signaling network, plays a pivotal role in lymphocyte development, proliferation and differentiation (Anderson and Longnecker, 2009; Cheng et al., 2001; Pui et al., 1999; Radtke et al., 2004). Lef1, a transcription factor participating in the Wnt signaling pathway, regulates B lymphocyte proliferation (Reya et al., 2000) and is aberrantly expressed in BLs (Hummel et al., 2006; Walther et al., 2013). Ptch1 is a transmembrane receptor for hedgehog signaling and plays an important role in lymphoid lineage commitment (Uhmann et al., 2007) and the germinal center reaction of B cells (Sacedón et al., 2005). Furthermore, recent publications show deregulations of the Hh signaling pathway in several lymphoma subtypes, including DLBCLs (Decker et al., 2012; Lin et al., 2010; Siggins et al., 2009; Singh et al., 2009, 2010). The α-IgM stimulation of BL cells led to reduction of expression of *NOTCH1*, *LEF1* and *PTCH1*, suggesting an active signaling in BL. Similarly, gene expression of *c-MYC*, the hallmark of BL was down regulated after BCR crosslink (gene set #14).

Taken together with the observation, that α-IgM stimulation of BL cells reduced the mBL index towards a more DLBCL-like index (compare chapter 3.1.1), the question arose whether the down regulation of those signaling pathways may give an explanation for essential differences between BL and DLBCLs. For a better understanding of the joint α-IgM mediated suppression of *PTCH1*, *LEF1*, *NOTCH1* and as well of *MYC*, I focused in this study on the role of *PTCH1* in aNHL. Recent publications suggest an important, but yet not clearly understood role for Hedgehog signaling in lymphoma genesis and progression (Decker et al., 2012; Singh et al., 2009, 2010). The role of *LEF1* and *MYC* in the diversion of BL and DLBCL is part of other projects in our group.

3.2 Ptch1 and Hedgehog signaling in lymphoma

Using qRT-PCR it was verified that the statistically modeled data are correct and that *MYC* as well as *PTCH1* and *LEF1* expression is down regulated after BCR crosslink. Therefore, RNA used for array hybridization (batches I-III, Figure 3-6) as well as independently collected data (data not shown) showed a marked down regulation of *PTCH1*, *LEF1* and *MYC* upon BCR activation. Although not postulated through the course of gene set #17, *PTCH1* expression showed a two-fold up regulation in the first hours after stimulation. This discrepancy between computed time course and time course collected through qRT-PCR may be due to the calculation of the mean time course of all genes in gene set #17. Additionally, the 3 batches of stimulated BL cells used for array hybridization differed strongly in their response to BCR activation regarding *PTCH1* mRNA expression especially in the first two hours of data collection. For statistical modeling an adaptive 3-point smoothing was applied, thus probably removing those differences in favor of the not-elevated mRNA expression data. However, an overall agreement of the computed to the experimental data could have been shown. *PTCH1*, *MYC* and *LEF1* mRNA expression was reduced in BL2 cells after 3 hours after α-IgM antibody treatment. This reduction lasted until 5 – 6 hours after stimulation and was then abolished (Figure 3-6).

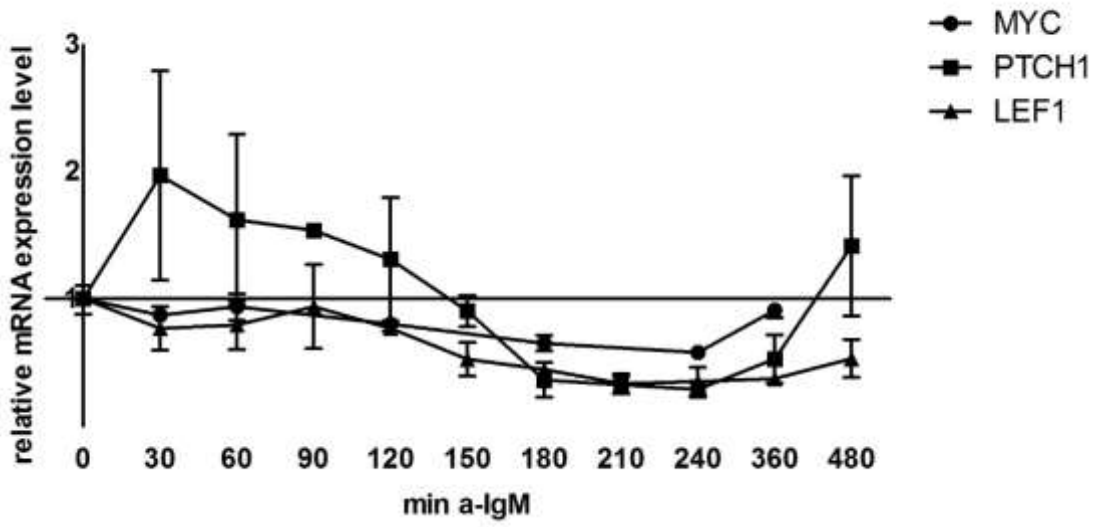

Figure 3-6 *MYC*, *PTCH1* and *LEF1* mRNA expression is suppressed in BL2 cells upon anti-IgM stimulation. Relative mRNA expression levels of *c-MYC*, *PTCH1* and *LEF1* as a function of time upon stimulation with α-IgM $F(ab)_2$ fragment. Data are represented as mean (±SEM) of three biological replicates (batches I-III, which were subjected to microarray analyses). $2^{-\Delta\Delta Ct}$ values were calculated using *ABL* as housekeeping gene.

3.2.1 Expression profile of Hedgehog signaling components

Recent findings suggest that hedgehog signals exerted from the microenvironment are important in hematologic malignancies, including lymphomas (Dierks et al., 2007; Hegde et al., 2008). All Hh ligands (Sonic hedgehog (Shh), Indian hedgehog (Ihh) and Desert hedgehog (Dhh)) share a common signaling pathway, where Patched (Ptch1) and Smoothened (Smo) are the membrane bound receptors. In the absence of ligand, Ptch1 exerts an inhibitory effect on Smoothened activity that is abrogated upon Hh ligand binding. Subsequent activation of the Gli transcription factors, Gli1, Gli2 and Gli3, leads to expression of *PTCH1* and *GLI1* amongst others. Recently, Singh et al. (2010) have shown that several DLBCL cell lines express *PTCH1*, *GLI1* and *SMO* and that inhibition of Hh signaling *via* inhibition of Smo through cyclopamine resulted in cell-cycle arrest and apoptosis in some of the tested DLBCL cell lines (Singh et al., 2010). To investigate whether Hh signaling components are expressed in a similar manner in Burkitt's and diffuse large B cell lymphoma cell lines, the mRNA expression profile of *PTCH1*, *GLI1*, *SMO*, *SHH* and *IHH* was comprehensively analyzed using qRT-PCR. Additionally, the reduction in mRNA expression levels of *PTCH1* upon 3 hours α-IgM $F(ab)_2$ fragment in BL2 cells was counterchecked in several cell lines of Burkitt's and diffuse large B cell lymphoma (Figure 3-7). mRNA expression levels are depicted as fold changes relative to the unstimulated cell line with the lowest expression level of the respective mRNA (marked with an asterisk in Figure 3-7).

As shown in Figure 3-7 A, the observed reduction of *PTCH1* mRNA upon α-IgM treatment for 3 hours in BL2 cells was not reproducible in other Burkitt's lymphoma cell lines tested, except BL30. All Burkitt's lymphoma cell lines tested did express *PTCH1* mRNA (Ct-values around 25 cycles, housekeeper *ABL* 21 cycles), but most of them showed slightly elevated *PTCH1* mRNA expression levels upon BCR crosslink. Diffuse large B cell lymphoma cell lines showed approximately the same overall expression levels as BL cell lines, however, the response to α-IgM treatment for 3 hours in terms of *PTCH1* mRNA expression levels differed. SuDHL5, SuDHL6 and OCI-Ly3 showed a slight to moderate decrease in *PTCH1* mRNA expression upon BCR activation, whereas the other DLBCL cell lines tested did not change or slightly increased their *PTCH1* mRNA expression levels (Figure 3-7E). *PTCH1* gene expression is amongst others activated through the successful activation of the Hh signaling pathway as a target gene of Gli1 transcription factor (Marigo and Tabin, 1996). The transcription factor *GLI1* itself is also a well-known target gene of Hh signaling (Lee et al., 1997). Therefore, the mRNA expression levels of *hGLI1* were investigated in BL and DLBCL cell lines before and 3 hours after BCR crosslink.

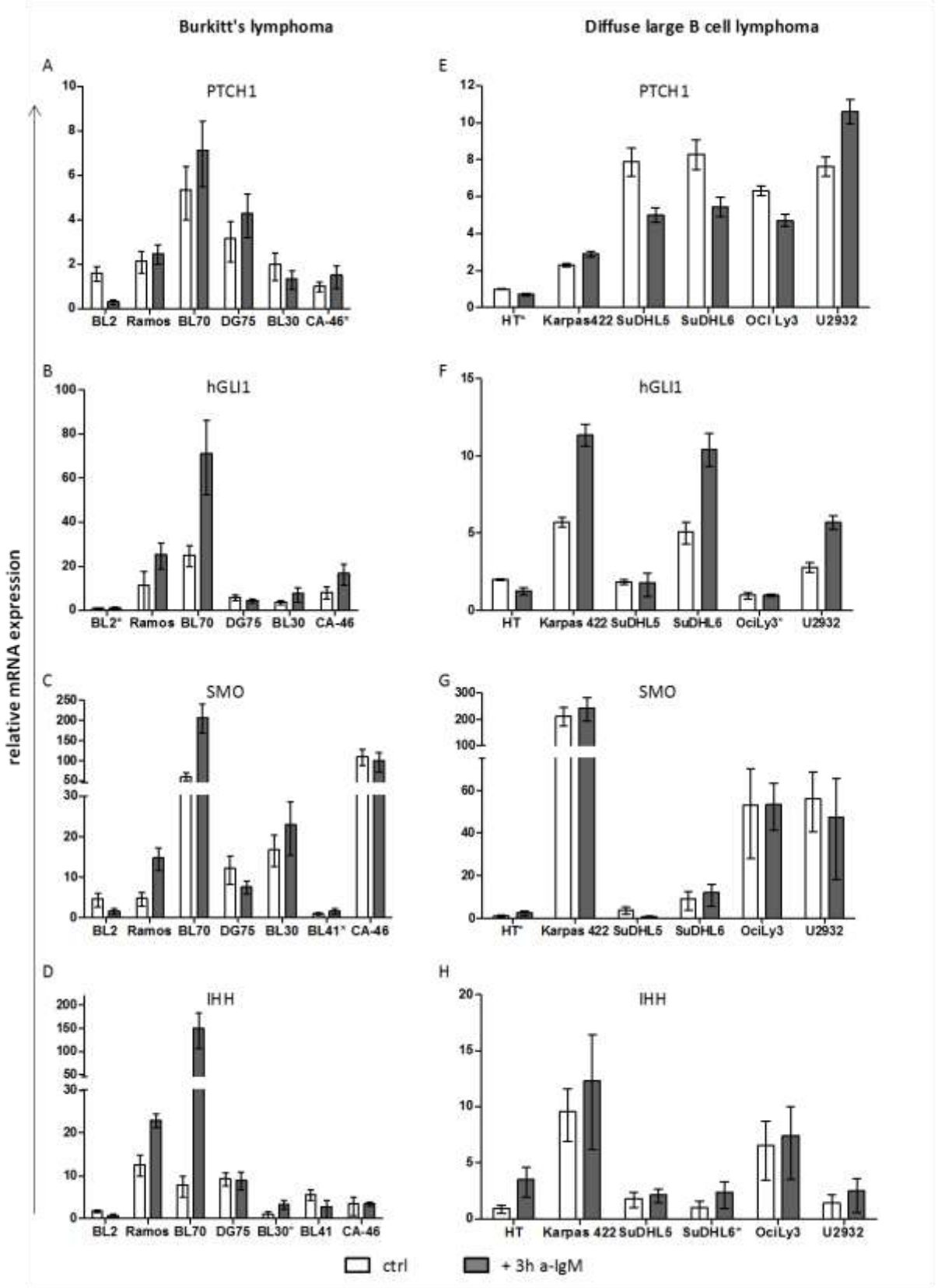

Figure 3-7 Differential expression and induction of Hh signaling components in Burkitt's and diffuse large B cell lymphoma cell lines through anti-IgM stimulation. Several Burkitt's lymphoma **(A-D)** and diffuse large B cell lymphoma **(E-H)** cell lines were tested for expression of hedgehog signaling pathway components by qRT-PCR. Additionally, cell lines were stimulated 3 hours with anti-IgM F(ab)$_2$ fragment and gene expression was compared to unstimulated control. Results are represented as $2^{-\Delta\Delta Ct}$-value relative to *ABL* housekeeper

expression and normalized to the cell line with the lowest expression (marked with an *). One representative experiment out of 3 biological replicates is shown. Expression of *SHH* mRNA could not be detected in any of the tested cell lines.

Overall mRNA expression levels were pretty low in most BL cell lines (Ct-values around 30 cycles, housekeeper Ct = 21) and differed largely between the cell lines (25-fold more basal *hGLI1* mRNA expression in BL70 than in BL2, Figure 3-7B). One could observe an increase of mRNA expression after BCR crosslink in nearly all BL cell lines (except DG-75), which is not correlated to the response to BCR in terms of *PTCH1* expression. Both genes are meant to be target genes of activated Hh signaling, but in BL2 cells *PTCH1* expression was reduced upon anti-IgM stimulation whereas *hGLI1* expression increased. In half of the BL cell lines tested (Ramos, BL70 and CA-46), one could observe a concomitant increase in mRNA expression, which would suggest an activation of Hh signaling pathway through BCR activation. In contrast, in 3 out of 6 BL cell lines (BL2, DG75, BL30) the regulation of these two target genes *PTCH1* and *hGLI1* was opposed (Figure 3-7 B). Similar observations have been made for the target gene expression of activated Hh signaling in DLBCL cell lines. The basal expression of *hGLI1* mRNA was in all DLBCL cell lines tested pretty low (Ct-values around 30 cycles), with differences of 5-fold higher expression in Karpass422 and SuDHL6 than in the DLBCL cell line with the lowest expression, OCI Ly3 (Figure 3-7 F). Here, the cell lines with the highest basal expression level (3/6) also showed an increase in *hGLI1* mRNA expression after 3 hours α-IgM stimulation, whereas the others did not respond in terms of *GLI1* mRNA expression level changes (OCI Ly3 and SuDHL5) or did show reduced levels (HT). Overall, one could not observe a consistent regulation of Hh signaling target genes upon BCR activation in the tested cell lines.

Furthermore, the intracellular signal transducer *SMO* was expressed in strongly diverse levels when comparing different BL cell lines (Figure 3-7 C). In some BL cell lines, expression of *SMO* was barely detectable (BL41, Ramos, Ct-values around 33 – 35 cycles), whereas in other BL cell lines a 60- to 100-fold higher basal expression level was observed (BL70, CA-46). The response to BCR induced signaling in terms of *SMO* regulation, regarding the different BL cell lines was comparatively differential. 2/7 cell lines (BL2 & DG75) showed an reduced expression level upon 3 hours α-IgM stimulation, 2/7 BL cell lines (BL41 & CA-46) did not show a regulation of *SMO* and the remaining 3 cell lines (Ramos, BL70 and BL30) increased the *SMO* expression levels upon BCR crosslink. In contrast, DLBCL cell lines, which also showed strong differences in basal *SMO* mRNA expression, showed no response to BCR induced signaling in terms of *SMO* expression (Figure 3-7 G).

When investigating the expression profile of Hh ligands, I focused on the expression of *SHH* and *IHH*, because of their implication in lymphocyte biology (Dierks et al., 2007; Lindemann, 2008; Sacedón et al., 2005; Siggins et al., 2009). Interestingly, no *SHH* mRNA expression was detectable at

all *via* use of SYBR based qRT-PCR and the expression levels of *IHH* were very low in BL and DLBCL cell lines tested. Investigating the expression changes of *IHH* mRNA after 3 hours α-IgM stimulation, differences ranging from more than 15-fold increase in *IHH* mRNA (BL70) to no change (DG75, CA-46) or reduction in *IHH* mRNA expression (BL2) were observable in BL cell lines (Figure 3-7 D). Overall, Burkitt's and diffuse large B cell lymphoma cell lines demonstrated very inconsistent basal levels as well as a very heterogeneous response to α-IgM stimulation regarding the expression profile of Hh signaling components. A clear activation or inactivation of the Hh signaling pathway through BCR induced signaling was not detectable.

Although literature concerning the expression and secretion of Hh ligands in hematologic malignancies is somewhat controversy, Dierks et al. showed that hedgehog ligands produced by stromal cells support proliferation and survival of B cell lymphomas (Dierks et al., 2007). Additionally, Singh et al. reported that DLBCL cell lines (OCI Ly3) expresses and secretes Hh ligands (Singh et al., 2010). Therefore, we decided to test BL and DLBCL cell lines for responsiveness to Shh and activatability of the Hh signaling pathway.

3.2.2 Lymphoma cell lines neither secrete nor respond to Sonic hedgehog

The murine B cell hybridoma cell line B9 (kind gift of Prof. Dr. H. Hahn), being highly responsive to Shh as Hh ligand, was used to investigate the capability of several lymphoma cell lines to produce Shh. A HEK293 cell line constitutively secreting Shh (HEK293SHH, a kind gift of Prof. Dr. H. Hahn) was used to produce conditioned media, enriched with soluble Shh. Subsequently, after having cultivated the murine B9 cells with conditioned media for 24 hours, the mRNA expression levels of *mGLI1* were measured using qRT-PCR as a mean of activated Hh signaling. As shown in Figure 3-8 A, expression of *mGLI1* markedly increased upon cultivation of B9 cells with Shh-containing conditioned media obtained from HEK293SHH. Simultaneously, conditioned media from BL2, Ramos and OCI Ly3 cells were tested for a comparable potency in activating Hh signaling in murine B9 cells, which would suggest a Shh secretion of the lymphoma cells. As clearly depicted in Figure 3-8 A, none of the tested B cell lymphoma cell lines was capable of activating *mGLI1* expression in B9 cells, thus indicating no Shh secretion into the medium.

To investigate the hypothesis that B cell lymphoma cells are sensitive to stroma-initiated Hh signaling, B cell lymphoma cell lines were incubated with Shh-containing media for 24 hours and the expression level of *hGLI1* was monitored as target gene of activated Hh signaling. As depicted in Figure 3-8 B, none of the tested cell lines changed the *hGLI1* expression levels upon Shh stimulation. Therefore, one can conclude that those B cell lymphoma cell lines are not sensitive to secreted Shh as potent activator of Hh signaling.

Several inhibitors of Hh signaling have been identified and are an extensive field of research for pharmaceutical companies and universities. The majority of the Hh pathway inhibitors reported today target Smoothened (Mar et al., 2011). One of the first inhibitors discovered is the Smo antagonist cyclopamine, which abrogates Hh signal transduction and therefore inhibits target gene expression (Incardona et al., 1998). To investigate the ability of cyclopamine to change gene expression levels of *PTCH1* and *hGLI1* upon stimulation with α-IgM antibody, Burkitt's lymphoma cell lines were treated for one hour with cyclopamine and subsequently stimulated for 3 hours with α-IgM antibody. *PTCH1* and *hGLI1* mRNA expression levels were subsequently analyzed by qRT-PCR (Figure 3-8 C & D).

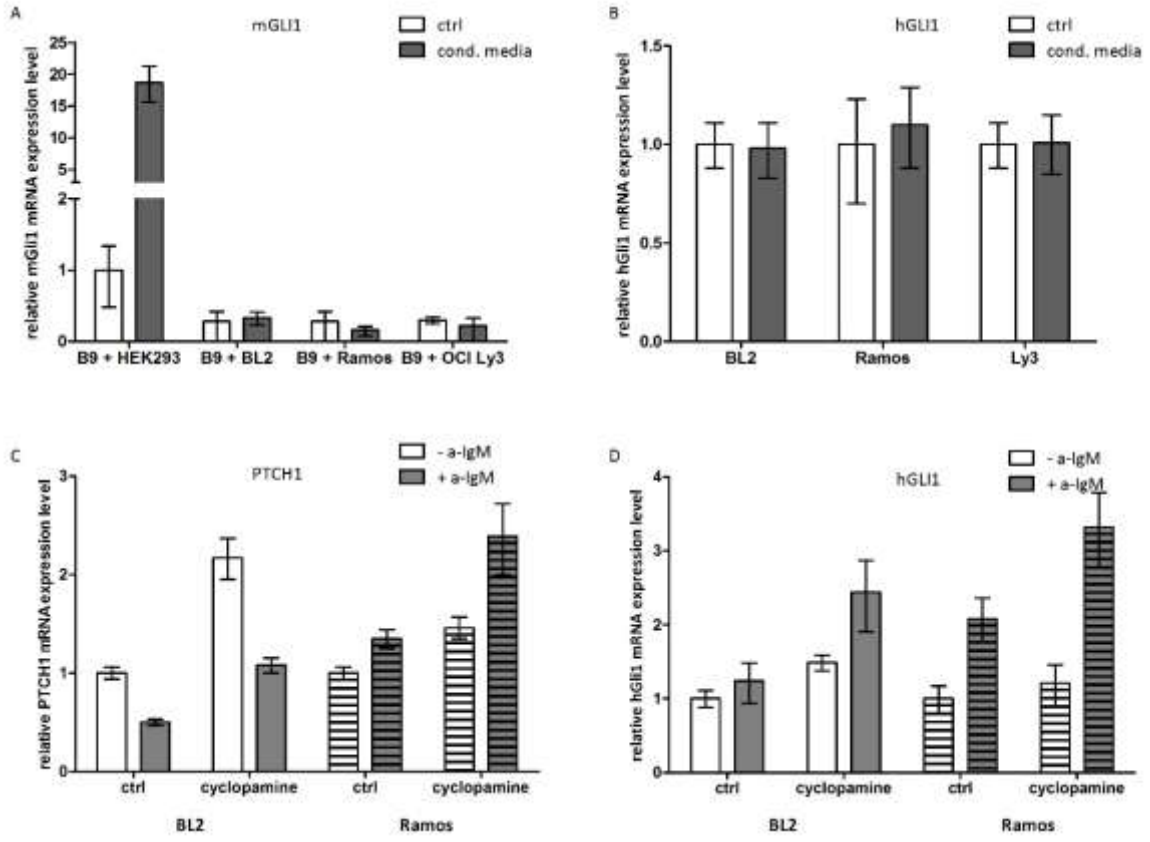

Figure 3-8 Lymphoma cell lines do not produce Shh, neither do they respond to Shh nor to cyclopamine. A Secretion of Shh through lymphoma cell lines was tested using the model cell line B9, being highly responsive to Shh. Murine B9 cells were 24 hours incubated with conditioned supernatant of Shh-secreting HEK293 cells as positive reference for *mGLI1* expression. Conditioned media of Burkitt's and diffuse large B cell lymphoma cell lines was also tested to induce *mGLI1* expression by qRT analysis. **B** Lymphoma cell lines are not responsive to secreted Shh in regard to Hh signaling pathway activation. BL2, Ramos and OCI Ly3 cells were incubated with conditioned media of Shh-producing HEK293 cells and their expression of *hGLI1* was determined by qRT analysis. **C + D** Neither BL2 nor Ramos cells are responsive to Cyclopamine. Cells were treated with 5 µM cyclopamine for 1 hour, and additionally stimulated with α-IgM $F(ab)_2$ fragment for 3 hours. Relative mRNA expression of *PTCH1* (**C**) and *hGLI1* (**D**) was measured using quantitative real-time PCR. Data were analysed for all samples using the ΔΔCt-method. Shown are representative results of at least two experiments, relative to *ABL* housekeeper expression.

As shown in Figure 3-8 C, the response of BL2 and Ramos cells to cyclopamine treatment differed with regard to *PTCH1* expression. In BL2 cells, basal *PTCH1* mRNA expression levels were elevated upon cyclopamine treatment (2-fold increase), but the BCR induced repression of *PTCH1* mRNA expression was not affected through cyclopamine treatment. In Ramos cells contrasting results were obtained. The BCR signal led to slight induction of *PTCH1* mRNA expression, but the cyclopamine treatment did not change the basal *PTCH1* expression. Instead an increase of *PTCH1* mRNA expression upon cyclopamine treatment and subsequent BCR crosslink was observable. This observation emphasizes once again the heterogeneity of Hh signaling responsiveness between different cell lines of one lymphoma subtype and leads to the overall conclusion that active canonical Hh signaling may not play an important role in Burkitt's lymphoma.

3.2.3 PI3K-mediated regulation of PTCH1, c-MYC and LEF1 mRNA expression

Initially, the observation that the α-IgM stimulation in BL2 cells led to a down regulation of *PTCH1* mRNA expression, raised the hypothesis that Burkitt's lymphoma harbor active Hh signaling. The transition of the mBL index from mBL towards DLBCL through BCR crosslink would then suggest an inactivation of Hh signaling in DLBCL. However, several publications have reported quite the opposite: active Hh signaling promoting lymphoma growth and progression, especially in DLBCLs (reviewed in Ok et al., 2012). Indeed, the results presented in the current study, showing enhanced *GLI1* expression upon BCR activation would favor the hypothesis of active Hh signaling in the transition to DLBCL instead of an inactivation. Nevertheless, the observation of reduced *PTCH*1 mRNA levels was accompanied by similarly reduced levels in *LEF1* and *c-MYC* mRNA expression. We therefore asked whether the regulation of these three genes may be directly targeted by BCR crosslink. Indeed, several very recent reports, being published in the course of the present study, supported our idea. Schmitz and coworkers reported about tonic BCR signaling and PI3K activity in Burkitt's Lymphoma (Schmitz et al., 2009) and Sander and colleagues established a new murine model supporting the view of synergistic action between c-Myc and PI3K signaling (Sander et al., 2012).

As shown in Figure 3-9 A, *PTCH1* mRNA expression was reduced upon α-IgM stimulation, whereas inhibition of the BCR signal transduction through the PI3K-inhibitors Ly294002, Compound15e (C15e) and BKM120 did not change *PTCH1* mRNA levels in comparison to unstimulated cells. Additionally, the PLCγ-inhibitor U73122 as well as the PKC-inhibitor Bisindolylmaleimide I abrogated the BCR induced decrease in *PTCH1* mRNA expression. Similar observations were made for the regulation of *c-MYC*, although here, an inhibition of the PKC seems to affect the basal *c-MYC* mRNA expression level positively (2.5-fold up regulation of *c-MYC* upon Bisindolymaleimide inhibitor use) (Figure 3-9 B). In former experiments, cells were treated 3 hours with inhibitor before subsequent stimulation.

This led to elevated *PTCH1* and *c-MYC* mRNA levels upon PI3K-inhibitor use (Ly294002, C15e and BKM120, respectively) in unstimulated BL2 cells (Schrader et al., 2012 and unpublished own data). To reduce these effects, the inhibitor treatment was reduced to 30 min prior to 3 hours stimulation together with respective inhibitor treatment.

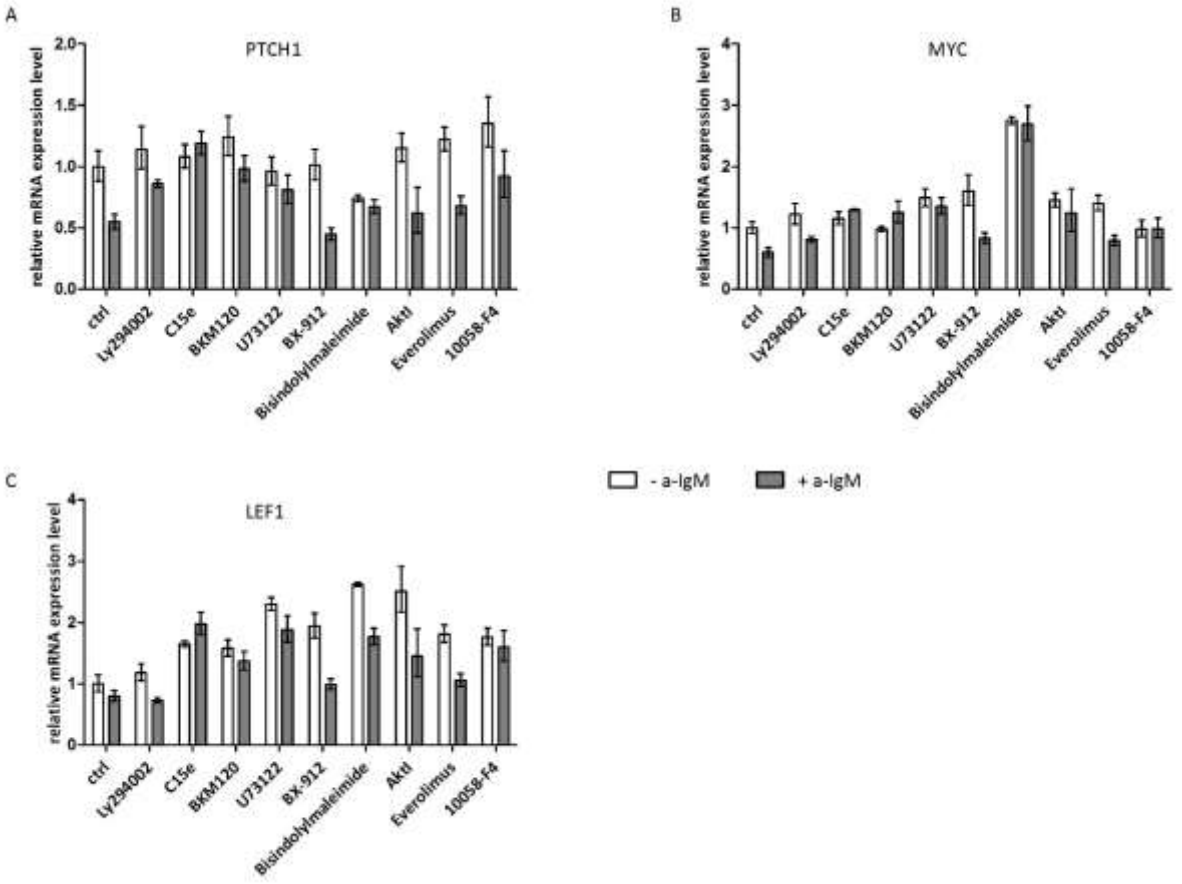

Figure 3-9 Regulation of *PTCH1*, *MYC* and *LEF1* is mediated through PI3K-PLCγ-PKC signaling. BL2 cells were subjected to 30 min treatment with inhibitors and subsequently 3 hours of stimulation with α-IgM $F(ab)_2$ fragment. mRNA expression levels of *PTCH1* (**A**), *c-MYC* (**B**) and *LEF1* (**C**) were determined using the ΔΔCt-method, relative to *ABL* housekeeping mRNA expression levels. Data are represented as mean of three biological replicates (± SEM), except for 10058-F4, which was used only twice.

Additionally, the reduction in *MYC* mRNA levels after BCR activation is abolished upon Akt inhibition. Thus the *c-MYC* regulation might be situated downstream of Akt-signaling, whereas *PTCH1*-regulation seems to be Akt-independent. Interestingly, none of both is regulated through the mTOR-pathway, interrupted by Everolimus. The inhibitor of Myc-Max dimerization 10058-F4 was used to investigate the effect of *c-MYC* regulation onto *PTCH1* and *LEF1* gene expression. α-IgM mediated *MYC* suppression is reversed by the Myc-inhibitor 10058-F4, whereas *PTCH1* repression seems to be only slightly affected. For *LEF* mRNA expression it is difficult to state a clear regulatory pathway, since all experiments did not show a strong α-IgM-mediated suppression of the *LEF1* gene (Figure 3-9 C). Additionally, basal *LEF1* expression levels were upregulated upon most inhibitors used

here. Nevertheless, an effect of the PI3K inhibitors Compound15e and BKM120 as well as the Myc-inhibitor 10058-F4 can be postulated, suggesting a positive regulation of the *LEF1* mRNA expression by PI3-kinase and c-Myc.

Overall, one can conclude that the BCR induced down regulation of all three genes is mediated *via* the PI3K-PLCγ-PKC signaling pathway. Although slight differences in the responsiveness to the different inhibitors are observable, the results presented here point towards a joint regulation of *PTCH1*, *MYC* and *LEF1* mRNA expression after BCR activation.

3.3 Analyzing intersections in signaling pathways *via* use of specific chemical inhibitors

Microenvironmental factors are a dominant source of influence for most B cell lymphomas. It is important to know and to understand signaling modules and their effectors, which are involved in the tumor-micromilieu interactions. It is likely, that several immune response associated signals, such as CD40 and BCR induced signaling events, are specific mediators in B cell transformation. Thus, our group was able to mimic oncogenic pathway activities in aNHL by investigating the major patterns of gene expression changes in response to different stimuli *in vitro* and to subsequently identify individual aNHL profiles reflecting those patterns (Schrader et al., 2012b).

We therefore asked whether we could get access to comprehensive insights into potential targets for future individually designed therapy, based on gene expression profiles of aggressive non-Hodgkin lymphoma. Thus, in this study a combination of *in vitro* stimulation with kinase inhibitors was used to delineate respective pathway interactions.

CD40 and α-IgM activated signaling involves both similar and diverging pathways. However, even similar pathways are activated in quantitative different manners (compare Figure 3-1). To investigate the branching points in this complex signaling network, several kinases regulating different parts of specific signaling pathways were targeted to interrupt CD40 and α-IgM mediated signaling and to determine subsequent changes in the gene expression profile.

As a first attempt, we meant to silence several transcription factors being crucial for signaling transduction on the gene expression level. We thought of targeting Bcl-6, c-Myc, Stat3 and p65 by RNAi mediated silencing. Unfortunately, previous work in our group showed strong difficulties to obtain differential gene expression profiles upon siRNA-mediated knock down of specific key players in diverging signaling pathways (unpublished data from K. Matulewicz). Even though an effective knock down was achievable in our model system, the Burkitt's lymphoma cell line BL2, we did not succeed to obtain comprehensive lists of specifically regulated genes. Although we could observe functional abrogation manifested in reduced proliferation or elevated apoptosis rates, current mathematical models did not succeed to exhibit differentially expressed genes. Controversially, we could even detect signaling pathway interruption on the protein level, but still the induced changes in gene expression were not strong enough to obtain lists of significant differentially expressed genes. Due to these complications, we decided to use chemical inhibitors instead of siRNA-mediated knock down. The major benefit of small molecule inhibitors is the active inhibition of enzymatic function, without inducing secondary effect by influencing the translational machinery. Another benefit of chemical (especially small molecule) inhibitors is the fast mode of action. When using

RNAi, we had to transfect cells twice or even three-times and waited for at least 24 hours to observe effects. With the use of inhibitors, changes in signal transduction were rapidly detectable. When using inhibitors of specific kinases, we were able to detect changes in following protein phosphorylation as early as 5 minutes after treatment (data not shown). Additionally we used the advantage of targeting kinases instead of transcription factors to intervene on different levels of the signaling tree. Thereby, we aimed to dissect jointly regulated and branching points of the signaling network induced through CD40L or α-IgM stimulation.

3.3.1 Inhibitors in use

To target kinases involved in both CD40 and BCR mediated signaling modules as well as kinases being specifically unique to BCR mediated signaling, we decided to target 6 different kinases in a way that we could perturb nearly the complete pathway and with use of a second and third inhibitor affect a single downstream effector. Thus, the use of one inhibitor aimed to directly affect the targets of one kinase, but the combination of several inhibitors affect the same targets as another inhibitor, targeting a more upstream kinase. Thereby, we were affecting only its direct targets, which are a subset of the phenotype obtained by blocking the complete pathway. A set of 6 different small molecule inhibitors were chosen based on literature and pretests in the group of D. Kube. We tried to choose inhibitors being already enrolled in clinical studies or having been described in research focused on hematological malignancies, mainly lymphomas.

The recombinant soluble CD40L, used to stimulate transformed germinal center B cells in this study, mimics the CD40L/CD154, that is expressed either at the surface of or as soluble form by $CD4^+$ T-helper cells, and activates its specific receptor CD40 (Aversa et al., 1993; Gascan et al., 1991; Hermann et al., 1993; Lane et al., 1992; Spriggs et al., 1992). CD40 mediated signaling mainly involves MAPK signaling *via* JNK and p38 and IKK activated canonical and non-canonical NF-κB signaling. The MAPKKK family member transforming growth factor-beta-activated kinase 1 (TAK1) has been reported to function as an 'upstream' molecule in IL-1R-mediated NF-κB and MAPK signaling pathways (Yamaguchi et al., 1995). Furthermore, Tak1 can be activated through latent membrane protein 1 from Epstein-Barr virus (Wan et al., 2004), which in turn is mimicking CD40 (Eliopoulos et al., 1996) and plays a pivotal role in EBV-positive Burkitt's lymphomas.

Antigen recognition through the B cell receptor activates protein tyrosine kinases as for example Syk, which functions as amplifier of the BCR signal and connects the BCR with multiple signaling pathways, such as PI3K/Akt (Pogue et al., 2000). Furthermore, formation of the CBM (CARMA1/BCL10/MALT1) complex triggers the activation of NF-κB through IKK linkage (Egawa et al., 2003; Gaide et al., 2002; Hara et al., 2003; Jun and Goodnow, 2003; Newton and Dixit, 2003; Ruefli-Brasse et al., 2003; Ruland et al., 2001, 2003). Additionally, it has been proposed that Tak1 facilitates

the IKK activation in response to BCR activation (Schuman et al., 2009; Shinohara and Kurosaki, 2009).

Likewise, B cell receptor crosslink also activates the MAPK signaling pathway by engagement of the Ras-Raf-mitogen-activated protein kinase/extracellular signal-regulated kinase kinase (MEK)-extracellular signal-regulated kinase (ERK) mitogen-activated protein (MAP) kinase pathway (DeFranco, 1997; Richards et al., 1996, 2001), thereby affecting MEK1/2, p38 and JNK.

Thus we chose to target TAK1 as a key diversifier of signaling in both CD40 and BCR mediated signaling pathways and to treat our model cell line of transformed germinal center B cells with 100 nM (5Z)-7-Oxozeanol (Arcipowski and Bishop, 2012; Ear et al., 2010; Ninomiya-Tsuji et al., 2003; Schrader et al., 2012b). The inhibitor was tested in BL2 cells for pathway interruption and a diminished phosphorylation of p38 upon CD40 and BCR activation could be proven by Western Blot analysis (Figure 3-10 B).

NF-κB signaling was attenuated by inhibiting IκBα kinase (IKK) through 7 µM IKK2 VIII-inhibitor (Murata et al., 2003). IKK is a large NF-κB-activating signaling complex, consisting of IKKα (IKK1), IKKβ (IKK2) and IKKγ-NEMO, whereby IKK1 and IKK2 serve as catalytic subunits phosphorylating IκBα, thereby promoting its degradation. The IKK2 inhibitor has been shown to abrogate phosphorylation of IκBα and NF-κB-DNA-binding as well as expression of NF-κB target genes leading to apoptosis in myeloma cells (Sanda et al., 2005). The inhibition of CD40 mediated NF-κB activation through IKK2 in transformed germinal center B cells was circumstantiated in OCI Ly1 cells. Nuclear translocation of p65 as activation characteristic for NF-κB signaling was abrogated upon inhibition with IKK2 inhibitor (Figure 3-10 D).

2 µM SB203580 was used to inhibit p38 activity (Craxton et al., 1998; Cuenda et al., 1995; Horie et al., 2007). This compound inhibits the activation of MAPKAP-2 by p38 and subsequent phosphorylation of HSP-27 (Cuenda et al., 1995). The efficiency of SB203580 has been shown before in pre-tests by other members in the group of D. Kube. Due to non-working antibody solutions a proof of principle by showing the inhibition of phosphorylation of HSP-27 through SB203580 in BL cells was not successful. Nonetheless, the specificity of this compound inhibiting p38 MAPK has been reported in several studies, including BL cell lines too (Birkenkamp et al., 2000; Cuenda et al., 1995; Fahmi et al., 2000; Horie et al., 2007; Schrantz et al., 2001; Vega et al., 2005; Vockerodt et al., 2001). To inhibit JNK activity 10 µM SP600125 were used as reported from other studies in B cells (Bennett et al., 2001; Ke et al., 2006; Nishimura et al., 2009; Schnidar et al., 2009; Wang et al., 2009). This compound was a recommendation from A. Kieser (Munich GER). In his lab, JNK kinase assays were

accomplished on lymphoblastoid cell lines (LCLs) to investigate the effect of SP600125 (Kutz et al., 2008).

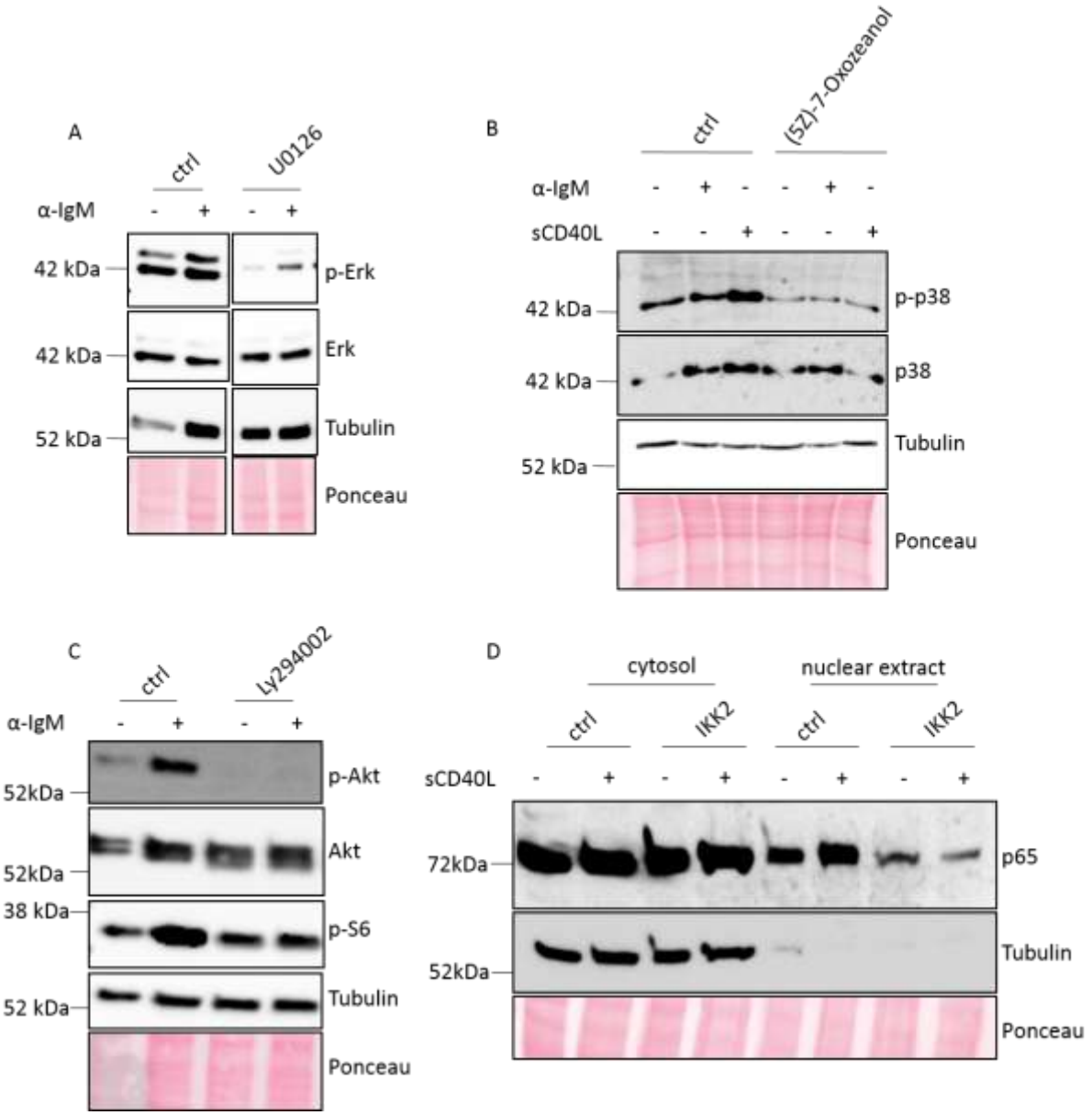

Figure 3-10 Proof of function of the inhibitors in use. BL2 cells were treated for 3 hours with respective inhibitors and subsequently 30 min stimulated with either α-IgM antibody or sCD40L. Samples were subjected to Western Blot analysis to detect pathway inhibition upon inhibitor use. **A** U0126 treatment inhibits MEK1/2 activity upon BCR crosslink. Cells were treated with 10 µM U0126 or dmso (ctrl) and inhibition of MEK1/2 was detected by diminished phosphorylation of Erk through phospho-specific antibodies detecting p-p42/p44. **B** The Tak1 inhibitor (5Z)-7-Oxozeanol reduces p-p38 levels in BL2 cells. Cells were treated with 100 nM (5Z)-7-Oxozeanol and phosphorylation of p38 was detected using specific antibodies. **C** 10 µM of the PI3K-inhibitor Ly294002 were used to inhibit BCR induced signaling, detected here by inhibited phosphorylation of Akt and S6. **D** IKK2 inhibitor ACHP prevents NF-κB activation. OCI Ly1 cells were pre-treated for 3 hours with 14 µM IKK2 inhibitor (ACHP) and subsequently CD40 signaling was activated *via* sCD40L. Nuclear extracts were analyzed for p65 translocation in the nucleus to monitor NF-κB activation.

To specifically dissect BCR mediated signaling modules, additionally PI3K and MEK1/2 activity was inhibited using 10 µM Ly294002 (PI3K) (Curnock and Knox, 1998; Uddin et al., 2006; Vlahos et al., 1994) and 10 µM U0126 (MEK1/2) respectively (Favata et al., 1998; Zheng et al., 2003). BL2 cells were pre-incubated for 3 hours with respective concentrations of specific inhibitor to ensure a complete mode of action of the inhibitor. To demonstrate the efficacy of U0126 in BL2 cells, the phosphorylation status of Erk1/2 upon α-IgM stimulation was monitored by WB using a phospho-specific antibody against p42/p44 (Erk1/2) (Figure 3-10 A). The activity of Ly294002 could be shown under similar conditions through abrogated phosphorylation of Akt upon inhibitor use as well as inhibition of phosphorylation of the downstream effector S6 (Figure 3-10 C).

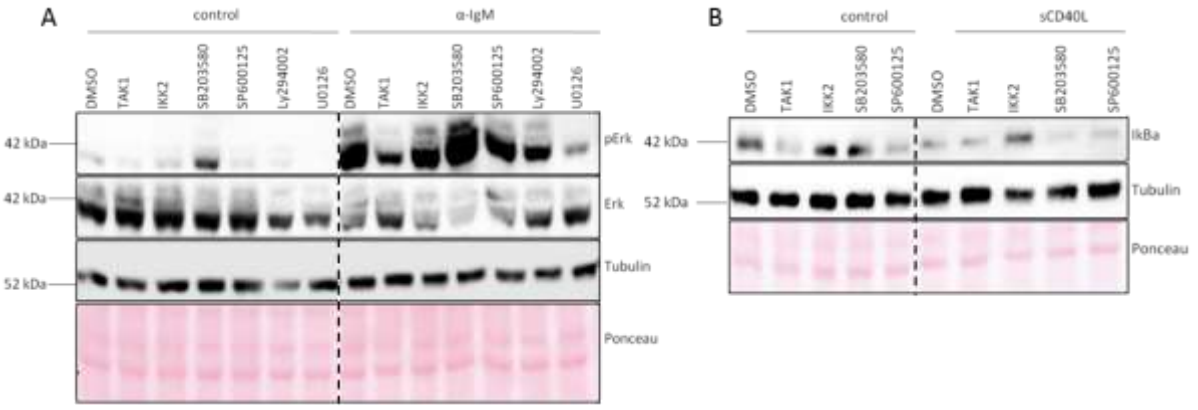

Figure 3-11 Effects of inhibitors used in microarray analyses. Western Blot analyses of 20 ng protein of samples of batch III, subjected to microarray hybridization, but harvested 30 min after stimulation to control successful activation of signaling pathways. Due to sample limitations, only one signaling pathway could have been analysed. **A** Samples subjected to α-IgM stimulation were verified for active phosphorylation of Erk upon stimulation using specific antibodies. **B** Samples subjected to CD40 activation were counterchecked for active NF-κB signaling *via* degradation of IκBα.

To verify the activity of the inhibitors and the successful stimulation of the BL cells in the specific samples dedicated for microarray hybridization, part of the samples were harvested upon 30 min stimulation to subject them to Western Blot analyses. As exemplified in Figure 3-11, the successful stimulation through α-IgM antibody was verified *via* phosphorylation of Erk (Figure 3-11 A) and the stimulation through sCD40L was verified by degradation of IκBα as marker for active NF-κB signaling (Figure 3-11 B). Figure 3-11 A depicts a strong phosphorylation of Erk upon α-IgM stimulation, which was inhibited by U0126. Additionally, a reduction in phosphorylation of Erk was observable after Tak1 inhibition (5Z-7-Oxozeanol). This was not expected, but may be supported by some few indirect hints proposing a connection between Tak1 and MEK1/Erk signaling (Ninomiya-Tsuji et al., 2003; Ohori et al., 2007; Schirmer et al., 2006). However, the effect of Tak1 inhibition on the phosphorylation status of Erk has not been shown before to our knowledge. Similar to Birkenkamp and coworkers in AML we observed an induction of phosphorylation of Erk upon p38 kinase inhibition through the use of SB203580 (Birkenkamp et al., 2000). CD40 activation led in turn to

active NF-κB signaling visualized by the degradation of IκBα (Figure 3-11 B). IKK2 inhibition abrogated the degradation of IκBα as expected. No activation of NF-κB signaling by inhibition of p38 or JNK (SB203580 or SP600125 respectively) was detected. The activation of NF-κB by the Tak1 inhibitor (5Z)-7-Oxozeanol was visible only once in all experiments conducted. Therefore we interpreted this as a technical artefact (compare Figure 3-13 A and Figure 3-14).

To conclude, the herein presented protein studies demonstrate that the chosen inhibitors interrupt the distinct signaling pathways they are aiming at. Thus we assume effects on the gene expression profile upon use of those inhibitors.

3.3.2 Differential gene expression on the whole genome level upon inhibitor use

To investigate the gene expression changes that are induced through specific pathway interruption under stimulation in a global way, gene expression profiling was performed. Samples of 3 independent biological replicates were hybridized to Affymetrix HG U133 Plus2.0 GeneChip arrays. Data were analysed with support from K. Meyer, M. Pirkl and Prof. Dr. R. Spang from the Institute of Functional Genomics in Regensburg. Differentially expressed genes were identified using linear models as implemented in the Bioconductor R package LIMMA (Smyth et al., 2005). Genes which show a significant (adj. p-value ≥ 0.05) change in expression were considered.

The stimulation of BL2 cells through BCR cross linking led to the differential expression of 16540 probes, mapping 9044 genes. CD40 stimulation of BL2 cells led to differential expression of 54654 probes, which are mapping 2634 genes. Due to the high number of significantly differentially expressed genes, in the following expression changes were sorted according to their absolute logarithmic fold changes (logFC) and only probe sets displaying logFC ≥ 0.75 or logFC ≤ -0.75 were taken into consideration. This process drops all genes with an expression less than 1.5-fold (0.5-fold respectively) of the control value.

The here conducted study comprises a large amount of comprehensive data. The numbers of differentially expressed genes upon each comparison between inhibitor, combination of inhibitors and stimulation are summarized in Table 3-1. A complete list of differentially expressed genes after BCR crosslink and CD40 stimulation can be found on the externally provided CD ROM (\\NEM\LimmaLists\).

Table 3-1 Differential expression in human transformed germinal center B cells in response to inhibition of B cell specific stimulations. Summarized are the numbers of differentially expressed genes in response to each inhibitor in comparison to unstimulated BL2 cells or BL2 cells stimulated for 3 hours with α-IgM antibody or sCD40L. The total number of affected genes comprises all genes significantly differentially expressed (adj. p-value ≤0.05) and is computed out of affected probes represented on the HG U133 Plus 2.0 microarray. Thus several genes are represented through probes which are marginally up as well as down regulated, which explains why the sum of up and down regulated genes does not necessarily correspond to the total number of affected genes. Due to high amounts of affected genes with very small effective fold change, genes exposing a logFC ≥ 0.75 or logFC ≤ -075 were regarded as differentially expressed.

	total # of affected genes (up/down)	**up regulated genes (logFC ≥ 0.75)**	**down regulated genes (logFC ≤ -0.75)**
Inhibitor Vs Ctrl			
Ly294002 (PI3K)	3875 (2025/1888)	73	84
U0126 (MEK1/2)	303 (234/62)	16	1
(5Z)-7-Oxozeanol (Tak1)	20 (20/2)	0	1
ACHP (IKK2)	4561 (2139/2535)	22	66
SB203580 (p38)	21 (18/3)	3	0
SP600125 (JNK)	1566 (1175/397)	130	6
IKK2/p38	4387 (2153/2383)	99	175
JNK/p38	4150 (2188/2038)	63	32
IKK2/JNK	5804 (2096/3087)	168	160
IKK2/JNK/p38	4574 (2609/2099)	151	53
α-IgM			
ctrl	9044 (3548/5770)	378	974
Ly294002 (PI3K)	5871 (4387/1558)	409	127
U0126 (MEK1/2)	6539 (4834/1795)	410	171
(5Z)-7-Oxozeanol (Tak1)	407 (167/241)	15	30
ACHP (IKK2)	2220 (1342/900)	56	60
SB203580 (p38)	36 (11/25)	0	1
SP600125 (JNK)	860 (690/171)	30	13
IKK2/p38	3477 (2320/1257)	195	103
JNK/p38	2513 (2114/410)	44	15
IKK2/JNK	4886 (3373/1640)	230	106
IKK2/JNK/p38	5512 (3817/1867)	365	139
sCD40L			
ctrl	2633 (1352/1323)	129	115
(5Z)-7-Oxozeanol (Tak1)	1838 (1001/862)	79	85
ACHP (IKK2)	4549 (2232/2575)	62	257
SB203580 (p38)	3453 (2137/1404)	198	175
SP600125 (JNK)	4589 (3051/1668)	280	121
IKK2/p38	5870 (3405/2929)	120	382
JNK/p38	6028 (3588/2789)	289	390
IKK2/JNK	5654 (3305/2765)	285	244
IKK2/JNK/p38	6113 (3316/3326)	239	373

In the present study, small molecule inhibitors were used to abrogate the function of specific kinases in order to obtain gene expression changes upon signaling pathway activation through CD40L or BCR cross linking. To investigate the effect of the specific inhibitor on the stimulated BL cells and to be aware of potential side-effects or effects without activation of the respective pathway two different experimental procedures were analyzed for each inhibitor: (1) cells treated with inhibitor alone and (2) stimulated cells treated with inhibitor. So, for each inhibitor or combination of inhibitors 3 lists of differentially expressed genes were obtained: (a) INHIBITOR-CTRL (contains all genes differentially regulated upon inhibitor use in unstimulated BL2 cells); (b) INHIBITORxBCR-CtrlBCR (shows all differentially expressed genes between BL2 cells incubated 3 hours with inhibitor and subsequently stimulated 3 hours with α-IgM antibody and BL2 cells incubated 3 hours with ctrl (dmso) and subsequently stimulated 3 hours with α-IgM antibody) and (c) INHIBITORxCD40-CtrlCD40 (exhibits all differentially expressed genes between BL2 cells incubated 3 hours with inhibitor and subsequent CD40 activation and the respective control: untreated/dmso-treated cells stimulated with sCD40L).

The list of differentially expressed genes upon inhibitor use on unstimulated cells compared with the unstimulated control BL2 cells, gives a first overview about the effects of the inhibitor on the cell type of Burkitt's lymphoma cells. Those effects observed here may include unspecific actions of the inhibitor as well as the exertion of inhibitory effects on already activated signaling pathways in the normal turnover of BL2 cells.

As shown in Table 3-1, most of the inhibitors used in this study did not exert large effects on the unstimulated BL2 cells. Major effects upon inhibitor use on unstimulated BL2 cells were detected upon PI3K, IKK2 and JNK inhibition. This may point towards active basal signaling of PI3K, NF-κB and JNK in Burkitt's lymphoma cells. Supporting this, a "tonic BCR signal" including augmented activity of PI3 kinase in Burkitt's lymphoma (Schmitz et al., 2012) and a synergistic action of c-Myc and PI3K signaling in Burkitt's lymphomagenesis (Sander et al., 2012) have been described recently. Although BL typically do not exhibit constitutive active NF-κB signaling in contrast to other lymphoma entitites (Dave et al., 2006; Klapproth et al., 2009), several hints point towards a sustained NF-κB activity in BL2 cells (see also chapter 3.3.4). In addition, our group could recently show a tonic activation of PI3K, NF-κB and JNK to regulate aberrant 'basal' c-Myc expression in BL (Schrader et al., 2012b).

This dataset comprises a highly comprehensive amount of data. Therefore, no specific single differentially expressed genes will be considered, but network analyses provided by M. Pirkl, K. Meyer and Prof. Dr. R. Spang (university of Regensburg) will be presented in the next paragraphs.

3.3.3 Nested Effects Models propose a controversial role of Tak1 in CD40 and BCR mediated signaling.

One of the main aims of the present study was to provide high-dimensional data to develop, establish and further improve computational methods. A key obstacle to infer signaling networks from perturbation screens is that gene expression profiles offer only an indirect view of pathway structure due to the high number of non-transcriptional regulatory events like protein modifications. A recent computational approach especially designed to learn from high-dimensional phenotypes and indirect information are *Nested Effects Models* (NEM) (Markowetz et al., 2005, 2007). NEMs are a class of probabilistic models, which reverse engineer upstream/downstream relations of cellular signaling cascades and are computed to return pathway structures explaining the perturbation effects.

The present study was designed in order to provide sufficient perturbations as well as upstream/downstream relations to infer signaling pathway structures with the use of NEMs.

As described above, CD40L and α-IgM antibody induce overlapping as well as specific signaling pathways in BL2 cells. Based on the high-dimensional gene expression data, consolidating several different perturbations in terms of pathway activation *via* stimulation and pathway interruption *via* kinase inhibition, nested effects models were generated returning pathway structures analyzing and comparing the role of Tak1 in CD40 and BCR mediated signaling. Prior knowledge based on literature discussed Tak1 as signal diversifier upstream of p38, NF-κB and JNK activation in CD40 activated signaling (Sato et al., 2005; Takaesu et al., 2003; Yamashita et al., 2008). Equally, an essential role as mediator for BCR induced NF-κB signaling has been reported for Tak1 (Schuman et al., 2009; Shinohara and Kurosaki, 2009). Additionally, a very recent report being published throughout the work on the present study demonstrates a pivotal role for Tak1 in regulating cell survival of mantle cell lymphoma, a lymphoma subtype being dependent on active NF-κB signaling (Buglio et al., 2012). However, the role of Tak1 in NF-κB-independent malignancies as Burkitt's lymphoma remains to be elucidated so far.

As shown in Figure 3-12, NEMs derived two independent pathway structures for CD40 and BCR mediated signaling, proposing individual roles for Tak1. The firstly provided nested effects models supposed a covalent activation of p38 and Tak1 both exerting effects on the activity of IKK2 (Figure 3-12 A). Furthermore, computed modeling resulted in an interchangeability of IKK2 and JNK, due to a strong overlap of target genes, when perturbing both kinases. However, Tak1 did not present as mediator that integrates signaling crosstalks. A similar surprising observation was made for BCR mediated signaling. Here, PI3K presented as expected as upstream signaling modifier. Nevertheless, Tak1 could not be modeled to be downstream of PI3K and upstream of NF-κB activation as already

described in literature (Schuman et al., 2009; Shinohara et al., 2005). Instead, p38, JNK and NF-κB signaling presented to be completely independent of Tak1 kinase function, but *vice versa* exerting effects on the shared target Erk1/2. The results proposed by the computed nested effects models were completely surprising, unexpected and contradictory to recent reports in other cell types, thus a biochemical proof was needed and several further experiments were conducted.

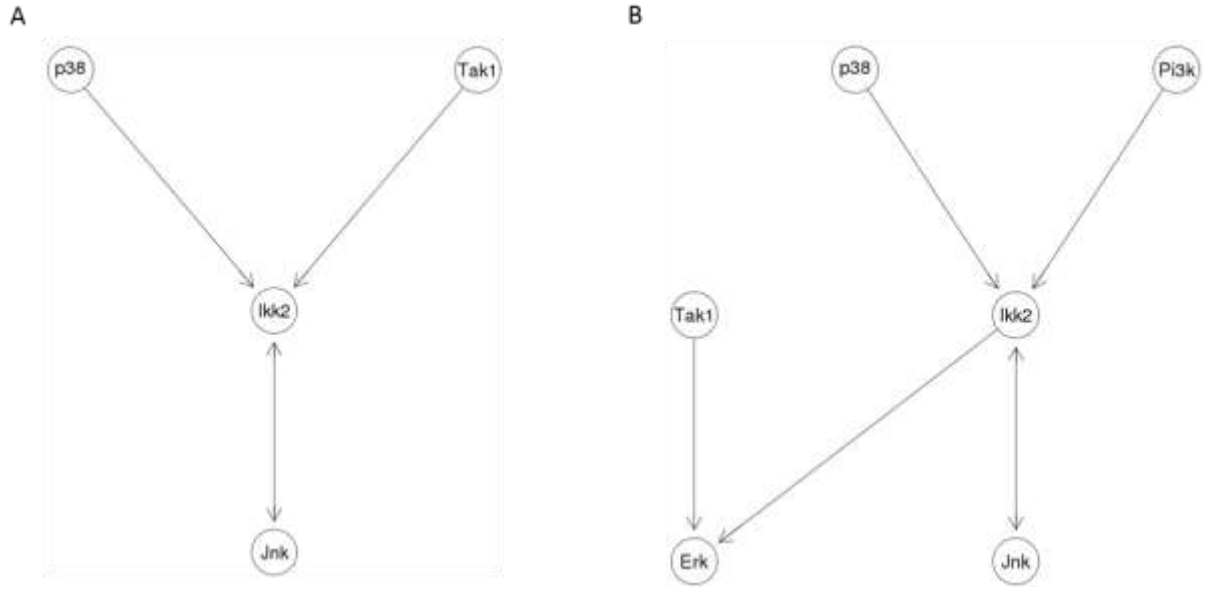

Figure 3-12 Role of Tak1 in CD40 and BCR mediated signaling proposed by a first generation Nested Effects Model. A Nested Effects Model (NEM) of CD40 mediated signaling suggests an influence of Tak1 on IKK2 and JNk, but the p38-excerted effect seems to be independent of Tak1. Furthermore are IKK2 inhibition and Jnk inhibition indistinguishable with regard to their gene expression profile. **B** NEM of BCR mediated signaling. p38, NF-kB and JNK signaling seem to be completely independent from Tak1 signaling, but PI3K inhibition leads to effects on NF-kB signaling. Additionally, Tak1 inhibition is proposed to be connected to Erk-pathway by sharing target genes.

To exclude probabilistic side effects of the used chemical inhibitor (5Z)-7-Oxozeanol, one additional small molecule inhibitor of Tak1 (AZ-TAK, Tocris, Bristol UK) and siRNA targeted against Tak1 was used in a comparative study (Figure 3-13). BL2 cells were transfected twice with a time lapse of 24 hours with control-siRNA (scrbl) or siRNA targeted against Tak1 (Silencer® Select, Ambion), respectively. Control-siRNA transfected cells were subsequently splitted and additionally pre-treated with (5Z)-7-Oxozeanol or AZ-TAK1 for 3 hours, before all cells were either stimulated with sCD40L or α-IgM antibody or left unstimulated. Stimulation was carried out for 30 min to analyze pathway activation signals *via* Western Blot analyses or for 3 hours respectively to analyzing target gene expression changes *via* qRT-PCR. In the following the activation of MAPK signaling (p38, Erk) and NF-κB signaling (IκBα degradation) was investigated using Western Blot analyses. JNK signaling was not contemplated due to the complexity of the here considered data, and non-working antibodies for phosphorylated JNK levels.

As clearly shown in Figure 3-13 A, (5Z)-7-Oxozeanol strongly inhibited CD40 and BCR induced phosphorylation of p38. Thus, Tak1 should be presented upstream of p38 both in CD40 as well as in BCR activated signaling models. Additionally, protein analyses of IκBα-levels in Tak1-inhibitor treated BL2 cells revealed a stabilization of IκBα upon inhibitor use and subsequent CD40 activation. In control-treated cells a marked degradation of IκBα after CD40 activation as hint for active NF-κB signaling was visible. BCR crosslink did not induce strong NF-κB activation, observable as IκBα degradation, in BL2 cells, therefore the effect of the inhibitor on BCR induced NF-κB signaling remains unclear upon analyses of protein modifications. The inhibitor AZ-TAK obtained from Tocris Bioscience (Bristol UK) did not seem to work properly in our hands. Buglio and coworkers could demonstrate reduced phosphorylation levels of p38 in an IL-1-induced HeLa cell line upon AZ-TAK1 treatment for 1 hour (Buglio et al., 2012), but here the phosphorylation status of p38 was already elevated upon AZ-TAK1 treatment of unstimulated BL2 cells compared to untreated BL2 cells. Same holds true for the use of siRNA mediated knock down of the gene of interest.

A strong reduction in protein levels of Tak1 was observable upon siRNA use, but the activation of p38 signaling through CD40L is still present. Similarly was the inhibition of NF-κB signaling, as visualized by IκBα degradation, most clearly detectable upon use of (5Z)-7-Oxozeanol and less convincing (but still observable) upon use of AZ-TAK or *TAK1*-targeting siRNA.

As already mentioned above the read out for BCR activated signaling on the protein level is more difficult. The p38 activation upon 30 min α-IgM stimulation was not as strong as after CD40L, but was nevertheless inhibited through (5Z)-7-Oxozeanol. IκBα degradation was not observable after 30 min of BCR crosslink, but a strong activation of Erk signaling was detectable *via* phosphorylation of Erk1/2. Upon use of Tak1 inhibitors and siRNA targeted against *TAK1*, the phosphorylation status of Erk1/2 seemed to be reduced.

Nevertheless, those analyses of protein modifications upon Tak1 inhibition and subsequent pathway activation led to the conclusion that Tak1 should be modeled as a signal modulator being situated upstream of p38 and NF-κB signals in CD40 mediated signaling as well as upstream of p38, NF-κB and Erk signals in the BCR pathway.

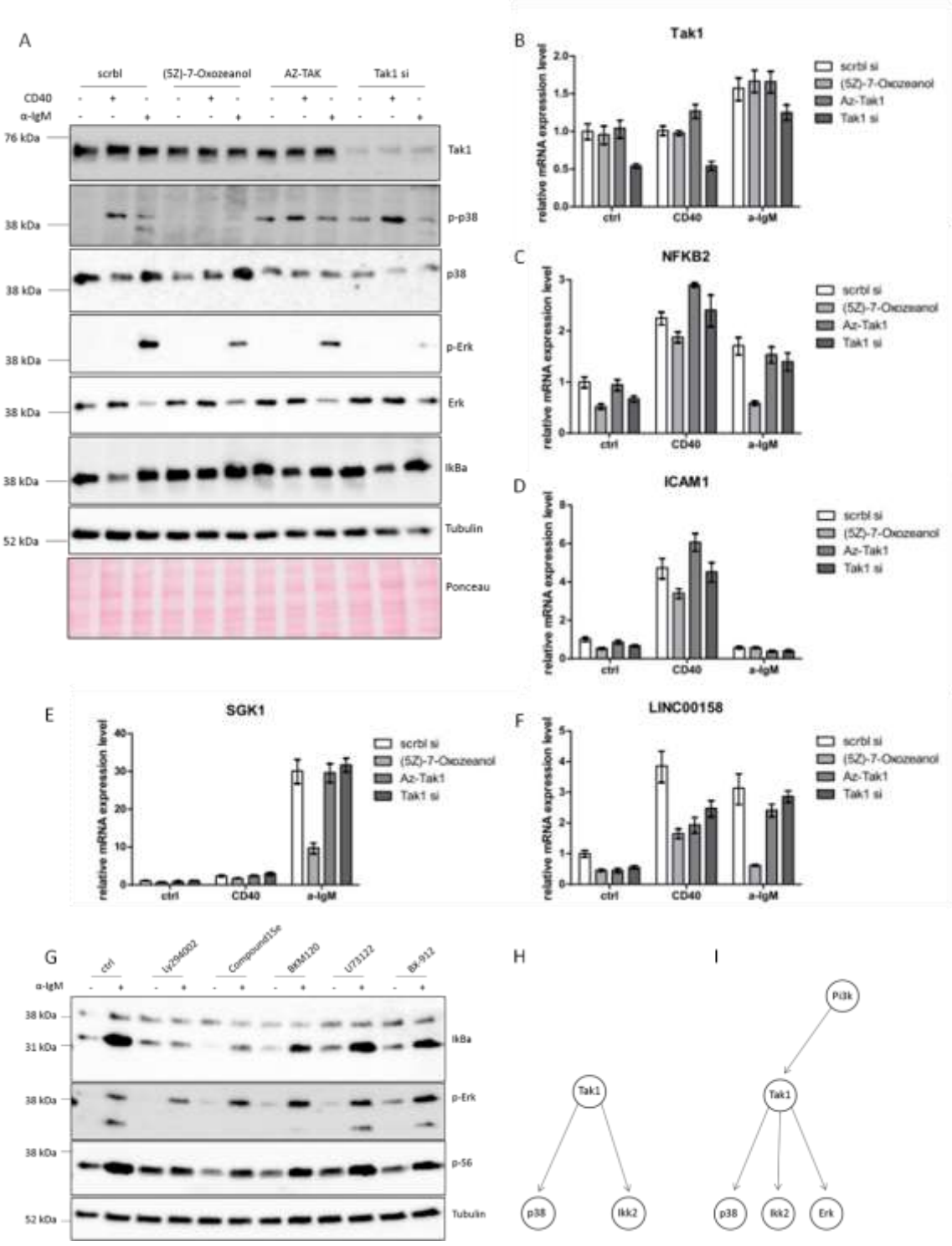

Figure 3-13 Tak1 presents as major signal modulator in CD40 and BCR mediated signaling. A Western Blot analysis of BL2 cells transfected twice for 24 hours with 4 µg scrbl siRNA or Tak1 siRNA. Samples transfected with scrbl siRNA were splitted 24 hours after second transfection for treatment with either 100 nM (5Z)-7-Oxozeanol or 250 nM Az-Tak1 for 3 hours and stimulated for 30 min afterwards. **B-F** qRT-analyses of transfected BL2 cells (same treatment as in **A**, apart from 3 hours of stimulation with either sCD40L or α-IgM $F(ab)_2$ fragment). Data are represented as $2^{-\Delta\Delta Ct}$ values relative to *ABL* housekeeping gene expression. **G** Western Blot analysis of several inhibitors of BCR mediated signaling in BL2 cells: PI3K (Ly294002, Compund15e, BKM120), PLC-γ (U73122), PDK1 (BX-912). **H** Model of CD40 mediated signaling based on experimental data involves Tak1 in p38 and NF-κB signaling. **I** Model of BCR mediated signaling based on

experimental data places Tak1 downstream of PI3K, but upstream of p38, NF-κB and Erk-signaling. The role of JNK in this context was not determined.

To further elucidate gene expression changes induced through Tak1 inhibition, qRT-PCR analyses were accomplished using the same experimental procedure as described above, except 3 hours of CD40/BCR stimulation before analysis. First of all, *TAK1* mRNA expression level were checked to prove a knock down of *TAK1* upon siRNA use. The results showed 50 % reduced expression levels upon siRNA, but not upon inhibitor use, as the chemicals inhibit kinase activity and not protein expression (Figure 3-13 A & B). To further investigate the NF-κB activation through BCR crosslink typical NF-κB target genes as *NFKB2* and *ICAM1* have been analyzed. One can observe an induction of *NFKB2* expression upon CD40 stimulation, which is much less pronounced upon BCR crosslink (Figure 3-13 C). However, (5Z)-7-Oxozeanol, but not AZ-TAK1 or Tak1 siRNA reduced the levels of *NFKB2* mRNA expression. Such a reduction in *NFKB2* expression level was even in the unstimulated BL2 cells detectable. Furthermore, the expression of *ICAM1* was markedly elevated upon CD40 activation, but not changed after α-IgM stimulation (Figure 3-13 D). The level of *ICAM1* activation was similarly suppressed through (5Z)-7-Oxozeanol treatment after pathway activation through CD40L as in unstimulated BL 2 cells. Figure 3-13 E & F shows the regulation of mRNA expression upon Tak1 inhibition and subsequent CD40/BCR stimulation of *SGK1* and *LINC00158*. SGK1, the serum- and glucocorticoid-induced kinase 1, is activated through the PI3K (Yan et al., 2008), thus *SGK1* mRNA expression level are highly up regulated upon α-IgM stimulation (Schrader et al., 2012b). *LINC00158* is a *long intergenic non-protein coding RNA 158,* which was found to be strongly regulated through CD40 and BCR activation (Schrader et al., 2012b) as well as IKK2 and Tak1 inhibition in CD40 activated BL cells (compare supplemental file \\NEM\combinedAnalyses_201211\IKK2_Tak1xCD40.int.xls on the provided CD ROM). For both genes a strong inhibition through the use of (5Z)-7-Oxozeanol was detectable, which confirms the microarray data by qRT-PCR and contradicts the proposed nested effects model for BCR. Additionally, similar to the NF-κB target genes *NFKB2* and *ICAM1,* a regulation by Tak1 inhibition in unstimulated BL2 cells for *LINC00158* was observed.

To further verify the proposed NEM for BCR activated signaling, the role of PI3K signaling in regard to its possibility to activate NF-κB signaling in BL cells was investigated. Several small molecule inhibitors targeting BCR induced signaling on different levels were used. Thus, BL2 cells were 3 hours pre-treated with Ly294002, Compound15e or BKM120 to inhibit PI3K activity with three independent inhibitors, as well as with inhibitors for PLC-γ (U73122) and PDK1 (BX-912) before subsequent stimulation with α-IgM antibody for 60 min (Kopp et al., 2012; Mogami et al., 1997; Vlahos et al., 1994; Walsh et al., 2013). As depicted in Figure 3-13 G, we could not detect a BCR induced degradation of IκBα in BL2 cells. Upon inhibition of basal ('tonic') and BCR induced PI3K activity *via* Ly294002 and Compound15e the stabilization of IκBα was abolished. Although not abolished, a

diminished stabilization of IκBα was also visible upon use of BX-912. The here demonstrated results raise the question if basal PI3K activity, as observed in BL (Schmitz et al., 2012), restrains NF-κB activatability. Therefore, one can conclude that NF-κB activity is also regulated through PI3K activation in BCR signaling. Similarly, a strong reduction in BCR induced phosphorylation levels of Erk were observed after PI3K-inhibition.

Summarizing the data presented in Figure 3-13, one can conclude that in CD40 mediated signaling Tak1 may indeed influence p38 and NF-κB signaling as upstream mediator, whereas in BCR mediated signaling Tak1 additionally modulates Erk signaling and may be interposed between PI3K influence upstream and p38, Erk and NF-κB signaling downstream (Figure 3-13 H & I). To further pinpoint the role of Tak1 in CD40 and BCR mediated signaling in BL cells, the experimental procedure as described above was expanded on another Burkitt's lymphoma cell line Ramos (Figure 3-14 B), thereby disclosing some particularities. In BL2 cells, p38 is activated upon both CD40L and α-IgM stimulation. (5Z)-7-Oxozeanol inhibited this activation markedly, whereas upon AZ-TAK treatment only diminished phosphorylation levels of p38 were detectable and the use of Tak1 siRNA did not affect the activation status of p38 (Figure 3-14 A). In Ramos cells, the p38 activation strongly appeared after CD40 pathway activation, but not upon BCR crosslink. Nevertheless, the effect of (5Z)-7-Oxozeanol was much stronger in Ramos cells than in BL2 cells, whereas the effect of AZ-TAK and Tak1 siRNA were comparable in both cell lines (Figure 3-14 B).

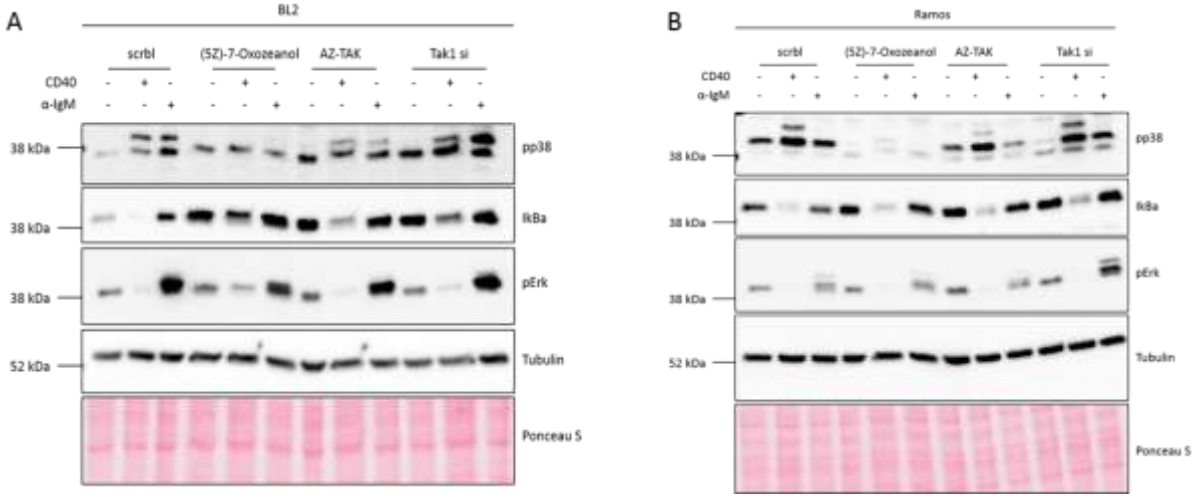

Figure 3-14 Comparison of two Burkitt's lymphoma cell lines with regard to signaling interruption upon Tak1 inhibition. A BL2 cells were transfected with Tak1 siRNA or respective control. Control transfected cells were splitted and additionally treated with Tak1 inhibitors (5Z)-7-Oxozeanol or AZ-TAK. After 3 hours of inhibitor treatment, cells were stimulated for 30 min with either sCD40L or α-IgM $F(ab)_2$ fragment or left as control. Samples were harvested and 20 µg protein were subjected to Western Blot analyses. **B** The Burkitt's lymphoma cell line Ramos was manipulated as in **A**. Shown is one representative result of at least 3 replicates.

NF-κB signaling was in both cell lines strongly activated upon CD40 activation and nearly not detectable *via* WB after 30 min BCR crosslink. In BL2 cells, (5Z)-7-Oxozeanol inhibited the NF-κB activation, whereas in Ramos cells still a strong IκBα degradation was detectable. Both AZ-TAK as well as Tak1-directed siRNA marginally led to an IκBα stabilization in BL2 as well as in Ramos cells.

Furthermore, the activation of the Erk pathway after BCR crosslink, displayed here through phosphorylation of Erk was much stronger in BL2 cells than in Ramos cells, thus the inhibitory effect of (5Z)-7-Oxozeanol is much easier to demonstrate in BL2 cells than in Ramos cells. All these observations point to a somehow particular role of BL2 cells, our model cell line for human transformed germinal center cells. Preliminary results from others in the group of D. Kube investigating further Burkitt's lymphoma cell lines, tend to confirm an outstanding role of the BL2 cell line in the scope of Burkitt's lymphoma cell lines. Nevertheless, the data used to compute nested effects models were obtained on perturbations of the BL2 cell line and in this cell line Tak1 seems to play its foretold role as mediator of p38 and NF-κB signaling upon CD40 activation as well as diversifier of signaling towards p38, NF-κB and Erk signaling after BCR crosslink.

Taken together, the biochemically collected data provide strong evidence that the primarily proposed nested effects models of the role of Tak1 in CD40 and BCR mediated signaling are inadequately describing the underlying signaling functions of Tak1. Thus, further computational advances have to be made to correctly model the here presented gene expression data.

3.3.4 NF-κB signaling upon BCR crosslink in Burkitt's lymphoma

Simultaneously to the question whether Tak1 plays its pivotal role as mediator for NF-κB signaling in BLs as well upon BCR signaling, the observation of generally low levels of NF-κB activation after α-IgM stimulation in BL cells was investigated. Generally, triggering of the B cell receptor leads to the activation of NF-κB signaling *via* protein kinase C (PKC) β and additional signal adaptors like CARMA1, Bcl10 and mucosal–associated lymphoid tissue 1 (MALT1) (Egawa et al., 2003; Li and Verma, 2002; Ruefli-Brasse et al., 2003; Ruland and Mak, 2003).

Interestingly, the results reported in the present study exhibit the contrasting observation of a reduced activatability of NF-κB signaling through B cell receptor signaling compared to CD40 mediated signaling in the BL cell lines BL2 and Ramos (compare Figure 3-14). Moreover, taking IκBα-degradation as a sign for NF-κB activation, the impression of reduced NF-κB signaling after BCR activation arises, as visualized by a sustained stabilization of IκBα (Figure 3-13 G and Figure 3-14 A).

To elucidate the reduced NF-κB signaling upon BCR crosslink in Burkitt's lymphoma, the different NF-κB family members and their activatability through CD40 or BCR were analyzed *via* WB. Upon activation of the NF-κB signaling pathway, the transcription factors belonging to the NF-κB family translocate into the nucleus, which can be monitored by extracting nuclear and cytosolic proteins separately after giving the stimulus to the cell. Thus, the model cell line for Burkitt's lymphoma in the present study, BL2, as well as a model cell line for DLBCLs, OCI Ly1, were compared with regard to the ability to translocate p65, c-Rel, or RelB to the nucleus 1 hour after activation with either sCD40L or α-IgM antibody (Figure 3-15 A & B). Yet, a more direct observation of NF-κB activation *via* nuclear translocation of the respective transcription factor was achieved in comparison to the indirect proof of NF-κB activation by IκBα-degradation.

Unexpectedly, in both cell lines, BL as well as DLBCL, a nuclear translocation of the NF-κB family members p65, c-Rel and RelB was mainly detectable after CD40 activation, but not after α-IgM stimulation. In the BL2 cell line, a remarkably strong nuclear signal for p65 was detectable in the unstimulated cells as well, thus favoring a completely new and contradicting theorem of constitutive active NF-κB signaling in the BL2 cell line. Indeed, when pre-treating BL2 cells with an IKK2-inhibitor, both the basal and the CD40 activated nuclear p65 signal was diminished (Figure 3-15 C). Unexpectedly, no BCR induced nuclear translocation of any investigated NF-κB family member was detectable in the DLBCL cell line OCI Ly1 (Figure 3-15 F). Instead, the BL cell line BL2 exhibits a faint NF-κB activation signal 60 min after α-IgM stimulation, which can be inhibited through either IKK2 or Tak1 inhibition (Figure 3-15 E). However, a low grade of NF-κB activation can be guessed in terms of nuclear translocation of p65, but not the other NF-κB family members c-Rel or RelB.

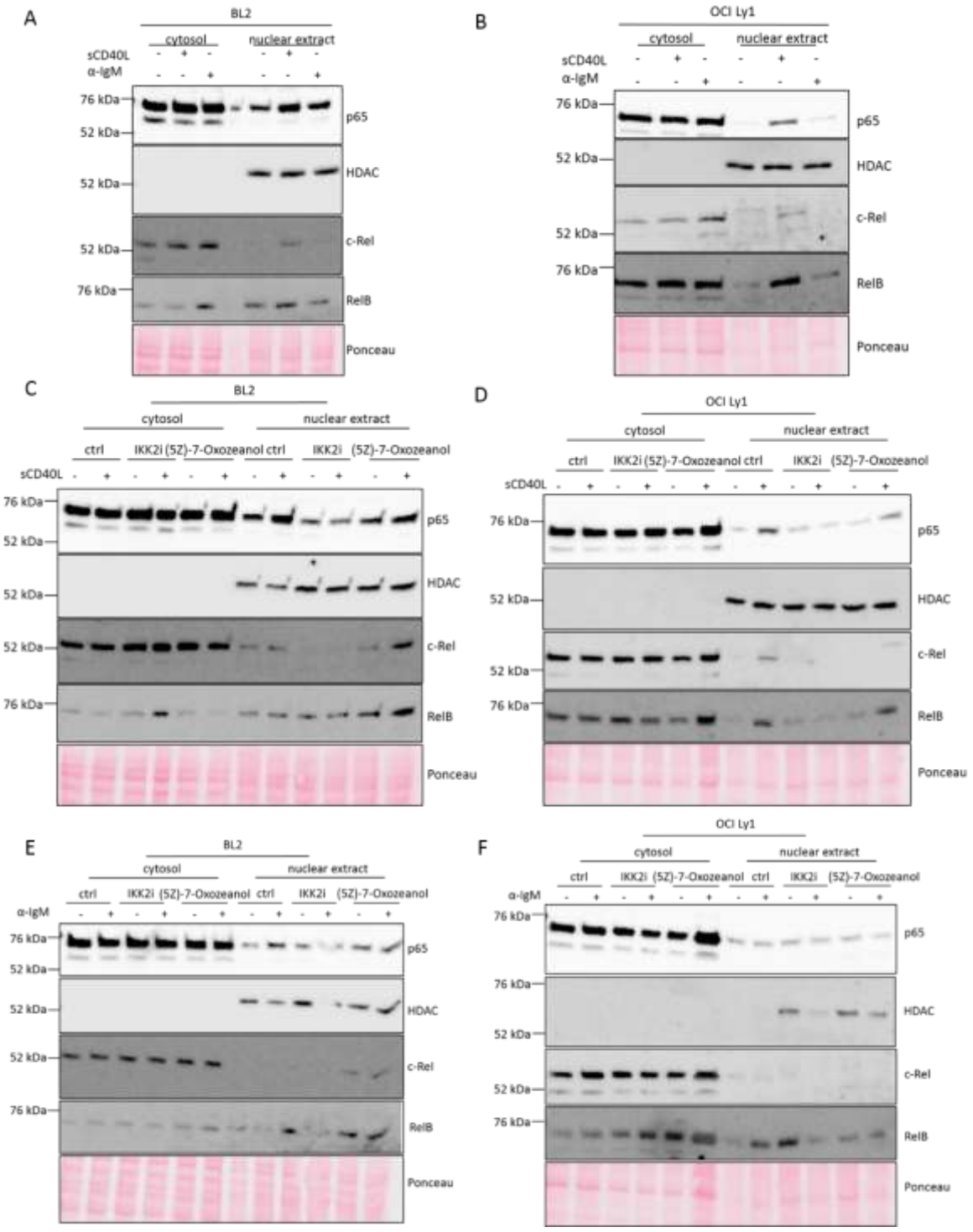

Figure 3-15 Differences in NF-kB activatability in Burkitt's lymphoma and Diffuse large B cell lymphoma. Nuclear translocation of NF-kB family member was monitored using specific antibodies against p65, c-Rel and Rel b. The nuclear extract was verified using a specific antibody against the nuclear marker HDAC1. To compare the differences between Burkitt' lymphoma and diffuse large B cell lymphoma, experiments were carried out in BL2 cells (BL) (**A, C, E**) and OCI Ly1 (DLBCL) (**B, D, F**). **A + B** show the general activatability of nuclear NF-kB translocation through CD40 stimulation and BCR crosslink with antibodies specific for NF-κB family members p65, c-Rel and RelB. **C + D** depict WB analyses of BL2 and OCI Ly1 cells upon NF-kB inhibition (IKK2i) and Tak1 inhibition ((5Z)-7-Oxozeanol) and 60 min CD40 stimulation. **E + F** show the same analyses as C + D upon stimulation with α-IgM $F(ab)_2$ fragment. 10 ng of protein were loaded for each fraction. The purity of the nuclear extracts was detected using a specific antibody against Histone Deacetylase 1 (HDAC).

To conclude, the nuclear translocation of p65 upon α-IgM stimulation demonstrates that NF-κB signaling seems to be slightly activated after BCR activation in the BL cell line BL2. This stands in contrast to the observed stabilization of IκBα 30 min and 60 min after BCR stimulation. However, CD40 mediated activation of NF-κB signaling is more pronounced when compared to BCR mediated NF-κB activation. Additionally, the BL2 cell line harbors high basal levels of nuclear p65 thus suggesting a basal NF-κB activity. Moreover, we observed for the first time, that BCR activation could not induce nuclear translocation of NF-κB family members in a DLBCL cell line. However, the molecular mechanisms of this phenomenon remain to be elucidated.

4 Discussion

We postulated that the differences between molecular BL and DLBCL are due to specific immune response associated signals mediated by the B cell microenvironment. Using *in vitro* stimulation of human transformed germinal center B cells as a model system to investigate pathway activation in aNHL, we could already demonstrate that both B cell receptor activation as well as CD40 activation lead to gene expression changes, which can be used to discriminate individual DLBCLs (Schrader et al., 2012b). However, these data are restricted to a specific time after giving the stimulus and may hide additional information about potential oncogenic pathway activities and their regulation. Thus, the present study aimed to provide gene expression data, which allow to investigate the relevant signaling pathways and their consequences in more detail. Therefore, this study used (a) time-resolved analysis of gene expression changes upon oncogenic pathway activation and (b) a combination of *in vitro* stimulation and kinase inhibition to provide data allowing the prediction of regulatory feedback loops and delineate respective pathway interactions on the whole genome gene expression level.

4.1 Analyzing the temporal pattern of gene expression changes

It was shown in this study that α-IgM as well as CD40 stimulation activate several signaling pathways in the BL cell line BL2. This includes overlapping signaling as the activation of p38 MAPK pathway through CD40 and α-IgM as well as distinct pathways, activated specifically through one of both stimuli. Thus, CD40 activation induces a strong and rapid activation of NF-κB signaling, whereas the BCR mediated NF-κB activation seems to be less pronounced and delayed in comparison to CD40 mediated activation (compare Figure 3-1 C & E). Activation of ERK/MAPK and PI3K/AKT pathway are unique to BCR mediated signaling and not triggered through CD40 induced signaling activation.

To our knowledge this study provides for the first time a global time-resolved investigation on the whole genome level of gene expression changes upon signaling pathway activation through CD40 or BCR crosslink on B lymphocytes. Both, BCR activation as well as CD40 activation induced a unique gene expression profile as revealed by microarray analyses. As shown before in another study, α-IgM stimulation of transformed germinal center B cells led to differential expression of significantly more genes than CD40 activation (Schrader et al., 2012b).

It was shown in this study that especially genes which are differentially expressed upon α-IgM stimulation shift the gene expression profile of mBL towards a gene expression profile of DLBCL (Figure 3-2). It becomes clear, that sustained activated signaling *via* the B cell receptor but not activation of CD40 mediated signaling leads to changes in gene expression which reduce the mBL index. This observation is supported by recent findings, which demonstrate chronic active BCR signaling in a subgroup of DLBCL, the ABC-like DLBCL (Davis et al., 2010; Kloo et al., 2011; Ngo et al.,

2006), thus defining the molecular profile of ABC DLBCL in comparison to other DLBCL subtypes (Alizadeh et al., 2000). In addition, our group could very recently demonstrate that the coherent expression of α-IgM affected genes characterizes individual NHL (Schrader et al., 2012b). In line with recent advances in the understanding of lymphoma pathogenesis, one can conclude that B cell receptor signaling has emerged as a central oncogenic pathway in lymphoma genesis and progression. The cascade of effectors downstream of the BCR includes many kinases diversifying the signal intensity, amplitude and outcome. Thus, it is not surprising that lymphomas adopt and spoil this signaling pathway, rendering it to an essential tool, which bears the potential of targeted therapy for patients with aNHL.

Due to the high-dimensionality and complexity of the generated data, statistical and bioinformatical analyses turned out to be challenging. In the present study, two different methods were used to analyze the temporal pattern of gene expression changes, thereby aiming at the disclosure of regulatory circuits, positively and negatively influencing signaling routes in their top-to-down signaling cascade. Even though using distinct mathematical models, both analyses are based on the integration of gene expression changes with similar time course to clusters of genes. It is not surprising that the computed clusters of genes are not identical to each other, since different mathematical approaches may result in different major findings, an observation which was demonstrated by others as well (de Matos Simoes et al., 2012). Apparently, in both models, BCR as well as CD40 activation induce a variety of different gene expression changes, including immediate-early activated and repressed genes as well as genes being changed in their expression profile after long-term stimulation or genes, displaying more-phasic time courses.

The first approach presented in this study demonstrates a causality network of α-IgM mediated gene expression correlations (Figure 3-3) and their conditional dependency, inferring an influence between connected clusters of genes (Chiquet et al., 2009). The network nicely demonstrates the complexity and connectivity of signaling pathways, which are induced upon crosslinking the BCR. A biological interpretation of this comprehensive network still remains to be fully elucidated. A first attempt to assign GO-terms and search for significant enrichment of specific biological processes identified the hub clusters of the causality network to be enriched for genes encoding kinases, G-proteins and related proteins as well as genes encoding for transcription factors thus playing crucial roles in cell signaling and cell proliferation processes. However, further analyses revealed that several clusters resemble each other not only in gene expression course but also in the biological processes the genes are encoded for. Furthermore, most clusters are composed of genes, which cannot be assembled to one specific function or process and whose composition remains difficult to interpret.

Tremendous advances have been made in the development of new mathematical and bioinformatical methods to construct gene regulatory networks (Friedman, 2004; Lee and Tzou, 2009; Markowetz and Spang, 2007). These methods often combine gene expression data with for example protein-DNA interaction data to recover the underlying networks. However, most methods focus on reconstructing networks from static data and do not contain any temporal information. Only very recent investigations dealed with time series expression data and provided some interesting new methods to engineer gene regulatory networks (Cooke et al., 2011; Darkins et al., 2013; Gonçalves et al., 2012; Haye et al., 2012; Nascimento et al., 2012; Schulz et al., 2012; Su et al., 2013; Titsias et al., 2012; Yeung et al., 2011; Zou and Conzen, 2005). Thus, the conflation of our time course specific gene expression data set with other sources of prior knowledge may be useful to fathom the biological meaning of such a causality network. In order to shed some light on the complexity of the gene expression changes and their causal correlation induced through α-IgM stimulation, ongoing analyses are supposed to integrate genome-wide chromatin immunoprecipitation assays in our cell perturbation assays. Therewith, we aim to use such a causality network for identification of, for example, transcription factor targets.

The mathematically further developed and refined method of testing for stationarity applied by J. Läuter and colleagues was used to build sets of genes which display distinct expression changes over time. Hereby, the clustering of genes is strictly mathematically justified and the biological interpretation relies on the assumption that genes, which exhibit a uniform process are also regulated through the same elicitor or display a similar biological function. Combining this method of time course analysis with Gene Ontology enrichment allowed the discrete characterization of stimuli-induced gene expression changes over time on a global level. One can conclude from the present study that activation of target genes affecting proliferation, differentiation and paracrine signaling occurs 2 hours after CD40L activation and thus, CD40 mediated signaling happens very rapidly on the proteome-level, leading to a fast feedback loop mediated by gene expression changes. In contrast, BCR mediated signals are also translated rapidly into gene expression changes but seem to induce a broader variety of signals. This is justified by the higher number of differentially expressed genes when compared to CD40 induced gene expression changes as well as longer lasting changes in gene expression. Taken together with the observation of the BCR mediated shift of originally mBL-index-bearing cells towards a gene expression pattern of non-mBL (chapter 3.1.1), the observations made in the present study underpin the particular importance of B cell receptor signaling in lymphoid malignancies. This is in line with recent assessments and the related investigations in the field of targeting the B cell receptor clinically (reviewed in Young and Staudt, 2013).

As described in chapter 3.1.3, time series analysis of α-IgM induced gene expression changes demonstrated the temporal expression pattern of many well-known and pivotal players in both normal and pathological BCR signaling. One example is CCR7, a chemokine receptor shown to be an essential regulator of leukemia cell infiltration into the central nervous system (Buonamici et al., 2009). Its high expression in T-cell leukemias was associated with tumor cell migration and invasion *in vitro* and *in vivo* (Yang et al., 2011). Further, CCR7 was recently described for regulating homing of lymphoma cells to T cell regions in lymph nodes, thus promoting lymphoma cell survival through facilitating the cross-talk to other microenvironmental non-tumor cells (Rehm et al., 2011). In addition, Rehm and colleagues suggested that T-cell zone location of their mouse-model-derived lymphoma cells awards resistance to spontaneous apoptosis through the proximity to fibroblastic reticular cells (FRCs), which provide the hedgehog protein Indian hedgehog, as shown by reduced viability of lymphoma cells upon use of the Hh signaling inhibitor Cyclopamine. This very interesting observation taken together with the simultaneous BCR mediated down regulation of the Hh-signaling receptor *PTCH1* as well as *LEF1* and *NOTCH1* (compare Figure 3-5 and Figure 3-6), both pivotal players in developmental biology as well as being associated with several types of lymphoid malignancies (Cheng et al., 2001; Pui et al., 1999; Radtke et al., 2004; Reya et al., 2000; Walther et al., 2013), strengthens the importance of paracrine and autocrine signaling in the tumor microenvironment and prompted us to a more profound analysis of the role of hedgehog signaling in lymphoma.

4.2 A non-canonical role of Hedgehog signaling in lymphoma

The statistical analyses of BCR mediated gene expression changes identified the BCR induced co-repression of *LEF1, NOTCH1* and *PTCH1*. Lef1, a transcription factor in the Wnt signaling pathway, has been shown to regulate normal B lymphocyte proliferation (Reya et al., 2000). Further, *LEF1* is one of the signature genes defining the mBL index (Hummel et al., 2006) and very recently our group could demonstrate an aberrant *LEF1* expression as well as its transcriptional activity in BLs (Walther et al., 2013). Notch1, the transmembrane receptor for the Notch signaling network plays not only a role in lymphocyte development, proliferation and differentiation (Anderson and Longnecker, 2009; Cheng et al., 2001; Pui et al., 1999; Radtke et al., 2004) but has also been implicated in a variety of hematological malignancies including chronic lymphatic leukemia (CLL) (Okuyama et al., 2012; Willander et al., 2013), acute lymphatic leukemia (ALL) (Schwanbeck and Just, 2011; Tosello and Ferrando, 2013) as well as DLBCL (Lohr et al., 2012). Further on, both genes are connected to c-*MYC* activation (Rakowski et al., 2013; Yochum et al., 2008), which in turn displayed a similar time course of mRNA decrease after BCR crosslink. However, the connection of Ptch1 and related hedgehog signaling and c-Myc in lymphoma signaling remained elusive so far. Studies in Hh-induced medulloblastoma formation suggested that c-Myc activates *GLI1* expression *in vitro* and thus promotes tumorigenesis (Rao et al.; Zwerner et al., 2008). Evidence for the role of Hh in lymphoma is limited but rapidly developing. Both, healthy germinal center B cells as well as myc-driven lymphoma cells have been found to be protected from apoptosis by Hh ligands secreted by stroma cells (Dierks et al., 2007; Sacedón et al., 2005). Further, expression of Hh signaling proteins and their contribution to survival was described for some DLBCL cell lines (Singh et al., 2010). However, the relevance of Hh signaling in BL cells was not determined. In the present study, the analyzed BL cell lines differed strongly in their basal expression level of Hh signaling components. Hh ligands as *SHH* and *IHH* were not or only barely expressed by BL cell lines. Further on, activation of the Hh signaling pathway could not be achieved through stimulation of the cells with Shh-enriched medium, thus suggesting that BL cells are not responsive to Hedgehog pathway activation. These results are supported by a very recent study, confirming that Burkitt's lymphoma cells do not seem to be Hedgehog responsive (Yoon et al., 2013). Instead, this group shows that c-Myc directly regulates *GLI1* expression more significantly than the canonical Hh signaling pathway. This finding circumstantiates the here presented data, which demonstrate no relevance of SMO inhibition on BL cells. Additionally, the BCR induced c-Myc repression occurs slightly earlier when compared to the time course of *PTCH1*. These findings suggest a c-Myc driven non-canonical regulation of Hh signaling in BL and implies new therapeutic approaches, which include the direct targeting of Gli1 or *GLI1* target genes.

This study could not reveal generally higher expression levels of Hh signaling components in the analyzed DLBCL cell lines, although several studies from one group around F. Vega suggest active Hh

signaling in ABC DLBCL, including expression and secretion of Hh ligands as well as responsiveness to Hh-inhibition (Ok et al., 2012; Ramirez et al., 2012; Singh et al., 2009, 2010, 2011). These findings are somewhat contradictory, even though they might be explainable by the diversity of the cell lines used for the investigations in the present and the recently published studies.

However, the observation of BCR mediated down regulation of *PTCH1* expression raised the initial hypothesis that Burkitt's lymphoma harbor active Hh signaling. As shown in Figure 3-6, the computed time course of *PTCH1* was verified by qRT-PCR and revealed an activation of *PTCH1* gene expression after α-IgM stimulation before its expression was down regulated. Thus, the observed reduction of *PTCH1* mRNA levels after 3 to 4 hours of BCR activation might contribute to a regulatory feedback loop, preventing an exaggeratory Hh response. However, activation of BCR signaling in the BL cell line BL2 led to reduced levels of *PTCH1* gene expression but no changes in expression levels of *GLI1* (Figure 3-7). Taken together with the contrasting results in other BL cell lines, we concluded that canonical Hh signaling is not active in BLs. Instead, the observed elevated *GLI1* expression levels upon BCR activation in most cell lines favor the hypothesis of active Hh signaling in DLBCLs. This especially holds true when taking into consideration that BCR activation induces a transition of the mBL index from mBL towards DLBCL.

Activation of Hh signaling in cancer has been attributed to aberrant activation of several signaling pathways resulting in the integration of multiple oncogenic signaling inputs. Interplay of TGF-β, NF-κB, Notch and the ERK/MAPK pathway is supported by multiple lines of evidence (Chang et al., 2010; Madhala-Levy et al., 2012; Mangelberger et al., 2012; Qu et al., 2013; Schnidar et al., 2009) Furthermore, a synergistic effect between Hh and PI3K signaling was suggested for several cancer entities including ALK (anaplastic lymphoma kinase)-positive anaplastic large cell lymphoma cells (Ju et al., 2009; Mizuarai et al., 2009; Singh et al., 2009; Wei and Xu, 2011). Very recently, a study defining causative factors for activation of Hh signaling in diffuse large B cell lymphoma supported this link, by demonstrating reduced Gli1 protein levels after PI3K inhibition in DLBCL cell lines (Ramirez et al., 2012). However, they could not reveal the precise mechanism by which PI3K regulates Hh signaling. Furthermore, in this study Gli1 protein expression was inhibited by very high concentrations of the PI3K inhibitor Ly294002 in GCB DLBCL cell lines, whereas in the ABC DLBCL cell line OCI Ly3, which exhibits chronic active BCR signaling (Davis et al., 2010), lower concentrations of Ly294002 were sufficient to effectively abrogate Gli1 protein expression (Ramirez et al., 2012). Similarly, long-lasting inhibition of PI3K through Ly294002 also increased *PTCH1* and additionally *c-MYC* expression levels in unstimulated BL2 cells (Schrader et al., 2012b and unpublished own data). This not only supports the already suggested link between PI3K and Hh signaling but additionally connects c-Myc activity to PI3K and Hh activity in lymphoma biology. Indeed, a synergistic mode of

action of c-Myc and PI3K has been recently described for lymphoma pathogenesis (Sander et al., 2012). Further on, a basal activity of PI3K and tonic BCR signaling was demonstrated in Burkitt's lymphoma (Schmitz et al., 2012).

Nonetheless, the present study revealed a strong heterogeneity between different BL cell lines regarding their BCR mediated Hh signaling activation. Furthermore, cell lines where the BCR activation led to *PTCH1* expression level reduction not necessarily displayed activation of Hh signaling as monitored by *GLI1* expression. These findings support a non-canoncial activation of Hh signaling in lymphoma cells as recently proposed by others (Yoon et al., 2013). Similarly, the cell lines tested in the present study did not show any responsiveness to canonical Hh signaling activation through stimulation by Shh. In summary, the here presented investigations could not reveal a clear BCR induced activation or inactivation of canonical Hh-signaling in lymphoma cells. Moreover, Burkitt's lymphoma cells as well as the one DLBCL cell line investigated here do not seem to be Hedgehog responsive. Above all, the present study could not exclusively determine the same regulatory factor behind the simultaneous decrease in expression levels of *c-MYC*, *PTCH1* and *LEF1*, although the regulation of all three genes is clearly dependent on the PI3K-PLCγ-PKC pathway. Taken together, the here presented results favor a non-canonical role of Hh signaling in lymphoma.

4.3 Analyzing pathway intersections

Our group was recently able to mimic oncogenic pathway activities in aNHL by investigating the major patterns of gene expression changes in response to different immune response-associated stimuli *in vitro* (Schrader et al., 2012b). We were also able to identify individual aNHL profiles reflecting those patterns and we concluded that future targeted therapies have to intervene into specific signaling modules to reverse pathway deregulations. Therefore it is of crucial relevance to understand the constellation of oncogenic activities in the context of their interplay and the cross talk of signaling pathways being involved in the pathogenesis of lymphomas. Thus, the present study aimed to use a combination of *in vitro* stimulation with specific kinase inhibitors in order to delineate respective pathway interactions. The genome-wide expression profile of BL2 cells was investigated in several conditions, depicting oncogenic signaling activation and its abrogation at specified intersections. Thus, a large amount of comprehensive data was generated, which is still subject to work in progress in order to establish suitable methods for analyzing the complexity, the connectivity and the biological relevance of gene expression changes.

Tak1 as major modulator in CD40 and BCR mediated signaling

A recent computational approach to infer signaling pathway structures from perturbation experiments and subsequent gene expression profiling, Nested Effects Modeling (NEM) (Markowetz et al., 2005, 2007), was used to compare the role of Tak1 in CD40 and BCR mediated signaling. In CD40 activated signaling in B cells, Tak1 has been described to act as pivotal signal regulator upstream of p38, JNK and NF-κB activation (Sato et al., 2005; Takaesu et al., 2003; Yamashita et al., 2008). BCR signaling also activates those signaling pathways, but the contribution of Tak1 is controversially debated. Sato and colleagues demonstrated murine Tak1-deficient B cells to be able to still activate NF-κB signaling, but not the kinase JNk in response to BCR stimulation (Sato et al., 2005), whereas a later study demonstrated that B cell-specific *TAK1*-deficiency disrupted BCR induced NF-κB activation (Schuman et al., 2009).

However, the NEMs derived from the gene expression data in the present study proposed an unexpected dispensable role for Tak1 in CD40 and BCR mediated signaling BL cells (Figure 3-12). Yet, subsequently conducted biochemical investigations provided strong evidence that the primarily proposed nested effects models are not sufficient to describe the role of Tak1 in CD40 and BCR mediated signaling. Comparative analysis of the two independent inhibitors of Tak1 activity, (5Z)-7-Oxozeanol and AZ-TAK1, as well as Tak1-directed siRNA revealed the indispensability of Tak1 for mediation of p38 and NF-κB activation in CD40 mediated signaling. In BCR activated signaling, the Tak1 mediated activation of Erk, besides p38 and NF-κB activation was demonstrated. Thus, former results from other studies can be transferred to BL cells. Tak1 is a pivotal modulator of p38, JNK and

NF-κB signaling in CD40 as well as BCR activated pathways. This includes a so far not recognized regulatory role of Tak1 in Erk1/2-signaling. The present results suggest, that inhibitors targeting Tak1 activity might be suitable treatment options for lymphoma subtypes, depending on NF-κB, JNK, p38 or Erk1/2 signaling activity. This is supported by a very recent report, which was published during the work on the current study and revealed a pivotal role for Tak1 in regulating cell survival of mantle cell lymphoma cells, a subtype of aNHL exhibiting active NF-κB signaling (Buglio et al., 2012).

The here conducted analysis highlights the limitations of NEMs to handle such complex high-dimensional data in order to correctly return upstream/downstream relations of cellular signaling cascades and demonstrates the need for adaptation of the existing method. The observed differences in signal intensity may lead to the construction of dissatisfactory graphs. The gene expression changes induced through BCR stimulation were much stronger than those induced through CD40 activation. Similar observations were made for use of the different inhibitors. Thus, less genes are significantly strong regulated upon p38 inhibition than upon Erk1/2 inhibition. Since a very stringent cut-off (p-value) for calculation of the NEMs is used, it is possible that such system-relevant effects cannot be spotted and lead to the omission of potential p38-exerted effects. Therefore, a new method of discretization has now been established to integrate the different signal intensities in future modeling processes (personal communication from M. Pirkl, Regensburg). Another possible cause for the limitations in the NEMs is lying within the off-target effects of the inhibitors. The difficulty in modeling signaling cascades with the help of intervention studies is concentrated on the possibility to smartly differentiate off-target effects from real pathway signaling. Therefore, we are now primarily interested in establishing new methods for learning regulatory networks from compendia of the perturbation expression data and combining this data with data sources that provide prior knowledge to the network structure. One source of such prior information is our collection of manually curated and experimentally validated data, obtained from Western Blot analyses, qRT-PCRs or reporter-gene assays. Additionally, literature-based prior information will also be included in the generation of a new model. Thus, adjustement of the existing statistical algorithms is in preparation in order to map a biologically comprehensive and perspicuous regulatory network of the here analyzed perturbations.

BCR dependent NF-κB signaling in BLs

Very recent studies demonstrated a so-called ‘tonic’ BCR signaling of Burkitt’s lymphoma cell lines, as shown through killing of BL cells by CD79A- or SYK-knock down (Schmitz et al., 2012). Consistent with these findings, conditional activation of PI3K along with Myc in mouse germinal center B cells leads to lymphoma genesis of strong BL phenotype (Sander et al., 2012). This ‘tonic’ BCR signaling in Burkitt’s lymphoma activates the PI3K pathway, but is interestingly not dependent on the NF-κB

signaling-mediators CARD11 or BTK. This demonstrates the qualitative difference to 'chronic active' BCR signaling in ABC DLBCL (Davis et al., 2010; Schmitz et al., 2012).

In contrast to other lymphoma entities as DLBCLs or mantle cell lymphoma, Burkitt's lymphoma are generally reported to be characterized through low expression levels of NF-κB activation modules (Dave et al., 2006; Hummel et al., 2006). Moreover, constitutive activation of the normally pro-survival factor NF-κB increased cell death in several BL cell lines (Klapproth et al., 2009).

Typically, antigen-mediated activation of the B cell receptor leads to activation of NF-κB signaling in B cells *via* activation of PKCβ and subsequent signal adaptors like CARMA1, Bcl10 and MALT1 (Egawa et al., 2003; Li and Verma, 2002; Ruefli-Brasse et al., 2003; Ruland and Mak, 2003). Contrarily, the current study demonstrates a reduced activatability of NF-κB signaling through BCR activation when compared to CD40 mediated signaling in the BL cell lines BL2 and Ramos (Figure 3-14). Moreover, the GCB DLBCL cell line OCI Ly1 did not exhibit a BCR inducible NF-κB activation either. A role for 'tonic' BCR signaling has been postulated for GCB DLBCLs as well (Chen et al., 2008), although genetic knockdown of BCR components did not affect the survival of various GCB DLBCL cell lines (Davis et al., 2010). Therefore, it seems possible that some so far unknown mechanisms of 'tonic' BCR signaling prevent a profound activatability of NF-κB signaling. Another possibility, which has to be elucidated, is a delayed activation of NF-κB signaling upon antigen-mediated BCR activation on the background of 'tonic' BCR activity, since BL2 cells exhibit low levels of nuclear translocation of NF-κB transcription factors after 60 min of α-IgM stimulation. Furthermore, time course analysis of α-IgM stimulated BL2 cells revealed a NF-κB activation after 60-90 min of BCR crosslink, as visualized by faint degradation of IκBα (Figure 3-1). However, when comparing the nuclear levels of NF-κB family members, remarkably high levels of nuclear p65 were detected in unstimulated BL2 cells, which were abolished through IKK2-inhibition. Thus, one can conclude that the BL2 cell line exhibits constitutive active NF-κB signaling. This completely new and former findings-contradicting hypothesis is sustained through preliminary data, which show reduced proliferation of BL2 cells upon IKK2-inhibition (data not shown). Further studies in several other BL cell lines should elucidate if the activation of NF-κB, including the translocation of its transcription factor molecules into the nucleus, is abrogated at a later time in BL signaling or if this phenomenon exclusively holds true for the BL2 cell line. As also shown in Figure 3-14, the CD40 mediated NF-κB activation is in Ramos cells not ablated through Tak1-inhibition as it is in BL2 cells. In spite of the confirmed pivotal role of Tak1 as major modulator of antigen and CD40 induced signaling pathways in BL cells, the direct comparison of the two BL cell lines Ramos and BL2 with regard to Tak1 mediated signaling exposed once again the heterogeneity of the available BL cell lines and the probably particular role of the BL2 cell line as model cell line for Burkitt's lymphoma (not published data from the group of D. Kube).

5 Conclusion

The analyses of the time course of global gene expression changes of BCR or CD40 stimulated human transformed germinal center B cells enabled us to describe distinct gene groups affected in a comparable way, being either activated or suppressed. Therewith, new regulatory circuits and perhaps feedback loops can be postulated. A co-repression of *LEF1*, *PTCH1* and *NOTCH1* mRNA expression through BCR activation was identified, which is slightly delayed when compared to the BCR induced c-Myc repression. This could represent one mechanistic explanation for the observed shift of the mBL signature of the BL2 lymphoma cell line towards the non-mBL gene expression profile. However, this needs to be proven by additional investigations, as for example testing different cell lines with differing c-Myc expression levels. The additional treatment with other factors of the DLBCL microenvironment or a combination of stimuli could be helpful to avoid the observed reversion of BCR mediated gene expression by so far unknown feedback loops. Furthermore, causal relationships within oncogenic pathways for BCR activated human transformed germinal center B cells were proposed but need further prior knowledge integration before experimental validation.

The current study provide evidence that, although *PTCH1* mRNA expression levels are changed upon BCR activation, active Hh signaling does not seem to be important for Burkitt's lymphoma. Instead, we suggest a non-canonical regulation of Hh signaling in cross talk with aberrant c-Myc expression. Furthermore, the biochemical validation of a computationally compiled model of Tak1-signaling revealed a context-dependent role of Tak1 in the modification of signaling transduction. Thus, a direct contribution of Tak1 to the BCR induced phosphorylation of Erk1/2 was demonstrated for the first time. In addition, the present study provides evidence for a constitutive active NF-κB signaling in the BL2 cell line and suggests reduced NF-κB activatability in tonic BCR signaling.

These global gene expression analyses offer comprehensive data collections, which can be used in lymphoma research but also modeling of oncogenic pathways in general. Therefore, herein created data provide a sophisticated basis to develop new bioinformatical and statistical methods fostering a better understanding of signaling pathways and their regulatory feedback mechanisms. However, the present study also elicits vigorously the balance between prediction of oncogenic pathway activites and prior knowledge integration to put forward corresponding new hypotheses for experimental validation. In addition, we conclude that isolated global gene expression profiling needs to be complemented by additional pathway analyses. As the cell fate is not only determined by gene expression changes but also by posttranslational protein modifications as phosphorylations, ubiquitinations, degradations and others, the integration with data sets obtained by other –omics may be helpful for future characterizations of oncogenic pathways in lymphoma pathogenesis and progression.

6 Bibliography

Ahn, T., Yim, S.K., Choi, H.I., and Yun, C.H. (2001). Polyacrylamide gel electrophoresis without a stacking gel: use of amino acids as electrolytes. Analytical Biochemistry *291*, 300–303.

Akiba, H., Oshima, H., Takeda, K., Atsuta, M., Nakano, H., Nakajima, A., Nohara, C., Yagita, H., and Okumura, K. (1999). CD28-independent costimulation of T cells by OX40 ligand and CD70 on activated B cells. Journal of Immunology (Baltimore, Md. : 1950) *162*, 7058–7066.

Alizadeh, A.A., Eisen, M.B., Davis, R.E., Ma, C., Lossos, I.S., Rosenwald, A., Boldrick, J.C., Sabet, H., Tran, T., Yu, X., et al. (2000). Distinct types of diffuse large B-cell lymphoma identified by gene expression profiling. Nature *403*, 503–511.

Amini, R.-M., Berglund, M., Rosenquist, R., Von Heideman, A., Lagercrantz, S., Thunberg, U., Bergh, J., Sundström, C., Glimelius, B., and Enblad, G. (2002). A novel B-cell line (U-2932) established from a patient with diffuse large B-cell lymphoma following Hodgkin lymphoma. Leukemia & Lymphoma *43*, 2179–2189.

Anderson, L.J., and Longnecker, R. (2009). Epstein-Barr virus latent membrane protein 2A exploits Notch1 to alter B-cell identity in vivo. Blood *113*, 108–116.

Antony, P., Petro, J.B., Carlesso, G., Shinners, N.P., Lowe, J., and Khan, W.N. (2004). B-cell antigen receptor activates transcription factors NFAT (nuclear factor of activated T-cells) and NF-kappaB (nuclear factor kappaB) via a mechanism that involves diacylglycerol. Biochemical Society Transactions *32*, 113–115.

Arcipowski, K.M., and Bishop, G. a (2012). Roles of the kinase TAK1 in TRAF6-dependent signaling by CD40 and its oncogenic viral mimic, LMP1. PloS One *7*, e42478.

Aszterbaum, M., Epstein, J., Oro, A., Douglas, V., LeBoit, P.E., Scott, M.P., and Epstein, E.H. (1999). Ultraviolet and ionizing radiation enhance the growth of BCCs and trichoblastomas in patched heterozygous knockout mice. Nature Medicine *5*, 1285–1291.

Aversa, G., Punnonen, J., and de Vries, J.E. (1993). The 26-kD transmembrane form of tumor necrosis factor alpha on activated CD4+ T cell clones provides a costimulatory signal for human B cell activation. The Journal of Experimental Medicine *177*, 1575–1585.

Baldwin, A.S. (2001). Control of oncogenesis and cancer therapy resistance by the transcription factor NF-kappaB. The Journal of Clinical Investigation *107*, 241–246.

Beckwith, M., Longo, D.L., O'Connell, C.D., Moratz, C.M., and Urba, W.J. (1990). Phorbol ester-induced, cell-cycle-specific, growth inhibition of human B-lymphoma cell lines. Journal of the National Cancer Institute *82*, 501–509.

Behrens, T.W., Jagadeesh, J., Scherle, P., Kearns, G., Yewdell, J., and Staudt, L.M. (1994). Jaw1, A lymphoid-restricted membrane protein localized to the endoplasmic reticulum. Journal of Immunology (Baltimore, Md. : 1950) *153*, 682–690.

Ben-Bassat, H., Goldblum, N., Mitrani, S., Goldblum, T., Yoffey, J.M., Cohen, M.M., Bentwich, Z., Ramot, B., Klein, E., and Klein, G. (1977). Establishment in continuous culture of a new type of

lymphocyte from a “Burkitt like” malignant lymphoma (line D.G.-75). International Journal of Cancer. Journal International Du Cancer *19*, 27–33.

Bennett, B.L., Sasaki, D.T., Murray, B.W., O’Leary, E.C., Sakata, S.T., Xu, W., Leisten, J.C., Motiwala, A., Pierce, S., Satoh, Y., et al. (2001). SP600125, an anthrapyrazolone inhibitor of Jun N-terminal kinase. Proceedings of the National Academy of Sciences of the United States of America *98*, 13681–13686.

Bentink, S., Wessendorf, S., Schwaenen, C., Rosolowski, M., Klapper, W., Rosenwald, A., Ott, G., Banham, A.H., Berger, H., Feller, A.C., et al. (2008). Pathway activation patterns in diffuse large B-cell lymphomas. Leukemia *22*, 1746–1754.

Berek, C., Berger, A., and Apel, M. (1991). Maturation of the immune response in germinal centers. Cell *67*, 1121–1129.

Bidère, N., Ngo, V.N., Lee, J., Collins, C., Zheng, L., Wan, F., Davis, R.E., Lenz, G., Anderson, D.E., Arnoult, D., et al. (2009). Casein kinase 1alpha governs antigen-receptor-induced NF-kappaB activation and human lymphoma cell survival. Nature *458*, 92–96.

Bild, A.H., Yao, G., Chang, J.T., Wang, Q., Potti, A., Chasse, D., Joshi, M.-B., Harpole, D., Lancaster, J.M., Berchuck, A., et al. (2006). Oncogenic pathway signatures in human cancers as a guide to targeted therapies. Nature *439*, 353–357.

Birkenkamp, K.U., Tuyt, L.M., Lummen, C., Wierenga, A.T., Kruijer, W., and Vellenga, E. (2000). The p38 MAP kinase inhibitor SB203580 enhances nuclear factor-kappa B transcriptional activity by a non-specific effect upon the ERK pathway. British Journal of Pharmacology *131*, 99–107.

Bishop, P.C., Rao, V.K., and Wilson, W.H. (2000). Burkitt’s lymphoma: molecular pathogenesis and treatment. Cancer Investigation *18*, 574–583.

Blum, K.A., Lozanski, G., and Byrd, J.C. (2004). Adult Burkitt leukemia and lymphoma. Blood *104*, 3009–3020.

Van den Bosch, C.A. (2004). Is endemic Burkitt’s lymphoma an alliance between three infections and a tumour promoter? The Lancet Oncology *5*, 738–746.

Brady, G., Macarthur, G.J., and Farrell, P.J. (2008). Epstein-Barr virus and Burkitt lymphoma. Postgraduate Medical Journal *84*, 372–377.

Brocker, T., Gulbranson-Judge, A., Flynn, S., Riedinger, M., Raykundalia, C., and Lane, P. (1999). CD4 T cell traffic control: in vivo evidence that ligation of OX40 on CD4 T cells by OX40-ligand expressed on dendritic cells leads to the accumulation of CD4 T cells in B follicles. European Journal of Immunology *29*, 1610–1616.

Buglio, D., Palakurthi, S., Byth, K., Vega, F., Toader, D., Saeh, J., Neelapu, S.S., and Younes, A. (2012). Essential role of TAK1 in regulating mantle cell lymphoma survival. Blood *120*, 347–355.

Buonamici, S., Trimarchi, T., Ruocco, M.G., Reavie, L., Cathelin, S., Mar, B.G., Klinakis, A., Lukyanov, Y., Tseng, J.-C., Sen, F., et al. (2009). CCR7 signalling as an essential regulator of CNS infiltration in T-cell leukaemia. Nature *459*, 1000–1004.

Burgering, B.M.T., and Medema, R.H. (2003). Decisions on life and death: FOXO Forkhead transcription factors are in command when PKB/Akt is off duty. Journal of Leukocyte Biology *73*, 689–701.

Burkitt, D. (1958). A sarcoma involving the jaws in African children. The British Journal of Surgery *46*, 218–223.

Calpe, E., Codony, C., Baptista, M.J., Abrisqueta, P., Carpio, C., Purroy, N., Bosch, F., and Crespo, M. (2011). ZAP-70 enhances migration of malignant B lymphocytes toward CCL21 by inducing CCR7 expression via IgM-ERK1/2 activation. Blood *118*, 4401–4410.

Cambier, J.C. (1995). New nomenclature for the Reth motif (or ARH1/TAM/ARAM/YXXL). Immunology Today *16*, 110.

Cambier, J.C., and Johnson, S.A. (1995). Differential binding activity of ARH1/TAM motifs. Immunology Letters *44*, 77–80.

Campo, E., Swerdlow, S.H., Harris, N.L., Pileri, S., Stein, H., and Jaffe, E.S. (2011). The 2008 WHO classification of lymphoid neoplasms and beyond: evolving concepts and practical applications. Blood *117*, 5019–5032.

Cancer Research UK (2010). Non-Hodgkin lymphoma incidence statistics. Http://www.cancerresearchuk.org/cancer-info/cancerstats/types/nhl/incidence/uk-nonhodgkin-lymphoma-incidence-statistics#world.

Cargnello, M., and Roux, P.P. (2011). Activation and function of the MAPKs and their substrates, the MAPK-activated protein kinases. Microbiology and Molecular Biology Reviews : MMBR *75*, 50–83.

Chalhoub, N., and Baker, S.J. (2009). PTEN and the PI3-kinase pathway in cancer. Annual Review of Pathology *4*, 127–150.

Challa, A., Eliopoulos, A.G., Holder, M.J., Burguete, A.S., Pound, J.D., Chamba, A., Grafton, G., Armitage, R.J., Gregory, C.D., Martinez-Valdez, H., et al. (2002). Population depletion activates autonomous CD154-dependent survival in biopsylike Burkitt lymphoma cells. Blood *99*, 3411–3418.

Chang, H., Blondal, J.A., Benchimol, S., Minden, M.D., and Messner, H.A. (1995). p53 mutations, c-myc and bcl-2 rearrangements in human non-Hodgkin's lymphoma cell lines. Leukemia & Lymphoma *19*, 165–171.

Chang, H., Li, Q., Moraes, R.C., Lewis, M.T., and Hamel, P.A. (2010). Activation of Erk by sonic hedgehog independent of canonical hedgehog signalling. The International Journal of Biochemistry & Cell Biology *42*, 1462–1471.

Charbonnier, C., Chiquet, J., and Ambroise, C. (2010). Weighted-LASSO for structured network inference from time course data. Statistical Applications in Genetics and Molecular Biology *9*, Article 15.

Chen, L., Monti, S., Juszczynski, P., Daley, J., Chen, W., Witzig, T.E., Habermann, T.M., Kutok, J.L., and Shipp, M.A. (2008). SYK-dependent tonic B-cell receptor signaling is a rational treatment target in diffuse large B-cell lymphoma. Blood *111*, 2230–2237.

Cheng, P., Zlobin, A., Volgina, V., Gottipati, S., Osborne, B., Simel, E.J., Miele, L., and Gabrilovich, D.I. (2001). Notch-1 regulates NF-kappaB activity in hemopoietic progenitor cells. Journal of Immunology (Baltimore, Md. : 1950) *167*, 4458–4467.

Chiquet, J., Smith, A., Grasseau, G., Matias, C., and Ambroise, C. (2009). SIMoNe: Statistical Inference for MOdular NEtworks. Bioinformatics (Oxford, England) *25*, 417–418.

Ci, W., Polo, J.M., and Melnick, A. (2008). B-cell lymphoma 6 and the molecular pathogenesis of diffuse large B-cell lymphoma. Current Opinion in Hematology *15*, 381–390.

Ci, W., Polo, J.M., Cerchietti, L., Shaknovich, R., Wang, L., Yang, S.N., Ye, K., Farinha, P., Horsman, D.E., Gascoyne, R.D., et al. (2009). The BCL6 transcriptional program features repression of multiple oncogenes in primary B cells and is deregulated in DLBCL. Blood *113*, 5536–5548.

Cooke, E.J., Savage, R.S., Kirk, P.D., Darkins, R., and Wild, D.L. (2011). Bayesian hierarchical clustering for microarray time series data with replicates and outlier measurements. BMC.Bioinformatics. *12*, 399–.

Craxton, A., Shu, G., Graves, J.D., Saklatvala, J., Krebs, E.G., and Clark, E.A. (1998). p38 MAPK is required for CD40-induced gene expression and proliferation in B lymphocytes. Journal of Immunology (Baltimore, Md. : 1950) *161*, 3225–3236.

Di Cristofano, A., Pesce, B., Cordon-Cardo, C., and Pandolfi, P.P. (1998). Pten is essential for embryonic development and tumour suppression. Nature Genetics *19*, 348–355.

Cuadrado, A., and Nebreda, A.R. (2010). Mechanisms and functions of p38 MAPK signalling. The Biochemical Journal *429*, 403–417.

Cuenda, A., Rouse, J., Doza, Y.N., Meier, R., Cohen, P., Gallagher, T.F., Young, P.R., and Lee, J.C. (1995). SB 203580 is a specific inhibitor of a MAP kinase homologue which is stimulated by cellular stresses and interleukin-1. FEBS Letters *364*, 229–233.

Cultrera, J.L., and Dalia, S.M. (2012). Diffuse large B-cell lymphoma: current strategies and future directions. Cancer Control : Journal of the Moffitt Cancer Center *19*, 204–213.

Curnock, A.P., and Knox, K.A. (1998). LY294002-mediated inhibition of phosphatidylinositol 3-kinase activity triggers growth inhibition and apoptosis in CD40-triggered Ramos-Burkitt lymphoma B cells. Cellular Immunology *187*, 77–87.

Dal Porto, J.M., Gauld, S.B., Merrell, K.T., Mills, D., Pugh-Bernard, A.E., and Cambier, J. (2004). B cell antigen receptor signaling 101. Molecular Immunology *41*, 599–613.

Darkins, R., Cooke, E.J., Ghahramani, Z., Kirk, P.D.W., Wild, D.L., and Savage, R.S. (2013). Accelerating bayesian hierarchical clustering of time series data with a randomised algorithm. PloS One *8*, e59795.

Dave, B.J., Nelson, M., Pickering, D.L., Chan, W.C., Greiner, T.C., Weisenburger, D.D., Armitage, J.O., and Sanger, W.G. (2002). Cytogenetic characterization of diffuse large cell lymphoma using multi-color fluorescence in situ hybridization. Cancer Genetics and Cytogenetics *132*, 125–132.

Dave, S.S., Fu, K., Wright, G.W., Lam, L.T., Kluin, P., Boerma, E.-J., Greiner, T.C., Weisenburger, D.D., Rosenwald, A., Ott, G., et al. (2006). Molecular diagnosis of Burkitt's lymphoma. The New England Journal of Medicine *354*, 2431–2442.

Davis, R.E., Brown, K.D., Siebenlist, U., and Staudt, L.M. (2001). Constitutive nuclear factor kappaB activity is required for survival of activated B cell-like diffuse large B cell lymphoma cells. The Journal of Experimental Medicine *194*, 1861–1874.

Davis, R.E., Ngo, V.N., Lenz, G., Tolar, P., Young, R.M., Romesser, P.B., Kohlhammer, H., Lamy, L., Zhao, H., Yang, Y., et al. (2010). Chronic active B-cell-receptor signalling in diffuse large B-cell lymphoma. Nature *463*, 88–92.

Decker, S., Zirlik, K., Djebatchie, L., Hartmann, D., Ihorst, G., Schmitt-Graeff, A., Herchenbach, D., Jumaa, H., Warmuth, M., Veelken, H., et al. (2012). Trisomy 12 and elevated GLI1 and PTCH1 transcript levels are biomarkers for Hedgehog-inhibitor responsiveness in CLL. Blood *119*, 997–1007.

DeFranco, A.L. (1997). The complexity of signaling pathways activated by the BCR. Current Opinion in Immunology *9*, 296–308.

Delgado, P., Cubelos, B., Calleja, E., Martínez-Martín, N., Ciprés, A., Mérida, I., Bellas, C., Bustelo, X.R., and Alarcón, B. (2009). Essential function for the GTPase TC21 in homeostatic antigen receptor signaling. Nature Immunology *10*, 880–888.

Dierks, C., Grbic, J., Zirlik, K., Beigi, R., Englund, N.P., Guo, G.-R., Veelken, H., Engelhardt, M., Mertelsmann, R., Kelleher, J.F., et al. (2007). Essential role of stromally induced hedgehog signaling in B-cell malignancies. Nature Medicine *13*, 944–951.

DiSanto, J.P., Bonnefoy, J.Y., Gauchat, J.F., Fischer, A., and de Saint Basile, G. (1993). CD40 ligand mutations in x-linked immunodeficiency with hyper-IgM. Nature *361*, 541–543.

Dogan, I., Bertocci, B., Vilmont, V., Delbos, F., Mégret, J., Storck, S., Reynaud, C.-A., and Weill, J.-C. (2009). Multiple layers of B cell memory with different effector functions. Nature Immunology *10*, 1292–1299.

Ear, T., Fortin, C.F., Simard, F. a, and McDonald, P.P. (2010). Constitutive association of TGF-beta-activated kinase 1 with the IkappaB kinase complex in the nucleus and cytoplasm of human neutrophils and its impact on downstream processes. Journal of Immunology (Baltimore, Md. : 1950) *184*, 3897–3906.

Egawa, T., Albrecht, B., Favier, B., Sunshine, M.-J., Mirchandani, K., O'Brien, W., Thome, M., and Littman, D.R. (2003). Requirement for CARMA1 in antigen receptor-induced NF-kappa B activation and lymphocyte proliferation. Current Biology : CB *13*, 1252–1258.

Elgueta, R., Benson, M.J., de Vries, V.C., Wasiuk, A., Guo, Y., and Noelle, R.J. (2009). Molecular mechanism and function of CD40/CD40L engagement in the immune system. Immunological Reviews *229*, 152–172.

Eliopoulos, A.G., Dawson, C.W., Mosialos, G., Floettmann, J.E., Rowe, M., Armitage, R.J., Dawson, J., Zapata, J.M., Kerr, D.J., Wakelam, M.J., et al. (1996). CD40-induced growth inhibition in epithelial cells is mimicked by Epstein-Barr Virus-encoded LMP1: involvement of TRAF3 as a common mediator. Oncogene *13*, 2243–2254.

Epstein, A.L., Herman, M.M., Kim, H., Dorfman, R.F., and Kaplan, H.S. (1976). Biology of the human malignant lymphomas. III. Intracranial heterotransplantation in the nude, athymic mouse. Cancer *37*, 2158–2176.

Epstein, A.L., Levy, R., Kim, H., Henle, W., Henle, G., and Kaplan, H.S. (1978). Biology of the human malignant lymphomas. IV. Functional characterization of ten diffuse histiocytic lymphoma cell lines. Cancer *42*, 2379–2391.

Fahmi, H., Cochet, C., Hmama, Z., Opolon, P., and Joab, I. (2000). Transforming growth factor beta 1 stimulates expression of the Epstein-Barr virus BZLF1 immediate-early gene product ZEBRA by an indirect mechanism which requires the MAPK kinase pathway. Journal of Virology *74*, 5810–5818.

Favata, M.F., Horiuchi, K.Y., Manos, E.J., Daulerio, A.J., Stradley, D.A., Feeser, W.S., Van Dyk, D.E., Pitts, W.J., Earl, R.A., Hobbs, F., et al. (1998). Identification of a novel inhibitor of mitogen-activated protein kinase kinase. The Journal of Biological Chemistry *273*, 18623–18632.

Ferlay, J., Parkin, D.M., and Steliarova-Foucher, E. (2010). Estimates of cancer incidence and mortality in Europe in 2008. European Journal of Cancer (Oxford, England : 1990) *46*, 765–781.

Ferry, J.A. (2006). Burkitt's lymphoma: clinicopathologic features and differential diagnosis. The Oncologist *11*, 375–383.

Feugier, P., Van Hoof, A., Sebban, C., Solal-Celigny, P., Bouabdallah, R., Fermé, C., Christian, B., Lepage, E., Tilly, H., Morschhauser, F., et al. (2005). Long-term results of the R-CHOP study in the treatment of elderly patients with diffuse large B-cell lymphoma: a study by the Groupe d'Etude des Lymphomes de l'Adulte. Journal of Clinical Oncology : Official Journal of the American Society of Clinical Oncology *23*, 4117–4126.

Friedberg, J.W. (2011). Relapsed/refractory diffuse large B-cell lymphoma. Hematology / the Education Program of the American Society of Hematology. American Society of Hematology. Education Program *2011*, 498–505.

Friedman, N. (2004). Inferring cellular networks using probabilistic graphical models. Science (New York, N.Y.) *303*, 799–805.

Fröhlich, H., Fellmann, M., Sueltmann, H., Poustka, A., and Beissbarth, T. (2007). Large scale statistical inference of signaling pathways from RNAi and microarray data. BMC Bioinformatics *8*, 386.

Fukuda, T., Yoshida, T., Okada, S., Hatano, M., Miki, T., Ishibashi, K., Okabe, S., Koseki, H., Hirosawa, S., Taniguchi, M., et al. (1997). Disruption of the Bcl6 gene results in an impaired germinal center formation. The Journal of Experimental Medicine *186*, 439–448.

Funakoshi, S., Longo, D.L., Beckwith, M., Conley, D.K., Tsarfaty, G., Tsarfaty, I., Armitage, R.J., Fanslow, W.C., Spriggs, M.K., and Murphy, W.J. (1994). Inhibition of human B-cell lymphoma growth by CD40 stimulation. Blood *83*, 2787–2794.

Gaide, O., Favier, B., Legler, D.F., Bonnet, D., Brissoni, B., Valitutti, S., Bron, C., Tschopp, J., and Thome, M. (2002). CARMA1 is a critical lipid raft-associated regulator of TCR-induced NF-kappa B activation. Nature Immunology *3*, 836–843.

Gallagher, E., Enzler, T., Matsuzawa, A., Anzelon-Mills, A., Otero, D., Holzer, R., Janssen, E., Gao, M., and Karin, M. (2007). Kinase MEKK1 is required for CD40-dependent activation of the kinases Jnk and p38, germinal center formation, B cell proliferation and antibody production. Nature Immunology *8*, 57–63.

Gascan, H., Gauchat, J.F., Aversa, G., Van Vlasselaer, P., and de Vries, J.E. (1991). Anti-CD40 monoclonal antibodies or CD4+ T cell clones and IL-4 induce IgG4 and IgE switching in purified human B cells via different signaling pathways. Journal of Immunology (Baltimore, Md. : 1950) *147*, 8–13.

Gille, H., Kortenjann, M., Thomae, O., Moomaw, C., Slaughter, C., Cobb, M.H., and Shaw, P.E. (1995). ERK phosphorylation potentiates Elk-1-mediated ternary complex formation and transactivation. The EMBO Journal *14*, 951–962.

Gonçalves, J.P., Aires, R.S., Francisco, A.P., and Madeira, S.C. (2012). Regulatory Snapshots: integrative mining of regulatory modules from expression time series and regulatory networks. PloS One *7*, e35977.

Goodrich, L. V, and Scott, M.P. (1998). Hedgehog and patched in neural development and disease. Neuron *21*, 1243–1257.

Graf, D., Müller, S., Korthäuer, U., van Kooten, C., Weise, C., and Kroczek, R.A. (1995). A soluble form of TRAP (CD40 ligand) is rapidly released after T cell activation. European Journal of Immunology *25*, 1749–1754.

Gunvén, P., Klein, G., Klein, E., Norin, T., and Singh, S. (1980). Surface immunoglobulins on Burkitt's lymphoma biopsy cells from 91 patients. International Journal of Cancer. Journal International Du Cancer *25*, 711–719.

Hara, H., Wada, T., Bakal, C., Kozieradzki, I., Suzuki, S., Suzuki, N., Nghiem, M., Griffiths, E.K., Krawczyk, C., Bauer, B., et al. (2003). The MAGUK family protein CARD11 is essential for lymphocyte activation. Immunity *18*, 763–775.

Haye, A., Albert, J., and Rooman, M. (2012). Robust non-linear differential equation models of gene expression evolution across Drosophila development. BMC Research Notes *5*, 46.

Hecht, J.L., and Aster, J.C. (2000). Molecular biology of Burkitt's lymphoma. Journal of Clinical Oncology : Official Journal of the American Society of Clinical Oncology *18*, 3707–3721.

Hegde, G. V, Peterson, K.J., Emanuel, K., Mittal, A.K., Joshi, A.D., Dickinson, J.D., Kollessery, G.J., Bociek, R.G., Bierman, P., Vose, J.M., et al. (2008). Hedgehog-induced survival of B-cell chronic lymphocytic leukemia cells in a stromal cell microenvironment: a potential new therapeutic target. Molecular Cancer Research : MCR *6*, 1928–1936.

Heisig, J., Weber, D., Englberger, E., Winkler, A., Kneitz, S., Sung, W.-K., Wolf, E., Eilers, M., Wei, C.-L., and Gessler, M. (2012). Target gene analysis by microarrays and chromatin immunoprecipitation identifies HEY proteins as highly redundant bHLH repressors. PLoS Genetics *8*, e1002728.

Heller, K.A., and Ghahramani, Z. (2005). Bayesian hierarchical clustering. In Proceedings of the 22nd International Conference on Machine Learning - ICML '05, (New York, New York, USA: ACM Press), pp. 297–304.

Hermann, P., Blanchard, D., de Saint-Vis, B., Fossiez, F., Gaillard, C., Vanbervliet, B., Brière, F., Banchereau, J., and Galizzi, J.P. (1993). Expression of a 32-kDa ligand for the CD40 antigen on activated human T lymphocytes. European Journal of Immunology *23*, 961–964.

Hommel, G., and Kropf, S. (2005). Tests for Differentiation in Gene Expression Using a Data-Driven Order or Weights for Hypotheses. Biometrical Journal *47*, 554–562.

Horie, K., Ohashi, M., Satoh, Y., and Sairenji, T. (2007). The role of p38 mitogen-activated protein kinase in regulating interleukin-10 gene expression in Burkitt's lymphoma cell lines. Microbiology and Immunology *51*, 149–161.

Horikawa, K., Martin, S.W., Pogue, S.L., Silver, K., Peng, K., Takatsu, K., and Goodnow, C.C. (2007). Enhancement and suppression of signaling by the conserved tail of IgG memory-type B cell antigen receptors. The Journal of Experimental Medicine *204*, 759–769.

Hu, Y., Baud, V., Delhase, M., Zhang, P., Deerinck, T., Ellisman, M., Johnson, R., and Karin, M. (1999). Abnormal morphogenesis but intact IKK activation in mice lacking the IKKalpha subunit of IkappaB kinase. Science (New York, N.Y.) *284*, 316–320.

Huber, W., von Heydebreck, A., Sultmann, H., Poustka, A., and Vingron, M. (2002). Variance stabilization applied to microarray data calibration and to the quantification of differential expression. Bioinformatics *18*, S96–S104.

Hummel, M., Bentink, S., Berger, H., Klapper, W., Wessendorf, S., Barth, T.F.E., Bernd, H.-W., Cogliatti, S.B., Dierlamm, J., Feller, A.C., et al. (2006). A biologic definition of Burkitt's lymphoma from transcriptional and genomic profiling. The New England Journal of Medicine *354*, 2419–2430.

Hurlin, P.J., Quéva, C., and Eisenman, R.N. (1997a). Mnt, a novel Max-interacting protein is coexpressed with Myc in proliferating cells and mediates repression at Myc binding sites. Genes & Development *11*, 44–58.

Hurlin, P.J., Qúeva, C., and Eisenman, R.N. (1997b). Mnt: a novel Max-interacting protein and Myc antagonist. Current Topics in Microbiology and Immunology *224*, 115–121.

Ikram, M.S., Neill, G.W., Regl, G., Eichberger, T., Frischauf, A.-M., Aberger, F., Quinn, A., and Philpott, M. (2004). GLI2 is expressed in normal human epidermis and BCC and induces GLI1 expression by binding to its promoter. The Journal of Investigative Dermatology *122*, 1503–1509.

Incardona, J.P., Gaffield, W., Kapur, R.P., and Roelink, H. (1998). The teratogenic Veratrum alkaloid cyclopamine inhibits sonic hedgehog signal transduction. Development (Cambridge, England) *125*, 3553–3562.

Iqbal, J., Gupta, S., Chen, Q.H., Brody, J.P., and Koduru, P. (2007). Diffuse large B-cell lymphoma with a novel translocation involving BCL6. Cancer Genetics and Cytogenetics *178*, 73–76.

Irie, T., Muta, T., and Takeshige, K. (2000). TAK1 mediates an activation signal from toll-like receptor(s) to nuclear factor-kappaB in lipopolysaccharide-stimulated macrophages. FEBS Letters *467*, 160–164.

Irizarry, R.A. (2003). Summaries of Affymetrix GeneChip probe level data. Nucleic Acids Research *31*, 15e–15.

Jacob, J., Kelsoe, G., Rajewsky, K., and Weiss, U. (1991). Intraclonal generation of antibody mutants in germinal centres. Nature *354*, 389–392.

Jaffe, E.S. (2009). The 2008 WHO classification of lymphomas: implications for clinical practice and translational research. Hematology / the Education Program of the American Society of Hematology. American Society of Hematology. Education Program 523–531.

Jaffe, E.S., Harris, N.L., Diebold, J., and Müller-Hermelink, H.K. (1998). World Health Organization Classification of lymphomas: a work in progress. Ann Oncol. *9*, -.

Johnson, W.E., Li, C., and Rabinovic, A. (2007). Adjusting batch effects in microarray expression data using empirical Bayes methods. Biostatistics (Oxford, England) *8*, 118–127.

Ju, B., Spitsbergen, J., Eden, C.J., Taylor, M.R., and Chen, W. (2009). Co-activation of hedgehog and AKT pathways promote tumorigenesis in zebrafish. Molecular Cancer *8*, 40.

Jun, J.E., and Goodnow, C.C. (2003). Scaffolding of antigen receptors for immunogenic versus tolerogenic signaling. Nature Immunology *4*, 1057–1064.

Katoh, M., and Katoh, M. (2009). Transcriptional mechanisms of WNT5A based on NF-kappaB, Hedgehog, TGFbeta, and Notch signaling cascades. International Journal of Molecular Medicine *23*, 763–769.

Kawabe, T., Naka, T., Yoshida, K., Tanaka, T., Fujiwara, H., Suematsu, S., Yoshida, N., Kishimoto, T., and Kikutani, H. (1994). The immune responses in CD40-deficient mice: impaired immunoglobulin class switching and germinal center formation. Immunity *1*, 167–178.

Ke, J., Gururajan, M., Kumar, A., Simmons, A., Turcios, L., Chelvarajan, R.L., Cohen, D.M., Wiest, D.L., Monroe, J.G., and Bondada, S. (2006). The role of MAPKs in B cell receptor-induced down-regulation of Egr-1 in immature B lymphoma cells. The Journal of Biological Chemistry *281*, 39806–39818.

Klapproth, K., Sander, S., Marinkovic, D., Baumann, B., and Wirth, T. (2009). The IKK2/NF-{kappa}B pathway suppresses MYC-induced lymphomagenesis. Blood *114*, 2448–2458.

Klein, U., and Dalla-Favera, R. (2008). Germinal centres: role in B-cell physiology and malignancy. Nature Reviews. Immunology *8*, 22–33.

Klein, G., Giovanella, B., Westman, A., Stehlin, J.S., and Mumford, D. (1975). An EBV-genome-negative cell line established from an American Burkitt lymphoma; receptor characteristics. EBV infectibility and permanent conversion into EBV-positive sublines by in vitro infection. Intervirology *5*, 319–334.

Kloo, B., Nagel, D., Pfeifer, M., Grau, M., Düwel, M., Vincendeau, M., Dörken, B., Lenz, P., Lenz, G., and Krappmann, D. (2011). Critical role of PI3K signaling for NF-kappaB-dependent survival in a subset of activated B-cell-like diffuse large B-cell lymphoma cells. Proceedings of the National Academy of Sciences of the United States of America *108*, 272–277.

Van Kooten, C., and Banchereau, J. (2000). CD40-CD40 ligand. Journal of Leukocyte Biology *67*, 2–17.

Kopp, F., Stratton, C.F., Akella, L.B., and Tan, D.S. (2012). A diversity-oriented synthesis approach to macrocycles via oxidative ring expansion. Nature Chemical Biology *8*, 358–365.

Kramer, M.H., Hermans, J., Wijburg, E., Philippo, K., Geelen, E., van Krieken, J.H., de Jong, D., Maartense, E., Schuuring, E., and Kluin, P.M. (1998). Clinical relevance of BCL2, BCL6, and MYC rearrangements in diffuse large B-cell lymphoma. Blood *92*, 3152–3162.

Kraus, M., Alimzhanov, M.B., Rajewsky, N., and Rajewsky, K. (2004). Survival of resting mature B lymphocytes depends on BCR signaling via the Igalpha/beta heterodimer. Cell *117*, 787–800.

Kube, D., Platzer, C., von Knethen, A., Straub, H., Bohlen, H., Hafner, M., and Tesch, H. (1995). Isolation of the human interleukin 10 promoter. Characterization of the promoter activity in Burkitt's lymphoma cell lines. Cytokine *7*, 1–7.

Küppers, R. (2005). Mechanisms of B-cell lymphoma pathogenesis. Nature Reviews. Cancer *5*, 251–262.

Küppers, R., and Dalla-Favera, R. (2001). Mechanisms of chromosomal translocations in B cell lymphomas. Oncogene *20*, 5580–5594.

Küppers, R., Klein, U., Hansmann, M.L., and Rajewsky, K. (1999). Cellular origin of human B-cell lymphomas. The New England Journal of Medicine *341*, 1520–1529.

Kusam, S., Munugalavadla, V., Sawant, D., and Dent, A. (2009). BCL6 cooperates with CD40 stimulation and loss of p53 function to rapidly transform primary B cells. International Journal of Cancer. Journal International Du Cancer *125*, 977–981.

Kutz, H., Reisbach, G., Schultheiss, U., and Kieser, A. (2008). The c-Jun N-terminal kinase pathway is critical for cell transformation by the latent membrane protein 1 of Epstein-Barr virus. Virology *371*, 246–256.

Laemmli, U.K. (1970). Cleavage of structural proteins during the assembly of the head of bacteriophage T4. Nature *227*, 680–685.

Lam, K.P., Kühn, R., and Rajewsky, K. (1997). In vivo ablation of surface immunoglobulin on mature B cells by inducible gene targeting results in rapid cell death. Cell *90*, 1073–1083.

Lam, L.T., Davis, R.E., Pierce, J., Hepperle, M., Xu, Y., Hottelet, M., Nong, Y., Wen, D., Adams, J., Dang, L., et al. (2005). Small molecule inhibitors of IkappaB kinase are selectively toxic for subgroups of diffuse large B-cell lymphoma defined by gene expression profiling. Clinical Cancer Research : an Official Journal of the American Association for Cancer Research *11*, 28–40.

Lam, L.T., Wright, G., Davis, R.E., Lenz, G., Farinha, P., Dang, L., Chan, J.W., Rosenwald, A., Gascoyne, R.D., and Staudt, L.M. (2008). Cooperative signaling through the signal transducer and activator of transcription 3 and nuclear factor-{kappa}B pathways in subtypes of diffuse large B-cell lymphoma. Blood *111*, 3701–3713.

Lane, P., Traunecker, A., Hubele, S., Inui, S., Lanzavecchia, A., and Gray, D. (1992). Activated human T cells express a ligand for the human B cell-associated antigen CD40 which participates in T cell-dependent activation of B lymphocytes. European Journal of Immunology *22*, 2573–2578.

Läuter, J., Glimm, E., and Kropf, S. (1996). New Tests for Data with an Inherent Structure. Biometrical Journal *38*, 1–23.

Läuter, J., Glimm, E., and Kropf, S. (1998). Multivariate tests based on left-spherically distributed linear scores. The Annals of Statistics *26*, 1972–1988.

Läuter, J., Rosolowski, M., and Glimm, E. (2012). Exact Multivariate Tests - A New Effective Principle of Controlled Model Choice. 18.

Lee, W.-P., and Tzou, W.-S. (2009). Computational methods for discovering gene networks from expression data. Briefings in Bioinformatics *10*, 408–423.

Lee, J., Platt, K.A., Censullo, P., and Ruiz i Altaba, A. (1997). Gli1 is a target of Sonic hedgehog that induces ventral neural tube development. Development (Cambridge, England) *124*, 2537–2552.

Lee, J.C., Laydon, J.T., McDonnell, P.C., Gallagher, T.F., Kumar, S., Green, D., McNulty, D., Blumenthal, M.J., Heys, J.R., and Landvatter, S.W. (1994). A protein kinase involved in the regulation of inflammatory cytokine biosynthesis. Nature *372*, 739–746.

Lee, J.K.J., Mathew, S.O.S., Vaidya, S. V, Kumaresan, P.R., and Mathew, P.A. (2007). CS1 (CRACC, CD319) induces proliferation and autocrine cytokine expression on human B lymphocytes. The Journal of … *179*, 4672–4678.

Lenoir, G.M., Vuillaume, M., and Bonnardel, C. (1985). The use of lymphomatous and lymphoblastoid cell lines in the study of Burkitt's lymphoma. IARC Sci.Publ. 309–318.

Lenz, G., Wright, G.W., Emre, N.C.T., Kohlhammer, H., Dave, S.S., Davis, R.E., Carty, S., Lam, L.T., Shaffer, a L., Xiao, W., et al. (2008). Molecular subtypes of diffuse large B-cell lymphoma arise by distinct genetic pathways. Proceedings of the National Academy of Sciences of the United States of America *105*, 13520–13525.

Li, Q., and Verma, I.M. (2002). NF-kappaB regulation in the immune system. Nature Reviews. Immunology *2*, 725–734.

Li, Z.W., Chu, W., Hu, Y., Delhase, M., Deerinck, T., Ellisman, M., Johnson, R., and Karin, M. (1999). The IKKbeta subunit of IkappaB kinase (IKK) is essential for nuclear factor kappaB activation and prevention of apoptosis. The Journal of Experimental Medicine *189*, 1839–1845.

Lin, T.L., Wang, Q.H., Brown, P., Peacock, C., Merchant, A. a, Brennan, S., Jones, E., McGovern, K., Watkins, D.N., Sakamoto, K.M., et al. (2010). Self-renewal of acute lymphocytic leukemia cells is limited by the Hedgehog pathway inhibitors cyclopamine and IPI-926. PloS One *5*, e15262.

Lindemann, R.K. (2008). Stroma-initiated hedgehog signaling takes center stage in B-cell lymphoma. Cancer Research *68*, 961–964.

Lohr, J.G., Stojanov, P., Lawrence, M.S., Auclair, D., Chapuy, B., Sougnez, C., Cruz-Gordillo, P., Knoechel, B., Asmann, Y.W., Slager, S.L., et al. (2012). Discovery and prioritization of somatic mutations in diffuse large B-cell lymphoma (DLBCL) by whole-exome sequencing. Proceedings of the National Academy of Sciences of the United States of America *109*, 3879–3884.

Van der Lugt, N.M., Domen, J., Verhoeven, E., Linders, K., van der Gulden, H., Allen, J., and Berns, A. (1995). Proviral tagging in E mu-myc transgenic mice lacking the Pim-1 proto-oncogene leads to compensatory activation of Pim-2. The EMBO Journal *14*, 2536–2544.

MacLennan, I.C. (1994). Germinal centers. Annual Review of Immunology *12*, 117–139.

Madhala-Levy, D., Williams, V.C., Hughes, S.M., Reshef, R., and Halevy, O. (2012). Cooperation between Shh and IGF-I in promoting myogenic proliferation and differentiation via the MAPK/ERK and PI3K/Akt pathways requires Smo activity. Journal of Cellular Physiology *227*, 1455–1464.

Magrath, I., Adde, M., Shad, A., Venzon, D., Seibel, N., Gootenberg, J., Neely, J., Arndt, C., Nieder, M., Jaffe, E., et al. (1996). Adults and children with small non-cleaved-cell lymphoma have a similar excellent outcome when treated with the same chemotherapy regimen. Journal of Clinical Oncology : Official Journal of the American Society of Clinical Oncology *14*, 925–934.

Mangelberger, D., Kern, D., Loipetzberger, A., Eberl, M., and Aberger, F. (2012). Cooperative Hedgehog-EGFR signaling. Frontiers in Bioscience : a Journal and Virtual Library *17*, 90–99.

Mar, B.G., Amakye, D., Aifantis, I., and Buonamici, S. (2011). The controversial role of the Hedgehog pathway in normal and malignant hematopoiesis. Leukemia *25*, 1665–1673.

Marigo, V., and Tabin, C.J. (1996). Regulation of patched by sonic hedgehog in the developing neural tube. Proceedings of the National Academy of Sciences of the United States of America *93*, 9346–9351.

Marino, S. (2005). Medulloblastoma: developmental mechanisms out of control. Trends in Molecular Medicine *11*, 17–22.

Markman, B., Atzori, F., Pérez-García, J., Tabernero, J., and Baselga, J. (2010). Status of PI3K inhibition and biomarker development in cancer therapeutics. Annals of Oncology : Official Journal of the European Society for Medical Oncology / ESMO *21*, 683–691.

Markowetz, F., and Spang, R. (2007). Inferring cellular networks--a review. BMC Bioinformatics *8 Suppl 6*, S5.

Markowetz, F., Bloch, J., and Spang, R. (2005). Non-transcriptional pathway features reconstructed from secondary effects of RNA interference. Bioinformatics (Oxford, England) *21*, 4026–4032.

Markowetz, F., Kostka, D., Troyanskaya, O.G., and Spang, R. (2007). Nested effects models for high-dimensional phenotyping screens. Bioinformatics (Oxford, England) *23*, i305–12.

Martin, S.W., and Goodnow, C.C. (2002). Burst-enhancing role of the IgG membrane tail as a molecular determinant of memory. Nature Immunology *3*, 182–188.

De Matos Simoes, R., Tripathi, S., and Emmert-Streib, F. (2012). Organizational structure and the periphery of the gene regulatory network in B-cell lymphoma. BMC Systems Biology *6*, 38.

Matsuzawa, A., Tseng, P.-H., Vallabhapurapu, S., Luo, J.-L., Zhang, W., Wang, H., Vignali, D.A.A., Gallagher, E., and Karin, M. (2008). Essential cytoplasmic translocation of a cytokine receptor-assembled signaling complex. Science (New York, N.Y.) *321*, 663–668.

Mazzei, G.J., Edgerton, M.D., Losberger, C., Lecoanet-Henchoz, S., Graber, P., Durandy, A., Gauchat, J.F., Bernard, A., Allet, B., and Bonnefoy, J.Y. (1995). Recombinant soluble trimeric CD40 ligand is biologically active. The Journal of Biological Chemistry *270*, 7025–7028.

Mead, G.M., Sydes, M.R., Walewski, J., Grigg, A., Hatton, C.S., Pescosta, N., Guarnaccia, C., Lewis, M.S., McKendrick, J., Stenning, S.P., et al. (2002). An international evaluation of CODOX-M and CODOX-M alternating with IVAC in adult Burkitt's lymphoma: results of United Kingdom Lymphoma Group LY06 study. Annals of Oncology : Official Journal of the European Society for Medical Oncology / ESMO *13*, 1264–1274.

Mizuarai, S., Kawagishi, A., and Kotani, H. (2009). Inhibition of p70S6K2 down-regulates Hedgehog/GLI pathway in non-small cell lung cancer cell lines. Molecular Cancer *8*, 44.

Mogami, H., Mills, C., and Gallacher, D. (1997). inhibitor, U73122, releases intracellular Ca2+, potentiates Ins (1, 4, 5) P3-mediated Ca2+ release and directly activates ion channels in mouse pancreatic acinar cells. Biochemical Journal *324 (Pt 2*, 645–651.

Monroe, J.G. (2006). ITAM-mediated tonic signalling through pre-BCR and BCR complexes. Nature Reviews. Immunology *6*, 283–294.

Murata, T., Shimada, M., Sakakibara, S., Yoshino, T., Kadono, H., Masuda, T., Shimazaki, M., Shintani, T., Fuchikami, K., Sakai, K., et al. (2003). Discovery of novel and selective IKK-beta serine-threonine protein kinase inhibitors. Part 1. Bioorganic & Medicinal Chemistry Letters *13*, 913–918.

Nascimento, M., Sáfadi, T., Fonseca e Silva, F., and Nascimento, A.C.C. (2012). Bayesian model-based clustering of temporal gene expression using autoregressive panel data approach. Bioinformatics (Oxford, England) *28*, 2004–2007.

Newton, K., and Dixit, V.M. (2003). Mice lacking the CARD of CARMA1 exhibit defective B lymphocyte development and impaired proliferation of their B and T lymphocytes. Current Biology : CB *13*, 1247–1251.

Ngo, V.N., Davis, R.E., Lamy, L., Yu, X., Zhao, H., Lenz, G., Lam, L.T., Dave, S., Yang, L., Powell, J., et al. (2006). A loss-of-function RNA interference screen for molecular targets in cancer. Nature *441*, 106–110.

Nilsson, K., and Pontén, J. (1975). Classification and biological nature of established human hematopoietic cell lines. International Journal of Cancer. Journal International Du Cancer *15*, 321–341.

Ninomiya-Tsuji, J., Kishimoto, K., Hiyama, A., Inoue, J., Cao, Z., and Matsumoto, K. (1999). The kinase TAK1 can activate the NIK-I kappaB as well as the MAP kinase cascade in the IL-1 signalling pathway. Nature *398*, 252–256.

Ninomiya-Tsuji, J., Kajino, T., Ono, K., Ohtomo, T., Matsumoto, M., Shiina, M., Mihara, M., Tsuchiya, M., and Matsumoto, K. (2003). A resorcylic acid lactone, 5Z-7-oxozeaenol, prevents inflammation by inhibiting the catalytic activity of TAK1 MAPK kinase kinase. The Journal of Biological Chemistry *278*, 18485–18490.

Nishimura, M., Shin, M.-S., Singhirunnusorn, P., Suzuki, S., Kawanishi, M., Koizumi, K., Saiki, I., and Sakurai, H. (2009). TAK1-mediated serine/threonine phosphorylation of epidermal growth factor receptor via p38/extracellular signal-regulated kinase: NF-{kappa}B-independent survival pathways in tumor necrosis factor alpha signaling. Molecular and Cellular Biology *29*, 5529–5539.

Nussenzweig, A., and Nussenzweig, M.C. (2010). Origin of chromosomal translocations in lymphoid cancer. Cell *141*, 27–38.

Nüsslein-Volhard, C., and Wieschaus, E. (1980). Mutations affecting segment number and polarity in Drosophila. Nature *287*, 795–801.

Ohori, M., Kinoshita, T., Yoshimura, S., Warizaya, M., Nakajima, H., and Miyake, H. (2007). Role of a cysteine residue in the active site of ERK and the MAPKK family. Biochemical and Biophysical Research Communications *353*, 633–637.

Ok, C.Y., Singh, R.R., and Vega, F. (2012). Aberrant activation of the hedgehog signaling pathway in malignant hematological neoplasms. The American Journal of Pathology *180*, 2–11.

Okuyama, K., Murata, A., Sudo, T., Yoshino, M., and Hayashi, S.-I. (2012). A checkpoint in B-lymphopoiesis related to Notch resistance. Biochemical and Biophysical Research Communications *417*, 141–146.

Oliveros, J.C. (2007). VENNY. An interactive tool for comparing lists with Venn Diagrams.

Parekh, S., Polo, J.M., Shaknovich, R., Juszczynski, P., Lev, P., Ranuncolo, S.M., Yin, Y., Klein, U., Cattoretti, G., Dalla Favera, R., et al. (2007). BCL6 programs lymphoma cells for survival and differentiation through distinct biochemical mechanisms. Blood *110*, 2067–2074.

Pattle, S.B., and Farrell, P.J. (2006). The role of Epstein-Barr virus in cancer. Expert Opinion on Biological Therapy *6*, 1193–1205.

Pearson, G. (2001). Mitogen-Activated Protein (MAP) Kinase Pathways: Regulation and Physiological Functions. Endocrine Reviews *22*, 153–183.

Pellat-Deceunynck, C., Amiot, M., Robillard, N., Wijdenes, J., and Bataille, R. (1996). CD11a-CD18 and CD102 interactions mediate human myeloma cell growth arrest induced by CD40 stimulation. Cancer Research *56*, 1909–1916.

Perkins, A.S., and Friedberg, J.W. (2008). Burkitt lymphoma in adults. Hematology / the Education Program of the American Society of Hematology. American Society of Hematology. Education Program 341–348.

Pham, L. V, Tamayo, A.T., Yoshimura, L.C., Lo, P., Terry, N., Reid, P.S., and Ford, R.J. (2002). A CD40 Signalosome anchored in lipid rafts leads to constitutive activation of NF-kappaB and autonomous cell growth in B cell lymphomas. Immunity *16*, 37–50.

Pogue, S.L., Kurosaki, T., Bolen, J., and Herbst, R. (2000). B cell antigen receptor-induced activation of Akt promotes B cell survival and is dependent on Syk kinase. Journal of Immunology (Baltimore, Md. : 1950) *165*, 1300–1306.

Polo, J.M., Dell'Oso, T., Ranuncolo, S.M., Cerchietti, L., Beck, D., Da Silva, G.F., Prive, G.G., Licht, J.D., and Melnick, A. (2004). Specific peptide interference reveals BCL6 transcriptional and oncogenic mechanisms in B-cell lymphoma cells. Nature Medicine *10*, 1329–1335.

Polo, J.M., Juszczynski, P., Monti, S., Cerchietti, L., Ye, K., Greally, J.M., Shipp, M., and Melnick, A. (2007). Transcriptional signature with differential expression of BCL6 target genes accurately identifies BCL6-dependent diffuse large B cell lymphomas. Proceedings of the National Academy of Sciences of the United States of America *104*, 3207–3212.

Powles, T., Matthews, G., and Bower, M. (2000). AIDS related systemic non-Hodgkin's lymphoma. Sexually Transmitted Infections *76*, 335–341.

Pui, J.C., Allman, D., Xu, L., DeRocco, S., Karnell, F.G., Bakkour, S., Lee, J.Y., Kadesch, T., Hardy, R.R., Aster, J.C., et al. (1999). Notch1 expression in early lymphopoiesis influences B versus T lineage determination. Immunity *11*, 299–308.

Qu, C., Liu, Y., Kunkalla, K., Singh, R.R., Blonska, M., Lin, X., Agarwal, N.K., and Vega, F. (2013). Trimeric G protein-CARMA1 axis links smoothened, the hedgehog receptor transducer, to NF-κB activation in diffuse large B-cell lymphoma. Blood 4718–4728.

Radtke, F., Wilson, A., and MacDonald, H.R. (2004). Notch signaling in T- and B-cell development. Current Opinion in Immunology *16*, 174–179.

Rakowski, L.A., Garagiola, D.D., Li, C.M., Decker, M., Caruso, S., Jones, M., Kuick, R., Cierpicki, T., Maillard, I., and Chiang, M.Y. (2013). Convergence of the ZMIZ1 and NOTCH1 pathways at C-MYC in acute T lymphoblastic leukemias. Cancer Research *73*, 930–941.

Raman, M., Chen, W., and Cobb, M.H. (2007). Differential regulation and properties of MAPKs. Oncogene *26*, 3100–3112.

Ramirez, E., Singh, R.R., Kunkalla, K., Liu, Y., Qu, C., Cain, C., Multani, A.S., Lennon, P.A., Jackacky, J., Ho, M., et al. (2012). Defining causative factors contributing in the activation of hedgehog signaling in diffuse large B-cell lymphoma. Leukemia Research *36*, 1267–1273.

Rao, G., Pedone, C.A., Coffin, C.M., Holland, E.C., and Fults, D.W. c-Myc enhances sonic hedgehog-induced medulloblastoma formation from nestin-expressing neural progenitors in mice. Neoplasia (New York, N.Y.) *5*, 198–204.

Rehm, A., Mensen, A., Schradi, K., Gerlach, K., Wittstock, S., Winter, S., Büchner, G., Dörken, B., Lipp, M., and Höpken, U.E. (2011). Cooperative function of CCR7 and lymphotoxin in the formation of a lymphoma-permissive niche within murine secondary lymphoid organs. Blood *118*, 1020–1033.

Reth, M. (1989). Antigen receptor tail clue. Nature *338*, 383–384.

Reya, T., O'Riordan, M., Okamura, R., Devaney, E., Willert, K., Nusse, R., and Grosschedl, R. (2000). Wnt signaling regulates B lymphocyte proliferation through a LEF-1 dependent mechanism. Immunity *13*, 15–24.

Richards, J.D., Gold, M.R., Hourihane, S.L., DeFranco, A.L., and Matsuuchi, L. (1996). Reconstitution of B cell antigen receptor-induced signaling events in a nonlymphoid cell line by expressing the Syk protein-tyrosine kinase. The Journal of Biological Chemistry *271*, 6458–6466.

Richards, J.D., Davé, S.H., Chou, C.H., Mamchak, a a, and DeFranco, a L. (2001). Inhibition of the MEK/ERK signaling pathway blocks a subset of B cell responses to antigen. Journal of Immunology (Baltimore, Md. : 1950) *166*, 3855–3864.

Rosenwald, A., Wright, G., Chan, W.C., Connors, J.M., Campo, E., Fisher, R.I., Gascoyne, R.D., Muller-Hermelink, H.K., Smeland, E.B., Giltnane, J.M., et al. (2002). The use of molecular profiling to predict survival after chemotherapy for diffuse large-B-cell lymphoma. The New England Journal of Medicine *346*, 1937–1947.

Rowley, R.B., Burkhardt, A.L., Chao, H.G., Matsueda, G.R., and Bolen, J.B. (1995). Syk protein-tyrosine kinase is regulated by tyrosine-phosphorylated Ig alpha/Ig beta immunoreceptor tyrosine activation motif binding and autophosphorylation. The Journal of Biological Chemistry *270*, 11590–11594.

Ruefli-Brasse, A.A., French, D.M., and Dixit, V.M. (2003). Regulation of NF-kappaB-dependent lymphocyte activation and development by paracaspase. Science (New York, N.Y.) *302*, 1581–1584.

Ruland, J., and Mak, T.W. (2003). Transducing signals from antigen receptors to nuclear factor kappaB. Immunological Reviews *193*, 93–100.

Ruland, J., Duncan, G.S., Elia, A., del Barco Barrantes, I., Nguyen, L., Plyte, S., Millar, D.G., Bouchard, D., Wakeham, A., Ohashi, P.S., et al. (2001). Bcl10 is a positive regulator of antigen receptor-induced activation of NF-kappaB and neural tube closure. Cell *104*, 33–42.

Ruland, J., Duncan, G.S., Wakeham, A., and Mak, T.W. (2003). Differential requirement for Malt1 in T and B cell antigen receptor signaling. Immunity *19*, 749–758.

Sacedón, R., Díez, B., Nuñez, V., Hernández-López, C., Gutierrez-Frías, C., Cejalvo, T., Outram, S. V, Crompton, T., Zapata, A.G., Vicente, A., et al. (2005). Sonic hedgehog is produced by follicular dendritic cells and protects germinal center B cells from apoptosis. J.Immunol. *174*, 1456–1461.

Saijo, K., Schmedt, C., Su, I.-H., Karasuyama, H., Lowell, C.A., Reth, M., Adachi, T., Patke, A., Santana, A., and Tarakhovsky, A. (2003). Essential role of Src-family protein tyrosine kinases in NF-kappaB activation during B cell development. Nature Immunology *4*, 274–279.

Saito, M., Novak, U., Piovan, E., Basso, K., Sumazin, P., Schneider, C., Crespo, M., Shen, Q., Bhagat, G., Califano, A., et al. (2009). BCL6 suppression of BCL2 via Miz1 and its disruption in diffuse large B cell lymphoma. Proceedings of the National Academy of Sciences of the United States of America *106*, 11294–11299.

Salmena, L., Carracedo, A., and Pandolfi, P.P. (2008). Tenets of PTEN Tumor Suppression. Cell *133*, 403–414.

Sanda, T., Iida, S., Ogura, H., and Asamitsu, K. (2005). Growth inhibition of multiple myeloma cells by a novel IκB kinase inhibitor. Clinical Cancer … *11*, 1974–1982.

Sander, S., Calado, D.P., Srinivasan, L., Köchert, K., Zhang, B., Rosolowski, M., Rodig, S.J., Holzmann, K., Stilgenbauer, S., Siebert, R., et al. (2012). Synergy between PI3K signaling and MYC in Burkitt lymphomagenesis. Cancer Cell *22*, 167–179.

Sarbassov, D.D., Guertin, D.A., Ali, S.M., and Sabatini, D.M. (2005). Phosphorylation and regulation of Akt/PKB by the rictor-mTOR complex. Science (New York, N.Y.) *307*, 1098–1101.

Sato, S., Sanjo, H., Takeda, K., Ninomiya-Tsuji, J., Yamamoto, M., Kawai, T., Matsumoto, K., Takeuchi, O., and Akira, S. (2005). Essential function for the kinase TAK1 in innate and adaptive immune responses. Nature Immunology *6*, 1087–1095.

Savage, R.S., Heller, K., Xu, Y., Ghahramani, Z., Truman, W.M., Grant, M., Denby, K.J., and Wild, D.L. (2009). R/BHC: fast Bayesian hierarchical clustering for microarray data. BMC Bioinformatics *10*, 242.

Schirmer, A., Kennedy, J., Murli, S., Reid, R., and Santi, D. V (2006). Targeted covalent inactivation of protein kinases by resorcylic acid lactone polyketides. Proceedings of the National Academy of Sciences of the United States of America *103*, 4234–4239.

Schmitz, R., Stanelle, J., Hansmann, M.-L., and Küppers, R. (2009). Pathogenesis of classical and lymphocyte-predominant Hodgkin lymphoma. Annual Review of Pathology *4*, 151–174.

Schmitz, R., Young, R.M., Ceribelli, M., Jhavar, S., Xiao, W., Zhang, M., Wright, G., Shaffer, A.L., Hodson, D.J., Buras, E., et al. (2012). Burkitt lymphoma pathogenesis and therapeutic targets from structural and functional genomics. Nature *490*, 116–120.

Schnidar, H., Eberl, M., Klingler, S., Mangelberger, D., Kasper, M., Hauser-Kronberger, C., Regl, G., Kroismayr, R., Moriggl, R., Sibilia, M., et al. (2009). Epidermal growth factor receptor signaling synergizes with Hedgehog/GLI in oncogenic transformation via activation of the MEK/ERK/JUN pathway. Cancer Research *69*, 1284–1292.

Schrader, A. (2011). Identification and functional characterization of oncogenic pathway signatures in malignant lymphoma. Georg-August University Göttingen.

Schrader, A., Bentink, S., Spang, R., Lenze, D., Hummel, M., Kuo, M., Arrand, J.R., Murray, P.G., Trümper, L., Kube, D., et al. (2012a). High Myc activity is an independent negative prognostic factor for diffuse large B cell lymphomas. International Journal of Cancer. Journal International Du Cancer *131*, E348–61.

Schrader, A., Meyer, K., von Bonin, F., Vockerodt, M., Walther, N., Hand, E., Ulrich, A., Matulewicz, K., Lenze, D., Hummel, M., et al. (2012b). Global gene expression changes of in vitro stimulated human transformed germinal centre B cells as surrogate for oncogenic pathway activation in individual aggressive B cell lymphomas. Cell Communication and Signaling : CCS *10*, 43.

Schrantz, N., Bourgeade, M.F., Mouhamad, S., Leca, G., Sharma, S., and Vazquez, A. (2001). p38-mediated regulation of an Fas-associated death domain protein-independent pathway leading to caspase-8 activation during TGFbeta-induced apoptosis in human Burkitt lymphoma B cells BL41. Molecular Biology of the Cell *12*, 3139–3151.

Schreiber, E., Matthias, P., Müller, M.M., and Schaffner, W. (1989). Rapid detection of octamer binding proteins with “mini-extracts”, prepared from a small number of cells. Nucleic Acids Research *17*, 6419.

Schulz, M.H., Devanny, W.E., Gitter, A., Zhong, S., Ernst, J., and Bar-Joseph, Z. (2012). DREM 2.0: Improved reconstruction of dynamic regulatory networks from time-series expression data. BMC Systems Biology *6*, 104.

Schuman, J., Chen, Y., Podd, A., Yu, M., Liu, H.-H., Wen, R., Chen, Z.J., and Wang, D. (2009). A critical role of TAK1 in B-cell receptor-mediated nuclear factor kappaB activation. Blood *113*, 4566–4574.

Schwanbeck, R., and Just, U. (2011). The Notch signaling pathway in hematopoiesis and hematologic malignancies. Haematologica *96*, 1735–1737.

Segal, G.H., Edinger, M.G., Owen, M., McNealis, M., Lopez, P., Perkins, A., Linden, M.D., Fishleder, A.J., Stoler, M.H., and Tubbs, R.R. (1991). Concomitant delineation of surface Ig, B-cell differentiation antigens, and HLADR on lymphoid proliferations using three-color immunocytometry. Cytometry *12*, 350–359.

Senftleben, U., Cao, Y., Xiao, G., Greten, F.R., Krähn, G., Bonizzi, G., Chen, Y., Hu, Y., Fong, A., Sun, S.C., et al. (2001). Activation by IKKalpha of a second, evolutionary conserved, NF-kappa B signaling pathway. Science (New York, N.Y.) *293*, 1495–1499.

Shinohara, H., and Kurosaki, T. (2009). Comprehending the complex connection between PKCbeta, TAK1, and IKK in BCR signaling. Immunological Reviews *232*, 300–318.

Shinohara, H., Yasuda, T., Aiba, Y., Sanjo, H., Hamadate, M., Watarai, H., Sakurai, H., and Kurosaki, T. (2005). PKC beta regulates BCR-mediated IKK activation by facilitating the interaction between TAK1 and CARMA1. The Journal of Experimental Medicine *202*, 1423–1431.

Shirogane, T., Fukada, T., Muller, J.M., Shima, D.T., Hibi, M., and Hirano, T. (1999). Synergistic roles for Pim-1 and c-Myc in STAT3-mediated cell cycle progression and antiapoptosis. Immunity *11*, 709–719.

Shkoda, A., Town, J. a, Griese, J., Romio, M., Sarioglu, H., Knöfel, T., Giehler, F., Kieser, A., and Knofel, T. (2012). The germinal center kinase TNIK is required for canonical NF-kappaB and JNK signaling in B-cells by the EBV oncoprotein LMP1 and the CD40 receptor. PLoS.Biol. *10*, e1001376–.

Siggins, S.L., Nguyen, N.-Y.N., McCormack, M.P., Vasudevan, S., Villani, R., Jane, S.M., Wainwright, B.J., and Curtis, D.J. (2009). The Hedgehog receptor Patched1 regulates myeloid and lymphoid progenitors by distinct cell-extrinsic mechanisms. Blood *114*, 995–1004.

Singh, R.R., Cho-Vega, J.H., Davuluri, Y., Ma, S., Kasbidi, F., Milito, C., Lennon, P.A., Drakos, E., Medeiros, L.J., Luthra, R., et al. (2009). Sonic hedgehog signaling pathway is activated in ALK-positive anaplastic large cell lymphoma. Cancer Research *69*, 2550–2558.

Singh, R.R., Kim, J.E., Davuluri, Y., Drakos, E., Cho-Vega, J.H., Amin, H.M., and Vega, F. (2010). Hedgehog signaling pathway is activated in diffuse large B-cell lymphoma and contributes to tumor cell survival and proliferation. Leukemia *24*, 1025–1036.

Singh, R.R., Kunkalla, K., Qu, C., Schlette, E., Neelapu, S.S., Samaniego, F., and Vega, F. (2011). ABCG2 is a direct transcriptional target of hedgehog signaling and involved in stroma-induced drug tolerance in diffuse large B-cell lymphoma. Oncogene *30*, 4874–4886.

Smyth, G.K. (2005). Limma: linear models for microarray data. In Bioinformatics and Computational Biology Solutions Using R and Bioconductor, R. Gentleman, V.J. Carey, W. Huber, R.A. Irizarry, and S. Dudoit, eds. (New York: Springer-Verlag), pp. 397–420.

Smyth, G.K., Michaud, J., and Scott, H.S. (2005). Use of within-array replicate spots for assessing differential expression in microarray experiments. Bioinformatics (Oxford, England) *21*, 2067–2075.

Sommer, A., Bousset, K., Kremmer, E., Austen, M., and Lüscher, B. (1998). Identification and characterization of specific DNA-binding complexes containing members of the Myc/Max/Mad network of transcriptional regulators. The Journal of Biological Chemistry *273*, 6632–6642.

Sorrentino, A., Thakur, N., Grimsby, S., Marcusson, A., von Bulow, V., Schuster, N., Zhang, S., Heldin, C.-H., and Landström, M. (2008). The type I TGF-beta receptor engages TRAF6 to activate TAK1 in a receptor kinase-independent manner. Nature Cell Biology *10*, 1199–1207.

Spriggs, M.K., Armitage, R.J., Strockbine, L., Clifford, K.N., Macduff, B.M., Sato, T.A., Maliszewski, C.R., and Fanslow, W.C. (1992). Recombinant human CD40 ligand stimulates B cell proliferation and immunoglobulin E secretion. The Journal of Experimental Medicine *176*, 1543–1550.

Stevenson, F.K., Sahota, S.S., Ottensmeier, C.H., Zhu, D., Forconi, F., and Hamblin, T.J. (2001). The occurrence and significance of V gene mutations in B cell-derived human malignancy. Advances in Cancer Research *83*, 81–116.

Su, C., Andrew, A., Karagas, M.R., and Borsuk, M.E. (2013). Using Bayesian networks to discover relations between genes, environment, and disease. BioData Mining *6*, 6.

Swerdlow, S.H., Campo, E., Harris, N.L., Jaffe, E.S., Pileri, S.A., Stein, H., Thiele, J., and Vardiman, J.W. (2008). WHO Classification of Tumours of Haematopoietic and Lymphoid Tissues (Lyon: IARC).

Taipale, J., Chen, J.K., Cooper, M.K., Wang, B., Mann, R.K., Milenkovic, L., Scott, M.P., and Beachy, P. a (2000). Effects of oncogenic mutations in Smoothened and Patched can be reversed by cyclopamine. Nature *406*, 1005–1009.

Takaesu, G., Surabhi, R.M., Park, K.-J., Ninomiya-Tsuji, J., Matsumoto, K., and Gaynor, R.B. (2003). TAK1 is critical for IkappaB kinase-mediated activation of the NF-kappaB pathway. Journal of Molecular Biology *326*, 105–115.

Takaesu, G., Inagaki, M., Takubo, K., Mishina, Y., Hess, P.R., Dean, G. a, Yoshimura, A., Matsumoto, K., Suda, T., and Ninomiya-Tsuji, J. (2012). TAK1 (MAP3K7) signaling regulates hematopoietic stem cells through TNF-dependent and -independent mechanisms. PloS One *7*, e51073.

Takata, M., and Kurosaki, T. (1996). A role for Bruton's tyrosine kinase in B cell antigen receptor-mediated activation of phospholipase C-gamma 2. The Journal of Experimental Medicine *184*, 31–40.

Tedoldi, S., Paterson, J.C., Cordell, J., Tan, S.-Y., Jones, M., Manek, S., Dei Tos, A.P., Roberton, H., Masir, N., Natkunam, Y., et al. (2006). Jaw1/LRMP, a germinal centre-associated marker for the immunohistological study of B-cell lymphomas. The Journal of Pathology *209*, 454–463.

Titsias, M.K., Honkela, A., Lawrence, N.D., and Rattray, M. (2012). Identifying targets of multiple co-regulating transcription factors from expression time-series by Bayesian model comparison. BMC Systems Biology *6*, 53.

Tosello, V., and Ferrando, A.A. (2013). The NOTCH signaling pathway: role in the pathogenesis of T-cell acute lymphoblastic leukemia and implication for therapy. Therapeutic Advances in Hematology *4*, 199–210.

Tweeddale, M.E., Lim, B., Jamal, N., Robinson, J., Zalcberg, J., Lockwood, G., Minden, M.D., and Messner, H.A. (1987). The presence of clonogenic cells in high-grade malignant lymphoma: a prognostic factor. Blood *69*, 1307–1314.

Uddin, S., Hussain, A.R., Siraj, A.K., Manogaran, P.S., Al-Jomah, N.A., Moorji, A., Atizado, V., Al-Dayel, F., Belgaumi, A., El-Solh, H., et al. (2006). Role of phosphatidylinositol 3'-kinase/AKT pathway in diffuse large B-cell lymphoma survival. Blood *108*, 4178–4186.

Uhmann, A., Dittmann, K., Nitzki, F., Dressel, R., Koleva, M., Frommhold, A., Zibat, A., Binder, C., Adham, I., Nitsche, M., et al. (2007). The Hedgehog receptor Patched controls lymphoid lineage commitment. Blood *110*, 1814–1823.

Vallabhapurapu, S., and Karin, M. (2009). Regulation and function of NF-kappaB transcription factors in the immune system. Annual Review of Immunology *27*, 693–733.

Vega, M.I., Huerta-Yepez, S., Jazirehi, A.R., Garban, H., and Bonavida, B. (2005). Rituximab (chimeric anti-CD20) sensitizes B-NHL cell lines to Fas-induced apoptosis. Oncogene *24*, 8114–8127.

Vlahos, C.J., Matter, W.F., Hui, K.Y., and Brown, R.F. (1994). A specific inhibitor of phosphatidylinositol 3-kinase, 2-(4-morpholinyl)-8-phenyl-4H-1-benzopyran-4-one (LY294002). The Journal of Biological Chemistry *269*, 5241–5248.

Vockerodt, M., Haier, B., Buttgereit, P., Tesch, H., and Kube, D. (2001). The Epstein-Barr virus latent membrane protein 1 induces interleukin-10 in Burkitt's lymphoma cells but not in Hodgkin's cells involving the p38/SAPK2 pathway. Virology *280*, 183–198.

Walsh, K., McKinney, M.S., Love, C., Liu, Q., Fan, A., Patel, A., Smith, J., Beaven, A., Jima, D.D., and Dave, S.S. (2013). PAK1 Mediates Resistance to PI3K Inhibition in Lymphomas. Clinical Cancer Research : an Official Journal of the American Association for Cancer Research.

Walther, N., Ulrich, A., Vockerodt, M., von Bonin, F., Klapper, W., Meyer, K., Eberth, S., Pukrop, T., Spang, R., Trümper, L., et al. (2013). Aberrant lymphocyte enhancer-binding factor 1 expression is characteristic for sporadic Burkitt's lymphoma. The American Journal of Pathology *182*, 1092–1098.

Wan, J., Sun, L., Mendoza, J.W., Chui, Y.L., Huang, D.P., Chen, Z.J., Suzuki, N., Suzuki, S., Yeh, W.-C., Akira, S., et al. (2004). Elucidation of the c-Jun N-terminal kinase pathway mediated by Estein-Barr virus-encoded latent membrane protein 1. Molecular and Cellular Biology *24*, 192–199.

Wang, M., Atayar, C., Rosati, S., Bosga-Bouwer, A., Kluin, P., and Visser, L. (2009). JNK is constitutively active in mantle cell lymphoma: cell cycle deregulation and polyploidy by JNK inhibitor SP600125. The Journal of Pathology *218*, 95–103.

Wei, L., and Xu, Z. (2011). Cross-signaling among phosphinositide-3 kinase, mitogen-activated protein kinase and sonic hedgehog pathways exists in esophageal cancer. International Journal of Cancer. Journal International Du Cancer *129*, 275–284.

Weston, C.R., and Davis, R.J. (2002). The JNK signal transduction pathway. Current Opinion in Genetics & Development *12*, 14–21.

Wichert, S., Fokianos, K., and Strimmer, K. (2003). Identifying periodically expressed transcripts in microarray time series data. Bioinformatics *20*, 5–20.

Wienands, J., Larbolette, O., and Reth, M. (1996). Evidence for a preformed transducer complex organized by the B cell antigen receptor. Proceedings of the National Academy of Sciences of the United States of America *93*, 7865–7870.

Willander, K., Dutta, R., Ungerbäck, J., Gunnarsson, R., Juliusson, G., Fredrikson, M., Linderholm, M., and Söderkvist, P. (2013). NOTCH1 mutations influence survival in chronic lymphocytic leukemia patients. BMC Cancer *13*, 274.

Wu, L., Chien, W.-M., Hartman, M.E., Moussavi-Harami, F., Liu, Y., and Chin, M.T. (2011). Regulation of MMP10 expression by the transcription factor CHF1/Hey2 is mediated by multiple E boxes. Biochemical and Biophysical Research Communications *415*, 662–668.

Xie, J., Murone, M., Luoh, S.M., Ryan, A., Gu, Q., Zhang, C., Bonifas, J.M., Lam, C.W., Hynes, M., Goddard, A., et al. (1998). Activating Smoothened mutations in sporadic basal-cell carcinoma. Nature *391*, 90–92.

Xu, J., Foy, T.M., Laman, J.D., Elliott, E.A., Dunn, J.J., Waldschmidt, T.J., Elsemore, J., Noelle, R.J., and Flavell, R.A. (1994). Mice deficient for the CD40 ligand. Immunity *1*, 423–431.

Yamaguchi, K., Shirakabe, K., Shibuya, H., Irie, K., Oishi, I., Ueno, N., Taniguchi, T., Nishida, E., and Matsumoto, K. (1995). Identification of a member of the MAPKKK family as a potential mediator of TGF-beta signal transduction. Science (New York, N.Y.) *270*, 2008–2011.

Yamamoto, Y., and Gaynor, R.B. (2004). IκB kinases: key regulators of the NF-κB pathway. Trends in Biochemical Sciences *29*, 72–79.

Yamashita, M., Fatyol, K., Jin, C., Wang, X., Liu, Z., and Zhang, Y.E. (2008). TRAF6 mediates Smad-independent activation of JNK and p38 by TGF-beta. Molecular Cell *31*, 918–924.

Yan, L., Mieulet, V., and Lamb, R.F. (2008). mTORC2 is the hydrophobic motif kinase for SGK1. The Biochemical Journal *416*, e19–21.

Yang, J., Wang, S., Zhao, G., and Sun, B. (2011). Effect of chemokine receptors CCR7 on disseminated behavior of human T cell lymphoma: clinical and experimental study. Journal of Experimental & Clinical Cancer Research : CR *30*, 51.

Yano, T., van Krieken, J.H., Magrath, I.T., Longo, D.L., Jaffe, E.S., and Raffeld, M. (1992). Histogenetic correlations between subcategories of small noncleaved cell lymphomas. Blood *79*, 1282–1290.

Yeung, K.Y., Dombek, K.M., Lo, K., Mittler, J.E., Zhu, J., Schadt, E.E., Bumgarner, R.E., and Raftery, A.E. (2011). Construction of regulatory networks using expression time-series data of a genotyped population. Proceedings of the National Academy of Sciences of the United States of America *108*, 19436–19441.

Yilmaz, Z.B., Weih, D.S., Sivakumar, V., and Weih, F. (2003). RelB is required for Peyer's patch development: differential regulation of p52-RelB by lymphotoxin and TNF. The EMBO Journal *22*, 121–130.

Yochum, G.S., Cleland, R., and Goodman, R.H. (2008). A genome-wide screen for beta-catenin binding sites identifies a downstream enhancer element that controls c-Myc gene expression. Molecular and Cellular Biology *28*, 7368–7379.

Yoon, S., and Seger, R. (2006). The extracellular signal-regulated kinase: multiple substrates regulate diverse cellular functions. Growth Factors (Chur, Switzerland) *24*, 21–44.

Yoon, J.W., Gallant, M., Lamm, M.L., Iannaccone, S., Vieux, K.-F., Proytcheva, M., Hyjek, E., Iannaccone, P., and Walterhouse, D. (2013). Noncanonical Regulation of the Hedgehog Mediator GLI1 by c-MYC in Burkitt Lymphoma. Molecular Cancer Research : MCR *11*, 604–615.

Young, R.M., and Staudt, L.M. (2013). Targeting pathological B cell receptor signalling in lymphoid malignancies. Nature Reviews. Drug Discovery *12*, 229–243.

Zheng, B., Fiumara, P., Li, Y. V, Georgakis, G., Snell, V., Younes, M., Vauthey, J.N., Carbone, A., and Younes, A. (2003). MEK/ERK pathway is aberrantly active in Hodgkin disease: a signaling pathway shared by CD30, CD40, and RANK that regulates cell proliferation and survival. Blood *102*, 1019–1027.

Zou, M., and Conzen, S.D. (2005). A new dynamic Bayesian network (DBN) approach for identifying gene regulatory networks from time course microarray data. Bioinformatics (Oxford, England) *21*, 71–79.

Zwerner, J.P., Joo, J., Warner, K.L., Christensen, L., Hu-Lieskovan, S., Triche, T.J., and May, W.A. (2008). The EWS/FLI1 oncogenic transcription factor deregulates GLI1. Oncogene *27*, 3282–3291.

Appendix

Table A-1 Clusters of genes identified upon BCR crosslinked BL2 cells (BHC, SIMoNe). Using Bayesian Hierarchical Clustering sets of genes were built, which show the same gene expression course after anti-IgM treatment of BL cells.

	Probe ID	Symbol
Cluster 4		
1	7902398	SNORD45A
2	7948908	SNORD26
3	7993664	CCP110
4	8043697	ANKRD36B
5	8068522	TTC3
6	8117330	HIST1H3A
7	8117580	HIST1H2AI
8	8127989	SNORD50B
9	8159004	SNORD24
Cluster 5		
1	7900119	THRAP3
2	7904974	PFN1P2
3	7908867	TMEM183A
4	7924923	NUP133
5	7957540	MRPL42
6	7959408	KNTC1
7	7969428	UCHL3
8	7969703	IPO5
9	7981335	HSP90AA1
10	7985829	FANCI
11	8014650	NPEPPS
12	8050565	PUM2
13	8059319	FARSB
14	8074925	GUSBP11
15	8085374	RAF1
16	8087874	WDR82
17	8091452	TMEM183B
18	8099926	PDS5A
19	8105523	KIF2A
20	8111455	GUSBP1
21	8112558	GUSBP2
22	8138670	HNRNPA2B1
23	8162313	IARS
24	8162514	FANCC
Cluster 6		
1	7897648	PEX14
2	7897849	MIIP
3	7899134	CEP85
4	7899244	PIGV
5	7900699	CDC20
6	7904812	PIAS3
7	7905198	TARS2
8	7907092	MPZL1
9	7909529	RCOR3
10	7909586	PPP2R5A
11	7909898	MIA3
12	7911591	SLC35E2B
13	7911600	NADK
14	7911862	LRRC47
15	7919825	ARNT
16	7921806	B4GALT3
17	7934477	CAMK2G
18	7941769	KDM2A
19	7941879	TBC1D10C
20	7941927	AIP
21	7945357	SIRT3
22	7948685	TUT1
23	7949518	FIBP
24	7949674	RBM4B
25	7951752	USP28
26	7952484	TMEM218
27	7952988	ERC1
28	7955217	SPATS2
29	7959777	BRI3BP
30	7960702	CDCA3
31	7961339	LRP6
32	7963851	KIAA0748
33	7964203	BAZ2A
34	7969935	ERCC5
35	7971039	FAM48A
36	7973732	KHNYN
37	7979849	DCAF5
38	7986186	RCCD1
39	7987405	RASGRP1
40	7989759	PARP16
41	7990757	CTSH
42	7995492	ADCY7
43	7996041	COQ9
44	7996744	NFATC3
45	7999304	FAM86A
46	7999596	KIAA2013
47	8000263	COG7
48	8000706	CDIPT
49	8002381	COG4
50	8002904	ADAT1
51	8003922	MED11
52	8005839	TMEM97
53	8009164	DCAF7
54	8014551	SYNRG
55	8014723	PIP4K2B

56	8016847	TRIM25
57	8017019	MTMR4
58	8018694	PRPSAP1
59	8025053	TNFSF9
60	8026982	MPV17L2
61	8029856	ARHGAP35
62	8032455	PLEKHJ1
63	8034122	SPC24
64	8034589	FARSA
65	8035249	NR2F6
66	8036483	YIF1B
67	8038117	DBP
68	8047288	SGOL2
69	8048175	SMARCAL1
70	8051012	PREB
71	8051298	GALNT14
72	8060705	MAVS
73	8065637	COMMD7
74	8065992	NFS1
75	8066964	TMEM189
76	8072529	DEPDC5
77	8078450	CRTAP
78	8080781	PXK
79	8087308	USP19
80	8089040	MINA
81	8093976	TBC1D14
82	8095574	DCK
83	8095751	PARM1
84	8098581	SNX25
85	8118116	MICB
86	8118863	ANKS1A
87	8124211	GPLD1
88	8125470	HLA-DOB
89	8131957	SNX10
90	8140107	DNAJC30
91	8143070	WDR91
92	8143863	FASTK
93	8145418	CDCA2
94	8149389	FAM86B1
95	8155327	ALDH1B1
96	8164304	ST6GALNAC6
97	8164481	C9orf114
98	8165064	UBAC1
99	8176245	F8A1
100	8177955	MICB
101	8178833	HLA-DOB
102	8180339	ST6GALNAC6
Cluster 7		
1	7908147	TSEN15
2	7911897	C1orf174
3	7942626	UVRAG
4	7947784	ARFGAP2
5	7956401	SHMT2
6	7968199	CDK8
7	7991406	PRC1
8	8002729	GLG1
9	8021727	CNDP2
10	8027139	RFXANK
11	8032525	SLC39A3
12	8051998	MCFD2
13	8064156	ZGPAT
14	8069933	MIS18A
15	8073379	L3MBTL2
16	8080645	APPL1
17	8093112	UBXN7
18	8093462	MAEA
19	8096688	GSTCD
20	8108861	NDFIP1
21	8110589	CNOT6
22	8111974	PAIP1
23	8132539	DBNL
24	8139356	NUDCD3
25	8143387	MKRN1
26	8145586	ELP3
27	8156897	C9orf30
28	8160953	PIGO
29	8164013	STRBP
30	8180394	POLR2M
Cluster 8		
1	7899604	ZCCHC17
2	7901479	ZYG11B
3	7902308	FPGT
4	7906652	NIT1
5	7907353	METTL13
6	7912292	LZIC
7	7914809	KIAA0319L
8	7915775	IPP
9	7915846	MKNK1
10	7921738	USF1
11	7935251	TCTN3
12	7935647	COX15
13	7939087	C11orf46
14	7946089	TRIM5
15	7948249	SLC43A1
16	7952914	CCDC77
17	7955450	LETMD1
18	7958275	POLR3B
19	7969374	BORA
20	7973036	PARP2
21	7974621	ARID4A
22	7980403	C14orf133
23	7982154	HERC2P2
24	7982723	IVD
25	7986569	HERC2P2
26	7986701	HERC2P2
27	7989834	C15orf44

28	7999889	GDE1
29	8006715	TADA2A
30	8007272	COASY
31	8007799	MGC57346
32	8053158	MOGS
33	8054702	CKAP2L
34	8059838	HJURP
35	8067167	AURKA
36	8068460	MORC3
37	8081362	CEP97
38	8083063	SLC25A36
39	8088092	RFT1
40	8088247	ARHGEF3
41	8098328	GALNT7
42	8106429	AGGF1
43	8119000	MAPK14
44	8119198	FTSJD2
45	8119858	POLH
46	8120251	FBXO9
47	8121161	UFL1
48	8126259	C6orf130
49	8128939	TRAF3IP2
50	8129181	GOPC
51	8138091	DAGLB
52	8140915	PEX1
53	8142019	ORC5
54	8143040	SLC35B4
55	8149673	REEP4
56	8151066	ARMC1
57	8168589	ZNF711
58	8175102	ENOX2
Cluster 9		
1	7898192	DNAJC16
2	7898679	NBPF3
3	7899829	S100PBP
4	7900833	KDM4A
5	7902883	LRRC8D
6	7903827	FAM40A
7	7904482	SRGAP2
8	7904755	PEX11B
9	7915516	MED8
10	7917120	USP33
11	7922707	RNASEL
12	7922823	EDEM3
13	7923812	RAB7L1
14	7927955	KIAA1279
15	7930577	CASP7
16	7930703	TRUB1
17	7930882	FAM45A
18	7931951	SFMBT2
19	7932703	ACBD5
20	7936817	C10orf88
21	7945979	TRIM68
22	7951422	KIAA1826
23	7954969	IRAK4
24	7959563	C12orf65
25	7960261	RAD52
26	7963935	DNAJC14
27	7967240	VPS33A
28	7969228	ALG11
29	7976307	GOLGA5
30	7985053	FBXO22
31	7985080	ISL2
32	7988838	LEO1
33	7991357	AP3S2
34	7995362	GPT2
35	7999478	TXNDC11
36	8000236	CDR2
37	8009552	C17orf80
38	8014264	PEX12
39	8016562	SPOP
40	8017555	ERN1
41	8021275	POLI
42	8021716	TIMM21
43	8034565	DNASE2
44	8042310	SLC1A4
45	8047443	STRADB
46	8050443	SMC6
47	8062545	ACTR5
48	8072108	ASPHD2
49	8072153	CCDC117
50	8073513	CCDC134
51	8080926	ARL6IP5
52	8081612	ABHD10
53	8081667	SLC35A5
54	8081953	GTF2E1
55	8083282	HPS3
56	8084360	ABCF3
57	8085852	NGLY1
58	8090420	TPRA1
59	8090577	MBD4
60	8091737	IFT80
61	8093936	MRFAP1
62	8095262	REST
63	8102745	PGRMC2
64	8108472	PURA
65	8109576	THG1L
66	8111960	C5orf34
67	8113733	CEP120
68	8113790	MARCH3
69	8121886	HINT3
70	8124280	FAM65B
71	8127787	IBTK
72	8132318	ANLN
73	8133114	VKORC1L1
74	8133809	RSBN1L

75	8136163	KLHDC10
76	8139244	C7orf44
77	8139737	PSPH
78	8140070	TBL2
79	8141024	BET1
80	8145652	LEPROTL1
81	8146159	AP3M2
82	8146278	SGK196
83	8152222	AZIN1
84	8154394	SNAPC3
85	8155696	FAM122A
86	8166382	MBTPS2
87	8166989	ZNF673
88	8170097	SLC9A6
Cluster 10		
1	7899087	PDIK1L
2	7902512	DNAJB4
3	7904469	SRGAP2
4	7913883	PAFAH2
5	7919780	GOLPH3L
6	7922870	TRMT1L
7	7928937	MINPP1
8	7947138	FANCF
9	7953765	RIMKLB
10	7979565	WDR89
11	7993298	ERCC4
12	8004266	SLC16A13
13	8011396	SHPK
14	8037144	DEDD2
15	8042576	NAGK
16	8058552	IDH1
17	8066786	ZMYND8
18	8083223	C3orf58
19	8084165	SOX2
20	8085788	NKIRAS1
21	8092177	NCEH1
22	8099696	SEPSECS
23	8102362	TIFA
24	8103226	TMEM154
25	8129590	STX7
26	8143188	CREB3L2
27	8171896	CXorf21
Cluster 11		
1	7897803	PLOD1
2	7898939	NIPAL3
3	7899870	ZNF362
4	7901102	MMACHC
5	7901592	TCEANC2
6	7901895	ATG4C
7	7903565	GPSM2
8	7904452	FAM72D
9	7904907	BCL9
10	7905299	PRUNE
11	7906671	USP21
12	7907058	POU2F1
13	7907079	RCSD1
14	7909146	FAM72D
15	7913682	HMGCL
16	7913694	FUCA1
17	7914917	LSM10
18	7915472	SLC2A1
19	7915787	PIK3R3
20	7919591	FAM72D
21	7923662	PIK3C2B
22	7923792	SLC45A3
23	7925773	ZNF692
24	7928491	KAT6B
25	7929322	CYP26A1
26	7933228	MARCH8
27	7938183	ZNF215
28	7941104	ARL2
29	7942562	NEU3
30	7944152	IL10RA
31	7945132	FLI1
32	7945875	FAM86B1
33	7952601	ETS1
34	7952707	PRDM10
35	7954717	BICD1
36	7955195	TROAP
37	7957167	TMEM19
38	7957759	APAF1
39	7958439	USP30
40	7959298	TMEM120B
41	7959354	BCL7A
42	7960910	AICDA
43	7961983	TM7SF3
44	7965565	USP44
45	7968789	RGCC
46	7971486	KIAA0226L
47	7974697	DAAM1
48	7975311	EXD2
49	7975361	KIAA0247
50	7975787	JDP2
51	7977868	C14orf93
52	7986463	LRRK1
53	7988426	SLC30A4
54	7988970	FAM214A
55	7994655	C16orf53
56	7997735	FOXL1
57	8001178	C16orf87
58	8006345	RHOT1
59	8007471	NBR1
60	8008339	RSAD1
61	8010139	SEC14L1
62	8011415	P2RX5
63	8013804	DHRS13

64	8015655	FAM134C
65	8019018	CBX4
66	8021565	PHLPP1
67	8026712	ANKLE1
68	8029465	BCL3
69	8031522	ZNF581
70	8037186	LIPE
71	8037495	ZNF296
72	8039928	FAM72D
73	8040365	TRIB2
74	8048898	SP140
75	8052669	SERTAD2
76	8056766	SLC25A12
77	8058161	ORC2
78	8058927	TMBIM1
79	8060977	C20orf94
80	8085233	RPUSD3
81	8087852	TLR9
82	8089261	CBLB
83	8092691	BCL6
84	8096070	BMP3
85	8097417	PHF17
86	8097867	KIAA0922
87	8098423	NEIL3
88	8102342	ELOVL6
89	8104901	IL7R
90	8105878	RAD17
91	8106107	PTCD2
92	8108301	KIF20A
93	8108447	CXXC5
94	8111136	FAM134B
95	8111552	NADKD1
96	8117120	ID4
97	8117165	SOX4
98	8117435	BTN3A2
99	8122013	L3MBTL3
100	8126018	STK38
101	8126428	TRERF1
102	8136341	BPGM
103	8138030	PMS2
104	8138088	C7orf70
105	8142096	ATXN7L1
106	8148158	WDR67
107	8148317	MYC
108	8149387	FAM86B1
109	8151074	PDE7A
110	8153935	ZNF252
111	8155332	C7orf70
112	8160835	C9orf23
113	8162438	BICD2
114	8164252	SH2D3C
115	8164314	ST6GALNAC4
116	8170998	F8A1
117	8171029	F8A1
118	8171136	P2RY8
119	8172088	BCOR
120	8173208	SPIN4
121	8173232	FAM123B
122	8177026	P2RY8
123	8177478	RAD17
124	8180336	SLC35E2
125	8180412	ST6GALNAC4
126	8180413	ST6GALNAC4
Cluster 12		
1	7897482	PIK3CD
2	7898677	HS6ST1
3	7901140	MAST2
4	7903719	AMPD2
5	7905831	FLAD1
6	7906061	SYT11
7	7906079	RAB25
8	7906767	FCGR2C
9	7912224	SLC2A5
10	7915567	ERI3
11	7916403	SSBP3
12	7920877	ARHGEF2
13	7920912	UBQLN4
14	7923824	SLC41A1
15	7925978	FAM208B
16	7926037	PFKFB3
17	7926170	DHTKD1
18	7927425	WDFY4
19	7929990	PPRC1
20	7931930	PRKCQ
21	7933760	CCDC6
22	7935968	LDB1
23	7937485	PNPLA2
24	7937892	PGAP2
25	7940349	CCDC86
26	7941302	FAM89B
27	7941457	CCDC85B
28	7941694	RBM14
29	7941743	LRFN4
30	7941797	ADRBK1
31	7942342	INPPL1
32	7944335	CXCR5
33	7945539	SLC25A22
34	7948565	CYBASC3
35	7949146	SF1
36	7949172	MAP4K2
37	7949206	MEN1
38	7949264	EHD1
39	7949383	SYVN1
40	7949746	POLD4
41	7949904	UNC93B1
42	7950086	NUMA1

43	7950248	FCHSD2
44	7951873	SIK3
45	7952132	SLC37A4
46	7952830	NCAPD3
47	7953651	PEX5
48	7953981	ETV6
49	7954104	ATF7IP
50	7955019	ARID2
51	7956220	OBFC2B
52	7957126	KCNMB4
53	7958950	C12orf52
54	7958960	TPCN1
55	7959025	RNFT2
56	7962659	HDAC7
57	7963988	SMARCC2
58	7964413	R3HDM2
59	7966542	RASAL1
60	7967358	PITPNM2
61	7967588	DHX37
62	7967789	PXMP2
63	7968126	LSP1
64	7969533	SLAIN1
65	7971015	SMAD9
66	7973709	NFATC4
67	7977319	PLD4
68	7977344	PACS2
69	7980327	ANGEL1
70	7980970	ITPK1
71	7981538	JAG2
72	7982326	KLF13
73	7982620	EIF2AK4
74	7987675	RPAP1
75	7990033	TLE3
76	7990487	SIN3A
77	7992402	NDUFB10
78	7992474	TSC2
79	7992775	PAQR4
80	7993478	ABCC1
81	7994109	PLK1
82	7994161	RBBP6
83	7995976	CPNE2
84	7996608	RLTPR
85	7996785	PRMT7
86	7997427	CMIP
87	7997680	KIAA0182
88	7998774	RNPS1
89	7999102	TFAP4
90	7999173	FAM100A
91	8004804	PFAS
92	8005978	TRAF4
93	8006063	ANKRD13B
94	8006298	RAB11FIP4
95	8006788	MLLT6
96	8007302	TUBG1
97	8010673	SLC25A10
98	8011093	SLC43A2
99	8011262	MNT
100	8011516	ATP2A3
101	8011747	SLC25A11
102	8012304	TRAPPC1
103	8012376	VAMP2
104	8012958	UBE2S
105	8013179	ATPAF2
106	8014700	C17orf96
107	8014706	PCGF2
108	8015412	JUP
109	8015526	KAT2A
110	8016546	ZNF652
111	8017511	CD79B
112	8018708	UBE2O
113	8019280	PCYT2
114	8019357	DCXR
115	8019778	PCYT2
116	8024111	CNN2
117	8024420	SF3A2
118	8024485	GADD45B
119	8024798	CCDC94
120	8025142	ARHGEF18
121	8025382	CERS4
122	8025601	ICAM1
123	8026047	JUNB
124	8026533	HSH2D
125	8026579	TMEM38A
126	8026830	FCHO1
127	8028286	SIPA1L3
128	8028397	FAM98C
129	8028930	RAB4B
130	8029521	TOMM40
131	8030525	PTOV1
132	8030671	SPIB
133	8031526	CCDC106
134	8031913	TRIM28
135	8032076	RNF126
136	8032365	KLF16
137	8032380	BTBD2
138	8032392	MKNK2
139	8032530	SGTA
140	8032755	ZBTB7A
141	8032899	TICAM1
142	8033190	SLC25A23
143	8033362	INSR
144	8034130	KANK2
145	8034454	DHPS
146	8034754	SAMD1
147	8034783	LPHN1
148	8035600	TMEM161A

149	8038261	GYS1
150	8039306	RDH13
151	8039316	PPP1R12C
152	8039413	PPP6R1
153	8039491	UBE2S
154	8040238	HPCAL1
155	8041617	MTA3
156	8041763	PRKCE
157	8041826	TTC7A
158	8045171	IMP4
159	8045182	PTPN18
160	8046815	ZNF804A
161	8047565	FAM117B
162	8048257	PNKD
163	8048452	WNT10A
164	8049246	INPP5D
165	8049317	DGKD
166	8049689	RNPEPL1
167	8051814	ZFP36L2
168	8052399	BCL11A
169	8053009	FBXO41
170	8055130	HS6ST1
171	8055208	CCDC115
172	8058973	ZNF142
173	8059650	SP110
174	8060353	RBCK1
175	8060675	CDC25B
176	8064100	PPDPF
177	8064790	RASSF2
178	8065683	SNTA1
179	8065693	NECAB3
180	8066939	B4GALT5
181	8070503	PRDM15
182	8070557	ZNF295
183	8070912	SLC19A1
184	8071339	ZDHHC8
185	8071566	PPIL2
186	8071691	BCR
187	8072757	CSF2RB
188	8074003	TRABD
189	8075430	MORC2
190	8075493	PATZ1
191	8075785	FOXRED2
192	8075910	RAC2
193	8076056	CSNK1E
194	8076690	KIAA0930
195	8077042	SBF1
196	8078729	MYD88
197	8079037	TRAK1
198	8079462	NBEAL2
199	8079796	RNF123
200	8080093	RBM15B
201	8080487	PRKCD
202	8081465	BBX
203	8082368	PODXL2
204	8084100	USP13
205	8086125	TRANK1
206	8087935	NT5DC2
207	8090433	MGLL
208	8093219	BDH1
209	8093440	FGFRL1
210	8093916	MAN2B2
211	8094240	CD38
212	8099965	ACOT7
213	8102232	LEF1
214	8108321	FAM53C
215	8109149	PCYOX1L
216	8112107	PPAP2A
217	8112940	SSBP2
218	8114215	PITX1
219	8114511	MZB1
220	8115543	EBF1
221	8115927	RNF44
222	8117243	LRRC16A
223	8119016	MAPK13
224	8119582	KIAA0240
225	8121076	PNRC1
226	8122971	ARID1B
227	8124813	MDC1
228	8125172	EHMT2
229	8126371	CCND3
230	8128818	WASF1
231	8130185	ZBTB2
232	8131091	MAFK
233	8133233	AUTS2
234	8133331	POM121
235	8135114	CUX1
236	8135149	SH2B2
237	8137225	REPIN1
238	8138504	RAPGEF5
239	8139057	ELMO1
240	8139270	RASA4
241	8140398	YWHAG
242	8141768	RASA4
243	8141803	RASA4
244	8142981	PODXL
245	8143327	PARP12
246	8145977	PLEKHA2
247	8147040	ZBTB10
248	8148694	GRINA
249	8149612	LZTS1
250	8149979	C8orf80
251	8152133	RRM2B
252	8153497	SCRIB
253	8153790	TONSL
254	8155707	TJP2

255	8156452	FAM120A
256	8158829	PRRC2B
257	8158839	PRRC2B
258	8159249	MRPS2
259	8160682	NOL6
260	8162533	PTCH1
261	8162729	TRIM14
262	8162803	ANKS6
263	8164131	SCAI
264	8164810	RALGDS
265	8165094	QSOX2
266	8165156	SDCCAG3
267	8165217	NOTCH1
268	8165552	NELF
269	8165711	PLCXD1
270	8170364	AFF2
271	8171837	KLHL15
272	8172471	PIM2
273	8173457	ZMYM3
274	8174692	SEPT6
275	8176286	PLCXD1
276	8178404	MDC1
277	8178727	ATF6B
278	8179884	EHMT2
279	8180362	MPRIP
280	8180363	MPRIP
281	8180411	ELMO1
Cluster 13		
1	7899192	RPS6KA1
2	7900426	SMAP2
3	7900911	DPH2
4	7901951	PGM1
5	7904137	HIPK1
6	7904742	LIX1L
7	7905444	SNX27
8	7905631	INTS3
9	7908779	RNPEP
10	7909708	CENPF
11	7912166	RERE
12	7912257	CLSTN1
13	7912374	SRM
14	7912412	MTOR
15	7913156	AKR7A2
16	7914603	RNF19B
17	7915695	MUTYH
18	7919940	VPS72
19	7919950	PI4KB
20	7919971	RFX5
21	7920000	POGZ
22	7920707	FAM189B
23	7921133	HDGF
24	7924669	PYCR2
25	7932109	SEPHS1
26	7935474	MMS19
27	7935639	SLC25A28
28	7937802	CD81
29	7939215	C11orf41
30	7940372	TMEM109
31	7940600	INCENP
32	7941148	TM7SF2
33	7941179	CAPN1
34	7941976	NDUFS8
35	7941985	TCIRG1
36	7944401	HMBS
37	7945573	POLR2L
38	7947861	SPI1
39	7949798	TMEM134
40	7950271	FAM168A
41	7953100	FKBP4
42	7955736	ESPL1
43	7956152	PA2G4
44	7959786	AACS
45	7963646	AAAS
46	7966570	DDX54
47	7966878	CIT
48	7967544	SCARB1
49	7968734	SLC25A15
50	7968890	DGKZ
51	7969438	LMO7
52	7972577	RPS26
53	7973067	PNP
54	7975459	SIPA1L1
55	7975815	TTLL5
56	7977820	PRMT5
57	7981494	AKT1
58	7982878	CHP
59	7983290	SERF2
60	7983843	TCF12
61	7985431	AGSK1
62	7987840	VPS39
63	7990361	UBL7
64	7990902	AGSK1
65	7990952	AGSK1
66	7991088	LOC388152
67	7991159	LOC388152
68	7991714	AGSK1
69	7992043	FAM173A
70	7992414	TBL3
71	7992737	FLYWCH2
72	7995655	FTO
73	7996137	KATNB1
74	7996685	EDC4
75	7997453	PLCG2
76	7998063	TUBB3
77	7998251	C16orf13
78	7998267	JMJD8

79	7998367	RPUSD1
80	8000869	SEPT1
81	8003357	PIEZO1
82	8003733	SGSM2
83	8004030	RNF167
84	8004057	KIF1C
85	8005407	LLGL1
86	8005994	ERAL1
87	8006655	DHRS11
88	8007188	CNP
89	8007197	NKIRAS2
90	8007505	DHX8
91	8007797	RPS26
92	8008922	PPM1D
93	8009382	BPTF
94	8010248	AFMID
95	8010664	MRPL12
96	8010747	GPS1
97	8011407	TAX1BP3
98	8013696	KIAA0100
99	8013788	FLOT2
100	8014882	MIEN1
101	8015460	ACLY
102	8015969	UBTF
103	8017460	SMARCD2
104	8018428	GALK1
105	8018511	MRPL38
106	8018849	TK1
107	8024089	WDR18
108	8024170	HMHA1
109	8024204	STK11
110	8024358	CSNK1G2
111	8024446	SPPL2B
112	8024497	THOP1
113	8024660	HMG20B
114	8024864	HDGFRP2
115	8025255	STXBP2
116	8026341	TECR
117	8026638	MYO9B
118	8026735	GTPBP3
119	8026751	FAM125A
120	8027117	ARMC6
121	8027621	GPI
122	8027701	GRAMD1A
123	8028851	SHKBP1
124	8028916	SNRPA
125	8029560	CLPTM1
126	8029814	PPP5C
127	8029831	CALM3
128	8030113	RUVBL2
129	8030470	AP2A1
130	8031097	NDUFA3
131	8031483	RPL28
132	8032106	MED16
133	8033479	ELAVL1
134	8033899	EIF3G
135	8033956	S1PR2
136	8034843	NDUFB7
137	8035553	COPE
138	8036010	PEPD
139	8036525	MAP4K1
140	8036938	ADCK4
141	8037537	ERCC2
142	8037647	FBXO46
143	8037991	LIG1
144	8038202	BCAT2
145	8042867	WBP1
146	8043377	WBP1
147	8048304	CTDSP1
148	8048595	GMPPA
149	8049582	SCLY
150	8051030	SLC5A6
151	8052803	AAK1
152	8053599	WBP1
153	8054092	TMEM131
154	8054888	CLASP1
155	8056545	STK39
156	8059177	TUBA4A
157	8059222	DNPEP
158	8059989	HES6
159	8060257	STK25
160	8062319	TGIF2
161	8064613	SLC4A11
162	8064739	C20orf27
163	8065817	GSS
164	8067361	TAF4
165	8069026	C21orf33
166	8071768	SMARCB1
167	8072744	NCF4
168	8072870	PDXP
169	8072979	POLR2F
170	8074020	SELO
171	8074388	SLC25A1
172	8075009	C22orf13
173	8075217	AP1B1
174	8076307	RANGAP1
175	8076393	CENPM
176	8076792	CERK
177	8079311	LARS2
178	8079563	DHX30
179	8079950	GNAI2
180	8080168	ACY1
181	8080714	FLNB
182	8082422	EEFSEC
183	8086754	SCAP
184	8087790	RRP9

185	8088106	TKT
186	8092457	ALG3
187	8093685	HTT
188	8094501	STIM2
189	8095216	KIAA1211
190	8101086	NAAA
191	8101622	TECR
192	8103188	PET112
193	8104506	TRIO
194	8107750	PRRC1
195	8108330	KDM3B
196	8109999	ERGIC1
197	8110327	RGS14
198	8110362	GRK6
199	8110982	DAP
200	8111286	DROSHA
201	8115524	CLINT1
202	8119627	PPP2R5D
203	8120585	SMAP1
204	8124828	FLOT1
205	8125125	LSM2
206	8125649	VPS52
207	8125775	MNF1
208	8127051	TRAM2
209	8128111	UBE2J1
210	8130916	PHF10
211	8131253	FOXK1
212	8131427	C7orf26
213	8133413	LIMK1
214	8134821	MEPCE
215	8137847	BRAT1
216	8139281	POLM
217	8139299	POLD2
218	8139468	TBRG4
219	8143988	MLL3
220	8148772	FAM203A
221	8148783	HEATR7A
222	8148799	FAM203A
223	8153652	SHARPIN
224	8153776	VPS28
225	8153838	RECQL4
226	8155699	FXN
227	8158123	FPGS
228	8158961	GTF3C5
229	8160036	C9orf123
230	8162462	FAM120A
231	8162502	FBP1
232	8165622	ZMYND19
233	8165630	C9orf37
234	8167042	RBM10
235	8167125	USP11
236	8167656	MAGED1
237	8167924	UBQLN2
238	8170865	TAZ
239	8172119	MED14
240	8172296	NDUFB11
241	8173009	PHF8
242	8175924	NAA10
243	8176117	FAM3A
244	8178419	FLOT1
245	8178641	LSM2
246	8178917	VPS52
247	8179688	FLOT1
248	8179839	LSM2
249	8180123	VPS52
Cluster 17		
1	7898549	MRTO4
2	7899703	TXLNA
3	7904000	DDX20
4	7910416	URB2
5	7913805	RUNX3
6	7915091	MTF1
7	7920766	ASH1L
8	7923503	ADIPOR1
9	7923778	ELK4
10	7924969	TAF5L
11	7928589	PPIF
12	7946201	ARFIP2
13	7947969	FNBP4
14	7948493	SLC15A3
15	7949916	CHKA
16	7967736	POLE
17	7970111	ARHGEF7
18	7971177	FOXO1
19	7972548	GPR18
20	7974455	MAPK1IP1L
21	7977105	TRMT61A
22	7980828	CCDC88C
23	7982185	DEXI
24	7986685	DEXI
25	7987584	INO80
26	7988687	GABPB1
27	7993148	PMM2
28	7993973	POLR3E
29	7994280	IL4R
30	7999120	CORO7
31	8000244	USP31
32	8003249	FBXO31
33	8004431	POLR2A
34	8005441	SMCR8
35	8006148	GOSR1
36	8006850	CDK12
37	8013486	USP22
38	8014214	NLE1
39	8014925	MED24
40	8019463	CSNK1D

41	8021866	NFATC1
42	8025458	ZNF317
43	8025563	PPAN-P2RY11
44	8027074	UPF1
45	8028119	WDR62
46	8028552	NFKBIB
47	8030035	GRWD1
48	8032137	C19orf6
49	8034482	TNPO2
50	8035007	AKAP8
51	8035023	AKAP8L
52	8035980	RHPN2
53	8037657	DMPK
54	8038624	C19orf48
55	8042381	PNO1
56	8042942	HK2
57	8052143	GPR75
58	8055183	SMPD4
59	8059996	PER2
60	8062286	C20orf4
61	8066641	ZNF335
62	8067563	DIDO1
63	8067593	YTHDF1
64	8068289	SON
65	8068551	DYRK1A
66	8068810	SLC37A1
67	8068974	TRAPPC10
68	8069174	FAM207A
69	8070194	RUNX1
70	8073039	GTPBP1
71	8073345	EP300
72	8074647	PI4KA
73	8075406	PES1
74	8077595	BRPF1
75	8080878	ATXN7
76	8083324	TSC22D2
77	8087271	QRICH1
78	8087748	VPRBP
79	8088128	DCP1A
80	8088642	LRIG1
81	8088776	FOXP1
82	8093590	RNF4
83	8097461	CCRN4L
84	8108099	SEC24A
85	8110841	LPCAT1
86	8115168	RBM22
87	8118228	LY6G5B
88	8118580	BRD2
89	8119712	SRF
90	8130116	LATS1
91	8133145	CRCP
92	8137542	RBM33
93	8140061	BCL7B
94	8142730	ZNF800
95	8145259	CHMP7
96	8159476	TRAF2
97	8160647	BAG1
98	8160722	UBAP2
99	8161192	RNF38
100	8162601	ZNF367
101	8164665	RAPGEF1
102	8164862	SURF6
103	8178059	LY6G5B
104	8179504	BRD2
Cluster 18		
1	7898602	OTUD3
2	7923659	PPP1R15B
3	7924526	TP53BP2
4	7925823	GTPBP4
5	7938331	ZNF143
6	7939839	PTPRJ
7	7940051	ZDHHC5
8	7940118	ZFP91-CNTF
9	7942439	RELT
10	7948229	SLC43A3
11	7955425	ATF1
12	7965918	NT5DC3
13	8003448	ANKRD11
14	8009932	SAP30BP
15	8022404	FAM210A
16	8031956	ZNF324
17	8069565	BTG3
18	8077612	TTLL3
19	8110734	BRD9
20	8115681	PANK3
21	8116548	DUSP22
22	8117128	E2F3
23	8119408	NFYA
24	8141241	SMURF1
25	8160756	DCAF12
26	8162850	TEX10
27	8173615	RLIM
Cluster 19		
1	7903321	RTCD1
2	7903619	SARS
3	7903908	CEPT1
4	7904340	MAN1A2
5	7906810	DUSP12
6	7907135	SFT2D2
7	7914180	SPCS2
8	7918255	CLCC1
9	7918284	TAF13
10	7922250	SCYL3
11	7923516	CYB5R1
12	7929012	STAMBPL1
13	7929634	ZDHHC16

14	7930162	C10orf26
15	7930614	NHLRC2
16	7932160	FAM107B
17	7942168	FADD
18	7942553	SPCS2
19	7943314	JRKL
20	7945058	FAM118B
21	7946742	CYP2R1
22	7950753	CCDC90B
23	7953211	C12orf5
24	7954492	FGFR1OP2
25	7954711	C12orf35
26	7958819	ERP29
27	7959282	RNF34
28	7964021	RNF41
29	7964347	TMEM194A
30	7967881	MPHOSPH8
31	7969626	GPR180
32	7969979	ABHD13
33	7971027	ALG5
34	7973530	PCK2
35	7974207	MGAT2
36	7974576	NAA30
37	7974725	JKAMP
38	7976571	C14orf129
39	7978932	SOS2
40	7979984	ZFYVE1
41	7980438	SPTLC2
42	7983744	TMOD3
43	7988753	SPPL2A
44	7989128	CNOT6L
45	7989224	ADAM10
46	7999553	CPPED1
47	8002347	AARS
48	8002523	FTSJD1
49	8018600	SRP68
50	8021187	SKA1
51	8021453	SEC11C
52	8035886	C19orf12
53	8036420	ZFP30
54	8036813	ZNF780B
55	8040503	UBXN2A
56	8041487	CCDC75
57	8041820	SOCS5
58	8042161	PEX13
59	8044613	CBWD1
60	8050278	PDIA6
61	8050474	RDH14
62	8055890	STAM2
63	8058221	TRAK2
64	8058985	RNF25
65	8061373	GZF1
66	8071274	SEPT5-GP1BB
67	8077993	TMEM43
68	8081115	ARL13B
69	8083310	RNF13
70	8083757	NMD3
71	8084016	PIK3CA
72	8088065	SFMBT1
73	8088151	ACTR8
74	8088700	TMF1
75	8088830	SHQ1
76	8090840	RYK
77	8091637	SLC33A1
78	8091941	PDCD10
79	8093961	KIAA0232
80	8095148	TMEM165
81	8095163	EXOC1
82	8096251	NUDT9
83	8097066	METTL14
84	8097704	TMEM184C
85	8099797	RELL1
86	8099834	TLR1
87	8100318	SGCB
88	8103834	AGA
89	8104760	TARS
90	8105862	CDK7
91	8106303	POLK
92	8106702	ZCCHC9
93	8106784	RASA1
94	8107520	TNFAIP8
95	8108847	RNF14
96	8110678	CCDC127
97	8111533	LMBRD2
98	8111952	C5orf28
99	8112182	MIER3
100	8112687	COL4A3BP
101	8114829	YIPF5
102	8115476	MED7
103	8116998	JARID2
104	8118613	SLC39A7
105	8120215	PAQR8
106	8120378	KIAA1586
107	8121525	KIAA1919
108	8121861	NCOA7
109	8121927	RNF146
110	8129254	MAN1A1
111	8130032	FBXO30
112	8130438	TFB1M
113	8130765	FAM103A1
114	8132292	Sep-07
115	8133167	KCTD7
116	8135464	DLD
117	8137464	PSPH
118	8137709	ZFAND2A
119	8141150	ASNS

120	8142540	FAM3C
121	8144774	VPS37A
122	8146000	ADAM9
123	8146649	MTFR1
124	8148658	ZNF623
125	8150219	BRF2
126	8150565	RNF170
127	8151436	PEX2
128	8151788	RBM12B
129	8155214	MELK
130	8155422	CBWD5
131	8155636	CBWD3
132	8156043	PSAT1
133	8158513	DOLPP1
134	8159815	CBWD1
135	8160405	KLHL9
136	8161537	CBWD3
137	8161587	CBWD3
138	8166098	RAB9A
139	8166140	MOSPD2
140	8166442	FAM3C
141	8169617	PGRMC1
142	8176230	RAB39B
143	8177462	CDK7
144	8178225	SLC39A7
145	8179525	SLC39A7
146	8180397	NT5C3
Cluster 20		
1	7899173	DHDDS
2	7899377	PPP1R8
3	7899486	TRNAU1AP
4	7901662	TTC4
5	7904883	CHD1L
6	7907124	TIPRL
7	7907445	KLHL20
8	7913242	MUL1
9	7922008	TADA1
10	7922391	CENPL
11	7926319	SUV39H2
12	7928752	GHITM
13	7929831	HIF1AN
14	7933115	SEPT7L
15	7934852	GLUD1
16	7939329	PDHX
17	7943218	PANX1
18	7943721	FDX1
19	7943842	C11orf57
20	7954279	AEBP2
21	7954382	PYROXD1
22	7959657	ATP6V0A2
23	7961829	BCAT1
24	7962185	AMN1
25	7967287	ZCCHC8
26	7970084	CARKD
27	7970716	LNX2
28	7971550	MED4
29	7974473	FBXO34
30	7975136	FUT8
31	7977127	KLC1
32	7978166	TM9SF1
33	7980523	GTF2A1
34	7988245	MFAP1
35	7989516	HERC1
36	7993833	METTL9
37	7997230	PSMD7
38	8001317	N4BP1
39	8004111	RABEP1
40	8004144	MIS12
41	8005512	PRPSAP2
42	8006477	ZNF830
43	8007435	RUNDC1
44	8015456	KLHL11
45	8017235	APPBP2
46	8021208	ME2
47	8023246	C18orf32
48	8023481	NARS
49	8026339	SNRPG
50	8027510	C19orf40
51	8027521	GPATCH1
52	8030991	LOC147804
53	8035193	C19orf42
54	8042830	MTHFD2
55	8048847	AGFG1
56	8053046	DUSP11
57	8054978	ERCC3
58	8061129	C20orf72
59	8061262	NAA20
60	8070215	SETD4
61	8073875	TRMU
62	8079869	RBM5
63	8084064	MTHFD2
64	8084904	SDHAP2
65	8084912	SDHAP2
66	8087634	TUSC2
67	8092534	TMEM41A
68	8092905	LSG1
69	8093039	SDHAP1
70	8097570	USP38
71	8101228	CNOT6L
72	8104422	MTRR
73	8113250	ERAP1
74	8113591	PGGT1B
75	8116867	TMEM14B
76	8116969	NOL7
77	8120698	MTO1
78	8124262	TDP2

79	8128650	SEC63
80	8131356	CCZ1
81	8132458	MRPL32
82	8134581	ARPC1A
83	8134621	ZKSCAN5
84	8135064	TRIM56
85	8138128	CCZ1
86	8141133	SHFM1
87	8141169	MGC72080
88	8144528	TNKS
89	8144931	ATP6V1B2
90	8146448	MRPL15
91	8146544	UBXN2B
92	8146930	TMEM70
93	8148941	ZNF7
94	8151118	VCPIP1
95	8155234	ZCCHC7
96	8157700	RABGAP1
97	8158112	CDK9
98	8162676	TSTD2
99	8163402	PTBP3
100	8163784	FBXW2
101	8163964	PDCL
102	8169920	RBMX2
103	8178090	C6orf48
104	8179326	C6orf48
105	8180257	CEP170
Cluster 21		
1	7897370	VAMP3
2	7905171	PRPF3
3	7906400	IFI16
4	7909782	RRP15
5	7911539	CCNL2
6	7922432	RC3H1
7	7925996	FBXO18
8	7926916	ZEB1
9	7927233	FAM21C
10	7927323	FAM21B
11	7927560	FAM21A
12	7935425	RRP12
13	7936596	C10orf46
14	7946635	ZBED5
15	7947894	CELF1
16	7953594	EMG1
17	7956524	PIP4K2C
18	7966202	KCTD10
19	7968999	NUDT15
20	7970858	HMGB1
21	7980998	BTBD7
22	7986411	MEF2A
23	7993341	BFAR
24	7998510	CLCN7
25	7999642	KIAA0430

26	8003298	SLC7A5
27	8006183	SUZ12P
28	8007904	GOSR2
29	8008530	UTP18
30	8014738	CWC25
31	8021228	SMAD4
32	8031899	ERVK3-1
33	8039909	CCNL2
34	8043105	KCMF1
35	8048940	SP100
36	8053388	TGOLN2
37	8053562	CHMP3
38	8061715	KIF3B
39	8063211	NCOA3
40	8063315	DDX27
41	8063607	RAB22A
42	8064976	DNAJC9
43	8067206	CTCFL
44	8073733	NUP50
45	8077931	MKRN2
46	8082408	SEC61A1
47	8087461	GMPPB
48	8091764	KPNA4
49	8099029	TNIP2
50	8103922	CASP3
51	8107353	ZRSR1
52	8107578	SRFBP1
53	8108510	ANKHD1-EIF4EBP3
54	8109528	CYFIP2
55	8110169	FAF2
56	8110894	NSUN2
57	8112312	DIMT1
58	8115765	FBXW11
59	8115783	STK10
60	8115895	KIAA1191
61	8122672	TAB2
62	8124022	DTNBP1
63	8124950	LTB
64	8125850	C6orf106
65	8130383	MTRF1L
66	8131044	GET4
67	8132188	AVL9
68	8134992	SRRT
69	8135363	PIK3CG
70	8136539	LUC7L2
71	8139859	GUSB
72	8142852	TNPO3
73	8144586	MTMR9
74	8145922	DDHD2
75	8147785	DCAF13
76	8150287	WHSC1L1
77	8150537	SLC20A2

78	8152628	DERL1
79	8154012	KANK1
80	8154856	UBE2R2
81	8157945	ZBTB34
82	8158686	FUBP3
83	8161632	PTAR1
84	8164587	TOR1A
85	8167790	TSR2
86	8177560	BDP1
87	8178512	LTB
88	8179768	LTB
Cluster 22		
1	7900438	ZNF643
2	7902166	MIER1
3	7903369	SLC30A7
4	7903893	CD53
5	7906819	ATF6
6	7907773	TOR1AIP1
7	7909628	FLVCR1
8	7912675	ZBTB17
9	7914202	SNHG12
10	7914214	SNORA44
11	7916135	CC2D1B
12	7917771	DNTTIP2
13	7919888	CDC42SE1
14	7920839	RIT1
15	7921667	CD48
16	7921970	ALDH9A1
17	7924701	ACBD3
18	7926021	RBM17
19	7926836	RAB18
20	7927513	FAM21C
21	7927767	ADO
22	7927972	VPS26A
23	7928171	SGPL1
24	7932885	ARHGAP12
25	7934122	SAR1A
26	7934459	NDST2
27	7934812	WAPAL
28	7936463	ABLIM1
29	7938762	GTF2H1
30	7947540	TRAF6
31	7953021	ADIPOR2
32	7959473	DENR
33	7960134	ZNF26
34	7962516	SLC38A1
35	7966638	RBM19
36	7967624	SLC15A4
37	7967794	ANKLE2
38	7970413	PSPC1
39	7970696	USP12
40	7972062	FBXL3
41	7972828	ANKRD10
42	7974249	ARF6
43	7975645	ZNF410
44	7975863	C14orf118
45	7978628	PPP2R3C
46	7979044	NIN
47	7979223	DDHD1
48	7980680	FOXN3
49	7980833	SMEK1
50	7986250	CHD2
51	7986665	NIPA2
52	7986675	NIPA1
53	7989013	RSL24D1
54	7991581	CHSY1
55	7993159	C16orf72
56	7993433	PDXDC1
57	7994102	DCTN5
58	7994518	SPNS1
59	7996341	PDP2
60	7996772	SLC7A6
61	7997381	CENPN
62	7998174	LUC7L
63	8001841	DYNC1LI2
64	8002878	TMEM170A
65	8003758	PAFAH1B1
66	8007885	NSF
67	8008087	NFE2L1
68	8008139	UBE2Z
69	8013908	NUFIP2
70	8015642	PSMC3IP
71	8017711	GNA13
72	8020149	NAPG
73	8021113	C18orf25
74	8022996	EPG5
75	8042291	AFTPH
76	8045398	RAB3GAP1
77	8046726	SSFA2
78	8047865	PIKFYVE
79	8048752	MRPL44
80	8049657	ASB1
81	8050128	KIDINS220
82	8050190	ADAM17
83	8050719	ITSN2
84	8052024	FBXO11
85	8052680	RAB1A
86	8053668	EIF2AK3
87	8054227	REV1
88	8054804	CCDC93
89	8054997	MAP3K2
90	8058182	FAM126B
91	8068062	USP16
92	8068919	PDXK
93	8070269	DSCR3
94	8072454	RNF185

95	8075130	PITPNB
96	8077450	ARL8B
97	8077458	EDEM1
98	8078350	TGFBR2
99	8078569	GOLGA4
100	8079021	CTNNB1
101	8081055	CHMP2B
102	8084717	ST6GAL1
103	8087473	IP6K1
104	8089299	CD47
105	8089584	C3orf17
106	8089999	KPNA1
107	8090490	RPN1
108	8092392	KLHL6
109	8092849	ATP13A3
110	8096938	LARP7
111	8098414	SPCS3
112	8099850	TMEM156
113	8101013	RCHY1
114	8103524	TMEM192
115	8105681	ERBB2IP
116	8107194	C5orf30
117	8109062	FBXO38
118	8109344	GM2A
119	8109350	SLC36A1
120	8110886	MED10
121	8111129	ZNF622
122	8113023	TMEM161B
123	8113616	FEM1C
124	8114083	AFF4
125	8114326	FAM13B
126	8114787	GNPDA1
127	8114814	NR3C1
128	8115022	CSNK1A1
129	8122202	MYB
130	8127425	LMBRD1
131	8128260	MAP3K7
132	8130071	C15orf29
133	8131292	RBAK
134	8132070	GARS
135	8133176	RABGEF1
136	8133914	DMTF1
137	8135955	CALU
138	8136259	MKLN1
139	8137833	SNX8
140	8138566	IGF2BP3
141	8138592	TRA2A
142	8138613	OSBPL3
143	8139592	HUS1
144	8139891	SBDS
145	8140311	PMS2P3
146	8143697	ZNF786
147	8144516	ERI1
148	8144658	NEIL2
149	8147548	POP1
150	8149258	MFHAS1
151	8149707	BIN3
152	8150126	PPP2CB
153	8150797	ATP6V1H
154	8152845	FAM49B
155	8158560	TOR1B
156	8162294	SPTLC1
157	8167573	GAGE1
158	8175360	MMGT1
159	8176698	TXLNG2P
160	8177137	UTY
161	8180323	USP12
Cluster 23		
1	7897322	PHF13
2	7897774	CLCN6
3	7899436	SESN2
4	7901054	PLK3
5	7902290	CTH
6	7902400	SNORD45B
7	7906564	PEA15
8	7907171	BLZF1
9	7910014	CNIH4
10	7910427	GALNT2
11	7911754	TNFRSF14
12	7914212	SNORA61
13	7915160	RRAGC
14	7915392	HIVEP3
15	7918157	VAV3
16	7918902	CD58
17	7923141	DENND1B
18	7923406	PTPN7
19	7924760	ITPKB
20	7927146	CSGALNACT2
21	7928308	DDIT4
22	7930927	INPP5F
23	7931353	PTPRE
24	7931479	INPP5A
25	7933877	JMJD1C
26	7940160	DTX4
27	7940191	STX3
28	7942289	RNF121
29	7943293	ENDOD1
30	7948332	LPXN
31	7948364	MPEG1
32	7950743	RAB30
33	7953878	CLEC2D
34	7957665	ELK3
35	7958884	OAS1
36	7960637	LPAR5
37	7960933	M6PR
38	7961151	KLRK1

39	7961371	DUSP16
40	7963174	CERS5
41	7964460	DDIT3
42	7965094	E2F7
43	7965964	SLC41A2
44	7968976	LRCH1
45	7969060	FNDC3A
46	7969651	DNAJC3
47	7970844	KATNAL1
48	7975068	ZBTB1
49	7980547	SEL1L
50	7982564	SPRED1
51	7983828	TEX9
52	7984112	RAB8B
53	7985482	WHAMM
54	7989069	PYGO1
55	7990345	SEMA7A
56	7992789	TNFRSF12A
57	7993167	ATF7IP2
58	7995895	HERPUD1
59	7996022	CCL22
60	7996954	NFAT5
61	8000028	DCUN1D3
62	8002322	PDXDC2P
63	8003611	FAM57A
64	8003875	SPNS2
65	8005707	MAP2K3
66	8005765	WSB1
67	8006123	CPD
68	8011875	DERL2
69	8013071	FLCN
70	8014233	SLFN11
71	8014391	CCL3L1
72	8014414	CCL3L1
73	8016088	CCDC43
74	8017843	SLC16A6
75	8019308	MAFG
76	8019731	CCL3L1
77	8019796	MAFG
78	8023646	BCL2
79	8026272	IL27RA
80	8027837	CD22
81	8032410	MOB3A
82	8035694	PBX4
83	8040440	GEN1
84	8042391	PLEK
85	8042416	ARHGAP25
86	8045289	RHOQ
87	8047854	CCNYL1
88	8050766	ADCY3
89	8051547	PRKD3
90	8056977	NFE2L2
91	8058824	MREG
92	8059361	WDFY1
93	8059854	ARL4C
94	8060344	TRIB3
95	8060418	SIRPA
96	8062964	SYS1
97	8063923	SLCO4A1
98	8064808	SLC23A2
99	8064868	GPCPD1
100	8067113	ZNF217
101	8069532	HSPA13
102	8071559	SDF2L1
103	8076533	PACSIN2
104	8079517	KLHL18
105	8082075	DTX3L
106	8083090	ZBTB38
107	8084045	MFN1
108	8084634	DNAJB11
109	8090018	PARP9
110	8096004	BMP2K
111	8096675	TET2
112	8097017	UGT8
113	8099760	ARAP2
114	8099897	UGDH
115	8101925	LAMTOR3
116	8102371	C4orf21
117	8102389	C4orf21
118	8103951	ACSL1
119	8104499	ANKRD33B
120	8105067	PTGER4
121	8106252	HEXB
122	8110569	SQSTM1
123	8112409	SGTB
124	8112428	CD180
125	8113064	LYSMD3
126	8113914	FNIP1
127	8118137	LTA
128	8118322	SNORD52
129	8119088	CDKN1A
130	8122343	HECA
131	8122756	PLEKHG1
132	8123181	IGF2R
133	8123609	SERPINB9
134	8123976	GFOD1
135	8125461	HLA-DQB1
136	8126542	ZNF318
137	8126666	NFKBIE
138	8128716	CD164
139	8129804	MAP3K5
140	8129861	IFNGR1
141	8131265	KIAA0415
142	8131479	MIOS
143	8132305	EEPD1
144	8135514	IFRD1

145	8135568	MDFIC
146	8135576	TES
147	8136591	ADCK2
148	8137091	ZNF398
149	8139003	HERPUD2
150	8145136	PPP3CC
151	8145954	TACC1
152	8147344	PDP1
153	8147439	PLEKHF2
154	8149330	CTSB
155	8149534	ASAH1
156	8152041	RNF19A
157	8153201	EIF2C2
158	8155930	GCNT1
159	8157524	TLR4
160	8157933	ZBTB43
161	8159554	UAP1L1
162	8163825	TRAF1
163	8164165	HSPA5
164	8164343	FAM102A
165	8164701	SETX
166	8167006	RP2
167	8168447	CXorf26
168	8177976	LTA
169	8179258	LTA
Cluster 24		
1	7899310	TMEM222
2	7900146	ZC3H12A
3	7907690	TOR3A
4	7912102	KLHL21
5	7913357	ECE1
6	7914021	SLC9A1
7	7920944	SMG5
8	7922717	RGS16
9	7923394	ARL8A
10	7926531	ARL5B
11	7930074	NFKB2
12	7948399	PATL1
13	7958749	SH2B3
14	7979813	ZFP36L1
15	7980051	C14orf43
16	7984952	C15orf39
17	7995258	ZNF267
18	8004671	KDM6B
19	8004691	TMEM88
20	8013312	FAM83G
21	8014956	NR1D1
22	8018937	USP36
23	8024228	MIDN
24	8026350	CLEC17A
25	8026915	ARRDC2
26	8030128	PPP1R15A
27	8035703	LPAR2
28	8036207	NFKBID
29	8040103	ID2
30	8049075	B3GNT7
31	8053882	DUSP2
32	8060427	STK35
33	8063156	CD40
34	8063583	RBM38
35	8066905	ZNFX1
36	8068280	IFNGR2
37	8071899	ADORA2A
38	8073960	PIM3
39	8077728	LOC442075
40	8082314	PLXNA1
41	8086330	CSRNP1
42	8091485	SIAH2
43	8096635	NFKB1
44	8103025	ZNF827
45	8109201	HMGXB3
46	8113761	ZNF608
47	8115806	UBTD2
48	8116559	IRF4
49	8116983	CD83
50	8123606	MGC39372
51	8152215	KLF10
52	8158147	SLC25A25
53	8164336	DPM2
Cluster 25		
1	7904361	FAM46C
2	7906622	LY9
3	7956287	NAB2
4	7965040	PHLDA1
5	7985493	TM6SF1
6	8044766	INSIG2
7	8082086	PARP15
8	8100231	TEC
9	8102800	SLC7A11
10	8113073	ARRDC3
11	8118142	TNF
12	8122265	TNFAIP3
13	8122334	CCRL1
14	8128123	RRAGD
15	8129677	SGK1
16	8131844	GPNMB
17	8151816	GEM
18	8177983	TNF
19	8179263	TNF
Cluster 26		
1	7906613	SLAMF7
Cluster 27		
1	7904726	TXNIP
2	7909214	RASSF5
3	7921625	SLAMF6
4	7922474	KIAA0040

5	7930139	TRIM8
6	7931863	ASB13
7	7947624	PHF21A
8	7955589	NR4A1
9	7963575	EIF4B
10	7966183	ALKBH2
11	7969677	MBNL2
12	7975626	C14orf43
13	7978644	NFKBIA
14	7988212	ELL3
15	7996571	FAM65A
16	8008263	PDK2
17	8028652	ZFP36
18	8029693	FOSB
19	8042811	TET3

20	8075673	RBFOX2
21	8084880	HES1
22	8088142	CHDH
23	8088180	WNT5A
24	8094743	RHOH
25	8108370	EGR1
26	8116910	HIVEP1
27	8117106	RNF144B
28	8119161	PIM1
29	8121850	HEY2
30	8132819	IKZF1
31	8149720	EGR3
32	8151101	MYBL1
33	8163629	TNFSF8
34	8165496	TUBB4B

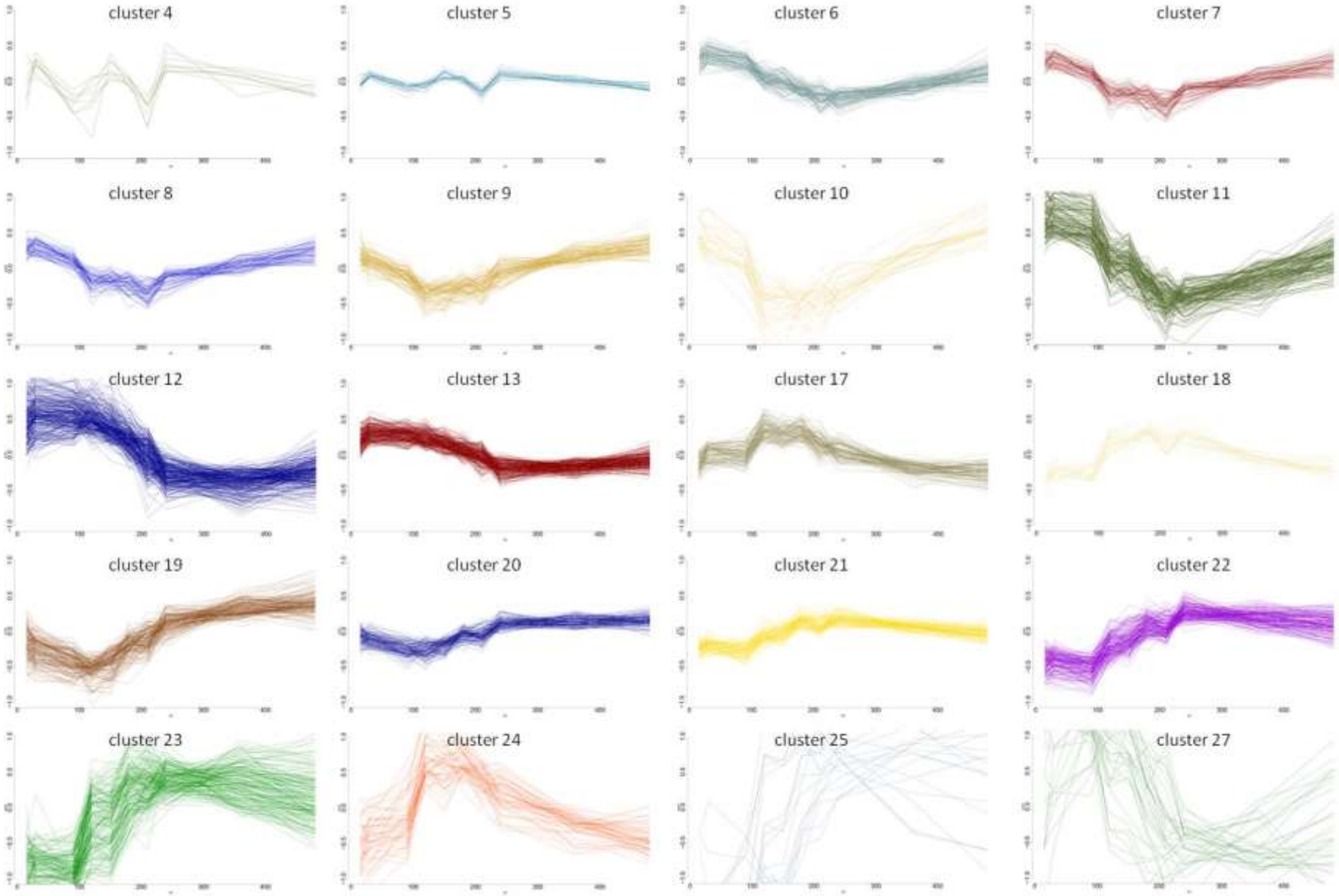

Figure A-1 (see next page for legend)

Figure A-1 Bayesian Hierarchical Clustering reveals 27 clusters of genes bearing differential expression over time. α-IgM stimulation of BL2 cells was monitored with regard to gene expression changes on the whole genome level for a period of 8 hours. Three biological replicates were hybridized to Human Gene ST 1.0 microarray chips (Affymetrix). Bayesian hierarchical clustering identified 21 clusters of genes with an expression range > 0.5. Clusters of genes with less than 10 % significantly enriched genes (FDR < 0.05) were excluded (cluster 26 contains only SLAMF7). Depicted are the time courses of each gene in one cluster.

Table A-2 Gene set enrichment analysis for manually picked clusters (cl 6, cl 8 and cl 11)

GOBPID	Pvalue	OddsRatio	ExpCount	Count	Size	Term
cluster 6						
GO:0044267	0.000	2.544	16	30	2926	cellular protein metabolic process
GO:0043153	0.000	191.784	0	2	4	entrainment of circadian clock by photoperiod
GO:0006464	0.000	2.492	12	24	2242	protein modification process
GO:0009648	0.000	95.878	0	2	6	photoperiodism
GO:0033235	0.001	76.697	0	2	7	positive regulation of protein sumoylation
GO:0043412	0.001	2.373	12	24	2335	macromolecule modification
GO:0033233	0.001	63.910	0	2	8	regulation of protein sumoylation
GO:0043501	0.001	63.910	0	2	8	skeletal muscle adaptation
GO:0009649	0.001	54.776	0	2	9	entrainment of circadian clock
GO:0019538	0.001	2.153	18	31	3472	protein metabolic process
GO:0071397	0.001	47.926	0	2	10	cellular response to cholesterol
GO:0014888	0.002	38.335	0	2	12	striated muscle adaptation
GO:0006486	0.004	5.136	1	5	197	protein glycosylation
GO:0043413	0.004	5.136	1	5	197	macromolecule glycosylation
GO:0070085	0.004	5.082	1	5	199	glycosylation
GO:0050691	0.005	22.539	0	2	19	regulation of defense response to virus by host
GO:0070723	0.005	22.539	0	2	19	response to cholesterol
GO:0044260	0.005	1.858	32	44	6081	cellular macromolecule metabolic process
GO:0006507	0.005	Inf	0	1	1	GPI anchor release
GO:0046092	0.005	Inf	0	1	1	deoxycytidine metabolic process
GO:0048213	0.005	Inf	0	1	1	Golgi vesicle prefusion complex stabilization
GO:0051754	0.005	Inf	0	1	1	meiotic sister chromatid cohesion, centromeric
GO:0061310	0.005	Inf	0	1	1	canonical Wnt receptor signaling pathway involved in cardiac neural crest cell differentiation involved in heart development
GO:0070159	0.005	Inf	0	1	1	mitochondrial threonyl-tRNA aminoacylation
GO:0071401	0.005	Inf	0	1	1	cellular response to triglyceride
GO:0071609	0.005	Inf	0	1	1	chemokine (C-C motif) ligand 5 production
GO:0071612	0.005	Inf	0	1	1	IP-10 production
GO:0071649	0.005	Inf	0	1	1	regulation of chemokine (C-C motif) ligand 5 production
GO:0071651	0.005	Inf	0	1	1	positive regulation of chemokine (C-C motif) ligand 5 production
GO:0071658	0.005	Inf	0	1	1	regulation of IP-10 production
GO:0071660	0.005	Inf	0	1	1	positive regulation of IP-10 production

GO:0090219	0.005	Inf	0	1	1	negative regulation of lipid kinase activity
GO:0097241	0.005	Inf	0	1	1	hematopoietic stem cell migration to bone marrow
GO:1900037	0.005	Inf	0	1	1	regulation of cellular response to hypoxia
GO:2000055	0.005	Inf	0	1	1	positive regulation of Wnt receptor signaling pathway involved in dorsal/ventral axis specification
GO:2000148	0.005	Inf	0	1	1	regulation of planar cell polarity pathway involved in ventricular septum morphogenesis
GO:2000149	0.005	Inf	0	1	1	negative regulation of planar cell polarity pathway involved in ventricular septum morphogenesis
GO:2000150	0.005	Inf	0	1	1	regulation of planar cell polarity pathway involved in cardiac muscle tissue morphogenesis
GO:2000151	0.005	Inf	0	1	1	negative regulation of planar cell polarity pathway involved in cardiac muscle tissue morphogenesis
GO:2000159	0.005	Inf	0	1	1	regulation of planar cell polarity pathway involved in heart morphogenesis
GO:2000160	0.005	Inf	0	1	1	negative regulation of planar cell polarity pathway involved in heart morphogenesis
GO:2000161	0.005	Inf	0	1	1	regulation of planar cell polarity pathway involved in cardiac right atrium morphogenesis
GO:2000162	0.005	Inf	0	1	1	negative regulation of planar cell polarity pathway involved in cardiac right atrium morphogenesis
GO:2000163	0.005	Inf	0	1	1	regulation of planar cell polarity pathway involved in outflow tract morphogenesis
GO:2000164	0.005	Inf	0	1	1	negative regulation of planar cell polarity pathway involved in outflow tract morphogenesis
GO:2000165	0.005	Inf	0	1	1	regulation of planar cell polarity pathway involved in pericardium morphogenesis
GO:2000166	0.005	Inf	0	1	1	negative regulation of planar cell polarity pathway involved in pericardium morphogenesis
GO:2000167	0.005	Inf	0	1	1	regulation of planar cell polarity pathway involved in neural tube closure

GO:2000168	0.005	Inf	0	1	1	negative regulation of planar cell polarity pathway involved in neural tube closure
GO:0016925	0.006	20.164	0	2	21	protein sumoylation
GO:0070887	0.006	2.306	7	15	1383	cellular response to chemical stimulus
GO:0071310	0.007	2.466	5	12	1015	cellular response to organic substance
GO:0006890	0.007	17.410	0	2	24	retrograde vesicle-mediated transport, Golgi to ER
GO:0044092	0.007	2.849	3	9	648	negative regulation of molecular function
GO:0019835	0.008	15.957	0	2	26	cytolysis
GO:0071396	0.009	15.318	0	2	27	cellular response to lipid
GO:0010907	0.010	14.728	0	2	28	positive regulation of glucose metabolic process
GO:0034381	0.010	14.728	0	2	28	plasma lipoprotein particle clearance
GO:0009101	0.010	4.094	1	5	245	glycoprotein biosynthetic process

Table A-3 List of genes, taken for comparison of CD40 and BCR stimulated BL cells by testing for stationarity.

	Gene ID	Probe ID	Gene Symbol	Gene Name
1	790	7906613	SLAMF7	SLAM family member 7
1	587	7904361	FAM46C	family with sequence similarity 46, member C
1	762	7906339	CD1A	CD1a molecule
1	763	7906348	CD1C	CD1c molecule
1	1169	7911754	TNFRSF14	tumor necrosis factor receptor superfamily, member
1	1216	7912496	MTHFR	methylenetetrahydrofolate reductase (NAD(P)H)
1	2072	7923917	FAIM3	Fas apoptotic inhibitory molecule 3
1	2548	7930413	DUSP5	dual specificity phosphatase 5
1	5066	7961891	BHLHE41	basic helix-loop-helix family, member e41
1	5207	7963911	CD63	CD63 molecule
1	5286	7965040	PHLDA1	pleckstrin homology-like domain, family A, member
1	5790	7972557	GPR183	G protein-coupled receptor 183
1	7130	7990345	SEMA7A	semaphorin 7A, GPI membrane anchor (John Milton Ha
1	7327	7992789	TNFRSF12A	tumor necrosis factor receptor superfamily, member
1	8388	8006608	CCL4L1	chemokine (C-C motif) ligand 4-like 1
1	8389	8006621	CCL4L1	chemokine (C-C motif) ligand 4-like 1
1	8623	8009476	MAP2K6	mitogen-activated protein kinase kinase 6
1	9420	8019651	CCL4L1	chemokine (C-C motif) ligand 4-like 1
1	10263	8030007	EMP3	epithelial membrane protein 3
1	12534	8059854	ARL4C	ADP-ribosylation factor-like 4C
1	13836	8075886	IL2RB	interleukin 2 receptor, beta
1	14768	8088848	PDZRN3	PDZ domain containing ring finger 3
1	15587	8100231	TEC	tec protein tyrosine kinase
1	17463	8125139	NEU1	sialidase 1 (lysosomal sialidase)
1	18005	8132725	UPP1	uridine phosphorylase 1
1	19132	8147344	PDP1	pyruvate dehyrogenase phosphatase catalytic subuni

1	19304	8149330	CTSB	cathepsin B
1	19510	8151816	GEM	GTP binding protein overexpressed in skeletal musc
1	21675	8178676	NEU1	sialidase 1 (lysosomal sialidase)
1	21798	8179851	NEU1	sialidase 1 (lysosomal sialidase)
3	13173	8068022	MIR155HG	MIR155 host gene (non-protein coding)
3	1056	7910427	GALNT2	UDP-N-acetyl-alpha-D-galactosamine:polypeptide N-a
3	1073	7910680	GPR137B	G protein-coupled receptor 137B
3	1347	7914202	SNHG12	small nucleolar RNA host gene 12 (non-protein codi
3	1348	7914212	SNORA61	small nucleolar RNA, H/ACA box 61
3	1601	7917754	BCAR3	breast cancer anti-estrogen resistance 3
3	1677	7918902	CD58	CD58 molecule
3	5457	7967624	SLC15A4	solute carrier family 15, member 4
3	6922	7986665	NIPA2	non imprinted in Prader-Willi/Angelman syndrome 2
3	7106	7989968	CALML4	calmodulin-like 4
3	9034	8015031	CCR7	chemokine (C-C motif) receptor 7
3	9716	8023646	BCL2	B-cell CLL/lymphoma 2
3	9922	8026007	ZNF791	zinc finger protein 791
3	10765	8035694	PBX4	pre-B-cell leukemia homeobox 4
3	12770	8062964	SYS1	SYS1 Golgi-localized integral membrane protein hom
3	13776	8075130	PITPNB	phosphatidylinositol transfer protein, beta
3	13965	8077450	ARL8B	ADP-ribosylation factor-like 8B
3	14296	8082086	PARP15	poly (ADP-ribose) polymerase family, member 15
3	15864	8103951	ACSL1	acyl-CoA synthetase long-chain family member 1
3	15939	8105067	PTGER4	prostaglandin E receptor 4 (subtype EP4)
3	16336	8110569	SQSTM1	sequestosome 1
3	16365	8110886	MED10	mediator complex subunit 10
3	16424	8111941	HMGCS1	3-hydroxy-3-methylglutaryl-CoA synthase 1 (soluble
3	16530	8113305	CHD1	chromodomain helicase DNA binding protein 1
3	16741	8116227	CLK4	CDC-like kinase 4
3	17286	8123181	IGF2R	insulin-like growth factor 2 receptor
3	17482	8125447	HLA-DQB1	major histocompatibility complex, class II, DQ bet
3	17583	8126666	NFKBIE	nuclear factor of kappa light polypeptide gene enh
3	19015	8145691	UBXN8	UBX domain protein 8
3	21736	8179258	LTA	lymphotoxin alpha (TNF superfamily, member 1)
4	9890	8025601	ICAM1	intercellular adhesion molecule 1
4	287	7900146	ZC3H12A	zinc finger CCCH-type containing 12A
4	606	7904702	NOTCH2NL	notch 2 N-terminal like
4	987	7909503	SERTAD4	SERTA domain containing 4
4	1697	7919193	NUDT4P1	nudix (nucleoside diphosphate linked moiety X)-typ
4	2071	7923907	IL10	interleukin 10
4	2450	7929032	FAS	Fas (TNF receptor superfamily, member 6)
4	2525	7930074	NFKB2	nuclear factor of kappa light polypeptide gene enh
4	2778	7933750	SLC16A9	solute carrier family 16, member 9 (monocarboxylic
4	6047	7975793	BATF	basic leucine zipper transcription factor, ATF-lik
4	6149	7977018	TRAF3	TNF receptor-associated factor 3
4	6493	7981530	GPR132	G protein-coupled receptor 132
4	6946	7987048	MTMR10	myotubularin related protein 10
4	7097	7989849	DENND4A	DENN/MADD domain containing 4A
4	7833	7999496	ZC3H7A	zinc finger CCCH-type containing 7A
4	8038	8002152	SLC12A4	solute carrier family 12 (potassium/chloride trans

4	8523	8008096	SNX11	sorting nexin 11
4	9345	8018922	CYTH1	cytohesin 1
4	9790	8024485	GADD45B	growth arrest and DNA-damage-inducible, beta
4	11145	8039545	NLRP11	NLR family, pyrin domain containing 11
4	11467	8043583	LOC285033	hypothetical protein LOC285033
4	12722	8062319	TGIF2	TGFB-induced factor homeobox 2
4	13294	8069541	SAMSN1	SAM domain, SH3 domain and nuclear localization si
4	14827	8089771	CD80	CD80 molecule
4	15907	8104580	FAM105B	family with sequence similarity 105, member B
4	15908	8104590	LOC100130744	hypothetical LOC100130744
4	16139	8108080	PHF15	PHD finger protein 15
4	17270	8122933	TIAM2	T-cell lymphoma invasion and metastasis 2
4	18253	8136067	TSPAN33	tetraspanin 33
4	20028	8158918	GTF3C4	general transcription factor IIIC, polypeptide 4,
5	16514	8113073	ARRDC3	arrestin domain containing 3
5	908	7908409	RGS2	regulator of G-protein signaling 2, 24kDa
5	2158	7925062	SIPA1L2	signal-induced proliferation-associated 1 like 2
5	4441	7953532	ENO2	enolase 2 (gamma, neuronal)
5	4992	7961075	CD69	CD69 molecule
5	8963	8014063	EVI2B	ecotropic viral integration site 2B
5	8964	8014066	EVI2A	ecotropic viral integration site 2A
5	12671	8061564	ID1	inhibitor of DNA binding 1, dominant negative heli
5	14645	8086961	PFKFB4	6-phosphofructo-2-kinase/fructose-2,6-biphosphatas
5	15286	8095870	CCNG2	cyclin G2
5	15296	8096070	BMP3	bone morphogenetic protein 3
5	15668	8101322	MOP-1	MOP-1
5	16475	8112615	ENC1	ectodermal-neural cortex 1 (with BTB-like domain)
5	16810	8117020	MYLIP	myosin regulatory light chain interacting protein
5	17049	8119898	VEGFA	vascular endothelial growth factor A
5	17197	8121861	NCOA7	nuclear receptor coactivator 7
5	17371	8124380	HIST1H1A	histone cluster 1, H1a
5	17884	8131069	GPER	G protein-coupled estrogen receptor 1
5	19666	8154100	VLDLR	very low density lipoprotein receptor
6	16808	8116983	CD83	CD83 molecule
6	1992	7922717	RGS16	regulator of G-protein signaling 16
6	2110	7924450	DUSP10	dual specificity phosphatase 10
6	2654	7931914	IL2RA	interleukin 2 receptor, alpha
6	3136	7938329	SNORA23	small nucleolar RNA, H/ACA box 23
6	3578	7943424	BIRC2	baculoviral IAP repeat-containing 2
6	4202	7950743	RAB30	RAB30, member RAS oncogene family
6	4515	7954436	LRMP	lymphoid-restricted membrane protein
6	6013	7975368	SRSF5	serine/arginine-rich splicing factor 5
6	6751	7984364	SMAD3	SMAD family member 3
6	7846	7999642	KIAA0430	KIAA0430
6	10766	8035703	LPAR2	lysophosphatidic acid receptor 2
6	10812	8036207	NFKBID	nuclear factor of kappa light polypeptide gene enh
6	12050	8052269	CCDC88A	coiled-coil domain containing 88A
6	12786	8063156	CD40	CD40 molecule, TNF receptor superfamily member 5
6	12796	8063351	SLC9A8	solute carrier family 9 (sodium/hydrogen exchanger
6	13225	8068551	DYRK1A	dual-specificity tyrosine-(Y)-phosphorylation regu

6	14291	8082035	CD86	CD86 molecule
6	14449	8084219	KLHL24	kelch-like 24 (Drosophila)
6	14763	8088776	FOXP1	forkhead box P1
6	14942	8091485	SIAH2	seven in absentia homolog 2 (Drosophila)
6	15555	8099760	ARAP2	ArfGAP with RhoGAP domain, ankyrin repeat and PH d
6	16561	8113761	ZNF608	zinc finger protein 608
6	17168	8121563	MARCKS	myristoylated alanine-rich protein kinase C substr
6	17232	8122343	HECA	headcase homolog (Drosophila)
6	17315	8123606	MGC39372	serpin peptidase inhibitor, clade B (ovalbumin), m
6	17347	8123981	C6orf114	chromosome 6 open reading frame 114
6	18983	8145136	PPP3CC	protein phosphatase 3, catalytic subunit, gamma is
6	19386	8150225	RAB11FIP1	RAB11 family interacting protein 1 (class I)
6	21458	8176384	ZFY	zinc finger protein, Y-linked
8	14277	8081838	ARHGAP31	Rho GTPase activating protein 31
8	785	7906564	PEA15	phosphoprotein enriched in astrocytes 15
8	1956	7922343	TNFSF4	tumor necrosis factor (ligand) superfamily, member
8	2819	7934367	ANXA7	annexin A7
8	2875	7935146	NOC3L	nucleolar complex associated 3 homolog (S. cerevis
8	4468	7953873	OVOS	ovostatin
8	4988	7961026	OVOS	ovostatin
8	5147	7963235	CSRNP2	cysteine-serine-rich nuclear protein 2
8	5377	7966356	HVCN1	hydrogen voltage-gated channel 1
8	7363	7993185	NUBP1	nucleotide binding protein 1 (MinD homolog, E. col
8	7968	8001185	DNAJA2	DnaJ (Hsp40) homolog, subfamily A, member 2
8	8679	8010243	SYNGR2	synaptogyrin 2
8	8735	8011027	MYO1C	myosin IC
8	9145	8016194	MAP3K14	mitogen-activated protein kinase kinase kinase 14
8	9493	8020495	CABLES1	Cdk5 and Abl enzyme substrate 1
8	9798	8024572	GNA15	guanine nucleotide binding protein (G protein), al
8	11850	8049271	ATG16L1	ATG16 autophagy related 16-like 1 (S. cerevisiae)
8	12201	8054192	MITD1	MIT, microtubule interacting and transport, domain
8	12503	8059413	DOCK10	dedicator of cytokinesis 10
8	14674	8087473	IP6K1	inositol hexakisphosphate kinase 1
8	15291	8096004	BMP2K	BMP2 inducible kinase
8	16766	8116548	DUSP22	dual specificity phosphatase 22
8	16908	8117890	HLA-E	major histocompatibility complex, class I, E
8	17325	8123717	RPP40	ribonuclease P/MRP 40kDa subunit
8	18070	8133459	CLIP2	CAP-GLY domain containing linker protein 2
8	20111	8159984	C9orf46	chromosome 9 open reading frame 46
8	20513	8164967	VAV2	vav 2 guanine nucleotide exchange factor
8	21197	8173444	IL2RG	interleukin 2 receptor, gamma
8	21584	8177788	HLA-E	major histocompatibility complex, class I, E
8	21721	8179103	HLA-E	major histocompatibility complex, class I, E
9	8447	8007228	ATP6V0A1	ATPase, H+ transporting, lysosomal V0 subunit a1
9	1075	7910706	LGALS8	lectin, galactoside-binding, soluble, 8
9	3655	7944560	ARHGEF12	Rho guanine nucleotide exchange factor (GEF) 12
9	4023	7948667	AHNAK	AHNAK nucleoprotein
9	4255	7951351	PDGFD	platelet derived growth factor D
9	4444	7953569	PTPN6	protein tyrosine phosphatase, non-receptor type 6
9	5549	7969060	FNDC3A	fibronectin type III domain containing 3A

9	6422	7980547	SEL1L	sel-1 suppressor of lin-12-like (C. elegans)
9	6443	7980958	LGMN	legumain
9	6474	7981290	WARS	tryptophanyl-tRNA synthetase
9	7051	7989037	CCPG1	cell cycle progression 1
9	8350	8006123	CPD	carboxypeptidase D
9	10652	8034304	ACP5	acid phosphatase 5, tartrate resistant
9	12500	8059361	WDFY1	WD repeat and FYVE domain containing 1
9	13957	8077270	CHL1	cell adhesion molecule with homology to L1CAM (clo
9	14367	8083092	ZBTB38	zinc finger and BTB domain containing 38
9	14471	8084634	DNAJB11	DnaJ (Hsp40) homolog, subfamily B, member 11
9	15358	8097017	UGT8	UDP glycosyltransferase 8
9	15434	8098121	RAPGEF2	Rap guanine nucleotide exchange factor (GEF) 2
9	16022	8106252	HEXB	hexosaminidase B (beta polypeptide)
9	16160	8108378	CTNNA1	catenin (cadherin-associated protein), alpha 1, 10
9	16492	8112841	HOMER1	homer homolog 1 (Drosophila)
9	17145	8121257	PRDM1	PR domain containing 1, with ZNF domain
9	17231	8122336	C6orf115	chromosome 6 open reading frame 115
9	17345	8123961	TBC1D7	TBC1 domain family, member 7
9	17683	8128123	RRAGD	Ras-related GTP binding D
9	17784	8129804	MAP3K5	mitogen-activated protein kinase kinase kinase 5
9	17787	8129861	IFNGR1	interferon gamma receptor 1
9	19810	8155930	GCNT1	glucosaminyl (N-acetyl) transferase 1, core 2
9	20881	8169541	DOCK11	dedicator of cytokinesis 11
10	1973	7922474	KIAA0040	KIAA0040
10	42	7897210	DFFB	DNA fragmentation factor, 40kDa, beta polypeptide
10	354	7901102	MMACHC	methylmalonic aciduria (cobalamin deficiency) cblC
10	661	7905299	PRUNE	prune homolog (Drosophila)
10	1312	7913787	C1orf201	chromosome 1 open reading frame 201
10	1646	7918457	KCNA3	potassium voltage-gated channel, shaker-related su
10	2529	7930139	TRIM8	tripartite motif-containing 8
10	3396	7941104	ARL2	ADP-ribosylation factor-like 2
10	3505	7942562	NEU3	sialidase 3 (membrane sialidase)
10	3762	7945875	FAM86C	family with sequence similarity 86, member C
10	4138	7949948	C11orf24	chromosome 11 open reading frame 24
10	4931	7960320	DCP1B	DCP1 decapping enzyme homolog B (S. cerevisiae)
10	6055	7975926	KIAA1737	KIAA1737
10	6343	7979505	SIX1	SIX homeobox 1
10	6910	7986463	LRRK1	leucine-rich repeat kinase 1
10	7308	7992594	CCNF	cyclin F
10	7736	7998336	NARFL	nuclear prelamin A recognition factor-like
10	8540	8008297	XYLT2	xylosyltransferase II
10	8543	8008339	RSAD1	radical S-adenosyl methionine domain containing 1
10	8764	8011396	SHPK	sedoheptulokinase
10	9234	8017186	HEATR6	HEAT repeat containing 6
10	9986	8026712	ANKLE1	ankyrin repeat and LEM domain containing 1
10	16165	8108447	CXXC5	CXXC finger 5
10	17196	8121850	HEY2	hairy/enhancer-of-split related with YRPW motif 2
10	18410	8138088	C7orf70	chromosome 7 open reading frame 70
10	20320	8162438	BICD2	bicaudal D homolog 2 (Drosophila)
10	20457	8164252	SH2D3C	SH2 domain containing 3C

10	20461	8164314	ST6GALNAC4	ST6 (alpha-N-acetyl-neuraminyl-2,3-beta-galactosyl
10	20489	8164644	FAM78A	family with sequence similarity 78, member A
10	21991	8180413	ST6GALNAC4	ST6 (alpha-N-acetyl-neuraminyl-2,3-beta-galactosyl
11	19176	8148059	DEPDC6	DEP domain containing 6
11	405	7901788	NFIA	nuclear factor I/A
11	771	7906386	PYHIN1	pyrin and HIN domain family, member 1
11	943	7908924	PRELP	proline/arginine-rich end leucine-rich repeat prot
11	1307	7913705	CNR2	cannabinoid receptor 2 (macrophage)
11	2311	7927215	ALOX5	arachidonate 5-lipoxygenase
11	3096	7938035	TRIM22	tripartite motif-containing 22
11	4061	7949021	RCOR2	REST corepressor 2
11	4168	7950307	UCP2	uncoupling protein 2 (mitochondrial, proton carrie
11	4208	7950810	SYTL2	synaptotagmin-like 2
11	4809	7958466	ACACB	acetyl-CoA carboxylase beta
11	5003	7961175	KLRC3	killer cell lectin-like receptor subfamily C, memb
11	6172	7977319	PLD4	phospholipase D family, member 4
11	6263	7978376	STXBP6	syntaxin binding protein 6 (amisyn)
11	6460	7981142	CLMN	calmin (calponin-like, transmembrane)
11	7111	7990033	TLE3	transducin-like enhancer of split 3 (E(sp1) homolo
11	7847	7999674	MYH11	myosin, heavy chain 11, smooth muscle
11	9261	8017599	PECAM1	platelet/endothelial cell adhesion molecule
11	10571	8033233	TUBB4	tubulin, beta 4
11	10909	8037205	CEACAM1	carcinoembryonic antigen-related cell adhesion mol
11	11579	8045182	PTPN18	protein tyrosine phosphatase, non-receptor type 18
11	12387	8057418	ZNF385B	zinc finger protein 385B
11	13106	8067185	BMP7	bone morphogenetic protein 7
11	13692	8074237	CECR1	cat eye syndrome chromosome region, candidate 1
11	14484	8084742	LPP	LIM domain containing preferred translocation part
11	16031	8106411	S100Z	S100 calcium binding protein Z
11	16542	8113504	C5orf13	chromosome 5 open reading frame 13
11	17432	8124806	NRM	nurim (nuclear envelope membrane protein)
11	19841	8156321	SYK	spleen tyrosine kinase
11	21058	8171493	CTPS2	CTP synthase II
12	9656	8022817	KLHL14	kelch-like 14 (Drosophila)
12	1867	7921319	FCRL1	Fc receptor-like 1
12	2779	7933760	CCDC6	coiled-coil domain containing 6
12	2780	7933772	ANK3	ankyrin 3, node of Ranvier (ankyrin G)
12	4014	7948565	CYBASC3	cytochrome b, ascorbate dependent 3
12	4491	7954104	ATF7IP	activating transcription factor 7 interacting prot
12	5077	7962151	DENND5B	DENN/MADD domain containing 5B
12	5323	7965541	FGD6	FYVE, RhoGEF and PH domain containing 6
12	5596	7969677	MBNL2	muscleblind-like 2 (Drosophila)
12	5972	7974653	KIAA0586	KIAA0586
12	6431	7980744	RPS6KA5	ribosomal protein S6 kinase, 90kDa, polypeptide 5
12	6900	7986383	IGF1R	insulin-like growth factor 1 receptor
12	6995	7987892	ZFP106	zinc finger protein 106 homolog (mouse)
12	8469	8007471	NBR1	neighbor of BRCA1 gene 1
12	9186	8016546	ZNF652	zinc finger protein 652
12	11738	8047565	FAM117B	family with sequence similarity 117, member B
12	14752	8088550	PRICKLE2	prickle homolog 2 (Drosophila)

12	14794	8089261	CBLB	Cas-Br-M (murine) ecotropic retroviral transformin
12	15401	8097657	SMAD1	SMAD family member 1
12	16038	8106516	JMY	junction mediating and regulatory protein, p53 cof
12	16437	8112107	PPAP2A	phosphatidic acid phosphatase type 2A
12	17003	8119161	PIM1	pim-1 oncogene
12	17209	8122071	ENPP3	ectonucleotide pyrophosphatase/phosphodiesterase 3
12	18799	8142930	TSGA14	testis specific, 14
12	20331	8162533	PTCH1	patched 1
12	20348	8162719	HEMGN	hemogen
12	20648	8166730	CYBB	cytochrome b-245, beta polypeptide
12	21096	8172088	BCOR	BCL6 corepressor
12	21127	8172471	PIM2	pim-2 oncogene
12	21228	8173869	POF1B	premature ovarian failure, 1B
13	20406	8163629	TNFSF8	tumor necrosis factor (ligand) superfamily, member
13	265	7899870	ZNF362	zinc finger protein 362
13	623	7904907	BCL9	B-cell CLL/lymphoma 9
13	2364	7927876	TET1	tet oncogene 1
13	2650	7931863	ASB13	ankyrin repeat and SOCS box-containing 13
13	2655	7931930	PRKCQ	protein kinase C, theta
13	2904	7935660	DNMBP	dynamin binding protein
13	3922	7947624	PHF21A	PHD finger protein 21A
13	4073	7949206	MEN1	multiple endocrine neoplasia I
13	4163	7950248	FCHSD2	FCH and double SH3 domains 2
13	4704	7956878	IRAK3	interleukin-1 receptor-associated kinase 3
13	4720	7957126	KCNMB4	potassium large conductance calcium-activated chan
13	4807	7958439	USP30	ubiquitin specific peptidase 30
13	4838	7958960	TPCN1	two pore segment channel 1
13	4843	7959025	RNFT2	ring finger protein, transmembrane 2
13	5277	7964852	BEST3	bestrophin 3
13	5363	7966183	ALKBH2	alkB, alkylation repair homolog 2 (E. coli)
13	5688	7971015	SMAD9	SMAD family member 9
13	7059	7989159	ZNF280D	zinc finger protein 280D
13	10640	8034130	KANK2	KN motif and ankyrin repeat domains 2
13	11313	8041617	MTA3	metastasis associated 1 family, member 3
13	12515	8059650	SP110	SP110 nuclear body protein
13	13235	8068671	BACE2	beta-site APP-cleaving enzyme 2
13	13820	8075673	RBM9	RNA binding motif protein 9
13	14721	8088142	CHDH	choline dehydrogenase
13	16500	8112940	SSBP2	single-stranded DNA binding protein 2
13	16854	8117476	BTN3A3	butyrophilin, subfamily 3, member A3
13	17590	8126770	CYP39A1	cytochrome P450, family 39, subfamily A, polypepti
13	19533	8152133	RRM2B	ribonucleotide reductase M2 B (TP53 inducible)
13	21179	8173208	SPIN4	spindlin family, member 4
16	16265	8109649	NA	NA
16	81	7897774	CLCN6	chloride channel 6
16	1082	7910950	KMO	kynurenine 3-monooxygenase (kynurenine 3-hydroxyla
16	2785	7933877	JMJD1C	jumonji domain containing 1C
16	4469	7953878	CLEC2D	C-type lectin domain family 2, member D
16	5000	7961151	KLRK1	killer cell lectin-like receptor subfamily K, memb
16	5100	7962516	SLC38A1	solute carrier family 38, member 1

16	6023	7975545	PSEN1	presenilin 1
16	6843	7985482	WHAMM	WAS protein homolog associated with actin, golgi m
16	7552	7995895	HERPUD1	homocysteine-inducible, endoplasmic reticulum stre
16	8319	8005765	WSB1	WD repeat and SOCS box-containing 1
16	9576	8021653	SERPINB8	serpin peptidase inhibitor, clade B (ovalbumin), m
16	11228	8040340	LPIN1	lipin 1
16	11234	8040440	GEN1	Gen homolog 1, endonuclease (Drosophila)
16	11300	8041447	CRIM1	cysteine rich transmembrane BMP regulator 1 (chord
16	12920	8064868	GPCPD1	glycerophosphocholine phosphodiesterase GDE1 homol
16	13182	8068105	BACH1	BTB and CNC homology 1, basic leucine zipper trans
16	14333	8082607	ATP2C1	ATPase, Ca++ transporting, type 2C, member 1
16	15718	8101992	SLC39A8	solute carrier family 39 (zinc transporter), membe
16	15744	8102389	C4orf21	chromosome 4 open reading frame 21
16	15974	8105506	ZSWIM6	zinc finger, SWIM-type containing 6
16	16569	8113914	FNIP1	folliculin interacting protein 1
16	18369	8137526	INSIG1	insulin induced gene 1
16	19031	8145954	TACC1	transforming, acidic coiled-coil containing protei
16	19076	8146550	SDCBP	syndecan binding protein (syntenin)
16	19905	8157216	UGCG	UDP-glucose ceramide glucosyltransferase
16	19926	8157524	TLR4	toll-like receptor 4
16	20355	8162833	ERP44	endoplasmic reticulum protein 44
16	20495	8164701	SETX	senataxin
16	21856	8180268	CYP51A1	cytochrome P450, family 51, subfamily A, polypepti

Table A-4 Testing for stationarity reveals 5 distinct and disjoint groups of genes, changing their expression after sCD40L stimulation.

	Gene ID	Probe ID	Gene Symbol	Gene Name
2	16514	8113073	ARRDC3	arrestin domain containing 3
2	903	7908376	RGS18	regulator of G-protein signaling 18
2	905	7908388	RGS1	regulator of G-protein signaling 1
2	908	7908409	RGS2	regulator of G-protein signaling 2, 24kDa
2	1897	7921625	SLAMF6	SLAM family member 6
2	2985	7936884	FAM53B	family with sequence similarity 53, member B
2	4441	7953532	ENO2	enolase 2 (gamma, neuronal)
2	4545	7954926	PDZRN4	PDZ domain containing ring finger 4
2	4992	7961075	CD69	CD69 molecule
2	5363	7966183	ALKBH2	alkB, alkylation repair homolog 2 (E. coli)
2	8674	8010139	SEC14L1	SEC14-like 1 (S. cerevisiae)
2	9011	8014706	PCGF2	polycomb group ring finger 2
2	12671	8061564	ID1	inhibitor of DNA binding 1, dominant negative heli
2	13494	8071691	BCR	breakpoint cluster region
2	14598	8086330	CSRNP1	cysteine-serine-rich nuclear protein 1
2	15035	8092691	BCL6	B-cell CLL/lymphoma 6
2	15296	8096070	BMP3	bone morphogenetic protein 3
2	15668	8101322	MOP-1	MOP-1
2	15726	8102135	CXXC4	CXXC finger 4

2	15806	8103226	TMEM154	transmembrane protein 154
2	16475	8112615	ENC1	ectodermal-neural cortex 1 (with BTB-like domain)
2	16684	8115490	ADAM19	ADAM metallopeptidase domain 19
2	16818	8117120	ID4	inhibitor of DNA binding 4, dominant negative heli
2	17371	8124380	HIST1H1A	histone cluster 1, H1a
2	17776	8129666	SLC2A12	solute carrier family 2 (facilitated glucose trans
2	19303	8149324	FAM167A	family with sequence similarity 167, member A
2	19666	8154100	VLDLR	very low density lipoprotein receptor
2	20566	8165711	PLCXD1	phosphatidylinositol-specific phospholipase C, X d
2	21237	8173999	XKRX	XK, Kell blood group complex subunit-related, X-li
2	21450	8176286	PLCXD1	phosphatidylinositol-specific phospholipase C, X d
4	9890	8025601	ICAM1	intercellular adhesion molecule 1
4	287	7900146	ZC3H12A	zinc finger CCCH-type containing 12A
4	606	7904702	NOTCH2NL	notch 2 N-terminal like
4	1348	7914212	SNORA61	small nucleolar RNA, H/ACA box 61
4	1601	7917754	BCAR3	breast cancer anti-estrogen resistance 3
4	1697	7919193	NUDT4P1	nudix (nucleoside diphosphate linked moiety X)-typ
4	2287	7926900	MAP3K8	mitogen-activated protein kinase kinase kinase 8
4	2450	7929032	FAS	Fas (TNF receptor superfamily, member 6)
4	4745	7957478	TMTC3	transmembrane and tetratricopeptide repeat contain
4	5448	7967456	RILPL2	Rab interacting lysosomal protein-like 2
4	5664	7970696	USP12	ubiquitin specific peptidase 12
4	7434	7994292	IL21R	interleukin 21 receptor
4	7833	7999496	ZC3H7A	zinc finger CCCH-type containing 7A
4	9034	8015031	CCR7	chemokine (C-C motif) receptor 7
4	9790	8024485	GADD45B	growth arrest and DNA-damage-inducible, beta
4	11145	8039545	NLRP11	NLR family, pyrin domain containing 11
4	13173	8068022	MIR155HG	MIR155 host gene (non-protein coding)
4	13294	8069541	SAMSN1	SAM domain, SH3 domain and nuclear localization si
4	15333	8096635	NFKB1	nuclear factor of kappa light polypeptide gene enh
4	15907	8104580	FAM105B	family with sequence similarity 105, member B
4	15908	8104590	LOC100130744	hypothetical LOC100130744
4	15939	8105067	PTGER4	prostaglandin E receptor 4 (subtype EP4)
4	16365	8110886	MED10	mediator complex subunit 10
4	16741	8116227	CLK4	CDC-like kinase 4
4	17221	8122202	MYB	v-myb myeloblastosis viral oncogene homolog (avian
4	17353	8124059	NUP153	nucleoporin 153kDa
4	17583	8126666	NFKBIE	nuclear factor of kappa light polypeptide gene enh
4	17901	8131292	RBAK	RB-associated KRAB zinc finger
4	18882	8143957	RHEB	Ras homolog enriched in brain
4	21908	8180323	USP12	ubiquitin specific peptidase 12
5	16808	8116983	CD83	CD83 molecule
5	191	7899018	TMEM57	transmembrane protein 57
5	571	7904086	LRIG2	leucine-rich repeats and immunoglobulin-like domai
5	3578	7943424	BIRC2	baculoviral IAP repeat-containing 2

5	4515	7954436	LRMP	lymphoid-restricted membrane protein
5	6751	7984364	SMAD3	SMAD family member 3
5	6825	7985259	ZFAND6	zinc finger, AN1-type domain 6
5	7846	7999642	KIAA0430	KIAA0430
5	9656	8022817	KLHL14	kelch-like 14 (Drosophila)
5	10766	8035703	LPAR2	lysophosphatidic acid receptor 2
5	10812	8036207	NFKBID	nuclear factor of kappa light polypeptide gene enh
5	11925	8050190	ADAM17	ADAM metallopeptidase domain 17
5	12050	8052269	CCDC88A	coiled-coil domain containing 88A
5	12074	8052689	SPRED2	sprouty-related, EVH1 domain containing 2
5	12786	8063156	CD40	CD40 molecule, TNF receptor superfamily member 5
5	12796	8063351	SLC9A8	solute carrier family 9 (sodium/hydrogen exchanger
5	14291	8082035	CD86	CD86 molecule
5	14449	8084219	KLHL24	kelch-like 24 (Drosophila)
5	14752	8088550	PRICKLE2	prickle homolog 2 (Drosophila)
5	14763	8088776	FOXP1	forkhead box P1
5	16637	8114814	NR3C1	nuclear receptor subfamily 3, group C, member 1 (g
5	17209	8122071	ENPP3	ectonucleotide pyrophosphatase/phosphodiesterase 3
5	17347	8123981	C6orf114	chromosome 6 open reading frame 114
5	18983	8145136	PPP3CC	protein phosphatase 3, catalytic subunit, gamma is
5	19342	8149720	EGR3	early growth response 3
5	19514	8151890	TP53INP1	tumor protein p53 inducible nuclear protein 1
5	19876	8156848	NR4A3	nuclear receptor subfamily 4, group A, member 3
5	20354	8162827	ALG2	asparagine-linked glycosylation 2, alpha-1,3-manno
5	21127	8172471	PIM2	pim-2 oncogene
5	21458	8176384	ZFY	zinc finger protein, Y-linked
7	14277	8081838	ARHGAP31	Rho GTPase activating protein 31
7	65	7897482	PIK3CD	phosphoinositide-3-kinase, catalytic, delta polype
7	533	7903592	KIAA1324	KIAA1324
7	785	7906564	PEA15	phosphoprotein enriched in astrocytes 15
7	1956	7922343	TNFSF4	tumor necrosis factor (ligand) superfamily, member
7	2819	7934367	ANXA7	annexin A7
7	4468	7953873	OVOS	ovostatin
7	5122	7962884	RND1	Rho family GTPase 1
7	5147	7963235	CSRNP2	cysteine-serine-rich nuclear protein 2
7	5377	7966356	HVCN1	hydrogen voltage-gated channel 1
7	6099	7976556	C14orf132	chromosome 14 open reading frame 132
7	8934	8013633	UNC119	unc-119 homolog (C. elegans)
7	9798	8024572	GNA15	guanine nucleotide binding protein (G protein), al
7	10628	8033996	TYK2	tyrosine kinase 2
7	11728	8047381	CFLAR	CASP8 and FADD-like apoptosis regulator
7	12201	8054192	MITD1	MIT, microtubule interacting and transport, domain
7	12503	8059413	DOCK10	dedicator of cytokinesis 10
7	12914	8064790	RASSF2	Ras association (RalGDS/AF-6) domain family member
7	12942	8065230	RBBP9	retinoblastoma binding protein 9

7	13575	8072757	CSF2RB	colony stimulating factor 2 receptor, beta, low-af
7	14725	8088180	WNT5A	wingless-type MMTV integration site family, member
7	15291	8096004	BMP2K	BMP2 inducible kinase
7	16002	8105949	SERF1A	small EDRK-rich factor 1A (telomeric)
7	16007	8105997	SERF1A	small EDRK-rich factor 1A (telomeric)
7	18070	8133459	CLIP2	CAP-GLY domain containing linker protein 2
7	19590	8153043	ZFAT	zinc finger and AT hook domain containing
7	20513	8164967	VAV2	vav 2 guanine nucleotide exchange factor
7	21565	8177658	SERF1A	small EDRK-rich factor 1A (telomeric)
7	21689	8178826	NA	NA
7	21810	8180022	NA	NA
8	15667	8101304	RASGEF1B	RasGEF domain family, member 1B
8	430	7902227	GADD45A	growth arrest and DNA-damage-inducible, alpha
8	974	7909332	CD55	CD55 molecule, decay accelerating factor for compl
8	1992	7922717	RGS16	regulator of G-protein signaling 16
8	3740	7945652	KRTAP5-3	keratin associated protein 5-3
8	5000	7961151	KLRK1	killer cell lectin-like receptor subfamily K, memb
8	5101	7962537	SLC38A2	solute carrier family 38, member 2
8	5313	7965423	BTG1	B-cell translocation gene 1, anti-proliferative
8	6135	7976844	NA	NA
8	6366	7979813	ZFP36L1	zinc finger protein 36, C3H type-like 1
8	9540	8021183	SCARNA17	small Cajal body-specific RNA 17
8	9935	8026163	IER2	immediate early response 2
8	11377	8042503	MXD1	MAX dimerization protein 1
8	11866	8049530	LRRFIP1	leucine rich repeat (in FLII) interacting protein
8	12150	8053576	RNF103	ring finger protein 103
8	12159	8053668	EIF2AK3	eukaryotic translation initiation factor 2-alpha k
8	12343	8056359	COBLL1	COBL-like 1
8	15560	8099834	TLR1	toll-like receptor 1
8	15741	8102362	TIFA	TRAF-interacting protein with forkhead-associated
8	16292	8110032	C5orf41	chromosome 5 open reading frame 41
8	17751	8129317	SERINC1	serine incorporator 1
8	17832	8130539	TAGAP	T-cell activation RhoGTPase activating protein
8	18203	8135392	HBP1	HMG-box transcription factor 1
8	18750	8142307	PNPLA8	patatin-like phospholipase domain containing 8
8	19111	8147040	ZBTB10	zinc finger and BTB domain containing 10
8	19147	8147573	OSR2	odd-skipped related 2 (Drosophila)
8	19380	8150186	RNF122	ring finger protein 122
8	20215	8161224	ZBTB5	zinc finger and BTB domain containing 5
8	20368	8162940	ABCA1	ATP-binding cassette, sub-family A (ABC1), member
8	21032	8171205	NLGN4X	neuroligin 4, X-linked

Table A-5 Testing for stationarity reveals 15 distinct and disjoint groups of genes in BCR-resolved time series analysis. Each group contains 30 genes, which are listed below. Each group of genes displays a unique expression course.

	Gene ID	Probe ID	Gene Symbol	Gene Name
1	790	7906613	SLAMF7	SLAM family member 7
1	587	7904361	FAM46C	family with sequence similarity 46, member C
1	762	7906339	CD1A	CD1a molecule
1	763	7906348	CD1C	CD1c molecule
1	1056	7910427	GALNT2	UDP-N-acetyl-alpha-D-galactosamine:polypeptide N-a
1	1169	7911754	TNFRSF14	tumor necrosis factor receptor superfamily, member
1	3735	7945620	TOLLIP	toll interacting protein
1	3995	7948332	LPXN	leupaxin
1	5286	7965040	PHLDA1	pleckstrin homology-like domain, family A, member
1	6630	7982564	SPRED1	sprouty-related, EVH1 domain containing 1
1	6730	7984112	RAB8B	RAB8B, member RAS oncogene family
1	7381	7993433	PDXDC1	pyridoxal-dependent decarboxylase domain containin
1	8319	8005765	WSB1	WD repeat and SOCS box-containing 1
1	8623	8009476	MAP2K6	mitogen-activated protein kinase kinase 6
1	9716	8023646	BCL2	B-cell CLL/lymphoma 2
1	12007	8051547	PRKD3	protein kinase D3
1	12017	8051707	MAP4K3	mitogen-activated protein kinase kinase kinase kin
1	12534	8059854	ARL4C	ADP-ribosylation factor-like 4C
1	14295	8082075	DTX3L	deltex 3-like (Drosophila)
1	14296	8082086	PARP15	poly (ADP-ribose) polymerase family, member 15
1	14768	8088848	PDZRN3	PDZ domain containing ring finger 3
1	15587	8100231	TEC	tec protein tyrosine kinase
1	17286	8123181	IGF2R	insulin-like growth factor 2 receptor
1	17428	8124742	GNL1	guanine nucleotide binding protein-like 1
1	18005	8132725	UPP1	uridine phosphorylase 1
1	18360	8137404	CHPF2	chondroitin polymerizing factor 2
1	18952	8144658	NEIL2	nei endonuclease VIII-like 2 (E. coli)
1	19304	8149330	CTSB	cathepsin B
1	19510	8151816	GEM	GTP binding protein overexpressed in skeletal musc
1	20495	8164701	SETX	senataxin
2	9034	8015031	CCR7	chemokine (C-C motif) receptor 7
2	791	7906622	LY9	lymphocyte antigen 9
2	2110	7924450	DUSP10	dual specificity phosphatase 10
2	2548	7930413	DUSP5	dual specificity phosphatase 5
2	4668	7956287	NAB2	NGFI-A binding protein 2 (EGR1 binding protein 2)
2	5377	7966356	HVCN1	hydrogen voltage-gated channel 1
2	5409	7966929	RAB35	RAB35, member RAS oncogene family
2	7405	7993825	RUNDC2B	RUN domain containing 2B
2	7452	7994576	RUNDC2C	RUN domain containing 2C
2	8886	8013071	FLCN	folliculin
2	9379	8019308	MAFG	v-maf musculoaponeurotic fibrosarcoma oncogene hom

2	9440	8019796	MAFG	v-maf musculoaponeurotic fibrosarcoma oncogene hom
2	9947	8026300	CD97	CD97 molecule
2	11228	8040340	LPIN1	lipin 1
2	12770	8062964	SYS1	SYS1 Golgi-localized integral membrane protein hom
2	13394	8070720	ICOSLG	inducible T-cell co-stimulator ligand
2	13964	8077441	BHLHE40	basic helix-loop-helix family, member e40
2	14505	8084951	LRRC33	leucine rich repeat containing 33
2	15939	8105067	PTGER4	prostaglandin E receptor 4 (subtype EP4)
2	16336	8110569	SQSTM1	sequestosome 1
2	16569	8113914	FNIP1	folliculin interacting protein 1
2	16572	8114010	IRF1	interferon regulatory factor 1
2	16748	8116316	MGAT4B	mannosyl (alpha-1,3-)-glycoprotein beta-1,4-N-acet
2	17583	8126666	NFKBIE	nuclear factor of kappa light polypeptide gene enh
2	17677	8128043	CNR1	cannabinoid receptor 1 (brain)
2	18369	8137526	INSIG1	insulin induced gene 1
2	19031	8145954	TACC1	transforming, acidic coiled-coil containing protei
2	19589	8153021	ST3GAL1	ST3 beta-galactoside alpha-2,3-sialyltransferase 1
2	19677	8154233	CD274	CD274 molecule
2	19905	8157216	UGCG	UDP-glucose ceramide glucosyltransferase
3	18760	8142452	TFEC	transcription factor EC
3	716	7905789	IL6R	interleukin 6 receptor
3	1601	7917754	BCAR3	breast cancer anti-estrogen resistance 3
3	1864	7921259	FCRL4	Fc receptor-like 4
3	4755	7957570	PLXNC1	plexin C1
3	5544	7968976	LRCH1	leucine-rich repeats and calponin homology (CH) do
3	5549	7969060	FNDC3A	fibronectin type III domain containing 3A
3	7869	8000028	DCUN1D3	DCN1, defective in cullin neddylation 1, domain co
3	9930	8026106	CALR	calreticulin
3	10652	8034304	ACP5	acid phosphatase 5, tartrate resistant
3	11686	8046726	SSFA2	sperm specific antigen 2
3	12500	8059361	WDFY1	WD repeat and FYVE domain containing 1
3	13383	8070584	TMPRSS3	transmembrane protease, serine 3
3	14155	8080084	MANF	mesencephalic astrocyte-derived neurotrophic facto
3	14471	8084634	DNAJB11	DnaJ (Hsp40) homolog, subfamily B, member 11
3	14874	8090490	RPN1	ribophorin I
3	15291	8096004	BMP2K	BMP2 inducible kinase
3	15358	8097017	UGT8	UDP glycosyltransferase 8
3	15561	8099841	TLR6	toll-like receptor 6
3	16022	8106252	HEXB	hexosaminidase B (beta polypeptide)
3	16095	8107474	DMXL1	Dmx-like 1
3	16160	8108378	CTNNA1	catenin (cadherin-associated protein), alpha 1, 10
3	17551	8126303	TREM1	triggering receptor expressed on myeloid cells 1
3	17683	8128123	RRAGD	Ras-related GTP binding D
3	17784	8129804	MAP3K5	mitogen-activated protein kinase kinase kinase 5
3	17936	8131844	GPNMB	glycoprotein (transmembrane) nmb

3	18217	8135576	TES	testis derived transcript (3 LIM domains)
3	19933	8157650	PTGS1	prostaglandin-endoperoxide synthase 1 (prostagland
3	20270	8161701	TMEM2	transmembrane protein 2
3	20448	8164165	HSPA5	heat shock 70kDa protein 5 (glucose-regulated prot
4	20135	8160332	MLLT3	myeloid/lymphoid or mixed-lineage leukemia (tritho
4	771	7906386	PYHIN1	pyrin and HIN domain family, member 1
4	943	7908924	PRELP	proline/arginine-rich end leucine-rich repeat prot
4	2243	7926170	DHTKD1	dehydrogenase E1 and transketolase domain containi
4	2655	7931930	PRKCQ	protein kinase C, theta
4	4208	7950810	SYTL2	synaptotagmin-like 2
4	4478	7953981	ETV6	ets variant 6
4	4720	7957126	KCNMB4	potassium large conductance calcium-activated chan
4	4843	7959025	RNFT2	ring finger protein, transmembrane 2
4	6735	7984174	SNX22	sorting nexin 22
4	6747	7984298	DIS3L	DIS3 mitotic control homolog (S. cerevisiae)-like
4	7012	7988212	ELL3	elongation factor RNA polymerase II-like 3
4	10640	8034130	KANK2	KN motif and ankyrin repeat domains 2
4	10909	8037205	CEACAM1	carcinoembryonic antigen-related cell adhesion mol
4	11456	8043465	IGKC	immunoglobulin kappa constant
4	12914	8064790	RASSF2	Ras association (RalGDS/AF-6) domain family member
4	13737	8074780	YPEL1	yippee-like 1 (Drosophila)
4	13820	8075673	RBM9	RNA binding motif protein 9
4	14179	8080562	IL17RB	interleukin 17 receptor B
4	14721	8088142	CHDH	choline dehydrogenase
4	16031	8106411	S100Z	S100 calcium binding protein Z
4	16829	8117243	LRRC16A	leucine rich repeat containing 16A
4	18441	8138489	CDCA7L	cell division cycle associated 7-like
4	18647	8140955	CDK6	cyclin-dependent kinase 6
4	18719	8141768	RASA4	RAS p21 protein activator 4
4	18722	8141803	RASA4	RAS p21 protein activator 4
4	19845	8156393	SUSD3	sushi domain containing 3
4	19953	8157804	OLFML2A	olfactomedin-like 2A
4	20348	8162719	HEMGN	hemogen
4	20526	8165156	SDCCAG3	serologically defined colon cancer antigen 3
5	19876	8156848	NR4A3	nuclear receptor subfamily 4, group A, member 3
5	109	7898070	PRDM2	PR domain containing 2, with ZNF domain
5	300	7900365	MFSD2A	major facilitator superfamily domain containing 2A
5	1047	7910261	C1orf69	chromosome 1 open reading frame 69
5	1992	7922717	RGS16	regulator of G-protein signaling 16
5	2398	7928429	PLAU	plasminogen activator, urokinase
5	2643	7931810	KLF6	Kruppel-like factor 6
5	5789	7972548	GPR18	G protein-coupled receptor 18
5	6366	7979813	ZFP36L1	zinc finger protein 36, C3H type-like 1
5	6386	7980051	C14orf43	chromosome 14 open reading frame 43
5	8665	8010050	FAM100B	family with sequence similarity 100, member B

5	9935	8026163	IER2	immediate early response 2
5	10003	8026915	ARRDC2	arrestin domain containing 2
5	10277	8030128	PPP1R15A	protein phosphatase 1, regulatory (inhibitor) subu
5	10744	8035445	JUND	jun D proto-oncogene
5	10812	8036207	NFKBID	nuclear factor of kappa light polypeptide gene enh
5	11834	8049075	B3GNT7	UDP-GlcNAc:betaGal beta-1,3-N-acetylglucosaminyltr
5	12107	8053022	EGR4	early growth response 4
5	12179	8053882	DUSP2	dual specificity phosphatase 2
5	13671	8073960	PIM3	pim-3 oncogene
5	14495	8084880	HES1	hairy and enhancer of split 1, (Drosophila)
5	14598	8086330	CSRNP1	cysteine-serine-rich nuclear protein 1
5	15667	8101304	RASGEF1B	RasGEF domain family, member 1B
5	16808	8116983	CD83	CD83 molecule
5	16819	8117128	E2F3	E2F transcription factor 3
5	17039	8119712	SRF	serum response factor (c-fos serum response elemen
5	17226	8122265	TNFAIP3	tumor necrosis factor, alpha-induced protein 3
5	19535	8152215	KLF10	Kruppel-like factor 10
5	20194	8160912	C9orf131	chromosome 9 open reading frame 131
5	21196	8173437	CXorf65	chromosome X open reading frame 65
6	19176	8148059	DEPDC6	DEP domain containing 6
6	405	7901788	NFIA	nuclear factor I/A
6	533	7903592	KIAA1324	KIAA1324
6	963	7909188	IKBKE	inhibitor of kappa light polypeptide gene enhancer
6	1302	7913644	E2F2	E2F transcription factor 2
6	1307	7913705	CNR2	cannabinoid receptor 2 (macrophage)
6	1816	7920552	KCNN3	potassium intermediate/small conductance calcium-a
6	1867	7921319	FCRL1	Fc receptor-like 1
6	1945	7922219	SELL	selectin L
6	5046	7961540	RERG	RAS-like, estrogen-regulated, growth inhibitor
6	6464	7981183	TCL1A	T-cell leukemia/lymphoma 1A
6	7058	7989146	MNS1	meiosis-specific nuclear structural 1
6	8905	8013319	GRAP	GRB2-related adaptor protein
6	9993	8026787	FAM129C	family with sequence similarity 129, member C
6	12385	8057377	CCDC141	coiled-coil domain containing 141
6	12678	8061668	HCK	hemopoietic cell kinase
6	12980	8065569	BCL2L1	BCL2-like 1
6	13106	8067185	BMP7	bone morphogenetic protein 7
6	13492	8071671	GNAZ	guanine nucleotide binding protein (G protein), al
6	14419	8083749	PPM1L	protein phosphatase, Mg2+/Mn2+ dependent, 1L
6	14487	8084766	TP63	tumor protein p63
6	14576	8085984	OSBPL10	oxysterol binding protein-like 10
6	16081	8107307	CAMK4	calcium/calmodulin-dependent protein kinase IV
6	16139	8108080	PHF15	PHD finger protein 15
6	16542	8113504	C5orf13	chromosome 5 open reading frame 13
6	17209	8122071	ENPP3	ectonucleotide pyrophosphatase/phosphodiesterase 3

6	17721	8128818	WASF1	WAS protein family, member 1
6	19841	8156321	SYK	spleen tyrosine kinase
6	21437	8176174	MPP1	membrane protein, palmitoylated 1, 55kDa
6	21884	8180299	PSIP1	PC4 and SFRS1 interacting protein 1
7	17196	8121850	HEY2	hairy/enhancer-of-split related with YRPW motif 2
7	661	7905299	PRUNE	prune homolog (Drosophila)
7	1633	7918300	PSRC1	proline/serine-rich coiled-coil 1
7	1646	7918457	KCNA3	potassium voltage-gated channel, shaker-related su
7	1973	7922474	KIAA0040	KIAA0040
7	2529	7930139	TRIM8	tripartite motif-containing 8
7	3627	7944152	IL10RA	interleukin 10 receptor, alpha
7	4536	7954717	BICD1	bicaudal D homolog 1 (Drosophila)
7	5723	7971486	C13orf18	chromosome 13 open reading frame 18
7	6012	7975361	KIAA0247	KIAA0247
7	6968	7987385	MEIS2	Meis homeobox 2
7	7736	7998336	NARFL	nuclear prelamin A recognition factor-like
7	8540	8008297	XYLT2	xylosyltransferase II
7	8947	8013804	DHRS13	dehydrogenase/reductase (SDR family) member 13
7	9001	8014551	SYNRG	synergin, gamma
7	9103	8015655	FAM134C	family with sequence similarity 134, member C
7	11798	8048489	ANKZF1	ankyrin repeat and zinc finger domain containing 1
7	12072	8052669	SERTAD2	SERTA domain containing 2
7	12622	8060977	C20orf94	chromosome 20 open reading frame 94
7	14725	8088180	WNT5A	wingless-type MMTV integration site family, member
7	15296	8096070	BMP3	bone morphogenetic protein 3
7	15382	8097417	PHF17	PHD finger protein 17
7	15454	8098423	NEIL3	nei endonuclease VIII-like 3 (E. coli)
7	15806	8103226	TMEM154	transmembrane protein 154
7	15931	8104901	IL7R	interleukin 7 receptor
7	16155	8108301	KIF20A	kinesin family member 20A
7	16602	8114365	BRD8	bromodomain containing 8
7	16817	8117106	RNF144B	ring finger protein 144B
7	16821	8117165	SOX4	SRY (sex determining region Y)-box 4
7	20457	8164252	SH2D3C	SH2 domain containing 3C
9	11444	8043363	NCRNA00152	non-protein coding RNA 152
9	540	7903703	GNAI3	guanine nucleotide binding protein (G protein), al
9	555	7903893	CD53	CD53 molecule
9	838	7907171	BLZF1	basic leucine zipper nuclear factor 1
9	4515	7954436	LRMP	lymphoid-restricted membrane protein
9	5501	7968297	POMP	proteasome maturation protein
9	6023	7975545	PSEN1	presenilin 1
9	6324	7979260	GMFB	glia maturation factor, beta
9	6712	7983828	TEX9	testis expressed 9
9	6954	7987172	C15orf24	chromosome 15 open reading frame 24
9	7650	7997272	GABARAPL2	GABA(A) receptor-associated protein-like 2

9	8087	8002878	TMEM170A	transmembrane protein 170A
9	8583	8008870	TMEM49	transmembrane protein 49
9	13298	8069574	C21orf91	chromosome 21 open reading frame 91
9	14333	8082607	ATP2C1	ATPase, Ca++ transporting, type 2C, member 1
9	14439	8084045	MFN1	mitofusin 1
9	16532	8113358	ST8SIA4	ST8 alpha-N-acetyl-neuraminide alpha-2,8-sialyltra
9	16600	8114326	FAM13B	family with sequence similarity 13, member B
9	17231	8122336	C6orf115	chromosome 6 open reading frame 115
9	17345	8123961	TBC1D7	TBC1 domain family, member 7
9	17484	8125463	HLA-DQB2	major histocompatibility complex, class II, DQ bet
9	17714	8128716	CD164	CD164 molecule, sialomucin
9	19076	8146550	SDCBP	syndecan binding protein (syntenin)
9	20355	8162833	ERP44	endoplasmic reticulum protein 44
9	20623	8166469	SAT1	spermidine/spermine N1-acetyltransferase 1
9	21243	8174076	GLA	galactosidase, alpha
9	21688	8178811	NA	NA
9	21809	8180003	NA	NA
9	21811	8180029	HLA-DQB2	major histocompatibility complex, class II, DQ bet
9	21856	8180268	CYP51A1	cytochrome P450, family 51, subfamily A, polypepti
10	10233	8029693	FOSB	FBJ murine osteosarcoma viral oncogene homolog B
10	357	7901140	MAST2	microtubule associated serine/threonine kinase 2
10	535	7903632	CELSR2	cadherin, EGF LAG seven-pass G-type receptor 2 (fl
10	1511	7916403	SSBP3	single stranded DNA binding protein 3
10	2234	7926037	PFKFB3	6-phosphofructo-2-kinase/fructose-2,6-biphosphatas
10	3064	7937823	KCNQ1	potassium voltage-gated channel, KQT-like subfamil
10	6045	7975779	FOS	FBJ murine osteosarcoma viral oncogene homolog
10	6175	7977344	PACS2	phosphofurin acidic cluster sorting protein 2
10	6280	7978644	NFKBIA	nuclear factor of kappa light polypeptide gene enh
10	6494	7981538	JAG2	jagged 2
10	7111	7990033	TLE3	transducin-like enhancer of split 3 (E(sp1) homolo
10	8751	8011262	MNT	MAX binding protein
10	8771	8011516	ATP2A3	ATPase, Ca++ transporting, ubiquitous
10	9094	8015526	KAT2A	K(lysine) acetyltransferase 2A
10	9790	8024485	GADD45B	growth arrest and DNA-damage-inducible, beta
10	9926	8026047	JUNB	jun B proto-oncogene
10	10696	8034783	LPHN1	latrophilin 1
10	11238	8040473	RHOB	ras homolog gene family, member B
10	11322	8041763	PRKCE	protein kinase C, epsilon
10	11474	8043657	CNNM4	cyclin M4
10	12024	8051814	ZFP36L2	zinc finger protein 36, C3H type-like 2
10	12269	8055130	HS6ST1	heparan sulfate 6-O-sulfotransferase 1
10	16719	8115927	RNF44	ring finger protein 44
10	17003	8119161	PIM1	pim-1 oncogene
10	17131	8121076	PNRC1	proline-rich nuclear receptor coactivator 1
10	17886	8131091	MAFK	v-maf musculoaponeurotic fibrosarcoma oncogene hom

10	19111	8147040	ZBTB10	zinc finger and BTB domain containing 10
10	19342	8149720	EGR3	early growth response 3
10	19848	8156452	FAM120A	family with sequence similarity 120A
10	20985	8170704	ABCD1	ATP-binding cassette, sub-family D (ALD), member 1
11	6845	7985493	TM6SF1	transmembrane 6 superfamily member 1
11	1624	7918157	VAV3	vav 3 guanine nucleotide exchange factor
11	1660	7918634	PHTF1	putative homeodomain transcription factor 1
11	2388	7928308	DDIT4	DNA-damage-inducible transcript 4
11	2531	7930162	C10orf26	chromosome 10 open reading frame 26
11	3218	7939465	HSD17B12	hydroxysteroid (17-beta) dehydrogenase 12
11	3840	7946504	TMEM41B	transmembrane protein 41B
11	4255	7951351	PDGFD	platelet derived growth factor D
11	6422	7980547	SEL1L	sel-1 suppressor of lin-12-like (C. elegans)
11	6474	7981290	WARS	tryptophanyl-tRNA synthetase
11	7051	7989037	CCPG1	cell cycle progression 1
11	7362	7993167	ATF7IP2	activating transcription factor 7 interacting prot
11	8563	8008646	SCPEP1	serine carboxypeptidase 1
11	9189	8016578	SLC35B1	solute carrier family 35, member B1
11	9560	8021453	SEC11C	SEC11 homolog C (S. cerevisiae)
11	12435	8058295	ALS2	amyotrophic lateral sclerosis 2 (juvenile)
11	13293	8069532	HSPA13	heat shock protein 70kDa family, member 13
11	13346	8070083	TMEM50B	transmembrane protein 50B
11	13604	8073088	APOBEC3G	apolipoprotein B mRNA editing enzyme, catalytic po
11	13688	8074204	XKR3	XK, Kell blood group complex subunit-related famil
11	14339	8082745	CCRL1	chemokine (C-C motif) receptor-like 1
11	14893	8090737	NPHP3	nephronophthisis 3 (adolescent)
11	15565	8099897	UGDH	UDP-glucose 6-dehydrogenase
11	15853	8103834	AGA	aspartylglucosaminidase
11	15924	8104760	TARS	threonyl-tRNA synthetase
11	17787	8129861	IFNGR1	interferon gamma receptor 1
11	18115	8134091	CLDN12	claudin 12
11	18474	8138789	JAZF1	JAZF zinc finger 1
11	19697	8154531	DENND4C	DENN/MADD domain containing 4C
11	20881	8169541	DOCK11	dedicator of cytokinesis 11
12	1897	7921625	SLAMF6	SLAM family member 6
12	903	7908376	RGS18	regulator of G-protein signaling 18
12	964	7909214	RASSF5	Ras association (RalGDS/AF-6) domain family member
12	2384	7928208	SLC29A3	solute carrier family 29 (nucleoside transporters)
12	3120	7938183	ZNF215	zinc finger protein 215
12	3698	7945132	FLI1	Friend leukemia virus integration 1
12	3762	7945875	FAM86C	family with sequence similarity 86, member C
12	4451	7953651	PEX5	peroxisomal biogenesis factor 5
12	4807	7958439	USP30	ubiquitin specific peptidase 30
12	4873	7959354	BCL7A	B-cell CLL/lymphoma 7A
12	5277	7964852	BEST3	bestrophin 3

12	6046	7975787	JDP2	Jun dimerization protein 2
12	6055	7975926	KIAA1737	KIAA1737
12	6224	7977868	C14orf93	chromosome 14 open reading frame 93
12	7059	7989159	ZNF280D	zinc finger protein 280D
12	8674	8010139	SEC14L1	SEC14-like 1 (S. cerevisiae)
12	9654	8022803	FAM59A	family with sequence similarity 59, member A
12	10907	8037186	LIPE	lipase, hormone-sensitive
12	12455	8058570	C2orf67	chromosome 2 open reading frame 67
12	14123	8079598	ZNF589	zinc finger protein 589
12	15401	8097657	SMAD1	SMAD family member 1
12	15518	8099200	JAKMIP1	janus kinase and microtubule interacting protein 1
12	16165	8108447	CXXC5	CXXC finger 5
12	16850	8117435	BTN3A2	butyrophilin, subfamily 3, member A2
12	16854	8117476	BTN3A3	butyrophilin, subfamily 3, member A3
12	17528	8126018	STK38	serine/threonine kinase 38
12	18011	8132819	IKZF1	IKAROS family zinc finger 1 (Ikaros)
12	19193	8148317	MYC	v-myc myelocytomatosis viral oncogene homolog (avi
12	20566	8165711	PLCXD1	phosphatidylinositol-specific phospholipase C, X d
12	21450	8176286	PLCXD1	phosphatidylinositol-specific phospholipase C, X d
13	16874	8117630	ZNF165	zinc finger protein 165
13	53	7897322	PHF13	PHD finger protein 13
13	306	7900438	ZNF643	zinc finger protein 643
13	869	7907690	TOR3A	torsin family 3, member A
13	1899	7921652	SLAMF1	signaling lymphocytic activation molecule family m
13	2654	7931914	IL2RA	interleukin 2 receptor, alpha
13	3247	7939839	PTPRJ	protein tyrosine phosphatase, receptor type, J
13	3306	7940118	ZFP91-CNTF	ZFP91-CNTF readthrough transcript
13	4625	7955943	PDE1B	phosphodiesterase 1B, calmodulin-dependent
13	7053	7989069	PYGO1	pygopus homolog 1 (Drosophila)
13	7145	7990555	NRG4	neuregulin 4
13	7417	7994058	SCNN1G	sodium channel, nonvoltage-gated 1, gamma
13	8147	8003611	FAM57A	family with sequence similarity 57, member A
13	8977	8014233	SLFN11	schlafen family member 11
13	9135	8016088	CCDC43	coiled-coil domain containing 43
13	9269	8017711	GNA13	guanine nucleotide binding protein (G protein), al
13	9951	8026350	CLEC17A	C-type lectin domain family 17, member A
13	10765	8035694	PBX4	pre-B-cell leukemia homeobox 4
13	10766	8035703	LPAR2	lysophosphatidic acid receptor 2
13	11708	8047086	NAB1	NGFI-A binding protein 1 (EGR1 binding protein 1)
13	12581	8060418	SIRPA	signal-regulatory protein alpha
13	15333	8096635	NFKB1	nuclear factor of kappa light polypeptide gene enh
13	15555	8099760	ARAP2	ArfGAP with RhoGAP domain, ankyrin repeat and PH d
13	16707	8115806	UBTD2	ubiquitin domain containing 2
13	16929	8118137	LTA	lymphotoxin alpha (TNF superfamily, member 1)
13	17232	8122343	HECA	headcase homolog (Drosophila)

13	17259	8122756	PLEKHG1	pleckstrin homology domain containing, family G (w
13	18983	8145136	PPP3CC	protein phosphatase 3, catalytic subunit, gamma is
13	21600	8177976	LTA	lymphotoxin alpha (TNF superfamily, member 1)
13	21736	8179258	LTA	lymphotoxin alpha (TNF superfamily, member 1)
14	453	7902512	DNAJB4	DnaJ (Hsp40) homolog, subfamily B, member 4
14	197	7899087	PDIK1L	PDLIM1 interacting kinase 1 like
14	612	7904755	PEX11B	peroxisomal biogenesis factor 11 beta
14	1322	7913883	PAFAH2	platelet-activating factor acetylhydrolase 2, 40kD
14	1617	7918008	DBT	dihydrolipoamide branched chain transacylase E2
14	1745	7919780	GOLPH3L	golgi phosphoprotein 3-like
14	1991	7922707	RNASEL	ribonuclease L (2',5'-oligoisoadenylate synthetase
14	2064	7923812	RAB7L1	RAB7, member RAS oncogene family-like 1
14	2720	7933092	ZNF248	zinc finger protein 248
14	2770	7933638	FLJ31958	hypothetical LOC143153
14	2860	7934945	PANK1	pantothenate kinase 1
14	4463	7953765	RIMKLB	ribosomal modification protein rimK-like family me
14	5288	7965060	BBS10	Bardet-Biedl syndrome 10
14	5577	7969374	C13orf34	chromosome 13 open reading frame 34
14	6768	7984626	SENP8	SUMO/sentrin specific peptidase family member 8
14	7373	7993298	ERCC4	excision repair cross-complementing rodent repair
14	10902	8037144	DEDD2	death effector domain containing 2
14	11666	8046502	SCRN3	secernin 3
14	12185	8053975	LMAN2L	lectin, mannose-binding 2-like
14	12454	8058552	IDH1	isocitrate dehydrogenase 1 (NADP+), soluble
14	12927	8064967	MKKS	McKusick-Kaufman syndrome
14	15551	8099696	SEPSECS	Sep (O-phosphoserine) tRNA:Sec (selenocysteine) tR
14	15741	8102362	TIFA	TRAF-interacting protein with forkhead-associated
14	16759	8116494	ZFP62	zinc finger protein 62 homolog (mouse)
14	16881	8117685	ZKSCAN3	zinc finger with KRAB and SCAN domains 3
14	16991	8119000	MAPK14	mitogen-activated protein kinase 14
14	17767	8129590	STX7	syntaxin 7
14	20547	8165486	TMEM203	transmembrane protein 203
14	20561	8165642	TMEM203	transmembrane protein 203
14	21087	8171896	CXorf21	chromosome X open reading frame 21
17	20331	8162533	PTCH1	patched 1
17	265	7899870	ZNF362	zinc finger protein 362
17	2924	7935968	LDB1	LIM domain binding 1
17	3452	7941797	ADRBK1	adrenergic, beta, receptor kinase 1
17	3466	7942007	LRP5	low density lipoprotein receptor-related protein 5
17	4073	7949206	MEN1	multiple endocrine neoplasia I
17	4075	7949264	EHD1	EH-domain containing 1
17	5108	7962659	HDAC7	histone deacetylase 7
17	6899	7986359	IGF1R	insulin-like growth factor 1 receptor
17	7421	7994109	PLK1	polo-like kinase 1
17	7680	7997680	KIAA0182	KIAA0182

17	8452	8007302	TUBG1	tubulin, gamma 1
17	9329	8018708	UBE2O	ubiquitin-conjugating enzyme E2O
17	9330	8018731	RHBDF2	rhomboid 5 homolog 2 (Drosophila)
17	9439	8019778	PCYT2	phosphate cytidylyltransferase 2, ethanolamine
17	9973	8026533	HSH2D	hematopoietic SH2 domain containing
17	10166	8028930	RAB4B	RAB4B, member RAS oncogene family
17	10582	8033362	INSR	insulin receptor
17	11854	8049317	DGKD	diacylglycerol kinase, delta 130kDa
17	13486	8071566	PPIL2	peptidylprolyl isomerase (cyclophilin)-like 2
17	13800	8075430	MORC2	MORC family CW-type zinc finger 2
17	14078	8079037	TRAK1	trafficking protein, kinesin binding 1
17	14177	8080487	PRKCD	protein kinase C, delta
17	15732	8102232	LEF1	lymphoid enhancer-binding factor 1
17	17465	8125172	EHMT2	euchromatic histone-lysine N-methyltransferase 2
17	18184	8135149	SH2B2	SH2B adaptor protein 2
17	19665	8154059	SMARCA2	SWI/SNF related, matrix associated, actin dependen
17	20529	8165217	NOTCH1	notch 1
17	21198	8173457	ZMYM3	zinc finger, MYM-type 3
17	21800	8179884	EHMT2	euchromatic histone-lysine N-methyltransferase 2
19	4234	7951077	SESN3	sestrin 3
19	525	7903507	FAM102B	family with sequence similarity 102, member B
19	889	7908041	LAMC1	laminin, gamma 1 (formerly LAMB2)
19	920	7908543	NEK7	NIMA (never in mitosis gene a)-related kinase 7
19	1629	7918255	CLCC1	chloride channel CLIC-like 1
19	2217	7925792	ZMYND11	zinc finger, MYND domain containing 11
19	2465	7929282	HHEX	hematopoietically expressed homeobox
19	2674	7932227	NMT2	N-myristoyltransferase 2
19	2689	7932512	DNAJC1	DnaJ (Hsp40) homolog, subfamily C, member 1
19	2901	7935627	GOT1	glutamic-oxaloacetic transaminase 1, soluble (aspa
19	5095	7962455	NELL2	NEL-like 2 (chicken)
19	7055	7989094	NEDD4	neural precursor cell expressed, developmentally d
19	8525	8008113	CALCOCO2	calcium binding and coiled-coil domain 2
19	9621	8022356	SPIRE1	spire homolog 1 (Drosophila)
19	11271	8040927	NRBP1	nuclear receptor binding protein 1
19	11833	8049044	ARMC9	armadillo repeat containing 9
19	13074	8066716	ELMO2	engulfment and cell motility 2
19	14105	8079334	LIMD1	LIM domains containing 1
19	14422	8083779	SERPINI1	serpin peptidase inhibitor, clade I (neuroserpin),
19	14427	8083839	GPR160	G protein-coupled receptor 160
19	16557	8113691	DTWD2	DTW domain containing 2
19	16945	8118310	HSPA1A	heat shock 70kDa protein 1A
19	17352	8124040	ATXN1	ataxin 1
19	17729	8128956	FYN	FYN oncogene related to SRC, FGR, YES
19	18711	8141688	PLOD3	procollagen-lysine, 2-oxoglutarate 5-dioxygenase 3
19	18883	8143961	PRKAG2	protein kinase, AMP-activated, gamma 2 non-catalyt

19	19050	8146243	HOOK3	hook homolog 3 (Drosophila)
19	19356	8149877	PNMA2	paraneoplastic antigen MA2
19	19675	8154178	JAK2	Janus kinase 2
19	21744	8179322	HSPA1A	heat shock 70kDa protein 1A

Curriculum vitae

Particulars

Name	Elisabeth Hand
Date of birth	14-06-1985 in Berlin - Pankow
Nationality	German
Marital status	Married

Tertiary and secondary education

Higher education

2009 Ph.D. candidate in Molecular Medicine, Department of Haematology and Oncology under the supervision of Prof. Dr. Dieter Kube, University Medicine Göttingen,

2007 - 2009 Molecular Medicine, M.Sc., Georg-August University, Göttingen

Master thesis: The influence of Ephrin B3 and Semaphorin 3A on CNS remyelination, Max Planck Institute for Experimental Medicine, Department for Neurogenetics, Göttingen,

2004 - 2007 Molecular Life Science, B.Sc., University of Lübeck

Bachelor thesis: Optimization of expression and purification of a Maltose-Binding-Protein-Falcipain2-fusionprotein, Institute for Biochemistry, University of Lübeck

Secondary school

2002 - 2004 Abitur, German School Istanbul, Turkey,

2001 - 2002 Exchange student, Collège Notre-Dame-de-l'Assomption, Nicolet, Québec, Canada,

1997 - 2001 Gerhart-Hauptmann-Gymnasium, Berlin

Other skills and experiences

Languages

German – native speaker
English – fluent
French – fluent

Publications

Global gene expression changes of in vitro stimulated human transformed germinal centre B cells as surrogate for oncogenic pathway activation in individual aggressive B cell lymphomas.

A. Schrader, K. Meyer, F. von Bonin, M. Vockerodt, N. Walther, E. Hand, A. Ulrich, K. Matulewicz, D. Lenze, M. Hummel, A. Kieser, M. Engelke, L. Trümper, D. Kube

Cell Communication and Signaling: CCS 2012 Dec 20. doi: 10.1186/1478-811X-10-43 PMID: 23253402

Inhibition of CNS remyelination by the presence of semaphorin 3A.

Y.A. Syed, E. Hand, W. Möbius, C. Zhao, M. Hofer, K.A. Nave, M.R. Kotter

The Journal of Neuroscience 2011 Mar 9; doi: 10.1523/JNEUROSCI.4930-10.2011 PMID: 21389227

Multikinase inhibitor sorafenib exerts cytocidal efficacy against Non-Hodgkin lymphomas associated with inhibition of MAPK14 and AKT phosphorylation.

B. Chapuy, N. Schuelper, M. Panse, A. Dohm, E. Hand, R. Schroers, L. Truemper, G.G. Wulf

British Journal of Haematology 2011 Feb; doi: 10.1111/j.1365-2141.2010.08526.x PMID: 21689083

Danksagung

Zunächst möchte ich Prof. Dr. Dieter Kube danken, der diese Arbeit ermöglicht hat. Er hat mir in den letzten 4 Jahren stets mit wertvollen Ratschlägen und Hinweisen zur Seite gestanden und mit seinen Ideen und seiner Diskussionsbereitschaft entscheidend diese Arbeit geprägt. Außerdem bin ich ihm sehr dankbar, dass er immer vollstes Verständnis für meine familiäre Situation hatte. Ich bin mir dessen bewußt, dass das keine Selbstverständlichkeit ist und danke ihm für sein Vertrauen, sein Entgegenkommen und seine moralische Unterstützung.

Ich danke auch den Mitgliedern meines Thesis Committees: Prof. Dr. Mika Simons für die durchgehende Unterstützung schon seit der Anfertigung meiner Masterarbeit, Prof. Dr. Steven Johnson für die immer wieder positiven Anmerkungen und Aufmunterungen, sowie Prof. Dr. Peter Burfeind für seine kurzfristige Einwilligung als neues drittes Mitglied im Thesis Committee mitzuwirken.

Großer Dank geht auch an den Verbund HaematoSys (gefördert durch das Bundesministerium für Bildung und Forschung (BMBF) und geleitet von Prof. Dr. Markus Löffler), in dessen Rahmen diese Arbeit durchgeführt wurde und dessen Verbundtreffen in Leipzig immer ein Erlebnis, sowohl wissenschaftlicher als auch kultureller Art waren. Besonderer Dank gilt an dieser Stelle auch den Verbundmitgliedern in Leipzig und Regensburg, die die statistische und bioinformatische Aufarbeitung der hier generierten Daten und Fragestellungen übernommen haben. Dr. Bernd Klaus und Prof. Dr. Korbinian Strimmer danke ich für die geduldigen Erklärungen zu den Netzwerkanalysen und die kurzweiligen Diskussionen in Leipzig. Prof. Dr. Jürgen Läuter danke ich für das beherzte „Drauf-Los-Rechnen“ bei den Zeitreihendaten und das stete Bemühen unsere Analysen voranzutreiben. Herzlicher Dank geht an Prof. Dr. Rainer Spang und seine Arbeitsgruppe *computational diagnostics* in Regensburg, ohne deren bioinformatische Expertise die vorliegenden Analysen nicht möglich gewesen wären, die aber auch immer ausreichend biologisches Verständnis gezeigt haben um eine anregende Diskussion zu ermöglichen. Besonderer Dank geht hierbei an Dr. Katharina Meyer und Martin Pirkl, die immer fleißig alle Berechnungen angefertigt haben, die ich angefordert habe und trotzdem nie müde wurden, mir ihre Vorgehensweisen zu erläutern.

Des Weiteren bedanke ich mich sehr bei Prof. Dr. Heidi Hahn und Dr. Anja Uhman aus dem Institut für Humangenetik für die ersten Einblicke ins Hedgehog-Signaling sowie die großzügige Bereitstellung aller Zelllinien, Plasmide, Assays und Primer, die die Bearbeitung des Hedgehog-Kapitels überhaupt erst ermöglichten.

Bei Prof. Dr. Arnd Kieser und seiner AG möchte ich mich für die Unterstützung bei dem Tak1-Projekt und die großzügige Bereitstellung aller Informationen, Plasmide und Antikörper zu TNIK bedanken, auch wenn diese Studien nicht den Eingang in diese Arbeit geschafft haben.

Herzlicher Dank geht an die Kollegen aus der AG Kube (auch und besonders an die Ehemaligen) für die unglaublich tolle Arbeitsatmosphäre, die stete Unterstützung moralischer wie auch technischer Natur sowie die regelmäßige Versorgung mit Kuchen. Besonders erwähnen möchte ich an dieser Stelle Frederike von Bonin, Susanne Hengst und Neele Walther, die mir nicht nur technisch im Labor durch erstaunliche Fähigkeiten geholfen. Sie haben mir immer wieder Arbeit abgenommen, wenn mal wieder die KiTa angerufen hat und waren stets eine große moralische Unterstützung. An Neele geht mein Dank auch für die unzähligen Stunden der Kinderbetreuung. An dieser Stelle möchte ich mich bei allen fleißigen Korrekturleserinnen bedanken: Franziska Linke, Dr. Sonja Eberth, Juliane Lippert, Natalie Klytta, Dr. Christina Heemann, Dr. Alexandra Schrader und Dr. Julia Bode.

Mein ganz besonderer Dank gilt Alexandra, die mich zu Beginn meiner Arbeit unter ihre Fittiche genommen hat und mir nicht nur eine sehr gute Kollegin war, sondern auch eine super Freundin geworden ist. Ihre Arbeiten waren nicht nur die Grundlage für die vorliegende Studie, die Diskussionen im Büro und gemeinsamen Stunden in der Zellkultur haben auch wesentlich zur Weiterentwicklung des Projektes beigetragen. Ich danke ihr und Julia besonders herzlich für das Korrekturlesen dieser Arbeit auch zu späten Nachtstunden und die vielen, unbezahlbaren Momente im Büro und in der Freizeit. Es ist schön, dass aus Kolleginnen auch Freundinnen werden können! Den Mädels vom ehemaligen Ost-Büro danke ich für die schöne Zeit und die vielen Anregungen aus den Kaffee-Pausen.

Meinen Eltern danke ich für ihren Glauben an mich und dass sie mir immer geholfen haben, meine Ziele zu erreichen. Außerdem danke ich ihnen, genauso wie meinen Schwiegereltern, für die unsagbar große Hilfe in den letzten Wochen vor der Abgabe dieser Arbeit. Meinem Ehemann Thomas und meinem Sohn Johann danke ich von ganzem Herzen für die schöne Ablenkung in Familie nach der Arbeitszeit und das große Verständnis und die Unterstützung wenn „Mama arbeiten muss“.